CATHETER ABLATION OF CARDIAC ARRHYTHMIAS

DEVELOPMENTS IN CARDIOVASCULAR MEDICINE

Perry, H.M., ed.: Lifelong management of hypertension. ISBN 0-89838-582-2.
Jaffe, E.A., ed.: Biology of endothelial cells. ISBN 0-89838-587-3.
Surawicz, B., Reddy, C.P., Prystowsky, E.N., eds.: Tachycardias. 1984. ISBN 0-89838-588-1.
Spencer, M.P., ed.: Cardiac doppler diagnosis. ISBN 0-89838-591-1.
Villareal, H.V., Sambhi, M.P., eds.: Topics in pathophysiology of hypertension. ISBN 0-89838-595-4.
Messerli, F.H., ed.: Cardiovascular disease in the elderly. 1984. ISBN 0-89838-596-2.
Simoons, M.L., Reiber, J.H.C., eds.: Nuclear imaging in clinical cardiology. ISBN 0-89838-599-7.
Ter Keurs, H.E.D.J., Schipperheym, J.J., eds.: Cardiac left ventricular hypertrophy. ISBN 0-89838-612-8.
Sperelakis, N., ed.: Physiology and pathophysiology of the heart. ISBN 0-89838-615-2.
Messerli, F.H., ed.: Kidney in essential hypertension. 1983. ISBN 0-89838-616-0.
Sambhi, M.P., ed.: Fundamental fault in hypertension. ISBN 0-89838-638-1.
Marchesi, D., ed.: Ambulatory monitoring: Cardiovascular system and allied applications. ISBN 0-89838-642-X.
Kupper, W., Macalpin, R.N., Bleifeld, W., eds.: Coronary tone in ischemic heart disease. ISBN 0-89838-646-2.
Sperelakis, N., Caulfield, J.B., eds.: Calcium antagonists: Mechanisms of action on cardiac muscle and vascular smooth muscle. ISBN 0-89838-655-1.
Godfraind, T., Herman, A.S., Wellens, D., eds.: Entry blockers in cardiovascular and cerebral dysfunctions. ISBN 0-89838-658-6.
Morganroth, J., Moore, E.N., eds.: Interventions in the acute phase of myocardial infarction. ISBN 0-89838-659-4.
Abel, F.L., Newman, W.H., eds.: Functional aspects of the normal, hypertrophied, and failing heart. ISBN 0-89838-665-9.
Sideman, S., and Beyer, R., eds.: Simulation and imaging of the cardiac system. ISBN 0-89838-687-X.
van de Wall, E., Lie, K.I., eds.: Recent views on hypertrophic cardiomyopathy. ISBN 0-89838-694-2.
Beamish, R.E., Singal, P.K., Dhalla, N.S., eds.: Stress and heart disease. ISBN 0-89838-709-4.
Beamish, R.E., Panagia, V., Dhalla, N.S., eds.: Pathogenesis of stress-induced heart disease. ISBN 0-89838-710-8.
Morganroth, J., Moore, E.N., eds.: Cardiac arrhythmias: New therapeutic drugs and devices. ISBN 0-89838-716-7.
Mathes, P., eds.: Secondary prevention in coronary artery disease and myocardial infarction. ISBN 0-89838-736-1.
Stone, H. Lowell, Weglicki, W.B., eds.: Pathology of cardiovascular injury. ISBN 0-89838-743-4.
Meyer, J., Erbel, R., Rupprecht, H.J., eds.: Improvement of myocardial perfusion. ISBN 0-89838-748-5.
Reiber, J.H.C., Serruys, P.W., Slager, C.J.: Quantitative coronary and left ventricular cineangiography. ISBN 0-89838-760-4.
Fagard, R.H., Bekaert, I.E., eds.: Sports cardiology. ISBN 0-89838-782-5.
Reiber, J.H.C., Serruys, P.W., eds.: State of the art in quantitative coronary arteriography. ISBN 0-89838-804-X.
Roelandt, J., eds.: Color doppler flow imaging. ISBN 0-89838-806-6.
van de Wall, E.E., eds.: Noninvasive imaging of cardiac metabolism. ISBN 0-89838-812-0.
Liebman, J., Plonsey, R., Rudy, Y., eds.: Pediatric and fundamental electrocardiography. ISBN 0-89838-815-5.
Higler, H., Hombach, V., eds.: Invasive cardiovascular therapy. ISBN 0-89838-818-X.
Serruys, P.W., Meester, G.T., eds.: Coronary angioplasty: a controlled model for ischemia. ISBN 0-89838-819-8.
Tooke, J.E., Smaje, L.H., eds.: Clinical investigation of the microcirculation. ISBN 0-89838-833-3.
van Dam, Th., van Oosterom, A., eds.: Electrocardiographic body surface mapping. ISBN 0-89838-834-1.
Spencer, M.P., ed.: Ultrasonic diagnosis of cerebrovascular disease. ISBN 0-89838-836-8.
Legato, M.J., ed.: The stressed heart. ISBN 0-89838-849-X.
Safar, M.E., ed.: Arterial and venous systems in essential hypertension. ISBN 0-89838-857-0.
Roelandt, J., ed.: Digital techniques in echocardiography. ISBN 0-89838-861-9.
Dhalla, N.S., Singal, P.K., Beamish, R.E., eds.: Pathophysiology of heart disease. ISBN 0-89838-864-3.
Dhalla, N.S., Pierce, G.N., Beamish, R.E., eds.: Heart function and metabolism. ISBN 0-89838-865-1.
Beamish, R.E., Panagia, V., Dhalla, N.S., eds.: Pharmacological aspects of heart disease. ISBN 0-89838-867-8.
Ter Keurs, H.E.D.J., Tyberg, J.V., eds.: Mechanics of the circulation. ISBN 0-89838-870-8.
Sideman, S., Beyar, R., eds.: Activation, metabolism and perfusion of the heart. ISBN 0-89838-871-6.
Aliot, E., Lazzara, R., eds.: Ventricular tachycardias. ISBN 0-89838-881-3.
Schneeweiss, A., Schettler, G.: Cardiovascular drug therapy in the elderly. ISBN 0-89838-883-X.
Chapman, J.V., Sgalambro, A., eds.: Basic concepts in doppler echocardiography. ISBN 0-89838-888-0.
Chien, S., Dormandy, J., Ernst, E., Matrai, A., eds.: Clinical hemorheology. ISBN 0-89838-807-4.
Morganroth, J., Moore, E.N., eds.: Congestive heart failure. ISBN 0-89838-955-0.
Heintzen, P.H., Bursch, J.H., eds.: Progress in digital angiocardiography. ISBN 0-89838-965-8.
Spaan, J.A.E., Bruschke, A.V.G., Gittenberger, A.C., eds.: Coronary circulation. ISBN 0-89838-978-X.
Bayes de Luna, A., eds.: Therapeutics in cardiology. ISBN 0-89838-981-X.

CATHETER ABLATION OF CARDIAC ARRHYTHMIAS

BASIC BIOELECTRICAL EFFECTS AND CLINICAL INDICATIONS

EDITED BY MELVIN M. SCHEINMAN

University of California, San Francisco

MARTINUS NIJHOFF PUBLISHING
A MEMBER OF THE KLUWER ACADEMIC PUBLISHERS GROUP
BOSTON/DORDRECHT/LANCASTER

Distributors

for North America: Kluwer Academic Publishers, 101 Philip Drive, Assinippi Park, Norwell, MA 02061, USA

for the UK and Ireland: Kluwer Academic Publishers, MTP Press Limited, Falcon House, Queen Square, Lancaster LA1 1RN, UK

for all other countries: Kluwer Academic Publishers Group, Distribution Centre, Post Office Box 322, 3300 AH Dordrecht, The Netherlands

Library of Congress Cataloging-in-Publication Data

Catheter ablation of cardiac arrhythmias.

(Developments in cardiovascular medicine)
Includes bibliographies and index.
1. Arrhythmia — Treatment. 2. Cardiac catheterization.
I. Scheinman, Melvin M. (Melvin Mayer), 1935–
II. Series. [DNLM: 1. Arrhythmia — Surgery. 2. Electrocardiography. 3. Heart catheterization. W1 DE997VME/WG 330 C363]
RC685.A65C295 1988 617'.412 87-22091

ISBN-13: 978-1-4612-8990-6 e-ISBN-13: 978-1-4613-1765-4

DOI: 10.1007/978-1-4613-1765-4

CONTENTS

CONTRIBUTING AUTHORS

Gust H. Bardy
Division of Cardiology
Harborview Medical Center
325 Ninth Avenue
Seattle, WA 98104

E.G. Boyd
Guy's Hospital
St. Thomas Street
London SE1 9RT
England

G. Thomas Evans, Jr.
University of California
Room 312 Moffitt Hospital
San Francisco, CA 94143-0214

Guy Fontaine
Cardiac Department
Hopital Jean-Rostand
39–41, rue Jean Le Galleu
94200
France

Paul C. Gillette
Director, Division of Pediatric Cardiology
Medical University of South Carolina
171 Ashley Avenue
Charleston, SC 29425

Phyllis M. Holt
5, Canonsfield Road, Oaklands
Welwyn Herts AL6 0PY
England

Joseph H. Levine
Assistant Professor of Medicine
Johns Hopkins University School of Medicine
600 N. Wolfe Street
Baltimore, MD 21205

Frank I. Marcus
Professor of Medicine
Chief of Cardiology Section
University of Arizona
Tucson, AZ 85724

Fred Morady
Division of Cardiology
University Hospital
University of Michigan Medical Center
UH/B1 F245/0022
1500 East Medical Center Drive
Ann Arbor, MI 48109-0022

E. Neil Moore
Department of Cardiology
Hospital of the University of Pennsylvania
669 White Building
3400 Spruce Street
Philadelphia, PA 19104

Bertrand Ross
Division of Pediatric Cardiology
Medical University of South Carolina
171 Ashley Avenue
Charleston, SC 29425

Michael A. Ruder
770 Welch Road
Suite 100
Palo Alto, CA 94304

Sanjeev Saksena
Newark Beth Israel Medical Center
201 Lyons Avenue
Newark, New Jersey 07112

Melvin M. Scheinman
Professor of Medicine
University of California
Room 312 Moffitt Hospital
San Francisco, CA 94143-0214

Vickie Zeigler
Division of Pediatric Cardiology
Medical University of South Carolina
171 Ashley Avenue
Charleston, SC 29425

DEDICATION

The use of electrode catheter techniques for treatment of cardiac arrhythmias has opened a new and exciting approach for management of patients with drug-refractory cardiac arrhythmias. As with any new advance, investigators properly focus on the safety and efficacy of the technique but often forgotten is the courage and emotional fortitude of the patients (and their families) who agree to walk with us through uncharted and potentially dangerous paths. It is for this reason that I dedicate this book to Paul Christian Anderson who was the first patient to undergo catheter ablative procedure. Paul was a retired machinist living in northern California who suffered from crippling arthritis and severe chronic obstructive lung disease as well as cardiac disease. He was plagued with recurrent episodes of atrial fibrillation associated with rapid ventricular rates, which often resulted in frank pulmonary edema. He proved refractory or intolerant to trials of all available drugs, including amiodarone. His case was discussed with our surgical colleagues who felt that surgical interruption of the His bundle constituted an unacceptably high risk procedure for this patient. At about this time, my colleague, Dr. Rolando Gonzalez, and I had just completed our canine studies using a catheter ablative technique to interrupt AV conduction. With some trepidation, we had decided to offer this technique to the appropriate patient.

The task of obtaining truly informed consent was particularly delicate since there was no prior clinical guidelines to define efficacy or potentially dangerous consequences of this procedure. I felt that it would be inappropriate for

me to obtain consent because of possible favorable biases that I might have for the procedure I helped develop. The task of obtaining consent was assigned to Dr. David Hess, an outstanding and sensitive clinical cardiologist who was a full-time faculty member in the Division of Cardiology (Electrophysiology). Dave, as an arrhythmia specialist, was in an excellent position to evaluate both the gravity of the clinical problem and was fully conversant with our animal experience. He spent many hours discussing the new procedure and counseling Mr. Anderson and his wife. Once the decision was made to proceed with ablation, I think Mr. Anderson sensed the apprehension of his physicians and turned out to be a tower of strength for us. He fully realized that this procedure would not cure his severe arthritis or prevent the relentless progression of his cardiac and pulmonary diseases. It was clear that the decision was taken as much for a chance of personal benefit as it was for a sincere desire to help other patients with similar debilitating cardiac arrhythmias. The procedure was performed on April 9, 1981 and, to our great relief, was both successful and uneventful. Although AV conduction subsequently resumed, his arrhythmia was now easily controlled with verapamil.

Paul died of severe cardiac failure several years ago, but I know that he and his wife shared enormous pride of having pioneered this procedure. He is fondly remembered for his magnificent altruism, emotional strength, and courage.

PREFACE

The field of catheter ablation has grown in a rather helter-skelter fashion. Ablative techniques were applied in patients before basic bioelectric and cellular electrophysiologic effects were fully defined. Since the introduction of this technique into clinical medicine in 1982, happily, a wealth of basic information has become available, and it was thought prudent to summarize existing data in the form of a text. The purpose of this text is to provide for a concise summary of both the basic and clinical experiences to date. It was simply not possible to include chapters from many workers who have made outstanding contributions in this area. For this, I offer my profound apologies. I do wish, however, to acknowledge the outstanding work of Drs. Bharati and Lev who provided us with a sound understanding of the histologic effects of various energy delivery systems. Their seminal observations allowed us to bring this technique to clinical fruition.

The book is divided into sections that allow for the clinician, physicist, basic electrophysiologist, or pathologist to extract relevant information. The first two chapters are devoted to exploring the physics of high-energy direct current discharge as well as the important cellular electrophysiologic changes incident to these discharges. This is followed by a series of chapters which focus on the histologic effects of both high-energy electrical shocks and laser and radiofrequency energy on atrial, AV junctional, and ventricular myocardial tissue. The final chapters summarize the clinical usage of this technique for patients with either supraventricular or ventricular arrhythmias. I am

delighted with and extremely appreciative of the outstanding contributions to this book by its world renowned group of authors. Their skill and patience made editing of this book both instructive and pleasant.

Clearly, the presently available catheter techniques represent the first small steps. We await with a great sense of excitement and anticipation the continued technical breakthroughs in terms of perfecting energy sources as well as exploring catheters. These technical advances will no doubt extend the clinical usefulness of these techniques. I sincerely hope this text serves as a catalyst for bright young clinicians, physicists and catheter engineers to expeditiously provide us with the needed technical advances.

CATHETER ABLATION OF CARDIAC ARRHYTHMIAS

1. BIOELECTRIC EFFECTS OF HIGH-ENERGY, ELECTRICAL DISCHARGES

PHYLLIS M. HOLT AND E.G. BOYD

Patients with paroxysmal supraventricular or ventricular tachycardias may find drug therapy ineffective or productive of unacceptable side effects. Until recently the therapeutic alternatives in this situation were antitachycardia pacemakers, which are unsuitable for some patients [1, 2], or surgery with its attendant hazards [3, 4]. The recent development of the high-energy, direct current endocardial ablation technique marked the beginning of a new era of the management of drug resistant tachyarrhythmias.

In 1979 Vedel et al [5] published the first report of atrioventricular block produced by electric shock. This occurred inadvertantly during an electrophysiological study. The patient required external cardioversion for refractory ventricular tachycardia and the shock was believed to have traveled via the His bundle catheter. Subsequent animal experiments by Scheinman et al showed that permanent complete heart block could be produced in dogs by delivering a direct current electrical discharge from a defibrillator via a catheter electrode to the atrioventricular node [6]. Such impulses produced localized myocardial damage [7].

This technique was then used to interrupt His bundle conduction in patients with drug-resistant paroxysmal supraventricular tachycardia [8, 9]. Its potential in the management of other tachyarrhythmias was soon recognized. High energy impulses were delivered by catheter electrodes positioned in the coronary sinus in patients with Wolff-Parkinson-White syndrome [10–12] and in the ventricles in patients with ventricular tachycardia [13, 14].

Using temporary catheter electrodes and standard defibrillators, the energies employed by different groups have varied considerably. For His bundle ablation, shocks have been delivered ranging in amplitude from 50 joules by McComb [15], 150 joules to 300 joules by Manz [16], 200 joules to 300 joules by Gallagher [9], 300 joules to 400 joules by Nathan [17] and 300 joules to 500 joules by Scheinman [8]. The total energy delivered to a single patient can be considerably higher, however, than these figures would suggest, e.g., 11 shocks with a maximum energy of 350 joules [17].

Energy delivery to the coronary sinus has ranged from 50 joules to 100 joules [12], 100 joules to 150 joules [10] and 400 joules at the coronary sinus ostium [11]. Attempted ablation of ventricular tachycardia foci have generally required higher energy impulses, e.g., 600 joules [13].

The rapid expansion of the endocardial ablation technique into all fields of tachyarrhythmia management has not been without complications. These include arrhythmias [17], cardiac tamponade [18], coronary sinus rupture and thrombosis [10], circumflex artery lesions [18], and impaired ventricular function [19, 20]. Efforts have been made to improve the efficiency of the energy delivery. These include the use of active fixation electrodes [21], suction electrodes [22], anodal instead of cathodal energy impulses [14, 23], bipolar energy delivery [24], or a second intracardiac electrode as the indifferent pole [25].

In order to further reduce energy requirements and improve the safety of the technique, it is essential that the biophysical effects of such high-energy impulses should be understood. This chapter discusses these effects. It is divided into three sections, the first discusses the physical and the second the physiological effects that occur during the delivery of high-energy impulses. Section three considers the energy delivery system and the catheter electrodes used in the endocardial technique and describes modifications that may reduce energy requirements clinically. These findings will then be used to try and identify the physical effects responsible for the interruption of conduction.

PHYSICAL EFFECTS OF HIGH-ENERGY DIRECT CURRENT SHOCKS

When performing His bundle ablation, most workers use the following technique. The high energy electrical impulse is delivered from the cathodal output of a standard defibrillator via the distal pole of a bipolar USCI catheter electrode, with an indifferent back plate connected to the anodal output.

If this technique is simply reproduced in the laboratory by immersing the back plate and distal end of the catheter electrode in a tank of normal saline, and energy is delivered from a defibrillator as described above, several phenomena will be noticed. First, a flash of light is produced from the electrode, a loud report will be heard, and gas bubbles may be seen in the fluid. All these events occur extremely rapidly.

A system has recently been described to investigate these effects in more detail [26]. A plastic tank with a side viewing port was filled with Ringer's solution and a standard defibrillator back paddle positioned adjacent to the wall inside the tank and connected to the anodal output of a cardioversion unit. The catheter under test was connected to the cathodal output and positioned so that its distal electrode was approximately at the center of the tank, 10 cm from the back paddle and visible through the viewing port. During these studies the pressure pulse in the tank was monitored using a simple piezoelectric crystal transducer mounted on a substantial back plate for mechanical support. The high voltage between the electrodes was measured from connections from the proximal end of the catheter and the back paddle. The current through the system was also recorded and stored on magnetic tape. Visual effects were recorded using 35 mm time exposures, video tape, and high-speed cine film at 4000 frames per second. The effects of different energies delivered via various catheter electrodes can all be evaluated using this system.

The sequence of events observed when a 400 joule impulse was delivered to the system using a 6F USCI bipolar catheter electrode is illustrated in the photographs in figure 1–1. Each picture is a print of single frames taken from the cine film.

During the delivery of the shock, an incandescent globe was produced around the electrode tip. The globe expanded to reach its maximum diameter in 5 milliseconds. This corresponded approximately to the peak flow of the current, thereafter the globe collapsed (figure 1–2). The incandescence continued during the contraction phase for the period of the flow of current. With the extinction of the glow, there remained a diffuse cloudlike structure around the electrode, which coalesced into minute bubbles. These became larger and fewer in number, moving away from the catheter tip. It was also observed that within two frames, 0.5 milliseconds, the globe had formed to almost half its maximum diameter. Oscillation of the pacing wire after the discharge of the defibrillator was also seen on the film.

The initial emission of energy from the catheter tip resembles an explosion, and during this phase, from 0 ms–2 ms, a positive pressure wave is generated. Following this phase a globe or fireball forms, which then condenses down into gas bubbles. The latter phase, up to the appearance of definite gas bubbles, lasts from 2 ms–7 ms and is accompanied by a negative pressure wave (figure 1–2). The ensuing oscillations of the pressure recording are thought to be due to reverberations of the pressure wave from the tank walls.

These pressure changes have been measured and found to be over 1 atmosphere, 3 centimeters from the electrode tip. Applying the inverse distance law, this suggests pressures of more than 3 atmospheres at the fireball surface [26]. Other workers have also attempted to measure pressure changes and found even higher values [27].

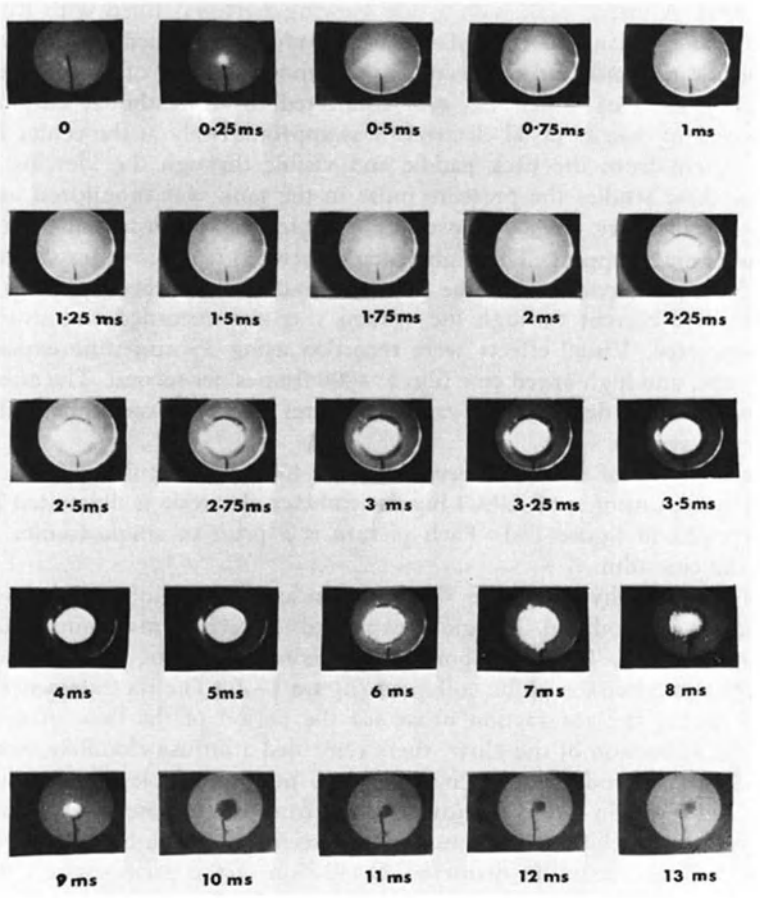

Figure 1–1. Photographs taken at 4000 frames per second of a 400 joule unipolar impulse delivered through a 6F USCI bipolar electrode in Ringer's solution.

Reliable and accurate measurements of temperature at the electrode tip are difficult, primarily because of the high voltages and currents present during the brief electrical impulse. Experiments in which electrode tips have been shielded by polytetrafluroethylene (PTFE) tubing have resulted in fusion and erosion of the electrodes, indicating temperatures in excess of 1700°C, the melting point of platinum. It is likely that even greater temperatures are present, see below.

Reducing the amount of energy delivered via the distal pole of a bipolar 6F USCI catheter reduces the size of the fireball obtained and the changes in

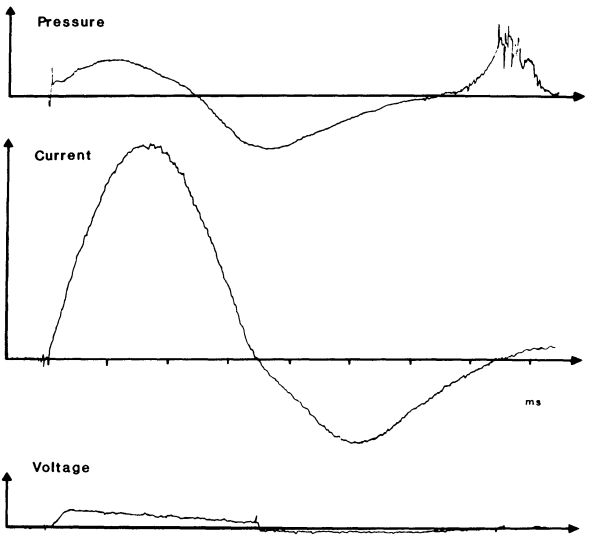

Figure 1–2. Voltage, current and pressure recordings of a 400 joule unipolar impulse delivered through a 6F USCI bipolar electrode in Ringer's solution.

pressure observed. Figure 1–3 shows photographs taken on 35 mm film using time exposures to give an integrated image of the electrode flash at different delivered energies. The corresponding changes in pressure, current, and voltage are shown in figure 1–4.

Using the observations above, it is possible to propose a detailed explanation of the sequence of events that occur during the delivery of a high-energy electrical impulse.

The current from the defibrillator passes between a small area electrode at the catheter tip and a large area electrode, the back paddle. The current density near the catheter electrode surface is therefore considerably higher than that near the back paddle. Thus, the effective resistance of the conducting medium around this electrode is also very high. As the current flows serially through the system, the energy dissipated will be proportional to the resistance of any individual element. The energy dissipated in the medium will be at a maximum near the catheter electrode surface.

This causes the temperature of the medium next to the catheter electrode surface to rise rapidly. When the temperature of any liquid in contact with the electrode surface reaches its boiling point, vapor forms on the electrode surface. As the last of the liquid in contact with the electrode vaporizes, it will be heated very rapidly due to the concentration of the current in this remaining liquid medium. The high field strength in the last of the vapor

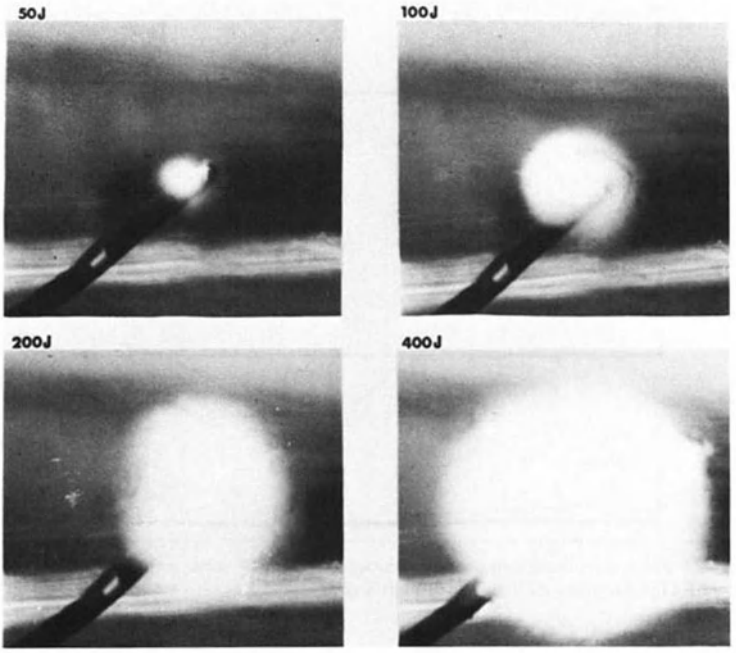

Figure 1–3. Time exposures for 50, 100, 200, and 400 joule unipolar impulses delivered through the distal pole of a 6F USCI bipolar electrode in Ringer's solution.

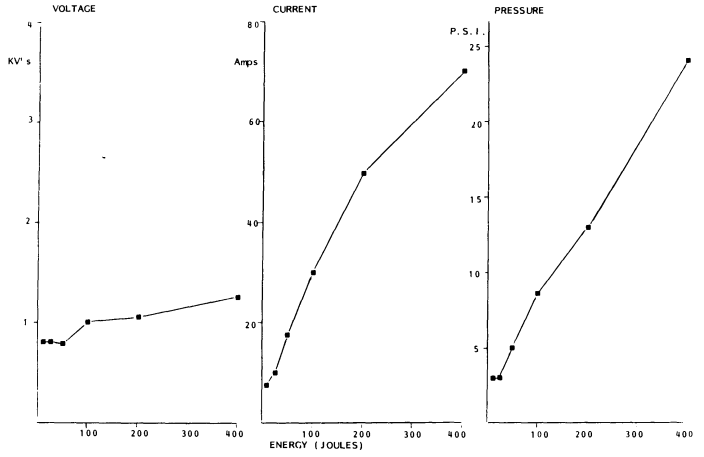

Figure 1–4. Graphs showing peak voltage, peak current, and peak pressure excursions versus energy for unipolar impulses delivered through a 6F USCI bipolar electrode in Ringer's solution.

film to be formed may initiate ionization, producing plasma tracks in the vapor volume surrounding the electrode.

Three phenomena should then occur,

1. The production of localized high temperatures.
2. Optical emission from the vapor film.
3. A discontinuity in the voltage-current relationship.

The observed effects confirm the presence of high temperatures within the fireball at the electrode surface. These are probably higher than 1700°C, since plasma arc temperatures are seldom less than 5000°C. The second phenomenon of optical emission is also observed. Since it is generated by electric arcs, it will be over a broad spectral band. The voltage-current relationships for the USCI electrode show pronounced discontinuities.

With a further increase in the current, more energy is dissipated in the liquid medium, producing further vaporization. This would account for the expanding incandescent globe. The initial rapid expansion of the bubble would generate a positive mechanical pressure wave.

Once the current has passed its peak value, the energy loss is no longer balanced by electrical energy input and the bubble growth can no longer be maintained. This accounts for the negative pressure wave. The gas bubbles seen in figure 1–1 may be produced from both heating and electrolysis of the medium.

These light, pressure, voltage, and current effects are all reduced by delivering smaller energy impulses, particularly if the shocks are less than 100 joules.

Effects on impedance

If a small spherical electrode, radius r, is emersed in a large volume of homogeneous medium and a large electrode is placed some distance away, the intra-electrode medium impedance is given by $\rho/4\pi r$, where ρ is the medium electrical conductivity. Using the same mathematical development, it can be shown that approximately 90% of the overall intra-electrode medium impedance is governed by the medium within ten radii of the electrode. Therefore, provided that the size of the small active electrode is below one-tenth of the dimensions of the tank, it would be operating in a semi-infinite medium environment. Initial investigations using small and large electrodes in various sized containers have shown that the fireball around the small electrode could reach over 2 cm in diameter at high-impulse energy. For such a fireball to remain within a semi-infinite medium, the linear dimension of the tank should be at least 20 cm.

Using the test tank described [26], the medium impedance has been measured for a range of spherical electrodes and the inverse relationship between electrode radius and intra-electrode impedance was found to be valid within 10%, up to 25 mm in diameter. Therefore, the growth of the fireball

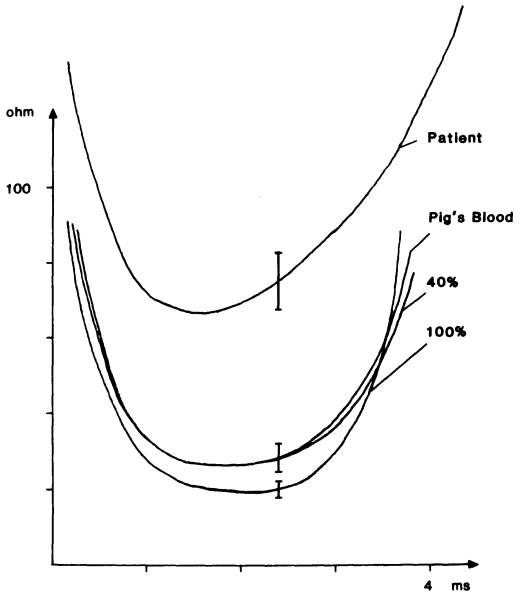

Figure 1–5. Impedance-time curves calculated from simultaneous voltage and current recordings for 100 joule unipolar impulses delivered through 6F USCI bipolar electrodes. The graph shows patient and tank measurements. The latter data are for a physiologically isotonic clear medium, a 40% dilution and heparinized pig's blood.

up to 25 mm in diameter would not be significantly constrained by this size of test tank. The use of tanks smaller than this size would be suitable for investigations employing lower impulse energies.

Using the voltage and current curves recorded over the impulse energy range 10 joules to 400 joules in the test tank, it was found that the impedance was grossly nonlinear and time dependent. Figure 1–5 shows a calculated impedance trace for the primary current pulse for 100 joules delivered through a physiologically normal clear solution. Traces for fresh heparinized pig's blood and a 40% solution are also shown. The uppermost trace is for a typical patient's unipolar recording. The difference in the results is due to the electrical conductivities of the fluid/tissue media.

The electrical conductivities of physiologically normal solutions, Ringer's or saline, is approximately three times that of whole blood. This is probably due to the red cells. At frequencies below several hundred kilohertz it is generally accepted that electrical conduction does not occur through the red cells [28], as the membrane acts as an insulator. With a typical hematocrit of 45%, it is expected that the isotonic concentration should be just over 50%. The random orientation of the disc-shaped red cells adds an additional path length for the current flow, which lowers the bulk electrical conductivity.

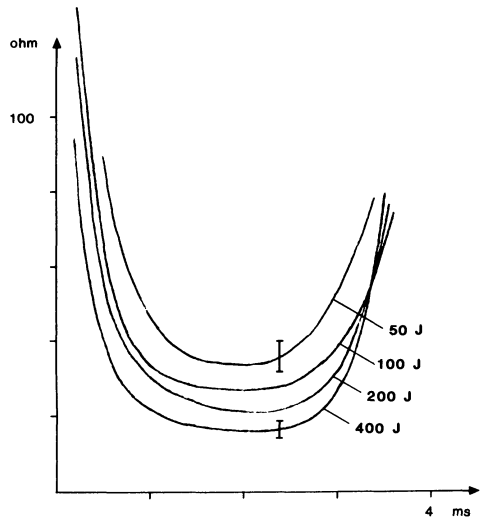

Figure 1–6. Impedance-time curves calculated from simultaneous voltage and current recordings for unipolar impulses delivered to a clear medium in the test tank over the energy range 50 joules to 400 joules. A 6F USCI bipolar electrode was used.

This effect was considered mathematically by Fricke [29]. The anisotropic nature of the electrical conductivity of moving blood was demonstrated practically by Leibman [30].

Figure 1–6 shows a family of impedance curves for a range of impulse energies for a 40% solution. It can be seen that as the impulse energy is increased, the impedance miminum falls to lower values. It has already been shown that the fireball increases in diameter as the energy is increased. Therefore the fireball growth is the dominant factor controlling the impedance non-linearity observed.

From measurements of the change in the fireball size with time using the high-speed cine film, it is possible to calculate the fireball/medium interface current density. Figure 1–7 shows the measured current and fireball diameter for a 50 joule impulse through a 40% solution. The calculated surface current density is also shown. It can be seen that, despite a considerable increase of current flow during the pulse, the current density at the fireball/medium interface actually falls progressively during the pulse. This is considered further in the energy delivery section.

The simple test tank is not an accurate patient analogue, but it does allow a comparative assessment of electrode performance. It is interesting to note that the impedance is not necessarily a useful parameter to monitor when considering the use of a regular defibrillator with an internal inductor. Figure 1–5 shows that the impedance at 100 joules for a unipolar patient ablation

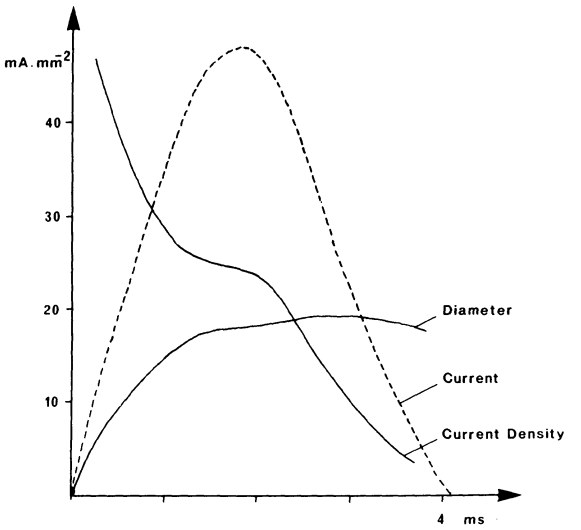

Figure 1–7. Current and fireball diameter measured for a 50 joule unipolar impulse delivered through a 6F USCI bipolar electrode. The calculated fireball surface current density is also shown.

impulse is 150% higher than the tank using 40% solution or whole blood. However, as the major controlling influence in the circuit is the inductor, the current is only 30% higher. Figure 1–8 shows a graph of the peak currents recorded versus energy for unipolar impulses via a 6F USCI catheter in the tank and in patients. The difference in currents is much lower than the relative impedances would suggest.

PHYSIOLOGICAL EFFECTS OF HIGH-ENERGY DIRECT CURRENT SHOCKS

During clinical endocardial ablation procedures, some of the energy will be delivered from the electrode surface adjacent to the endocardium and conducting tissue, while the remainder is delivered away from the endocardium into the blood. Therefore, this section considers both the hematological and tissue/membrane effects produced during the delivery of high-energy impulses.

Hematological effects

The presence of high temperatures and large pressure changes is likely to produce red cell damage. A study in which impulses were delivered to a small volume of fresh human blood showed that hemolysis and gas production occurred [31]. This was later confirmed in vivo. [32].

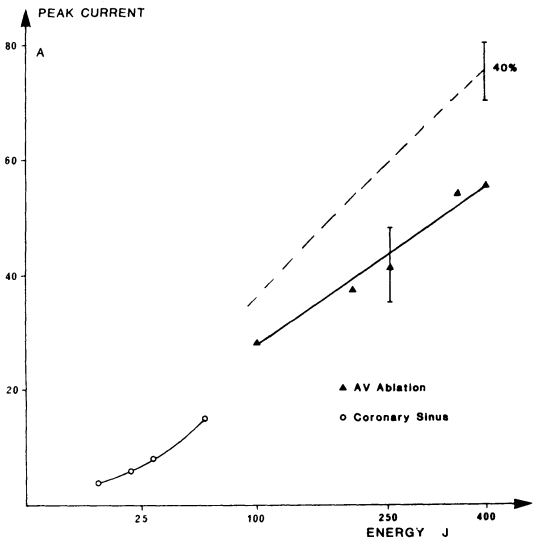

Figure 1–8. Peak current recordings for unipolar impulses delivered through a 6F USCI bipolar electrode over the energy range 10 joules to 400 joules for patients. The dashed line represents the peak currents during tank tests using a 40% solution.

Recent work using fresh heparinized pig's blood has attempted to quantify the hematological damage that occurs during delivery of high-energy impulses [33]. Using a plastic tank and a gas collecting assembly, cathodal and anodal shocks were delivered via the distal electrode of 6F USCI catheters immersed in the blood. Multiple shocks at energies of 10, 25, 50, 100, 200, and 400 joules were delivered. Hemolysis and gas production was assessed for each energy value.

Gas production

A quantity of energy may be delivered as a single large shock or as several smaller impulses. Figure 1–9 illustrates the effects on the volume of gas produced when a total of 400 joules is delivered as single or multiple impulses. The volume of gas liberated per single impulse at each energy was calculated for anodal and cathodal deliveries and is illustrated in figure 1–10. Using cathodal impulses mean gas production over the energy range 10 joules to 50 joules was 0.50 ul/J falling to 0.29 ul/J in the higher range of 100 joules to 400 joules. Anodal impulses liberated greater gas volumes, at a rate of 4.34 ul/J from 10 joules to 200 joules. Greater energies could not be assessed because the gas collecting apparatus could not withstand the pressure shock wave produced when 400 joules was delivered anodally.

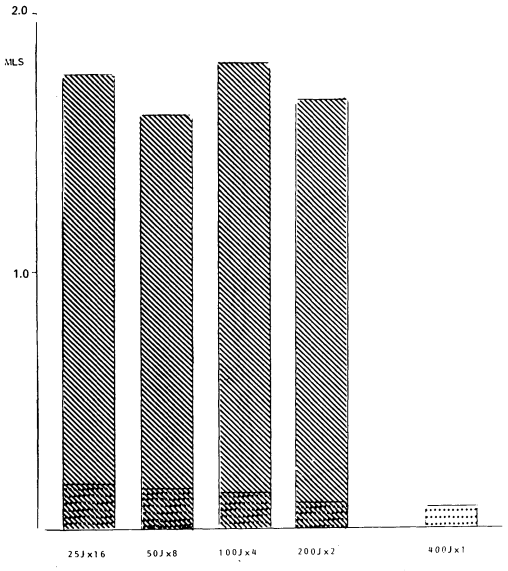

Figure 1–9. Variation in gas volumes produced when 400 joules is delivered as single or multiple shocks.

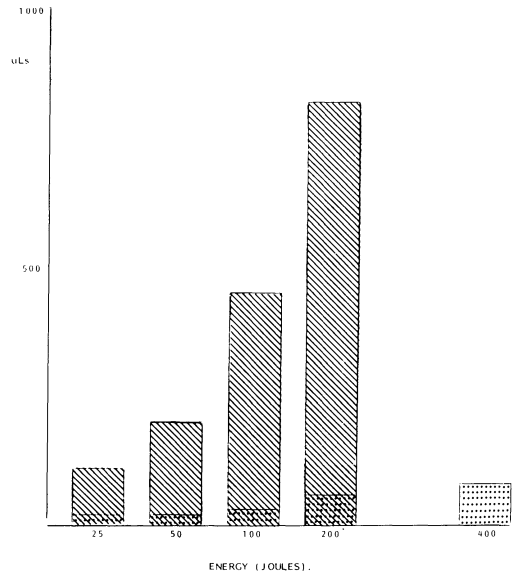

Figure 1–10. Volume of gas liberated per impulse for unipolar anodal and cathodal impulses.

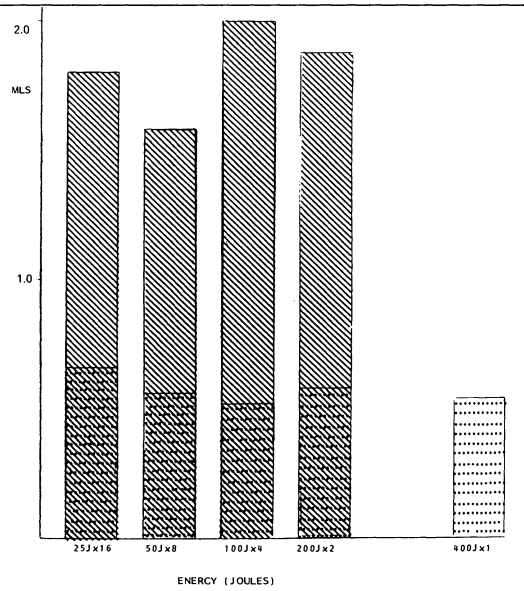

Figure 1–11. Graph of the amount of hemolysis occurring in 7 litres of fresh pig's blood per 400 joules delivered at various impulse energies.

Analysis of the gas samples showed that they were composed predominantly of hydrogen and nitrogen. Values of hydrogen for cathodal and anodal energy delivery, respectively, were 50% to 69% and 66% to 69%. The corresponding figures for nitrogen were 21% to 39% and 12% to 17%. Oxygen and carbon dioxide were present in much smaller amounts. As the impulse energy increased, the percentage of nitrogen and oxygen rose, and hydrogen and carbon dioxide fell.

For anodal delivery, in addition to the gases mentioned above, small quantities of carbon monoxide were present.

Hemolysis

Using either electrode polarity hemolysis was found to be directly proportional to the impulse energy. The volume hemolyzed per 400 joules delivered, either as a single shock or multiple shocks of smaller energies is shown in figure 1–11. The hemolysis produced per single impulse is illustrated in figure 1–12. Expressed as blood hemolyzed per joule delivered, the rates were 1.37 ul/J for cathodal electrodes and 4.48 ul/J for anodal electrodes.

Analysis of blood films after delivery of high-energy impulses showed

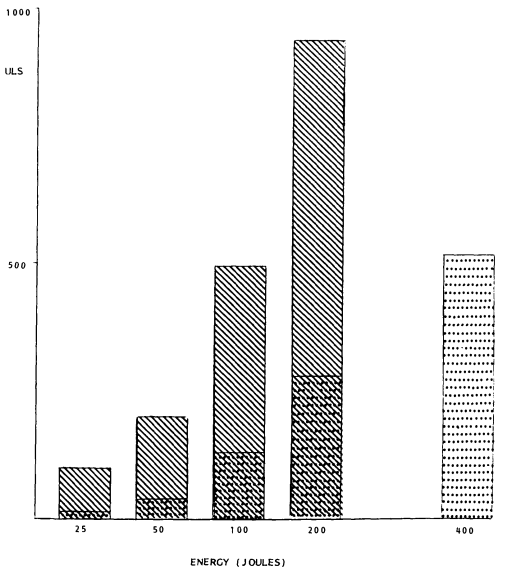

Figure 1–12. Graph of the amount of hemolysis per single high energy impulse. The quantity of blood hemolysed rises as the energy of the shock increases from 10 joules to 400 joules.

evidence of cellular clumping and aggregation. However, there was no significant change in hematocrit or hemoglobin.

The results of delivering energy anodally differ markedly from those produced by cathodal energy delivery. Gas production is 8.7–15.0 times greater using anodal energy delivery, and hemolysis is three times greater using anodal compared to cathodal polarity. The effects of anodal versus cathodal impulses will be discussed in more detail below.

Faraday's law of electrolysis predicts the formation of hydrogen around a negative electrode. Calculations based on the charge transported per impulse suggest the volume of hydrogen evolved would be 2.1 ul to 13.2 ul for 10 joules to 400 joules impulses. The amount detected was considerably greater. Theoretically no hydrogen should be evolved with a positive electrode, whereas it forms more than 60% of the total volume. Both these findings provide evidence of plasmas within the fireball around the electrode. Plasma temperatures may be high enough to promote direct thermal dissociation of water, releasing hydrogen, oxygen, and various species of free radicals. With cathodal electrode polarity oxygen would be released only after establishment of the electrical plasma (i.e., after fireball production), whereas with anodal electrode polarity oxygen would be produced initially by electrolysis before the fireball had formed and be available immediately for oxidation processes during the latter process. The heat of reaction of this anodal process would

increase the local environmental temperature around the electrode and enhance the initial energy dissipation. This effect could account for the more violent effects observed when using anodal electrodes.

Although carbon monoxide is produced during anodal discharges, the maximum volume produced was 0.16 ml for 400 joules. The volume produced for single shocks of 10 joules to 200 joules is therefore below that producing clinical toxicity [34]. However, the volume of gas produced experimentally during anodal delivery of high-energy impulses may prove a potential source of emboli. This would be important in procedures involving the left ventricle.

Tissue effects of high-energy direct current impulses

The effects of high-energy impulses on the myocardium will be considered in two sections: firstly, impairment of cellular membrane function and structure, and, secondly, gross, macroscopic effects on cardiac tissue. Histological changes will be discussed in subsequent chapters.

Effects on the cell membrane

Work on the response of myocardial cells to electric field stimulation was originally performed during the investigation of electric countershock treatment for defibrillation. Jones et al [35, 36] developed a method for growing myocardial cells from chick embryos. These cells were subject to electric field stimulation to examine the relationship between the shock intensity and cellular effects observed. Jones developed the concept of shock strength (f) expressed in terms of potential gradient V/L where V equals the voltage applied and L the distance between electrode plates.

Low levels of stimulation (6 V/cm–20 V/cm) elicit action potentials of normal amplitude followed by complete repolarization. At 40 V/cm an action potential of larger amplitude than the control was produced, followed by incomplete repolarization. At 60 V/cm–80 V/cm these high amplitude action potentials were followed by incomplete repolarization and a number of rapid action potentials of reduced amplitude. At 100 V/cm the induced action potential was reduced in amplitude and followed by a period of arrest. The arrest was terminated by the appearance of slow oscillations, which developed into a rapid sequence of action potentials.

Cellular contraction was also studied. Following a single shock of 80 V/cm the amplitude of contraction was diminished but gradually returned to normal over 20 seconds. A shock of 200 V/cm produced an extrasystole followed by temporary arrest. A contracture of approximately 75% of the normal contraction amplitude developed, acompanied by cellular fibrillation [35–37]. This gradually subsided over three minutes.

Accompanying these effects in action potentials and cellular contraction were associated changes in the cellular ultrastructure [38]. Cells receiving low

intensity shocks (80 V/cm) showed some changes in the mitochondria. Cells receiving high intensity shocks (200 V/cm) exhibited pronounced alterations, including aggregation of mitochondria, with alteration of mitochondrial structure. Other changes include contracture with occasional disorganization of myofibrils, separation of the nuclear membranes, and swelling of the endoplasmic reticulum. In addition to this swelling of cellular organelles, cellular edema also occurs. These changes are consistent with those reported following application of shocks of similar voltage gradients to dogs [39] and guinea pig myocardium [40], and exhibit dose dependency similar to that reported by other workers [41, 42].

One hypothesis to explain these findings is that transient microlesions are produced in the sarcolemma [43]. This could occur due to compression of the membrane by the electric field [44]. The membrane has a high resistance, therefore, membrane areas parallel to the field, where the current enters and leaves the cell, are subjected to the highest transmembrane voltage gradient. Microlesions are produced in those areas where a critical membrane potential is exceeded. Therefore, the size of the microlesions and area of the membrane over which they occur, increase with shock intensity. During and post-shock these lesions would allow an indiscriminate exchange of ions to take place. This would lead to membrane depolarization and post-shock arrest. Support for this hypothesis comes from two pieces of evidence. First, prolonged depolarization occurs in the presence of tetrodotoxin and verapamil in concentrations which block the excitation channels [35]. Secondly, dextrans labeled with fluorescein-isothiocyanate (FITC) and having a molecular diameter less than 50 Å, enter the myocardial cell during 200 V/cm, 5 ms rectangular wave shocks, although larger dextrans are excluded [44].

Although the above findings resulted from work on electric counter shock for defibrillation, they are relevant to the endocardial ablation technique, since this consists simply of electrical energy delivered between two electrodes.

Macroscopic effects

The histological findings occurring during the ablation technique will be reported in subsequent chapters. However, the gross cardiovascular effects of this procedure will be considered, since they provide evidence which helps identify the physical effect producing the therapeutic result, i.e., abolition of conduction in the cardiac conducting tissue.

Experiments in which shocks of 100 joules were delivered to isolated perfused guinea pig hearts and 400 joules to dog hearts perfused using the Langendorff technique [45] failed to show any macroscopic endocardial lesion acutely [46]. A study was subsequently performed in which energies of 50 joules to 400 joules were delivered cathodally to the left and right ventricles of dogs who were sacrificed 30 minutes later. Macroscopic endocardial

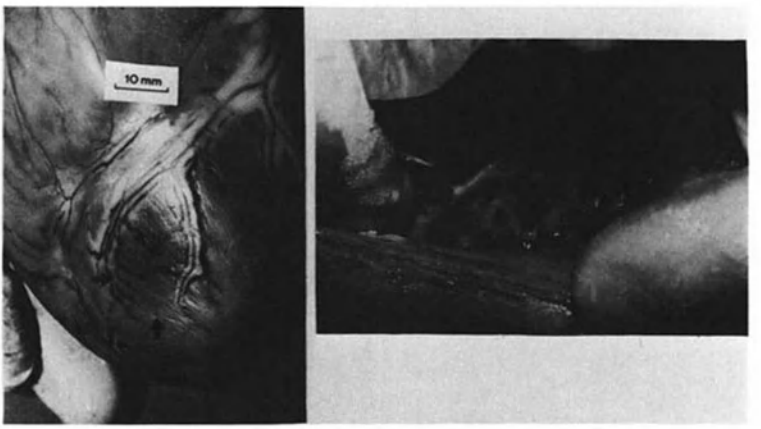

Figure 1–13. This illustrates the epicardium (on the left) and endocardium (on the right) of the right ventricle of a canine heart. Four hundred joules were delivered via a USCI electrode, and the dog died 30 minutes later. No macroscopic endocardial lesion is visible, athough a hemorrhagic epicardial lesion is apparent.

lesions were not invariably present, even when areas of epicardial damage were visible (figure 1–13). A similar absence of macroscopic endocardial damage has also been reported in some humans who have died shortly after ablation procedures [47].

Attempts have also been made to measure the temperature in vitro at the endocardium and at different depths within the myocardium [31]. This study showed that as long as the endocardium remained in contact with liquid, e.g., saline or blood, then tissue temperatures remained low. Earlier, Anderson et al [41] had measured temperature changes under defibrillator electrodes and did not find any substantial temperature increase at the site of injury. A recent study has compared the thermal effects of laser and electrical ablation and found much smaller endocardial temperature changes with the latter technique [48].

Physical effect responsible for abolition of conduction in the endocardial ablation technique

There are four physical effects produced by the high-energy ablation technique which could be responsible for the therapeutic effects on the conducting system. They are,

1. light
2. heat
3. pressure
4. current intensity.

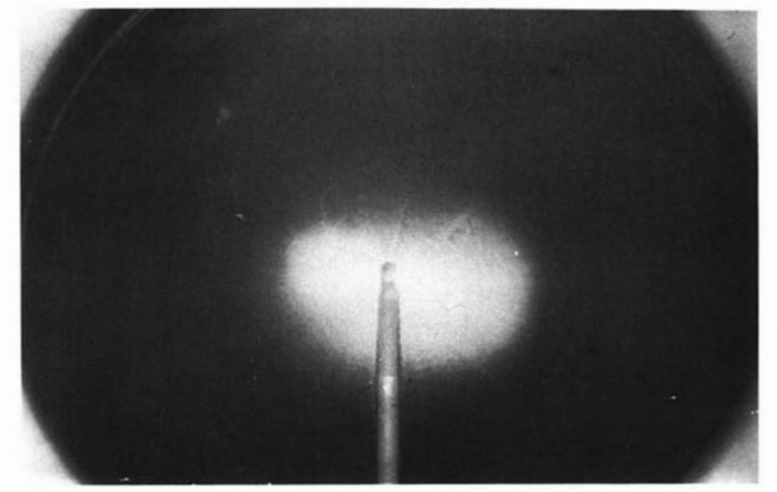

Figure 1–14. Effect of delivering the equivalent of 400 joules as a cathodal impulse via the distal pole of a USCI electrode. The electrode is submerged in pig's blood. Light from the fireball can be seen.

These will be considered, in turn, to assess the evidence for their significance in the clinical ablation procedure.

The delivery of high-energy impulses via standard pacing catheter electrodes releases radiant energy in the visible spectrum even in blood (figure 1–14). Light energy in the form of Nd: YAG lasers [49] has been investigated in coronary artery disease [50] and cardiac arrhythmias [51]. The therapeutic effects produced acutely by these lasers (especially argon) have the appearance of vaporized craters. These lesions are not seen following electrical ablation. Thermal effects are unlikely to be implicated in the acute therapeutic response, since the rise in tissue temperature beneath the endocardium are very small and would not account for the endocardial and epicardial effects observed.

Speculation has occurred on the role of barotrauma in the ablation of conduction [52]. Mechanical shock waves have been shown to initiate depolarization in conducting tissue [53].

Experiments on mechanical shock or blast injuries have shown that the pressure changes generated by the shock waves can produce myocardial lesions [54]. Such lesions are due to shearing stresses. These produce myocardial contusions, which occur not only immediately under the point of impact, but are also apparent distant from the impact, most commonly adjacent to major coronary vessels along the interventricular groove [55]. The pathological findings in animal experiments involving the high-energy ablation technique are localized to the site of energy delivery. These acute lesions

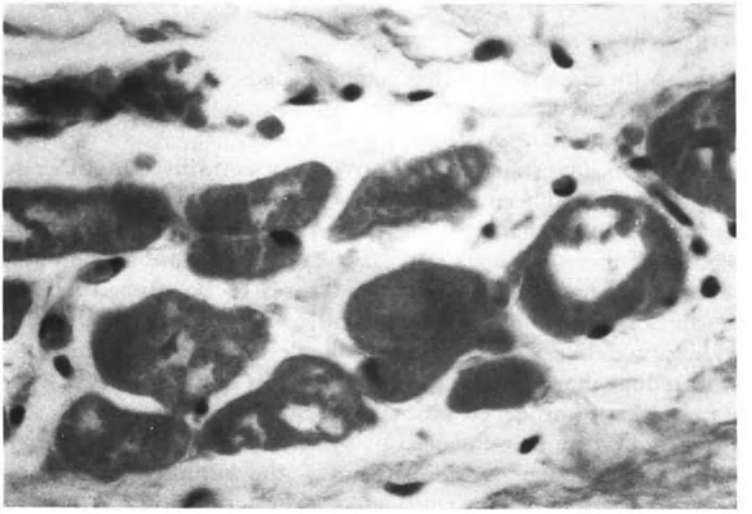

Figure 1–15. Section of myocardium from canine ventricle underlying electrode. One shock of 400 joules had been delivered. The myocardial cell membranes are intact. Some loss of cell nuclei can be seen.

showed no signs of rupture of the myocardial cells (figure 1–15). In addition, where electrical impulses have been delivered between two catheter electrodes, equal tissue damage has occurred around the cathodal and anodal electrodes [56]. If the shock wave were responsible for the acute effects, the lesion should be greater around the anodal electrode. These histological appearances, although not conclusive, suggest that barotrauma is not responsible for the acute lesion and alteration or abolition of conduction in the high-energy ablation technique.

The current density is probably responsible for the acute effect on cardiac conducting tissue seen during delivery of high energy electrical impulses. This may explain why successful ablation of atrioventricular nodal conduction can occur using much lower energies, when shielded USCI electrodes [7] or active fixation electrodes [21] are used.

The dramatic acute pathological effects of coronary sinus [10, 57] or right atrial perforation are undoubtedly due to the pressure waves generated. Depression of myocardial function [19, 20] may be related to barotrauma but could be related to "overdose" of the current density [58]. In both instances, measures designed to decrease the amount of energy required to produce successful ablation of the His bundle, accessory pathway, or ventricular tachycardia foci will reduce the pathological effects of this technique. Such changes can be directed at the energy delivery system or the catheter electrodes, and these are discussed in detail below.

ENDOCARDIAL ABLATION EQUIPMENT

The energy delivery system

The work by Jones and colleagues established in vitro the characteristics of the delivered energy wave form which should allow successful cardioversion with the maximum margin of safety [44, 59–61].

Laboratory tank investigations are now being conducted by other workers on modifications of the energy waveform in the ablation technique [27]. There is interest in methods of delivering the electrical ablation energy that do not produce pressure shock waves. Very short duration, high amplitude pulses in the laboratory allow higher voltages to be applied before shock wave generation occurs [62]. Multiple pulses at short pulse width also allow greater energy delivery rate before voltage breakdown occurs [63]. An attempt to reduce the energy requirements in His bundle ablation by increasing the pulse duration proved unsuccessful [64].

Energy delivery can be influenced by 1) the waveform of the energy pulse, 2) whether it is unipolar or bipolar, and 3) the impulse electrical polarity, anodal or cathodal. These are considered separately below.

Waveform

Most groups use the standard DC defibrillator to store and deliver the high-energy electrical charge during transcatheter ablation procedures. The development of the modern defibrillator is given in several published texts [65–67] and many waveforms have been investigated [68–72]. Lown and coworkers developed the form of the modern DC defibrillator by using a capacitor discharging through an inductor. This produced a damped sinusoidal current flow through the subject [72]. Alterations in the degree of damping in the Lown waveform, produce the Edmark and Pantridge current profiles. In addition to the damped sine wave, there are two other wave shapes, the exponential and the truncated exponential, which have been investigated and incorporated into commercial units. These three waveforms are considered separately below.

THE DAMPED SINUSOIDAL WAVE FORM. The majority of the defibrillators currently available use this waveform. The damped sine wave current pulse is produced by completing a circuit containing a capacitor, an inductor and an energy dissipating resistive element. The latter consists of the sum of the transthoracic resistance of the patient and the internal resistance of the defibrillator. For test standards [73, 74] the patient resistance is assumed to be a nominal 50 ohms with a range of 25 ohms to 100 ohms. In practice, however, it can vary over an even wider range of 14 ohms, to 140 ohms [75]. Figure 1–16(A) shows the Lown current pulse calculated for the standard 50 ohm and the extreme range of subject loads specified in the standards. It can be seen that the damping can vary considerably. To minimize the negative current flow, the more highly damped Edmark and Pantridge wave forms

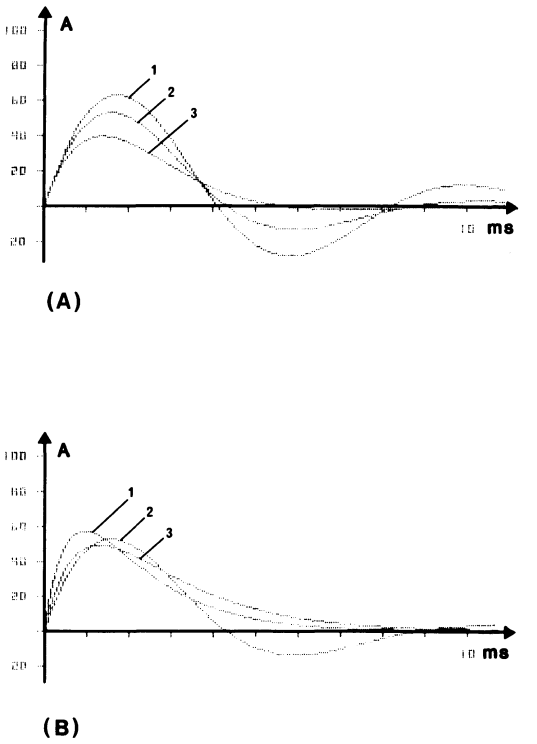

Figure 1–16. Calculated defibrillator current time graphs for the Lown, Edmark, and Pantridge profiles.
(A) Shows the Lown discharging into (1) 25, (2) 50, and (3) 100 ohms.
(B) Shows (1) the Edmark, (2) the Lown, and (3) the Pantridge circuits discharging into the standard 50 ohm load.

have been incorporated in the majority of modern designs [76]. Figure 1–16(B) shows the relative current profiles of these three wave forms discharging into 50 ohm resistive loads.

THE EXPONENTIAL WAVE FORM. This waveform has been used clinically [77] and has been available in a commercial defibrillator [76]. There is some doubt in its value because Schuder et al [69] have suggested that the long tail can produce post shock refibrillation. It has been also reported [78] that this waveform has the ability to produce AV block.

THE TRUNCATED EXPONENTIAL WAVEFORM. This waveform does not suffer from the extended current pulse tail problem. Since it is relatively easy to generate, its clinical effectiveness has been extensively investigated [65]. It is a specified standard waveform [73], but there is only one manufacturer supplying units to date.

Unipolar versus bipolar impulses

In unipolar ablation all the current passes through the heart muscle and the thoracic structures. The energy density is highest near the electrode surface of the intracardiac catheter. In a bipolar ablation procedure, both electrodes are within the heart, and the current is restricted to the tissue adjacent to the path between the electrode surfaces. There are two methods of applying bipolar ablation impulses. Some investigators use two electrodes on the same catheter [24], while others use an electrode on two separate catheters [25]. The former method is usually employed for coronary sinus procedures, while the latter is used in transseptal ventricular ablation procedures.

Bipolar catheters have been shown to withstand energies up to 400 joules when the distal electrode is used in unipolar mode ablation. Unfortunately, the internal conductor to the proximal electrode is less electrically robust, and using these electrodes in single catheter bipolar ablation mode energies above approximately 50 joules can cause conductor and insulation failures.

Figure 1–17 illustrates 25 joule unipolar and bipolar discharges through 6F catheters in the test tank. Bipolar catheters were used in (A) and (B), and the two most distal electrodes energized on a quadrapolar catheter in (C). There is color difference between the anodal and cathodal flashes. The cathodal light has bluish color, whereas the anodal light is distinctly red. This is further evidence that the discharge mechanisms are different for the two polarities [33].

Figure 1–17 also shows the voltage and current recordings taken during the flash photographs. It can be seen that there are marked differences between the unipolar and bipolar records. The latter current waveforms show an overdamped characteristic. The exact source of the shapes of the voltage profiles is not known at present and requires further investigation.

Ablation procedures have been performed using shocks delivered between two catheter electrodes instead of one catheter and a back plate. Intercatheter energy delivery produces higher peak currents and greater tissue damage than catheter-to-back-plate energy delivery [56]. Therefore, much smaller energies should be used clinically where impulse delivery is performed between two catheter electrodes.

Anodal and cathodal impulses

Although unipolar energy delivery with the catheter electrode connected to the cathodal output of a defibrillator is widely used, some groups are employing anodal energy delivery [14, 23]. As discussed in the section on hematological effects, a comparison has been made of anodal versus cathodal energy delivery [33]. Hemolysis and gas production are much greater for anodal than cathodal impulses. Anodal energy delivery produces three times more hemolysis and 8.7 to 15 times more gas than cathodal impulses. The composition of the gas varies depending upon the electrode polarity.

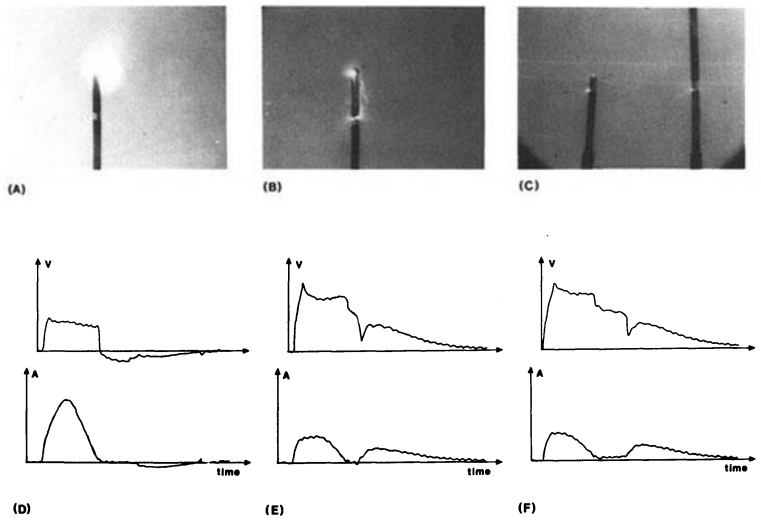

Figure 1–17. These photographs illustrate 25 joule unipolar and bipolar impulses in the test tank and the voltage and current waveforms recorded for,
(A) Unipolar impulse from the distal electrode of a 6F USCI bipolar catheter.
(B) Bipolar impulse from the electrodes of a 6F USCI bipolar catheter.
(C) Bipolar impulse from the two most distal electrodes of a 6F USCI quadripolar catheter.
(D) Voltage and current recordings of (A)
(E) Voltage and current recordings of (B)
(F) Voltage and current recordings of (C)

More importantly, anodal energy delivery produces much larger mechanical shock waves than cathodal impulses [33]. The current and voltage records for both polarities are shown in figure 1–18. The peak values of voltage and current for anodal electrodes are slightly higher on average than those for cathodal electrodes. The most obvious difference is the pronounced peak in the voltage graphs. This moves progressively earlier in the waveform as the energy is increased. The rate of rise of voltage for the 200 joule anodal impulse is extremely steep (4000 V/msec) and is maintained until peak voltage is attained. The cathodal electrode graph shows a much smoother waveform.

The effects on the electrode are markedly different depending on the polarity used. When a total of 48,000 joules had been delivered via the distal electrode of a 6F USCI catheter electrode connected cathodally, the electrode had an overall dull finish. The same energy delivered anodally via a different catheter electrode produced a bright shining appearance. Optical and scanning electron micrographs (figure 1–19) confirmed this impression and showed that both electrode surfaces had fused. The cathodal electrode had a pitted, splashed appearance, whereas the anodal electrode had smooth circu-

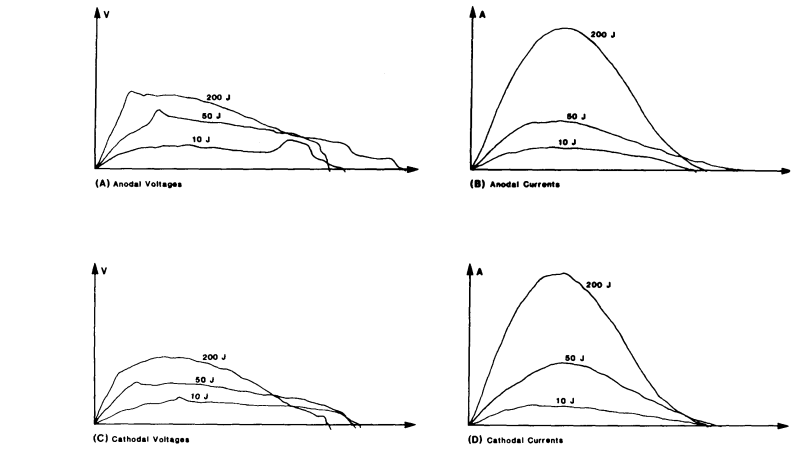

Figure 1–18. The current and voltage records for anodal and cathodal electrode polarities for impulse energies of 10, 50, and 200 joules delivered to fresh pig's blood in the test tank.

lar areas of lavalike appearance. Within most of the circular areas there were one or two deep cavities.

The surface appearance of the two electrodes suggests that the plasma discharges are different for the two electrode polarities. The anodal electrode surface appears to have a relatively small number of discrete foci, suggesting a small number of stable arc initiation points. The cathodally eroded electrode shows a more uniform surface appearance, which suggests a sheet-type discharge mechanism. The significance of these observations warrants further attention.

Platinum assay results show that for 20,000 joules delivered to a seven litre volume of blood in the test tank, there were increases in blood platinum levels of 0.42 ug/ml and 0.12 ug/ml for cathodal and anodal electrodes, respectively. This indicates total electrode platinum losses of 2.94 mg and 0.84 mg. Therefore the amount of platinum released during clinical ablation procedures is not significant for either electrode polarity.

In summary, the increased hemolysis, gas production, and, more importantly, the greater shock waves produced using positive electrode polarity make cathodal energy delivery preferable.

Catheter electrodes

Although the USCI catheter electrodes used in most clinical ablation procedures were designed and manufactured for low current and low voltage pacing applications, they safely withstand repeated delivery of high energy, direct current impulses from a standard defibrillator. Nevertheless, it is essential that any electrode intended for use in clinical ablation procedures

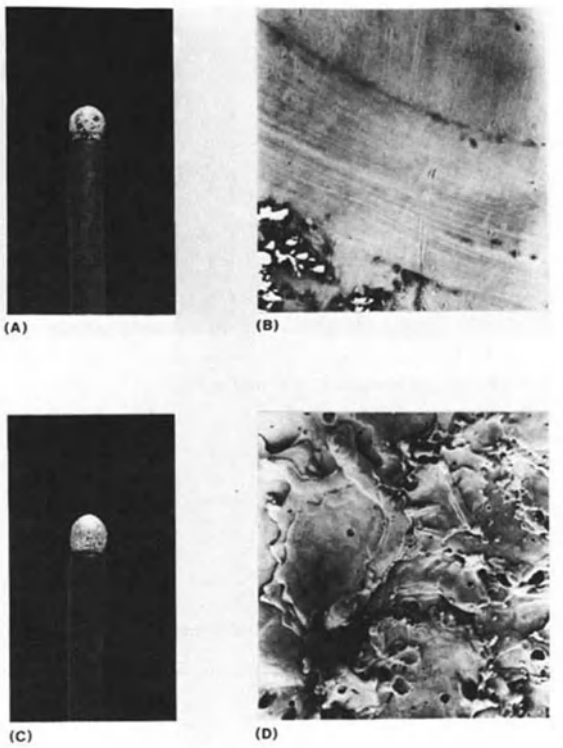

Figure 1–19. Optical and electron micrographs of the distal electrodes of two USCI 6F bipolar catheters. Both delivered a total of 48,000 joules. (A) and (B) illustrate the anodal electrode. The former is magnified × 5 and the latter × 1200. (C) and (D) illustrate the cathodal electrode with magnifications as above. The latter has a pitted, splashed appearance, whereas the former has smooth circular fused areas.

should undergo extensive in vitro investigation, possibly using the technique described above [26]. This is necessary since testing different leads has revealed considerable intermanufacturer and intramanufacturer differences in their ability to withstand high energy shocks [79]. Figure 1–20 illustrates the effects of energy impulses via different electrodes.

The highest electrical field strength in a dielectric is produced by the smallest radius of curvature of a conductor in contact with the dielectric. This is usually at the base of the electrode in the case of standard nonactive fixation leads. The sharpest part or parts of this ring are likely to be flash initiators. Therefore, if the shape of the electrode is altered so that the sharpest radius of curvature is not at its base, then the sites of flash initiation and direction could be changed.

Different catheter electrodes, currently marketed for temporary or perma-

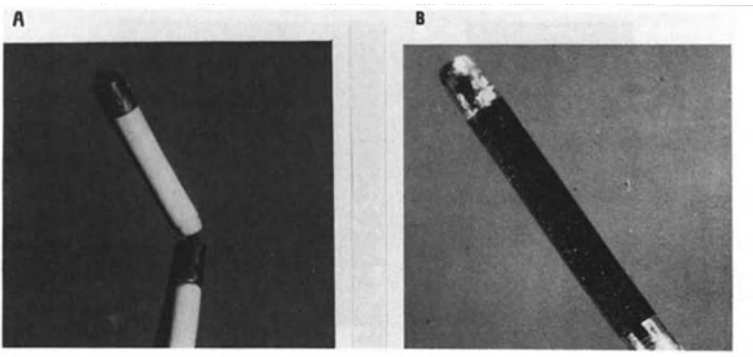

Figure 1–20. Cathodal unipolar shocks of 400 joules via,
(A) a 6F APC electrode
(B) a 6F USCI electrode.

Table 1–1. Effects of energy delivery through various temporary and permanent pacing catheter electrodes.

Electrode	Energy Stored (Joules)	Lead Impedance (ohms)	Fireball Size (mm)	Fireball shape	Tissue gel lesion size dia × depth (mm) × (mm)	Comments
USCI 6F	50	2.0	12	Plate from base of electrode	2 × 0.5	Slight roughening at electrode base
Vitatron Helifix	50	117		Several flash centers near distal end	2 × 2	Slight roughening at end of helix
Sorin S 90	50	47.7	6	Elipse emerging from end of electrode	14 × 2.5	—
Screw-in electrode screw length 0.5 mm	50	49	9	Small globe centered approx. at electrode tip	1.5 × 3	Screw electrode fractured and separated from lead
Screw-in electrode screw length 2 mm	50	64.8	7	Small globe centered approx. at electrode tip	2 × 4.5	—
Osypka 6F	50	0.2	6	Globe from base of electrode	3 × 1	—
Teletronics Dish electrode	50	75.5	6	Globe from dish surface	1 × 1	—

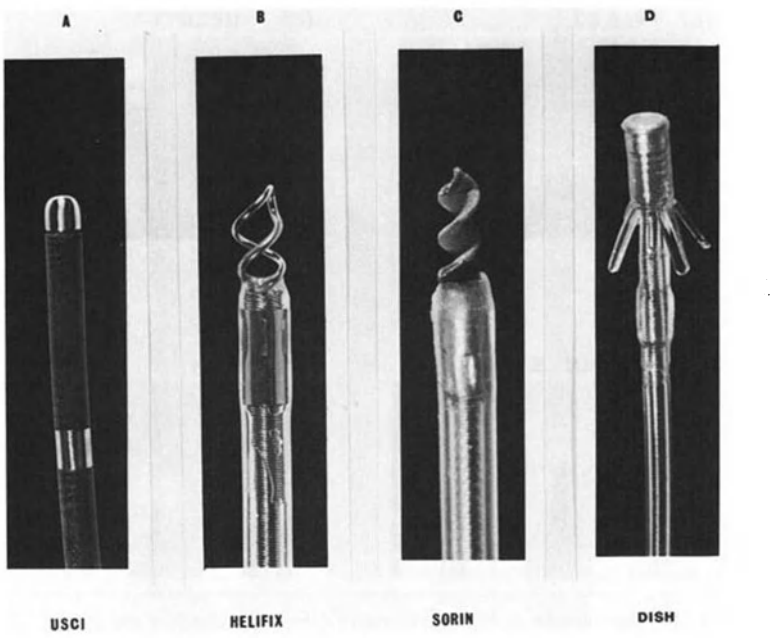

Figure 1–21. This shows the different geometries of,
(A) a USCI 6F electrode
(B) a Vitatron Helifix electrode
(C) a Sorin S 90 electrode
(D) a Teletronics Dish electrode.

nent pacing, have been evaluated to assess their ability to withstand high energy impulses and also to investigate whether the geometry of the electrode influenced the position and direction of the flash produced. Seven electrodes were studied. These are listed in table 1–1.

Using the plastic tank described above in the section, "Physical effect of high energy impulses" [26], a series of different energies were delivered via each electrode. The shocks were unipolar, and the electrodes were connected to the cathodal output of a standard defibrillator.

Using electrical input connections at the proximal end of the catheter and the back paddle, as described previously, the voltage across, and current through, the catheter electrode and fluid medium were measured. Energies of 50 joules and then 400 joules were delivered to each catheter, in turn, and the results recorded on 35 mm film, video tape, and high-speed cine film at 4000 frames per second. Figure 1–21 illustrates four of the electrodes investigated.

The results show that, whatever the electrode geometry, the shape of the fireball is always nearly spherical when the higher energy of 400 joules is

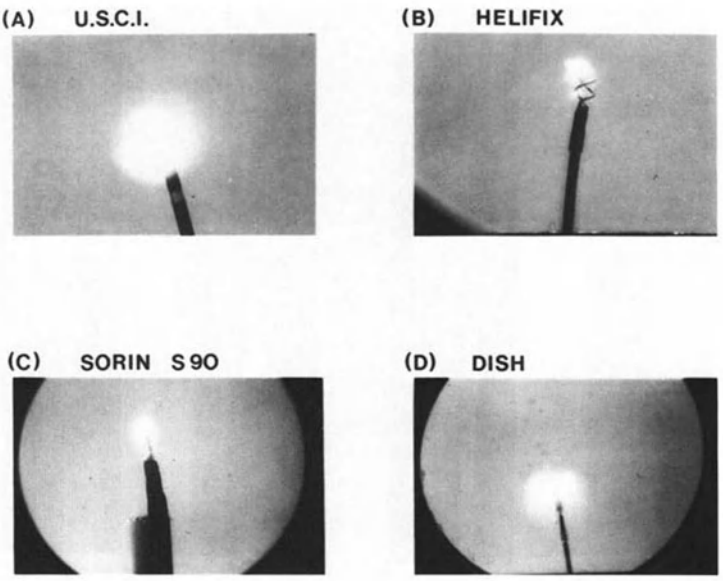

Figure 1–22. Photographs of 50 joule impulses delivered cathodally to,
(A) a USCI 6F electrode
(B) a Vitatron Helifix electrode
(C) a Sorin S 90 electrode
(D) a Teletronics Dish electrode.
The flash from the Helifix, the S 90, and the Dish emerge forward from the distal parts of the electrodes.

delivered. However, at the lower energy of 50 joules, the flash is different depending on the shape of the electrode under test. The flash appearances at 50 joules are summarized in table 1–1 and illustrated in figure 1–22. All shocks were delivered without the guide wire in place in those leads where a guide wire is supplied for electrode placement.

These pictures suggested that some of the active fixation or screw-type of electrode would deliver low energies more efficiently to the tissue than the plain rounded electrode, i.e., directing the energy forward towards the endocardium rather than retrogradely away from the tissue.

This hypothesis was tested using a tissue substitute gel supplied by the Ministry of Defense (Dr. G. Cooper, Head of Trauma Section, Porton Down, Wilts., England). The gel and catheter electrode were submerged in the tank of Ringer's solution. The electrodes were in contact with the gel and

Figure 1–23. This illustration shows the lesions produced in a tissue simulation gel block when unipolar shocks of 50 joules are delivered cathodally via (A) a USCI, (B) a Helifix, (C) a Sorin S 90, and (D) a Teletronics Dish. The Sorin produces the largest lesion with greatest depth of penetration.

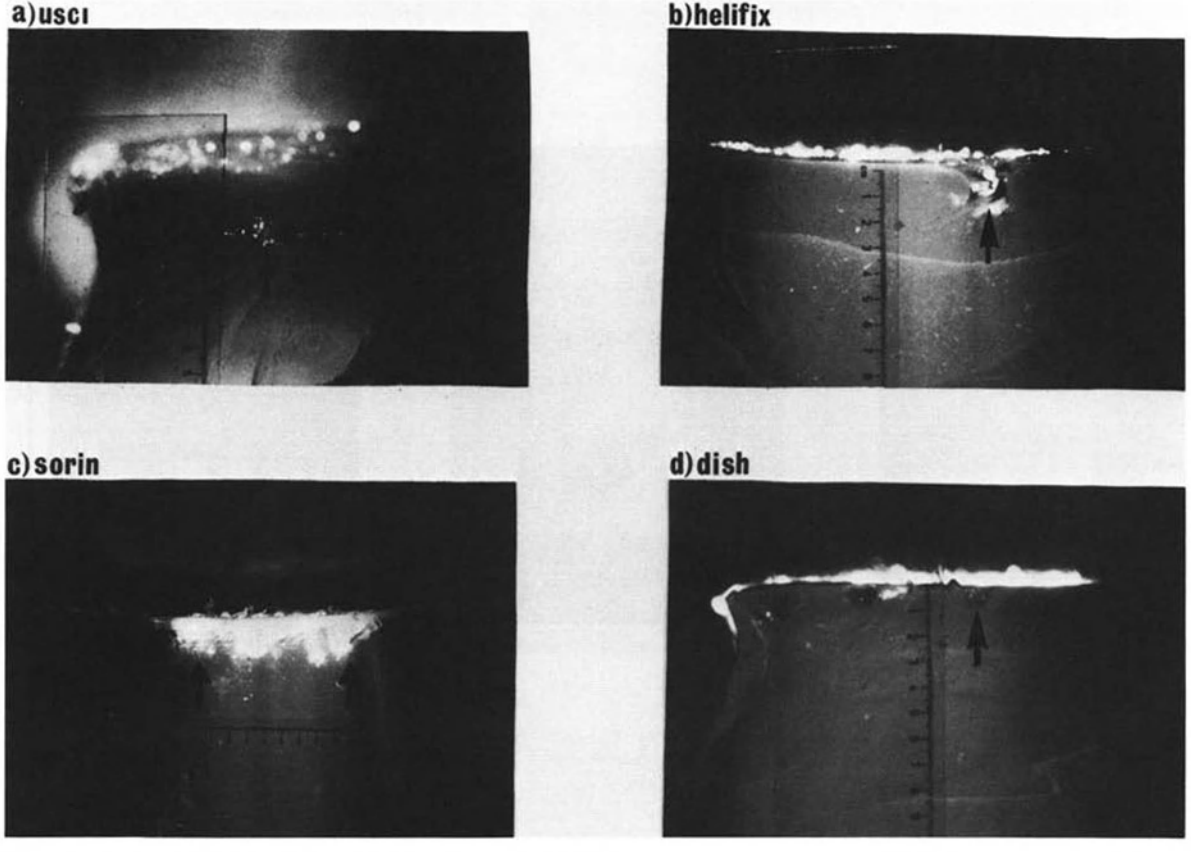
a) usci
b) helifix
c) sorin
d) dish


a)usci
b)helifix
c)usci

normal to the surface. Active fixation electrodes were screwed into the surface of the gel to attempt to simulate their insertion in vivo. A single shock of 50 joules was delivered. Lesions were visible in all cases, ranging from a superficial crater to large-scale disruption of the gel block. This data is summarized in table 1–1. Figure 1–23 illustrates the lesions produced by 50 joules via the USCI Helifix and Sorin S 90 electrodes. These results suggest that electrode geometry does affect the shape of the flash produced and the direction of the energy delivered.

However, the catheter electrodes with active fixation properties are designed for use in permanent pacing systems, and their torque characteristics render the accurate positioning required for successful ablation difficult and time consuming.

Temporary pacing wires (e.g., USCI) are much easier to position. Shielding the USCI tip, using a heat resistant device, could direct the energy distally from the electrode end. Figure 1–24 illustrates the effect on the electrode and tissue when 400 joules was delivered via a USCI electrode and a Vitatron Helifix electrode shielded with PTFE tubes. The flash emerged distally. This appeared to penetrate the canine myocardial tissue section suspended in the saline tank when a Helifix electrode was used. There was considerable electrode erosion.

Recently a method of fixing the smooth rounded electrode type has been devised using suction. This appears to be more efficient, allowing ablation of His bundle conduction with lower energy requirements [22]. This is as yet an experimental lead and further reports are awaited with interest.

The search for a catheter electrode which is easy to position accurately and yet will deliver electrical energy efficiently and safely has most relevance for patients with accessory pathways requiring ablation from the coronary sinus. Using currently available leads and energies over 100 joules there is a considerable risk of coronary sinus rupture, and most workers do not advocate attempting ablation procedures from the mid or distal coronary sinus, especially where this is a small structure. An attempt has been made in this department to produce a catheter electrode capable of directing energy laterally, as a focused beam (See figure 1–25). This catheter electrode is a 16-pole device and is intended to deliver low energies. It has been repeatedly tested with 400 joules impulses and has not failed. However, this device is not yet capable of ablating conduction in accessory AV pathways using energies less than 100 joules.

Figure 1–24. The effects of shielding the distal pole of a 6F USCI bipolar catheter and a Helifix electrode.
(A) Illustrates the flash produced by 400 joules delivered via a shielded USCI electrode in contact with a section of fresh myocardium.
(B) Illustrates the flash produced by 400 joules delivered via a shielded Helifix electrode.
(C) Shows the electrode tip fusion produced by one 400 joule impulse.

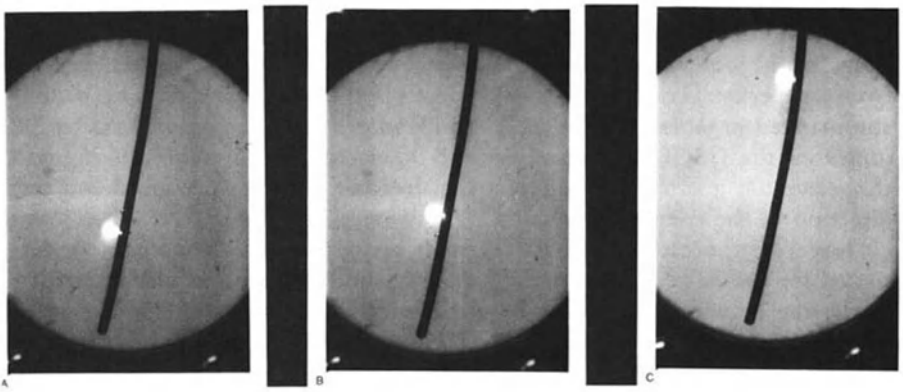

Figure 1–25. An experimental 16 pole electrode with radial energy directing properties,
(A) shows 10 joules delivered via pole 3
(B) shows 10 joules delivered via pole 4
(C) shows 10 joules delivered via pole 10.

Catheter electrode designs continue to be investigated. No definitive solution has yet been achieved, and it is likely that electrodes of different designs will be required to satisfy the different requirements of His Bundle, accessory pathway, and ventricular tachycardia foci ablation.

SUMMARY

The high-energy endocardial ablation technique is extremely valuable in the management of drug-resistant tachyarrhythmias. The physical effects produced during delivery of such high energy impulses are light, heat, mechanical shock waves, and high current density. The latter may be responsible for the therapeutic effects on conduction, while barotrauma causes the acute pathological effects such as coronary sinus rupture. In order to reduce these complications and render the technique safer, energy delivery must be made more efficient. This could be achieved by modifying the energy delivery system or catheter electrodes used. Work is continuing in both these areas and the results are being awaited with interest.

REFERENCES

1. German LD, Strauss HC: Electrical termination of tachyarrhythmias by discrete pulses. *PACE* 7: 514–540, 1984.
2. Fisher JD, Kim SG, Furman S, Matos JA: Role of implantable pacemakers in control of recurrent ventricular tachycardia. *Am J Cardiol* 49: 194–206, 1982.
3. Sealy WC, Gallagher JJ, Pritchett LC: The surgical anatomy of Kent bundles based on electrophysiological mapping and surgical exploration. *J Thorac Cardiovasc Surg* 76: 804, 1978.

4. Boineau JP, Cox JL: Rationale for a direct surgical approach to control ventricular arrhythmias. *Am J Cardiol* 49:381–396, 1982.
5. Vedel J, Frank R, Fontaine G, et al: Bloc auriculo-ventriculaire intra-Hisien definitif induit au cours d'une exploration endoventriculaire droite. *Arch Mal Coeur* 72: 107, 1979.
6. Gonzales R, Scheinman M, Margaretten W, Rubinstein M: Closed-chest electrode-catheter technique for His bundle ablation in dogs. *Am J Physiol*, (*Heart Circ Physiol*, 10) 241: H283–H287, 1981.
7. Gonzales R, Scheinman M, Bharati S, Lev M: Closed chest permanent atrioventricular block in dogs. *Am Heart J* 105: 461–470, 1983.
8. Scheinman MM, Morady F, Hess DS, Gonzales R: Catheter-induced ablation of the atrioventricular junction to control refractory supraventricular arrhythmias. *JAMA* 248: 851–855, 1982.
9. Gallagher JJ, Svenson RH, Kassell JH, German LD, Bardy GH, Broughton A, Critelli G: Catheter technique for closed chest ablation of the atrioventricular conduction system. *N Engl J Med* 306: 194–200, 1982.
10. Fisher JD, Brodman R, Kim SG, et al: Attempted non-surgical electrical ablation of accessory pathways via the coronary sinus in the Wolff Parkinson White syndrome. *JACC* 4: 685–694, 1984.
11. Morady F, Scheinman MM: Transvenous catheter ablation of an accessory pathway in a patient with Wolff Parkinson White Syndrome. *N Engl J Med* 310: 705–707, 1984.
12. Ward D, Drysdale M, Redwood D: Interruption of anomalous atrioventricular conduction using a transvenous electrode catheter to deliver shocks in the coronary sinus. (abstract) *Br Heart J* 51: 686–687, 1984.
13. Harzler GO: Electrode catheter ablation of refractory focal ventricular tachycardia. *JACC* 2: 1107–1113, 1983.
14. Tonet JL, Fontaine G, Frank R, Grosgogeat Y: Treatment of refractory ventricular tachycardias by endocardial fulguration. *Circulation* 72: (4): III 388 (abstract.), 1985.
15. McComb JM, McGovern BA, Garen H, Ruskin JW: Modification of atrioventricular conduction using low energy transcatheter shocks. *JACC* (abstract) 5: 454, 1985.
16. Manz M, Steinbeck G, Luderitz B: His bundel-ablation Eine Methode zur Behandling bedrohlicher supraventrikularer Herzrhthmusstorungen. *Ler Internist* 24: 95–98, 1983.
17. Nathan AW, Ward DE, Bennett DH, Bexton RS Camm AJ: Catheter ablation of atrioventricular conduction. *Lancet* 1: 1280–1284, 1984.
18. Conde AX, Perez Gomerz F, Harguindey LS: Endocardial ablation. In: *Cardiac Pacing, Electrophysiology, Tachyarrhythmias*. Perez-Gomez, ed. Madrid. Editorial Group pp. 1545–1558, 1985.
19. Abbott JA, Eldar M, Segar JJ, Ruder MA, et al: Noninvasive assessment of myocardial function following attempted catheter ablation of ventricular tachycardia foci. *Circulation* 72, (4): III 388 (abstract), 1985.
20. Bennett DH: from Symposium on Endocardial Ablation British Pacing Group, Royal College of Physicians, London, June 1985.
21. Holt P, Boyd EGCA, Crick JCP, Sowton E: Low energies and Helifix electrodes in the successful ablation of atrioventricular conduction. *PACE* 8: 639–645, 1985.
22. Polgar P, Bolnar P, Worum F, Bekassy Sz, Kovacs P, Lorinerz I: Closed chest ablation of the His Bundle; a new technique using suction electrode catheter and DC shock. In *Cardiac Pacing* Steinbach K., ed. Verlag-Darstdat: Dr.D.Steinkopff 883–890, 1983.
23. Breithardt G, Borggrefe M, Karbenn U, Schwartzmaler J, Rohner D: Catheter ablation of ventricular tachycardia. *Eur Heart J* 6 (Suppl 1): 19, 1985.
24. Morady F, Scheinman M, Winston S, et al: Efficacy and safety of transcatheter ablation of posteroseptal accessory pathways. *Circulation* 72 (Suppl III): III–389 (abstract), 1985.
25. de la Asuncion MA Guillen L, Almeria C, Farinas J, Brandau D, Sanchez Harguindelf L: Low energy endocardial His Bundle ablation method using two intracardiac electrodes. Preliminary results. In: *Cardiac Pacing, Electrophysiology, Tachyarrhythmias* F. Perez-Gomez, ed. Madrid: Editorial Group pp. 1605–1610, 1985.
26. Boyd EG, Holt P: An investigation into the electrical ablation technique and a method of electrode assessment. *PACE* 8: 815–824, 1985.
27. Bardy GH, Coltorti F, Rackson MM, Hanson K, Greene HL, Ivey TD: Current waveform

modulation to avoid plasma-arcing and barotrauma with catheter mediated electrode discharges. *Circulation* 72 (Suppl III): III 474, 1985.
28. Schwan HP: Electrical properties of body tissues and impedance. *IRE Trans Med Electronics* 3: 32–46, 1955.
29. Fricke H: The electric conductivity and capacity of disperse systems. Physics 1: 106–115, 1931.
30. Leibman FM, Pearl ME, et al: The electrical conductance of blood in motion. *Phys Med Biol* 7: 177–194, 1962.
31. Boyd E, Holt P: Haematological and tissue effects of high energy ablation. *Br Heart J* 53(1): 99 (abstract), 1985.
32. Rowland E, Foale R, Nihoyannopoulos P, Perelman M, Krikler DM: Intracardiac contrast echoes during transvenous His bundle ablation. *Br Heart J* 53: 240–242, 1985.
33. Holt P, Boyd EG: Haematological effects of the high energy endocardial ablation technique. *Circulation* 73: 1029, 1986.
34. Koch-Weser J: Common Poisons. In: *Harrison's Principles of Internal Medicine*. Wintrobe, Thorn, Adams, Braunwald, Isselbacher, Petersdorf, eds., 1974.
35. Jones JL, Lepeschkin E, Jones RE, Rush S: Response of cultured myocardial cells to countershock-type electric field stimulation. *Am J Physiol* 235(2): H214–H222, 1978.
36. Jones JL, Lepeschkin E, Jones R, Rush S: Cellular fibrillation appearing in cultured myocardial cells after application of strong capacitor discharges. *Am J Cardiol* 39: 273 (abstract), 1977.
37. Jones JL, Lepeschkin E, Rush S, Jones R: Depolarization induced arrhythmias following high intensity electric field stimulation of cultured myocardial cells. *Med Instrum* 12: 54, 1978.
38. Jones JL, Proskauer CC, Paull WK, Lepeschkin C, Jones RG: Ultrastructural injury to chick myocardial cells in vitro following "Electric Countershock". *Circ Res* 46: 387–394, 1980.
39. Davis JS, Lie JT, Bentinck DC, Titus JL, Tacker WA, Geddes LA: Cardiac damage due to electric current and energy: Light microscopic and ultrastructural observations of acute and delayed myocardial cellular injuries. *Proceedings Cardiac Defibrillation Conference*, Purdue University, West Lafayette, Indiana (Engineering Station Document No. 00147) pp. 27–32, 1975.
40. Homburger H, Rossner JA, Antoni H: Ultrastructural findings after injury of isolated heart muscle tissue of the guinea pig by direct currents (German) *Bietr Ersten Hife Bahandl Unfallen Elektr Strom* 7: 140–181, 1976.
41. Anderson HN, Reichenback D, Steinmetz GP Jr, Merendino KA: An evaluation and comparison of effects of alternating and direct current electrical discharges on canine hearts. *Ann Surg* 160: 251–262, 1966.
42. Dahl CF, Gwy GA, Warner ED, Thomas ED: Myocardial necrosis from direct current countershock. Effect of paddle electrode size and time interval between discharges. *Circulation* 50: 956–961, 1974.
43. Jones JL, Jones RE: Decreased defibrillator induced dysfunction with biphasic rectangular waveforms. Am J Physiol 247 (*Heart Circ Physiol 16*): H792–H796, 1984.
44. Jones JL, Jones RE: Determination of safety factor for defibrillator waveforms in cultured heart cells. *Am J Physiol* 242 (*Heart Circ Physiol* 11): H662–H670, 1982.
45. Hoerter JH, Opie LH: Perinatal changes in glycolytic function in response to hypoxia in the incubated or perfused rat heart. *Biol Neonate* 33: 144–161, 1978.
46. Holt PM, Boyd EG: Endocardial ablation: The background to its use in ventricular tachycardia. *Br Heart J* 51: 687 (abstract), 1984.
47. Henthorn RW, Cohen MD, Anderson PG, Epstein AE, Plumb VJ, Olshansky B, Waldo AL: Pathological and clinical observations after catheter fulguration in man. *JACC* 7(2): 236A, 1986.
48. Lee NI, Notargiacoma A, Fletcher RD, Rodriguerz ER, Ferrans VJ, Chen Y-W: The thermal response of ventricular endocardium to laser and electrical ablation and the disparate effects of different suferfusion media. *JACC* 7(2): 37A, 1986.
49. Colles MJ: Lasers in medicine. *Physics Bull* 35: 430–432, 1984.
50. Lee G, Ikeda RM, Theis JH, Chan MC, Stobbe D, Ogata C, Kumagai A: Acute and chronic complications of laser angioplasty: Vascular wall damage and formation of aneurysms in the atherosclerotic rabbit. *Am J Cardiol* 53: 290–293, 1984.

51. Svenson RH, Gallagher JJ, Selle JG, Sealy WC, Zimmern SH, Fedor JM, Marroum MC, Tatis GP, Seifert KT, Robicsek MD: Successful intraoperative Nd: YAG laser ablation of ventricular tachycardia. *JACC* 7(2): 237A, 1986.
52. Ward DE, Davis M: Transvenous high energy shock for ablating atrioventricular conduction in man. Observations on the histological effects. *Br Heart J* 51: 175–178, 1984.
53. Wehner HD, Sellier K: Compound action potentials in the peripheral nerve induced by shock waves. *Acta Chir Scand* Suppl 508: 179–184, 1982.
54. Cooper GJ, Maynard RC, Pearse BP, Stainer MC, Taylor DE: Cardiovascular distortion in experimental nonpenetrating chest impacts. *J Trauma* 24(3): 188–200, 1984.
55. Cooper GJ, Pearse BP, Strainer MC, et al: The biomechanical response of the chest wall to impact with particular reference to cardiac injuries. *J Trauma* 22: 994–1008, 1982.
56. Kadish AH, Spear JF, Prood C, Levine JH, Moore GN: Intercatheter energy delivery for ablation of ventricular myocardium. *JACC* 7(2): 237A, 1986.
57. Brodman R, Fisher JD: Evaluation of a catheter technique for ablation of accessory pathways near the coronary sinus using a canine model. *Circulation* 67(4): 923–929, 1983.
58. Geddes LA, Niebauer MJ, Babbs CF, Bourland JD: Fundamental criteria underlying the efficiency and safety of defibrillating current waveforms. *Med & Biol Engng & Computing* 23: 122–130, 1985.
59. Jones JL, Jones RE: Post shock arrhythmias — a possible cause of unsuccessful defibrillation. *Critical Care Medicine* 8(3): 167–171, 1980.
60. Jones JL, Jones RE: Decreased defibrillator-induced dysfunction with biphasic rectangular waveforms. *Am J Physiol* 247 (*Heart Circ Physiol* 16): H729–H796, 1984.
61. Jones JL, Jones RE: Improved defibrillator waveform safety factor with biphasic waveforms. *Am J Physiol* 245 (*Heart Circ Physiol* 14): H60–H65, 1983.
62. Bardy GH, Coltonti F, Rackson M, Hanson K, Greene HL, Ivey TD: Catheter mediated electrical ablation: The relation between current and pulse width on voltage breakdown and shock wave generation. *JACC* 7(2): 99A, 1986.
63. Bardy GH, Coltonti F, Rackson M, Hanson K, Greene L, Ivey TD: Multiple vs single pulses to avoid voltage breakdown and shock-wave generation with catheter mediated electrical pulses. *JACC* 7(2): 242A, 1986.
64. Boyd EG, Holt PM, Sowton E: A modified energy delivery system for lower energy ablation. *Br Heart J* 7: 651, 1985.
65. Tacker WA, Jr, Geddes LA: *Electrical Defibrillation*. Boca Raton, Florida: CRC Press Inc 1980.
66. O'Dowd WJ: Defibrillator design and development — a review. *J Med Eng & Tech* 7(1): 5–15, 1983.
67. Higgins S: *Defibrillation: What you should know*. Redmond, WA: Physio-Control Corp., 1978.
68. Kugelberg JE: Ventricular defibrillation with double square pulse. *Med Biol Eng* 6: 167–169, 1968.
69. Schuder JC, Rahmoeller GA, Stoeckle H: Transthoracic ventricular defibrillation with triangular and trapezoidal waveforms. *Circ Res* 19: 689–694, 1966.
70. McFarland J, Milnor W, Geddes LA, et al: Ventricular defibrillation in the dogs using single half-wave sinusoidal current pulses of various durations. *Cardiovasc Res Cent Bull* 7: 151–157, 1969.
71. Schuder JC, Rahmoeller GA, Nellis SH, et al: Transthoracic ventricular defibrillation with very high amplitude rectangular pulses. *J Gen Physiol* 22: 1110–1114, 1967.
72. Lown B, Neuman J, Amarasingham R, Berkovits BV: Comparison of alternating current with direct current electroshock across the chest. *Am J Cardiol* 10: 223, 1962.
73. Association for the advancement of medical instrumentation. Cardiac defibrillator devices. ANSI. Arlington, VA: AAMI, 1981.
74. International Electrotechnical Commission. Particular requirements for safety of cardiac defibrillators and cardiac defibrillator-monitors. IEC 601; Part 2.4 Geneva: IEC, 1983.
75. Kerber R, Hoyt R: Human transthoracic resistance in emergency defibrillation: Range and relationships to body weight. *Circulation* 57 (Suppl II): 204, 1978.
76. Riethorst J: Portable defibrillators: A comparative evaluation. MFI-TEST 83.366 *Adviescentrum Medische Technologie*, Institute of Medical Physics TNO, PO Box 5011, 3502 JA Utrecht, The Netherlands, 1983.

77. Bouvrain PY, Saumont R, Berthier Y: Etude clinique de la fibrillation ventriculaire, resultat des chocs electrique transthoraciques. *Ext Arch Mal Coeur* 2: 213, 1967.
78. Tacker WA, Geddes LA, Hoff HE: Defibrillation without A-V block using capacitor discharge with added inductance. *Circ Res* 22: 633–638, 1968.
79. Fisher JD, Brodman R, Johnston DR, Waspe LE, Kim SG Matos JA, Scavin G: Non-surgical electrical ablation of tachycardias: Importance of prior in vitro testing of catheter leads. *PACE* 7: 74–81, 1984.

2. CELLULAR ELECTROPHYSIOLOGY OF ELECTRICAL DISCHARGES

JOSEPH H. LEVINE*, JOSEPH F. SPEAR, JOHN C. MERILLAT, HARLAN F. WEISMAN, ALAN H. KADISH AND E. NEIL MOORE

Myocardial ablation is a new therapeutic option for arrhythmia management. High-energy electrical ablation has been successfully applied to the atrium [1], atrioventricular node [2–6], and accessory pathways [7, 8] for control of automatic and reentrant supraventricular tachycardias. More recently, ventricular ectopic foci have been ablated using high-energy electrical shocks [9–15].

Although myocardial ablation has been associated with successful control of chronic refractory tachycardias, it has also caused life-threatening arrhythmias in some patients [13–15]. If the morbidity and mortality of the procedure is to be reduced, it is necessary to understand the possible mechanisms of these ablation-induced arrhythmias. In this chapter, we will first review the clinical and animal data regarding ablation induced arrhythmias and then present in vitro data which demonstrate that a potentially arrhythmogenic substrate of injured, non-necrotic myocardium develops in the border zone surrounding the site of ablation in normal canine hearts.

*Dr. Levine is the recipient of a Clinician Scientist Research Award sponsored by the Johns Hopkins Medical Institutions.

This work was supported in part by grants from the National Institutes of Health (HL–28393, HL–25213, HL–07220) and the W.W. Smith Charitable Trust.

We thank Charles Prood, Ralph Iannuzzi, and William Moore for their expert technical assistance; Cynthia O. Siu for statistical support; and Joanne Howell for typing the manuscript.

In normal animal hearts, high-energy electrical shocks have been associated with the development of spontaneous ventricular tachyarrhythmias [16–19]. When electrical shocks are applied in situ to canine hearts, ventricular tachycardia and fibrillation may develop. Lee and coworkers [16] noted a 100% incidence of sustained ventricular tachycardia or fibrillation immediately following the delivery of high-energy electrical shocks of 100 joules to 200 joules via an electrode catheter. In these studies, the ectopic beats and runs of ventricular tachycardia persisted up to seven minutes after the delivery of the high-energy shocks. These investigators also found that higher energies led to a greater number of premature ventricular contractions per minute [16–19]. Arrhythmias appeared to be energy dose related; that is, the data suggested that the greater the energy delivered, the more likely it was that significant ventricular arrhythmias would develop. Similarly, Lerman and coworkers [17] found a high incidence of ventricular tachyarrhythmias in the 48 hours immediately following direct current shocks delivered via catheters to normal dogs. A dose-response relationship was present between energy delivered and survival (48 hours). Holter monitors demonstrated sustained ventricular tachycardia in all dogs. In addition, sudden death in these animals was associated with documented ventricular fibrillation recorded on the monitors. Of note is that there was a trend toward a diminished frequency of extra systoles beginning the third day after DC shock, suggesting that the arrhythmogenic mechanisms were transient and self-limiting. The findings of an early proarrhythmic period followed by gradual reduction in spontaneous arrhythmias was also demonstrated by Westveer and coworkers [18], as well as by Kempf and coworkers [19]. They too found a high incidence of spontaneous ventricular tachyarrhythmias early post-ablation. In addition, Kempf and coworkers demonstrated that programmed electrical stimulation two weeks post-shock failed to induce ventricular tachyarrhythmias, suggesting that although high-energy shocks are acutely arrhythmogenic, a chronic substrate capable of supporting inducible ventricular tachyarrhythmias is not produced.

Ventricular tachyarrhythmias have also been noted following high-energy electrical shocks delivered to ventricular myocardium in man. Hartzler and Giorgi [13] noted ventricular fibrillation in a patient undergoing ablation for refractory ventricular tachycardia. Ruffy and coworkers [14] reported a life-threatening new form of ventricular tachycardia, which resolved 24 hours after ablation for ventricular tachycardia and did not require further therapy. Similarly, Belhassen and coworkers [15] observed nonclinical ventricular tachycardia in two of eight patients undergoing ablation for ventricular tachycardia; the nonclinical tachycardia required cardioversion in one of the two patients. These transient but malignant ventricular arrhythmias have been frequently seen immediately following high-energy shocks to ventricular myocardium and remain a major cause of morbidity in patients undergoing ablation for control of ventricular tachycardia.

Thus the results of clinical and animal investigations suggest that high-energy electrical shocks are associated with the development of an arrhythmogenic substrate. The self-limited nature of these arrhythmias indicate that the myocardial changes which develop are temporary. However, the mechanisms of the arrhythmias which occur are unknown. Recent work has shown that cultured myocardial cells subjected to electrical field stimulation develop microlesions in the sarcolemma [20–22]. These microlesions are thought to be caused by the compression of the membrane due to the large voltage gradients produced across it secondary to its high resistance. These conditions lead to temporary depolarization of the membrane as well as to transient cellular dysfunction, arrhythmias, and cell contractures. The authors of these studies have provided evidence for nonselective cation flow following microlesion formation in the cell membranes and have suggested that the sequelae of electric field stimulation may be due to these current-voltage-related phenomena of cell disruption via this membrane breakdown hypothesis. In these studies, significant cellular changes were noted even with relatively low-energy, electric field stimulation; that is, with an electric field comparable in strength to that produced by standard defibrillation. It follows that the application of a stronger field associated with high-energy electrical ablative shocks would result in more extensive and significant cellular electrophysiologic changes. In addition, the consequences of cell depolarization as well as nonselective cation flux would be expected to lead to abnormalities of refractoriness, impulse conduction, and impulse initiation. Thus, potential arrhythmogenic mechanisms in this setting include reentry, abnormal automaticity, and triggered activity. Experimental data are available to implicate each of these mechanisms in the genesis of the arrhythmias that develop following high-energy ablation.

REENTRY

Arrhythmias caused by reentry are dependent upon abnormal impulse conduction, refractoriness, and excitability. Although reentry has not been directly demonstrated following high-energy electrical ablation, abnormalities in conduction and refractoriness have been identified in myocardium after electrical shocks, suggesting that some arrhythmias following high-energy ablation are undoubtably due to reentry.

ABNORMAL IMPULSE CONDUCTION

Abnormal impulse conduction and conduction block are present in isolated Purkinje fibers exposed to local damage as a result of low-level electrical shocks [23]. The experimental arrangement used to produce local electrical damage is presented in figure 2–1, where bipolar stimulating electrodes were located on the proximal (St_p) and distal (St_d) ends of the fiber perpendicular to its long axis. A third bipolar electrode (arrow) was positioned on the

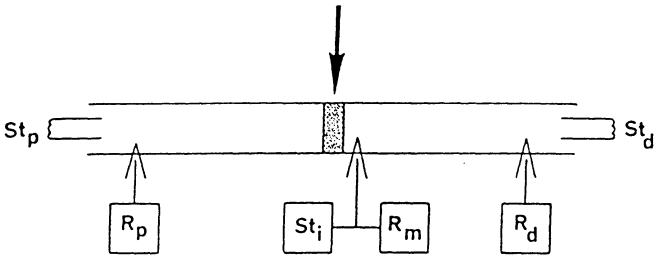

Figure 2–1. Diagram illustrating the Purkinje fiber and the arrangement of the stimulating and recording electrodes. The central area (large arrow) represents the zone of conduction block induced with electrocautery. St_p and St_d are the proximal and distal stimulating electrodes, respectively. R_p and R_d are the proximal and distal recording microelectrodes, respectively. R_m is the recording microelectrode impaled immediately distal to the zone of conduction block. (With permission, John C. Bailey, MD; modified from reference 23).

midportion of the Purkinje fiber so that its poles spanned the breadth of the fiber. Local, low-level electrical shocks to the Purkinje fiber resulted in varying degrees of bidirectional conduction block; the block was monitored by recording from intracellular microelectrodes positioned proximal (R_p) and distal (R_d) to the area of block. In addition, a third microelectrode (R_m) was positioned just distal to the area of block [23].

An example of the effect of local electrical damage on the conduction characteristics of a Purkinje fiber are presented in figure 2–2. Shown are microelectrode recordings from cells proximal (R_p), immediately distal (R_m), and further distal (R_d) to the site of electrocautery. The S_1 and S_3 stimuli were delivered simultaneously at both ends of the Purkinje fiber, while the S_2 stimulus was delivered from only the proximal (St_p) extracellular stimulating electrode. Action potentials developed in all three Purkinje cells consequent to the S_1 and S_3 stimuli. The S_2 stimulus, however, resulted in an action potential only at the proximal end of the Purkinje fiber (R_p). A subthreshold depolarization was noted immediately distal to the site of local electrical damage, while no response was observed at the far distal (R_d) end of the fiber. Thus, local local low-level electrical energy may lead to focal conduction block.

It was unclear whether high-energy electrical shocks as used in catheter ablation would also be associated with similar changes. As noted, previous data suggested the presence of a border zone of transiently depressed but non-necrotic tissue surrounding the ablating site, which might be arrhythmogenic. Therefore we developed an in vitro model of high-energy electrical ablation to study the properties of impaired conduction in the border zone as well as to identify the mechanisms involved. In addition, the in vitro model allowed other potentially arrhythmogenic mechanisms, such as abnormal automaticity or triggered activity, to be identified if present.

In these studies, the cellular electrophysiologic consequences of high-energy electrical ablation were investigated in normal canine myocardium.

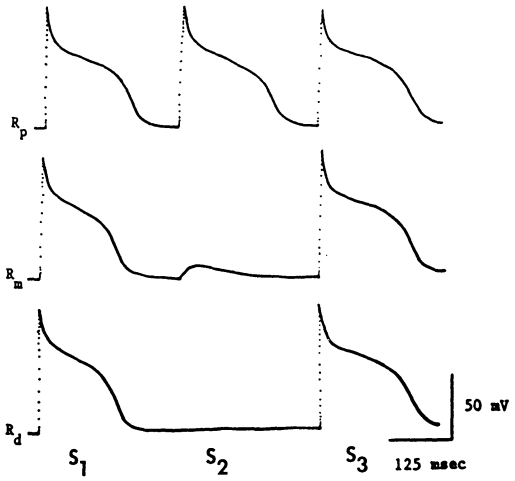

Figure 2–2. The S_1 and S_2 stimuli were delivered simultaneously at both ends of the Purkinje fiber. The S_2 stimulus was applied only via the proximal stimulating electrode. The cell proximal to the zone of conduction block (R_p) responded to the S_2 stimulus with a full amplitude depolarization. The cell immediately distal to the zone of conduction block (R_m) responded to the S_2 stimulus with a subthreshold depolarization. No activity was noted in the most distal cell (R_d). (With permission, John C. Bailey, MD; modified from reference 23).

Following the delivery of the shock, action potential characteristics were recorded at varying distances from the cathode to determine the pattern of injury which developed proximal and distal to the cathode. This allowed us to identify injured but non-necrotic myocardium using electrophysiological measurements of action potential characteristics which are more sensitive to reversible injury than are pathologic methods. Thus, the in vitro model allowed us to quantitatively evaluate changes in conduction and refractoriness that developed post-shock as well as to identify potential membrane phenomena such as afterdepolarizations that developed.

IN VITRO ABLATION

Techniques

In these experiments, isolated canine epicardial tissues superfused with oxygenated Tyrode's solution underwent high-energy electrical ablation in vitro [24]. A 1.5 mm or 1.9 mm cathode (silver) was positioned above each tissue and a 25 mm anode (platinum) was centered beneath each tissue. A single shock (5 joules to 20 joules) was delivered between the cathode and anode. Shocks were delivered from a standard defibrillator (Hewlett-Packard 78670A). Immediately following the shock, the cathode and anode were removed from the tissue bath, and the tissues were allowed to equilibrate for 30 minutes. Five to fifteen action potentials were then recorded at varying distances, 0 mm–10 mm from the position of the cathode edge, and the

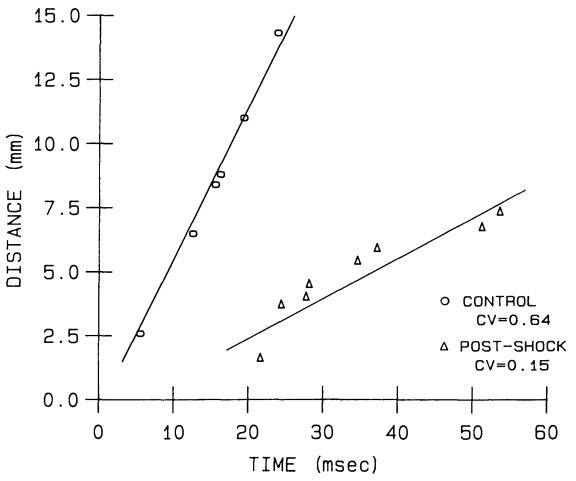

Figure 2–3. Conduction velocity determinations in an epicardial strip prior to (○) and following (△) a high-energy electrical shock. Plotted are the activation times of action potentials recorded from impalements made at the stated distances. Note that the slope of the regression of distance versus time is shallower for the post-shock tracing, demonstrating a slow conduction velocity. The measured conduction velocities for the control and post-shock recordings are 0.64 m/sec and 0.15 m/sec, respectively.

action potential characteristics from these impalements were compared with those from impalements made in the control state prior to the delivery of the shock. The location of each impalement was determined by observing the midpoint of the dimple produced at the site of impalement using an optical micrometer (resolution = 0.08 mm).

Conduction velocity was determined by recording the activation time of impalements made parallel to fiber orientation, calculated as the time difference between the stimulus artifact and the time of maximum rate of depolarization of the action potential. Impalements were made over a distance of 1 cm in line with the pacing electrode and passed within 5 mm of the edge of a 1.5 mm or 1.9 mm cathode used for ablation. Conduction velocity was determined from the linear regression of a plot of activation time versus distance. Control determinations obtained before the delivery of a high-energy shock were compared with those obtained 30 minutes following the delivery of 5 joules to 20 joules in vitro.

Results

When high-energy electrical shocks were delivered to normal canine myocardium, abnormal impulse conduction developed. Examples of a conduction velocity determination in a control tissue and in a tissue following a high-energy electrical shock are shown in figure 2–3. Note that the post-shock

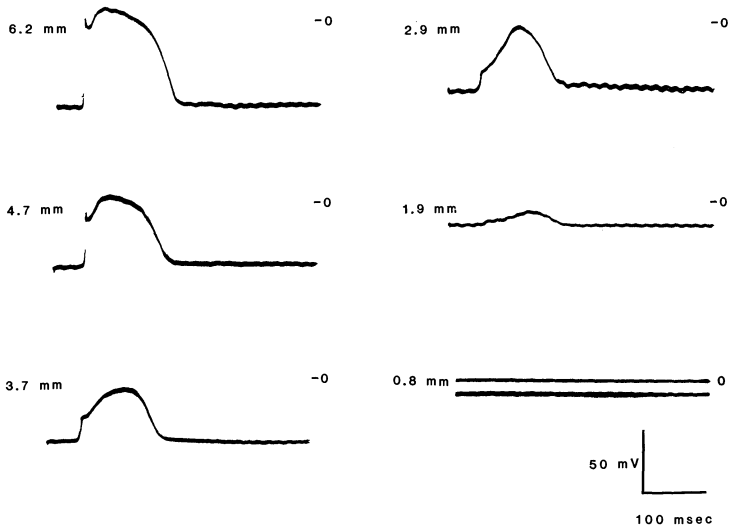

Figure 2–4. Shown are analog recordings of action potentials from cells at varying distances from the cathode (1.5 mm diameter) following a high-energy electrical shock (5 joules). There was a progressive decrement in resting membrane potential, action potential amplitude, and dV/dT as the distance of the impalement from the cathode decreased. At very close distances (< 2 mm), no action potentials were recorded. (From Levine, JH et al.: The cellular electrophysiologic changes induced by high-energy electrical ablation in canine myocardium. *Circulation* 73: 818, 1986; with permission, American Heart Association).

plot of activation time versus distance has a shallower slope, indicating slower conduction compared to the normal, control tissue. A decrease in conduction velocity in the affected border zone around the ablation site was noted in each experiment and the mean conduction velocity (13 tissues) decreased from 0.40 ± 0.17 m/sec to 0.18 ± 0.14 m/sec ($p < 0.001$) after in vitro ablation. In addition, conduction became nonlinear in most of the tissues subjected to high-energy shocks; that is, conduction time between points close to each other was prolonged in some parts of the tissue, while conduction velocity was relatively normal in other parts of the tissue. Thus, abnormal, slow conduction in the border zone around the crater was noted post-shock. The cellular mechanisms of this slow conduction, however, are unclear.

Conduction depends upon source and sink factors [25]. The source is the inward current of the action potential and can be estimated by measuring the maximum rate of depolarization and amplitude of the action potential. When normal canine myocardium was subjected to high-energy electrical shocks in vitro, abnormal source factors were identified in a large border-zone of depressed but non-necrotic myocardium. Analog recordings from one tissue are presented in figure 2–4. Shown are action potentials recorded from

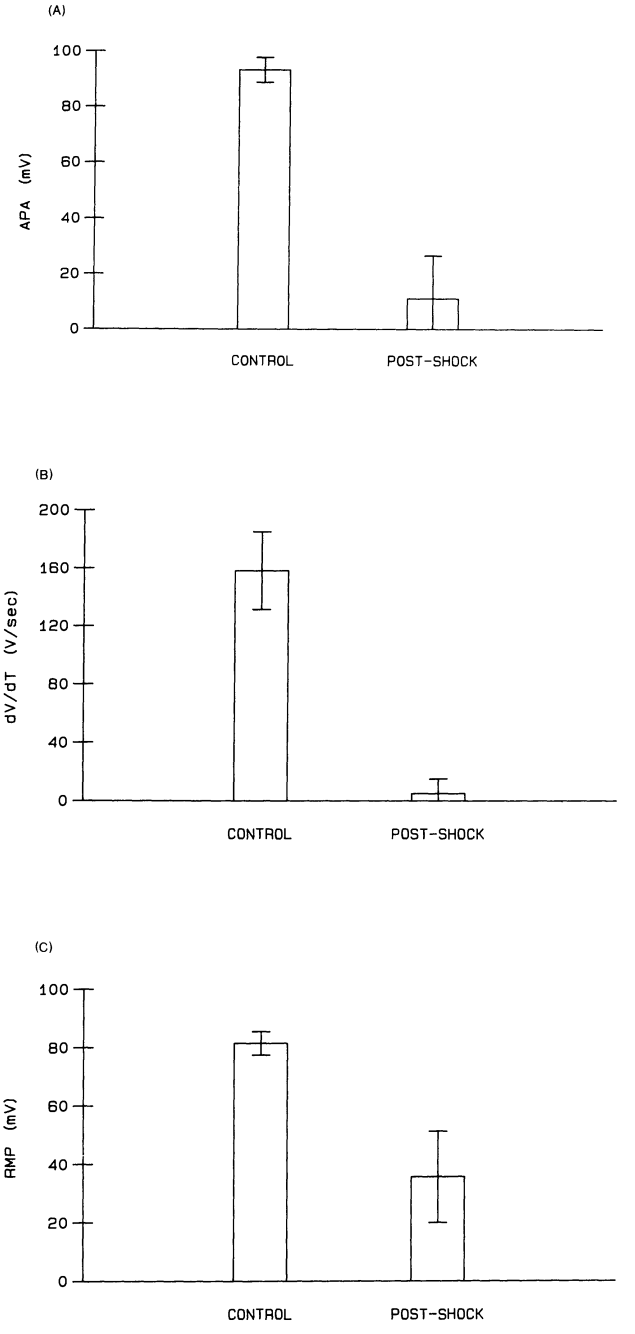
(A)
APA (mV)
100
80
60
40
20
0
CONTROL
POST-SHOCK
(B)
dV/dT (V/sec)
200
160
120
80
40
0
CONTROL
POST-SHOCK
(C)
RMP (mV)
100
80
60
40
20
0
CONTROL
POST-SHOCK

impalements made at the varying distances from the cathode. Following a high-energy shock, a depression in action potential amplitude and the maximum rate of depolarization was noted. The extent of the abnormality of action potential characteristics was related to the distance of the impalement from the cathode; that is, the depression in action potential characteristics was most severe close to the cathode and was of graded severity at increasing distances from the cathode. In addition, the extent of the abnormalities were large relative to the size of the cathode.

The depressed action potential characteristics were noted in each of the tissues studied (figure 2–5). In these experiments, for all impalements within 5 mm of the cathode, mean action potential amplitude decreased from 93.0 ± 4.5 mV to 11.0 ± 15.5 mV and the maximum rate of depolarization from 157.8 ± 26.7 V/sec to 5.0 ± 10.0 V/sec ($p < 0.001$). Thus, source factors, as indexed by action potential amplitude and the maximum rate of depolarization, are reduced in a large border zone around the cathode following high-energy electrical ablation in vitro and may contribute to the decrement in conduction velocity measured.

Sink factors may also be abnormal following electrical energy delivery to myocardium. The sink is the complex interaction among passive membrane properties, tissue geometry, and architecture and other factors which influence transmission of the action potential. We have previously demonstrated that resting membrane potential is an independent factor which influences conduction [26]. In those experiments, conduction velocity was directly related to the level of resting membrane potential and was independent of the method used to alter it; the more depolarized the resting potential, the slower the conduction velocity. In addition, changes in conduction velocity were independent of alterations in the maximum rate of depolarization. Post-shock, the mean resting potential for all impalements within 5 mm of the cathode decreased from 81.2 ± 4.0 mV to 35.5 ± 15.6 mV ($p < 0.001$). The severity of the changes in resting membrane potential was inversely related to the distance of the impaled cell from the ablation site. This interaction between the change in resting membrane potential and distance was statistically significant ($p < 0.05$). Thus, since conduction is dependent in part upon resting membrane potential, the decrease in resting potential of cells located in the border zone following a high-energy shock may contribute to the decreased conduction velocity and nonlinear conduction noted.

Another factor which may effect the sink and hence alter conduction is the presence of necrotic myocardium following high-energy shocks in vitro.

Figure 2–5. Shown are summary data for (A) action potential amplitude (APA), (B) the maximum rate of depolarization (dV/dT), and (C) resting membrane potential (RMP) for impalements within 5 mm of the cathode before and after the high-energy electrical discharge. The mean values of each of these parameters was significantly depressed following a high-energy shock ($p < 0.001$).

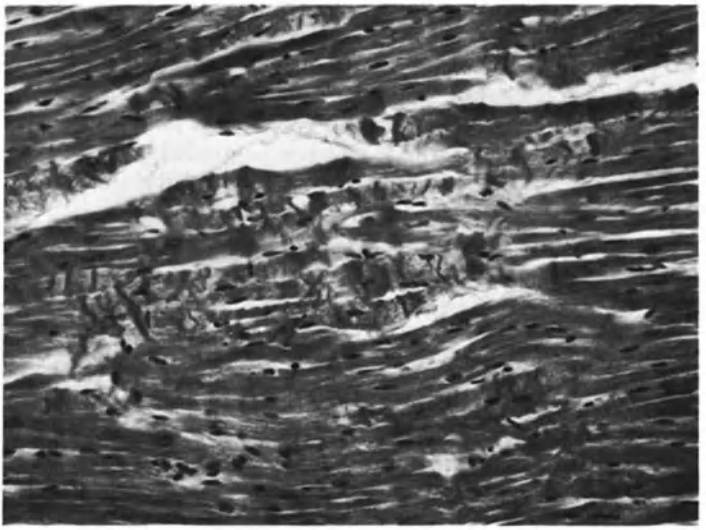

Figure 2–6. An example demonstrating the histopathologic changes seen after high-energy ablation. Distal from the crater, focal areas of contraction band necrosis were seen (center).

Studies from this laboratory as well as from other investigators have demonstrated contraction band necrosis following high-energy shocks delivered to normal myocardium. The necrosis is not uniform in the border zone which develops between the crater at the shock site and distant normal myocardium [24, 28]. Rather, islands of necrotic myocardium are interspersed with viable tissue. An example of one such tissue is shown in figure 2–6. This tissue had undergone a 20 joule ablative shock in vitro. Note that contraction band necrosis developed but that it was not uniform. An island of contraction band necrosis is present, surrounded by normal myocardium. This type of mottled tissue architecture (necrotic tissue intermingled with surviving myocytes) has been seen in other settings (infarcts) and has been associated with an increased resistance to passive current flow [27]. The mottled architecture may be, in part, responsible for the impaired conduction noted post-shock.

Thus, abnormal source and sink factors are both present in normal canine myocardium subjected to high-energy electrical discharge. The impaired conduction noted is likely due to the complex interplay between these factors.

REFRACTORINESS

Abnormalities of tissue refractoriness also occur following high-energy shocks delivered in vitro. Action potential duration, a measure of cellular

refractoriness, was measured before and after the delivery of a high-energy shock. The results of these measurements are presented in figure 2–7. Mean action potential duration decreased from 193.1 ± 24.7 ms to 147.3 ± 31.8 ms ($p < 0.001$). The changes in action potential duration were not uniform and considerable heterogeneity developed. We quantitated the heterogeneity that developed in each tissue as a coefficient of variation for each tissue; that is, the standard deviation divided by the mean for all impalements in a given tissue. In our experiments, the mean coefficient of variation for all the tissues increased from 4.0 ± 2.5% to 18.2 ± 11.0% after ablation in vitro ($p < 0.001$). Thus, in addition to changes in conduction, alterations in tissue refractoriness also are observed in the border zone surrounding the ablation site. Although we have not directly demonstrated the presence of reentrant arrhythmias in these tissues, the abnormalities of conduction and cellular refractoriness as well as mottled heterogeneous cellular damage provide an appropriate electrophysiologic and anatomic substrate for reentry.

ABNORMAL IMPULSE INITIATION

Afterdepolarizations and phase 4 diastolic depolarization may also be implicated in some arrhythmias following ablation. In some experiments we observed secondary depolarizations occurring during phase 2 of the action potential, which developed immediately following a high-energy shock delivered in vitro (figure 2–8). These secondary depolarizations may represent true early afterdepolarizations or may be a result from electrotonic interactions between cells separated by myocardium exhibiting varying degrees of conduction block. In these experiments, early afterdepolarizations occurring during phase 3 of the action potential were also seen, albeit less frequently, and were associated with the propagation of spontaneous ectopic activity.

In studies of canine myocardium excised and studied 24 hours following high-energy ablation in situ, abnormal impulse initiation also has been documented [28]. In those studies, delayed afterdepolarizations and typical triggered activity were observed in some regions of affected myocardium. In addition, abnormal automaticity due to phase 4 diastolic depolarization has also been recorded. In these tissues, islands of cells exhibiting depressed action potentials and abnormal impulse initiation were intermixed with necrotic myocardium. Thus, as in the experiments in which the ablative shock was delivered in vitro, a zone of injured potentially arrhythmogenic, but non-necrotic tissue developed around the site of ablation.

CONCLUSIONS

Catheter-mediated high-energy electrical ablation is a promising new therapeutic option for control of refractory tachyarrhythmias. Unfortunately, at present, it remains somewhat unrefined and has been associated with an incidence of proarrhythmic complications. Data regarding the occurence and

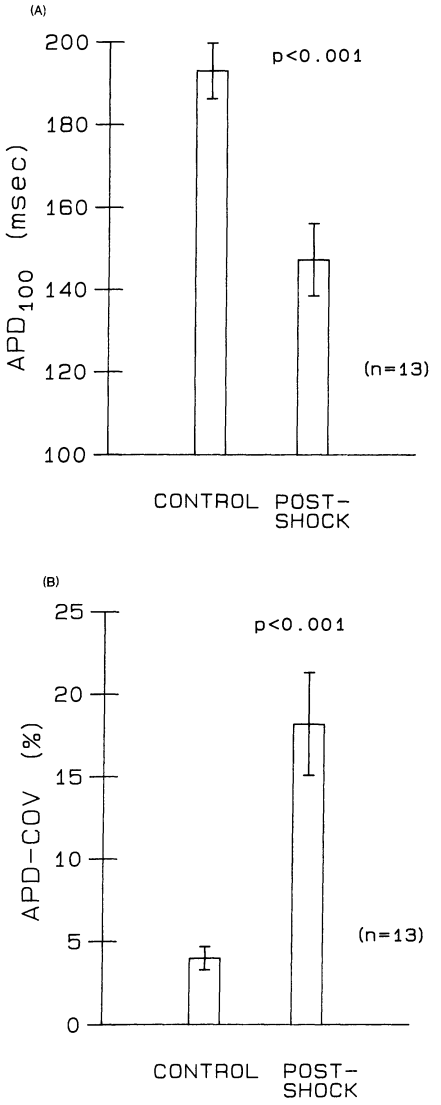

Figure 2–7. (A) Shown are summary data from 13 experiments for action potential duration (APD) changes before and after high-energy electrical ablation. Mean action potential duration decreased from 193.1 ± 24.7 ms to 147.3 ± 31.8 ms ($p < 0.001$).
(B) The changes in action potential duration were not uniform. The heterogeneity within each tissue was quantitated as a coefficient of variation (COV), and the mean coefficient of variation for all the tissues was compared before and after a high-energy shock. The mean APD-COV increased significantly following a high-energy shock.

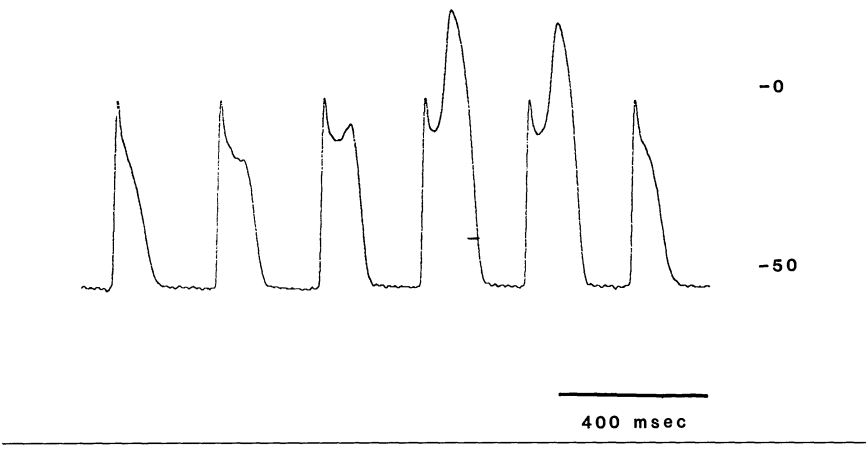

Figure 2–8. Secondary depolarizations that may represent early afterdepolarizations of varying amplitude or that may be electrotonic phenomena were common and occasionally associated with the propagation of premature extrastimuli. (From Levine, JH et al.: The cellular electrophysiologic changes induced by high-energy electrical ablation in canine myocardium. *Circulation* 73: 818, 1986; with permission AHA.)

frequency of these ablation induced tachyarrhythmias in animal models and in man have been summarized and in vitro data suggesting potential proarrhythmic mechanisms presented. Further study is needed to refine ablative techniques in order to maximize and focus ablative energy upon specific target tissues, while avoiding undesirable injury to surrounding myocardium.

REFERENCES

1. Silka MJ, Gillette PC, Garson A, Zinner A: Transvenous catheter ablation of a right atrial automatic ectopic tachycardia. *JACC* 5: 999, 1985.
2. Beazell J, Tan K, Criley J, Schulman J: The electrosurgical production of heart block without thoracotomy. *Clin Res* 24: 137A, 1976.
3. Scheinman MM, Morady F, Hess DS, Gonzalez R: Catheter-induced ablation of the atrial-ventricular function to control refractory supraventricular arrhythmias. *JAMA* 248: 851, 1982.
4. Gallagher JJ, Svenson RH, Kasell JH, German LD, Bardy GH, Broughton A, Critelli G: Catheter technique for closed chest ablation of the atrioventricular conduction system: A therapeutic alternative for the treatment of refractory supraventricular tachycardia. *N Engl J Med* 306: 194, 1984.
5. Trantham JL, Gallagher JJ, German LD, Broughton A, Guarnieri T, Kassel J: Effects of energy delivery via a His-bundle catheter during closed chest ablation of the atrioventricular conduction system. *J Clin Invest* 72: 1563, 1983.
6. Gonzales R, Scheinman MM, Margaretter W: Closed-chest electrode catheter technique for His-bundle ablation in dogs. *Am J Physiol* 241: H283, 1981.
7. Morady F, Scheinman MM: Transvenous catheter ablation of a posteroseptal accessory pathway in patient with the Wolff-Parkinson-White Syndrome. *N Eng J Med* 310: 705, 1984.
8. Brodman R, Fisher JD: Evaluation of a catheter technique for ablation of accessory pathways near the coronary sinus using a canine model. *Circulation* 67: 923, 1983.
9. Hartzler GO: Electrical catheter ablation of refractory focal ventricular tachycardia. *JACC* 2: 1107, 1983.

10. Winston SA, Davis JC, Morady F, DiCarlo LA, Matsubara T, Wexman MP, Scheinman MM: A new approach to electrode catheter ablation for ventricular tachycardia arising from the intraventricular septum. *Circulation* 70(Suppl II): II–412, 1984.
11. Winston SA, Morady F, Davis JC, Di Carlo LA, Wexman MP, Scheinman MM: Catheter ablation of ventricular tachycardia.*Circulation* 70(Suppl II): II–412, 1984.
12. Steinhaus D, Whilford E, Stavens C, Schneller S, McComb J, Carr J, McGovern B, Garan H, Ruskin J: Percutaneous transcatheter electrical ablation for recurrent sustained ventricular tachycardia. *Circulation* 70(Suppl II): II–100, 1984.
13. Harztler GO, Giorgi LV: Electrode catheter ablation of refractory ventricular tachycardia. Continued experience (abstract) *JACC* 3: 512, 1984.
14. Ruffy R, Kim SS, Lal R: Paroxysmal fascicular tachycardia: Electrophysiologic characteristics and treatment by catheter ablation. *J Am Coll Cardiol* 5: 1008, 1985.
15. Belhassen B, Miller HI, Geller E, Laniado S: Transcatheter electrical shock ablation of ventricular tachycardia. *JACC* 7: 1347, 1986.
16. Lee BI, Gottdiener JS, Fletcher RD, Rodriguez ER, Ferrans VJ: Transcatheter ablation: Comparison between laser photoablation and electrode shock ablation in the dog. *Circulation* 71: 579, 1985.
17. Lerman BB, Weiss JL, Bulkley BH, Becker LC, Weisfeldt ML: Myocardial injury and induction of arrhythmia by direct current shock delivered via endocardial catheters in dogs. *Circulation* 69: 1006, 1984.
18. Westveer DC, Nelson T, Stewart JR, Thornton EP, Gordon S, Timmis GC: Sequelae of left ventricular electrical endocardial ablation, *JACC* 5: 956, 1985.
19. Kempf FC, Falcone RA, Marchlinski FE, Josephson ME: The electrophysiologic effects of high-energy electrical discharges in the ventricle (abstract) *JACC* 3(2): 554A.
20. Jones JL, Lepeschkin E, Jones RE, Rush S: Response of cultured myocytes to countershock-type electric field stimulation. *Am J Physiol* 235: H214, 1978.
21. Jones JL, Jones RE: Decreased defibrillator-induced dysfunction with biphasic rectangular wave forms. *Am J Physiol* 247: H792, 1984.
22. Jones JL, Jones RE: Improved defibrillator waveform safety factor with biphasic waveforms. *Am J Physiol* 245: H60, 1983.
23. Bailey JC, Spear JF, Moore EN: Microelectrode demonstration of Wedensky facilitation in canine cardiac Purkinje fibers. *Circ Res* 33: 48, 1973.
24. Levine JH, Spear JF, Weisman HF, Kadish AH, Prood C, Siu CO, Moore EN: The cellular electrophysiologic changes induced by high-energy electrical ablation in canine myocardium. *Circulation* 73: 818, 1986.
25. Fozzard HA: Conduction of the action potential. In: *Handbook of Physiology*. RM Berne, N Sperelakis, SR Geiger, eds. Wash DC: Am Physiol Soc, pp 335–392, 1979.
26. Spear JF, Moore EN: Supernormal excitability and conduction in the His-Purkinje system of the dog. *Circ Res* 35: 782, 1974.
27. Spear JF, Michelson EL, Moore EN: Reduced space constant in slowly conducting regions of chronically infarcted canine myocardium. *Circ Res* 53: 176, 1983.
28. Friedman R, Moak JP, Garson A: Endocardial catheter ablation of ventricular muscle induces arrhythmias: Reentry, abnormal automaticity and triggered activity (abstract) *JACC* 7(2): 38A, 1986.

3. EFFECTS OF HIGH-ENERGY ELECTRICAL SHOCKS DELIVERED TO ATRIAL OR ATRIOVENTRICULAR JUNCTIONAL TISSUE

MICHAEL A. RUDER AND MELVIN M. SCHEINMAN

For more than a decade, patients with drug-refractory supraventricular tachycardias have been treated with disruption of the normal atrioventricular conducting system or by division of anomalous atrioventricular connections at the time of open-heart surgery. In order to avoid the need for a thoracotomy, nonoperative techniques to modulate conduction have recently been developed.

High-energy electrical discharges were used first to interrupt normal conduction across the atrioventricular junction [1–7]. With the success of this method in both animals and man, the technique was broadened to include the possibility of disrupting anomalous conduction. Accordingly, the response of canine hearts to shocks delivered within the coronary sinus [8] (as a model for left free wall accessory pathway ablation), just outside the coronary sinus [9] (for posteroseptal pathways), and around the tricuspid annulus (for right free wall pathways) has been examined.

This chapter will review the investigative work examining the hemodynamic, pathologic, and electrophysiologic effects of high-energy discharges in a canine model delivered at the AV node-His bundle axis and along the tricuspid annulus. Other chapters will focus on the effects of discharges within or just outside the coronary sinus.

HIGH ENERGY DISCHARGES

Near the atrioventricular node

Early techniques used to achieve complete AV block involved thoracotomy with subsequent surgical dissection of the AV node-His bundle area [10, 11]. Further developments included the direct injection of formalin [12] and other caustic substances into the junctional area or the use of electrocautery at the time of open heart surgery [13, 14]. Gallagher and colleagues have refined the use of cryoablation of the AV node-His bundle with the region exposed through a right atriotomy [15]. More recent efforts were directed at avoiding thoracotomy and, indeed, several investigators achieved complete AV block in as many as 60% of animals by injecting formalin via a percutaneously inserted needle catheter [16, 17].

The use of high-energy discharges was first described by Beazell and colleagues, who modified a transseptal catheterization needle by insulating it with Teflon [18, 19]. The catheter was placed via an internal jugular vein in a series of dogs and was positioned under flouroscopic, but not electrocardiographic, guidance near the area defined as the third angle in an equilateral triangle whose remaining two angles were the fossa ovalis and the coronary sinus. There was no attempt to record a His bundle electrogram. A direct current pulse was delivered between this catheter and a hip plate, with no mention of the "polarity" used. Delivered energies ranged from 30 joules to 40 joules. Complete AV block was achieved in 45 of 46 dogs, 14 with 1 shock, the remainder requiring 2 to 8 shocks. There were no acute complications and 17 dogs were observed chronically.

Following sacrifice of the animal, small (0.5 mm to 2 mm diameter) areas of damage were seen. Histologically, the injury consisted of coagulative necrosis acutely and dense connective tissue chronically.

Gonzalez and colleagues simplified this approach further by making use of a modified version of a readily available electrode catheter [1, 2]. In this study, a quadripolar catheter with partially insulated electrodes was inserted into the femoral vein and positioned across the tricuspid valve for His bundle recording and delivery of the discharge. The electrode with the largest unipolar His bundle potential was identified, and a direct current pulse was delivered between this electrode (cathode) and a patch (anode) positioned between the animal's spine and left scapula. The effective delivered energy was 35 joules. A single shock was effective in five animals, whereas four animals required a total of two to four shocks. The animals were observed for a period of three months before sacrifice. All continued with complete AV block with ventricular escape rates between 34 and 51 bpm's and none required chronic pacing.

In six animals, right atrial and ventricular pressure were recorded before the shocks and just prior to sacrifice. There was no evidence of right heart

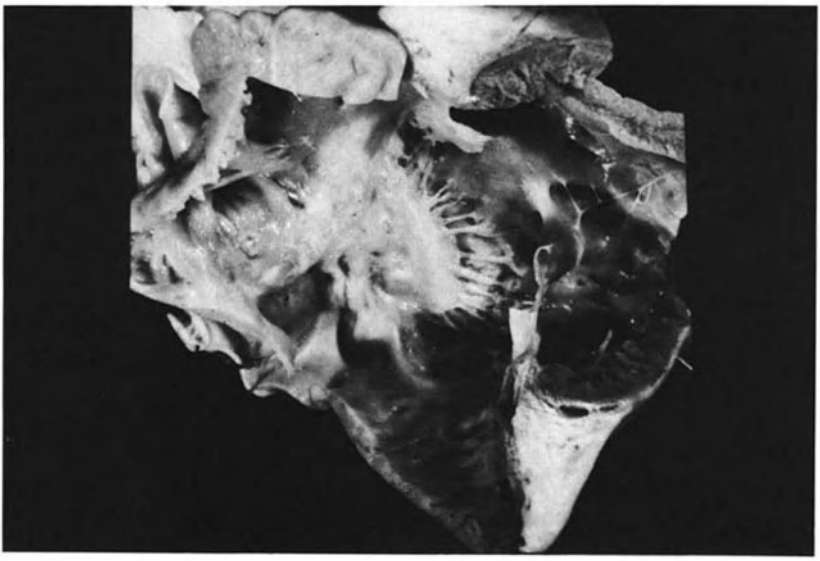

Figure 3–1. Gross examination of a canine heart after multiple direct-current shocks delivered to the junctional area. Note the wide band of scarring involving the atrial muscle as well as the summit of the ventricular septum in the region of the tricuspid valve.

injury or tricuspid regurgitation. Similarly, right ventriculograms performed before sacrifice were normal.

Following the death of the animals, there was no evidence of perforations, and gross and histologic examination revealed no evidence of damage to the heart valves or valvular apparatus. In those animals requiring only one shock, the area of visible damage consisted of a whitened area at the AV junction (figure 3–1). When multiple shocks were employed, the area of visible damage was consistently larger and extended into atrial and ventricular musculature.

Microscopic examination showed marked damage in the AV node as well as in the approaches to the node, the penetrating bundles, and, in some cases, the bundle branches (figure 3–2). For those animals who received a single shock, histologic damage was less extensive and injury of the penetrating bundle tended to be minimal. Fibrosis and fatty infiltration with some instances of giant cell inflammation was primarily seen. The atrial septum and ventricular summit was involved to a certain extent in some animals.

There was no precise correlation between the escape rhythm QRS morphology and histologic injury to a specific bundle branch. It was, in fact, recognized that either bundle branch pattern in the escape rhythm may have been caused by injury within the His bundle or penetrating bundle.

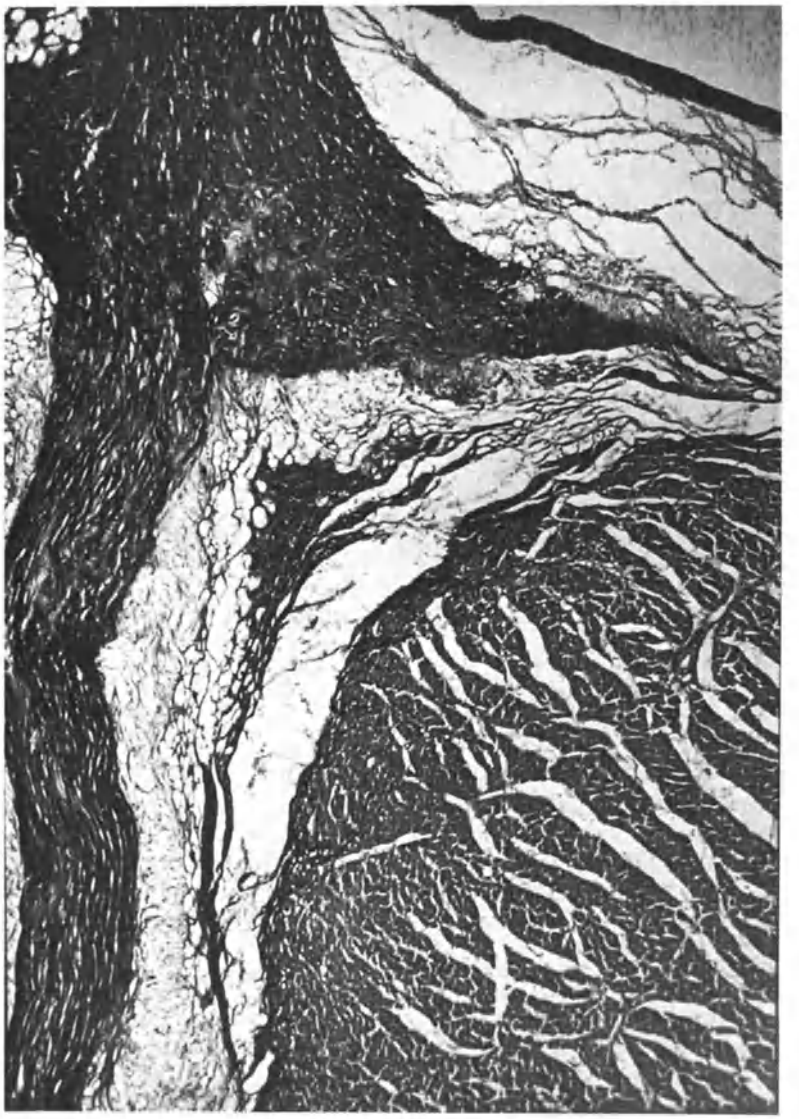

Figure 3–2. Microscopic examination showing necrosis of the bundle branches at their division to the summit of the ventricular septum.

Bardy et al delivered single 280 joule (delivered) shocks to the AV junction in ten dogs [3]. A standard tripolar electrode catheter (USCI) was used. The electrode with the largest unipolar His bundle deflection was connected to the cathode and a left scapular patch to the anode. All of the dogs tolerated the shock but five dogs resumed AV conduction within one week. At the time of sacrifice, in four weeks, the dogs were well, without evidence of perforation or valvular injury. In those dogs with complete heart block, extensive fibrosis was seen in the AV node, the approaches to the node, and the penetrating bundles. In those animals in which conduction returned, the extent and severity of histologic damage was considerably less. The estimated mass of myocardial damage was 0.068 grams or $< 1\%$ of the total myocardial mass.

These studies suggested that normal AV conducting could be reliably disrupted using a nonsurgical technique. The method used appeared to be safe, at least for the short term. Histologic damage appeared limited enough that long-term effects on ventricular, atrial, and tricuspid function seemed unlikely.

The technique has since been applied to man with excellent results [4, 5, 20]. However, a number of questions remain about the optimum technique of disrupting normal AV conduction. First, it would clearly be desirable to significantly alter conduction without producing complete AV block. Scheinman and others examined the effects of shocks delivered through tissue-fixation catheters in the region of the AV node with the hope of altering conduction [21]. In a series of dogs, low-energy discharges (20 joules to 180 joules) resulted in damage to the approaches to the AV node and the node itself, whereas shocks of higher energy created diffuse damage to the His bundle and penetrating bundles as well. However, minimal changes in AV conduction were seen at follow-up electrophysiologic study two to three weeks after delivery of the discharges. (This was true even in face of up to 50% necrosis of the AV node.) Although the observed electrophysiological changes in AV nodal function were small and inconsistent, it is possible that the observed histologic changes might produce a beneficial effect in patients with supraventricular tachycardia. Experiences in man with techniques designed to modify but not produce complete AV conduction block is limited. Attempts by McComb et al, using standard catheters but low energies, have not produced consistent results [22].

Secondly, a rigorous examination of the effect of pre-shock catheter position, as determined by amplitudes of atrial, His, and ventricular electrograms, on the post-ablation escape rhythm has not been conducted. Theoretically, shocks in the AV node might be expected to yield a faster, more reliable escape rhythm. Bardy et al suggest that an atrial to His bundle deflection amplitude ratio of 4 to 10 appears desirable, but this is not at all established [3]. Indeed, earlier surgical investigations by Sealy imply that the anatomic location of induced AV block might not consistently correlate with the rate of the escape rhythm [14].

The ideal form of energy for AV junction ablations has not been established. Laser has been used but probably offers no advantage over high-energy discharges [23]. Radiofrequency energies, currently undergoing investigation, may offer more control than single pulse discharges of electrical energy [24]. In addition, radiofrequency application appears to be safer in terms of the production of concussive waves or bubbles compared with DC shock.

Similarly, the varying effects produced by discharges of different energy waveforms is now being studied. Whereas most defibrillators deliver discharges with a damped sinusoidal waveform of a relatively long duration (35 ms), it appears that a truncated exponential waveform with a much shorter duration (6 ms–10 ms) may deliver similar amounts of current (presumably the element that causes most deep tissue destruction) with much less barotrauma (which is felt to be undesirable). In addition, the advantages and disadvantages of "cathodal" versus "anodal" discharges have not been examined for AV junctional ablations. There are theoretical reasons why cathodal shocks (for which the chest wall patch is connected to the defibrillator current sink) might be preferable, including the probability that less barotrauma is produced [25].

Near the Tricuspid Annulus

With the success of altering AV nodal conduction in humans, the technique was broadened to include the interruption or modification of accessory pathways. Brodman and Fisher studied the effects of discharges within the coronary sinus as a means of affecting the conduction of left free wall pathways [8, 26]. However, rupture of the coronary sinus and lesions produced in the adjacent coronary artery appears to limit the usefulness of this approach [8, 26]. Conversely, shocks delivered outside the coronary sinus os have proven to be apparently safe and reasonably effective in disrupting posteroseptal accessory pathways [9, 27]. Other investigators have delivered high-energy discharges near the site of right free wall bypass tracts in man, although the experience with this approach has been limited [28–31]. To explore this technique further, we analyzed the hemodynamic, pathologic, and electrophysiologic effects of shocks delivered via an electrode catheter to areas immediately above the tricuspid annulus in a series of dogs. Our goals were not only to formally assess the use of a specific technique which might prove adaptable to disrupting conduction in right free wall bypass tracts in man, but also to analyze the effects of high-energy discharges on right atrial endocardium, to examine the correlation between pre-shock endocardium-electrode contact and subsequent lesion size, and examine the association between energy delivered and subsequent lesion size.

Nine adult mongrel dogs were studied. Venous access was obtained using the right internal jugular vein and right femoral vein, and pressures from the right atrium and right ventricle were obtained. Programmed ventricular stimulation was then performed at the right ventricular apex in the usual fashion.

Table 3–1. Acute effects of shocks

Dog No.	Site	Energy delivered (Joules)	Acute effects
1	AL	200	VF; 3° AVB (30 min)
	AM	50	VT (10 sec); 3° AVB (15 min)
2	PM	50	VT (3 sec)
	AL	50	VT (3 sec)
	AM	50	
3	PM	50	VT (3 sec)
	AL	100	3° AVB (30 sec)
	AM	200	3° AVB (10 min)
4	AL	50	VT (11 sec)
	AM	100	VT (9 sec); 3° AVB (10 min)
	PM	200	3° AVB (35 sec)
5	AL	200	VT (12 sec); 3° AVB (20 sec)
	PM	300	3° AVB (> 1 hr)+
6	PM	200	3° AVB (3 min)
	AL	300	3° AVB (7 min)
7	PM	300	VT (3 sec); 3° AVB (20 min)
	AL	200 × 2*	VT (25 sec); 3° AVB (> 1 hr)
8	AL	200 × 2	3° AVB (5 min)
	AM	300	VT (13 sec); 3° AVB (28 min)
9	AL	200 × 2	VT (4 sec); 3° AVB (3 min)
	AM	300	VT (45 sec); 3° AVB (> 1 hr)

Abbreviations: AL = anterolateral, AM = anteromedial, PM = posteromedial, 3° AVB = complete atrioventricular block, VF = ventricular fibrillation, VT = ventricular tachycardia.
* Indicates 200 joule shocks given twice without moving the catheter.
+ Indicates that the animal was caged with complete heart block (see text for discussion)

A standard quadripolar electrode catheter was placed through the right internal jugular vein and positioned under fluoroscopic guidance such that the tip of the catheter made firm contact with the atrial endocardium near the estimated level of the tricuspid annulus. The sites chosen for shocks were in the anteromedial, anterolateral, or posteromedial area of the right atrium. To determine the adequacy of contact between the endocardial wall and electrode catheter, the atrial pacing threshold was determined. The endocardial electrograms from the distal two poles of the catheter were also recorded, and the amplitudes of the atrial and ventricular electrograms were compared. To deliver the shock as closely as possible to the tricuspid annulus, the catheter was positioned such that the ratio of the amplitudes of atrial and ventricular electrograms (the A:V ratio) was between 1.0 and 1.5. For six of the shocks, a pacing threshold below 1.5 mA could not be obtained.

A series of 24 shocks were delivered in the nine dogs. Six dogs received a single shock at each of two to three different sites, whereas three dogs received a single shock at one site and then, at a different site, two shocks delivered twice without moving the catheter. The scheme of these discharges are outlined in table 3–1.

The discharges were delivered using a direct-current defibrillator with the distal pole of the catheter connected to the cathode of the defibrillator and a chest wall patch as the anode (current sink). The patch was placed so that the intended area of ablation was between the catheter and patch. For anteromedial, anterolateral, and posteromedial ablations, the patch was therefore placed at the left of the sternum, the right of the sternum, and under the right scapula, respectively. Twenty minutes were allowed to elapse between successive shocks in the same animal. When AV block occurred, the ventricle was paced until conduction returned or until the rhythm stabilized.

After seven to ten days, under general anesthesia, pressures were again measured in the right atrium and right ventricle, and a right ventriculogram was obtained in the 30° RAO projection. Programmed ventricular stimulation was also repeated.

The heart was removed and examined. The area of the lesions produced were measured, and the distance of the center of the lesion from the tricuspid annulus determined. Tissue blocks were taken of each lesion, sectioned, and stained with hematoxylin and eosin.

The dogs tolerated the shocks well without deaths or hemodynamic deterioration. Brief (< 15 second) periods of nonsustained ventricular tachycardia were common. One dog developed ventricular fibrillation and required chest-wall direct-current countershock. Transient complete AV block occurred frequently with shocks greater than 200 joules (table 3–1). The escape rhythm was of a wide QRS complex (rate 41 bpm's–105 bpm's), which did not accelerate with atropine. Normal AV conduction returned within 60 minutes in six of the nine dogs, whereas three dogs were caged with AV block. This uniformly resolved within seven to ten days.

There was no change in the right atrial or ventricular pressures recorded at the time of sacrifice. Tricuspid regurgitation was not seen and there were no inducible arrhythmias before and seven to ten days later. Myocardial perforation or pericardial reactions were not seen. The lesions caused by the shock were discrete and consisted of a central hemorrhagic focus surrounded by a raised indurated area (figure 3–3). When pre-shock atrial pacing thresholds were less than 1.5 mA (indicating adequate electrode-endocardial surface contact), the area of the lesion correlated with the stored energy ($r = 0.78$) (figure 3–4). Conversely, when the pre-shock pacing threshold was greater than 1.5 mA, the lesions were significantly smaller. Thus, the size of the lesion produced was dependent not only on the amount of energy delivered but also on the adequacy of pre-shock electrode-endocardial surface contact.

The distance of the center of the lesion from the tricuspid annulus correlated with pre-shock ratio of the amplitude of the atrial and ventricular electrograms (table 3–2, figure 3–5). All shocks delivered with the catheter in such a position that the pre-shock ratios were between 1.0 and 1.5 produced lesions that were at or within 5 mm of the upper border of the annulus. When the ratio was above 1.5, the lesions were higher in the atrium,

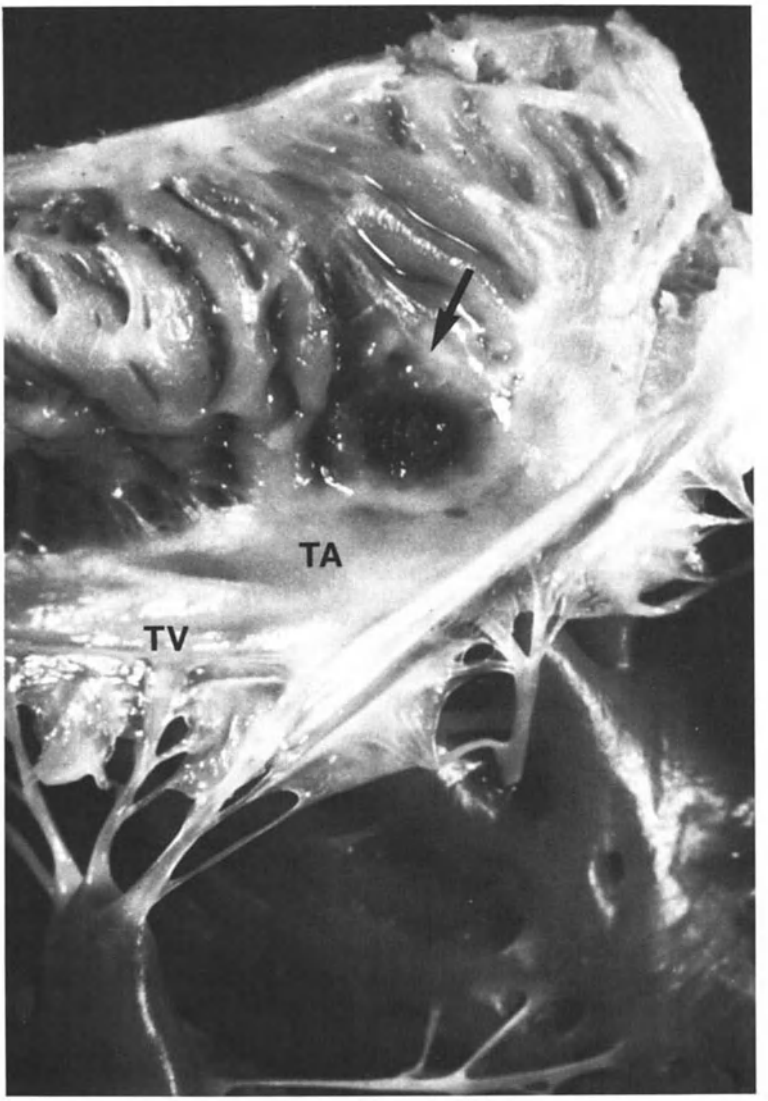

Figure 3–3. Ablation lesion caused by a 50 joule discharge in the anterolateral right atrium, consisting of a central hemorrhagic area surrounded by a raised, edematous collar. There is no involvement of the tricuspid valve. Histologically, there was transmural damage at the level of the annulus. The area of the lesion is 57 mm^2.

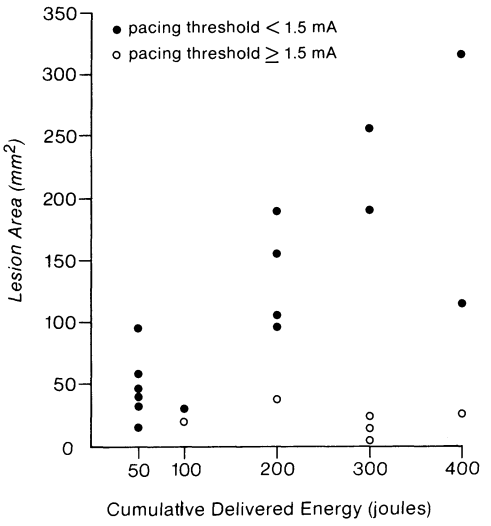

Figure 3–4. Lesion area (mm^2) versus cummulative delivered energy (joules). When the pre-shock atrial pacing threshold was less than 1 mA–5 mA (closed circles), the lesion area correlated with the total delivered energy ($r = 0.78$, $p < 0.001$). When the pre-shock electrode-endocardial surface contact was poor (threshold greater than 1.5 mA, open circles), little or no damage was seen.

whereas when the ratio was below 1.0, the lesions were lower on the annulus, on the tricuspid valve, or even within the ventricle (table 3–2). The location of the lesion produced could therefore be determined by the pre-shock ratio of atrial and ventricular electrograms.

On histologic examination, the lesions, in general, consisted of a central area of hemorrhage and necrosis surrounded by a region of early scarring and peripheral inflammation (figure 3–6). Transmural necrosis was present with 17 (81%) of the 21 lesions and transmural necrosis at the annulus in 15 (71%) of the lesions. Transmural necrosis at the annulus was uniformly seen when the catheter position met the proposed criteria of a pre-shock ratio of atrial and ventricular electrograms between 1.0 and 1.5 and low atrial pacing threshold, even with stored energies as low as 50 joules. The extent of damage to the atrial wall was clearly related to the amount of energy delivered. With higher energy discharges, the histologic damage tended to extend up into the atrium and down to the ventricular summit. The fat in the coronary sulcus was also involved in the necrotic process to a degree varying with the energy involved. With low discharge energies, minimal inflammation of the adipose tissue immediately adjacent to the epicardium was seen. With higher energies, extensive necrosis of large amounts of the fat in the nearby coronary sulcus occurred. Similarly, with higher discharge energies, there frequently was inflammation at the base of the tricuspid valve.

Table 3–2. Examination of lesion produced

Dog No.	Site	Energy delivered (Joules)	A:V ratio	Pacing threshold (mA)	Lesion area (mm^2)	Center of lesion to annulus (mm)
1	AL	200	1.1	0.6	154	0
	AM	50	3.2	0.7	33	18
2	PM	50	0.8	0.3	38	−10
	AL	50	1.0	0.7	95	−1
	AM	50	6.2	1.0	44	10
3	PM	50	0.6	0.2	13	−10
	AL	100	1.0	0.9	28	2
	AM	200	1.2	1.5	38	3
4	AL	50	1.3	1.0	57	3
	AM	100	0.9	5.4	20	−4
	PM	200	4.0	0.3	188	6
5	AL	200	1.4	0.7	104	3
	PM	300	3.2	1.8	24	8
6	PM	200	1.7	1.3	95	6
	AL	300	1.2	1.0	188	0
7	PM	300	1.4	0.9	254	5
	AL	200 × 2	1.2	1.2	133	0
8	AL	200 × 2	1.2	1.7	24	0
	AM	300	1.0	1.7	13	0
9	AL	200 × 2	1.0	0.6	314	0
	AM	300	1.3	3.6	3	0

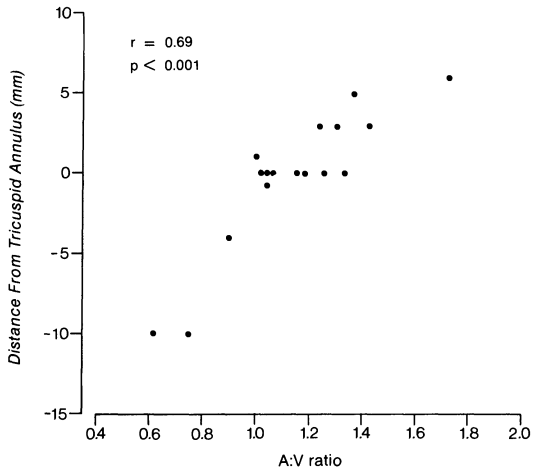

Figure 3–5. Graph of the distance of the center of the lesion from the top of the tricuspid annulus plotted against the ratio of the amplitude of the pre-shock atrial and ventricular electrograms (A:V ratio). The location of the lesion produced could be predicted by the measured A:V ratio. When the pre-shock A:V ratio was between 1.0 and 1.5, transmural necrosis at the annulus was produced by the shock.

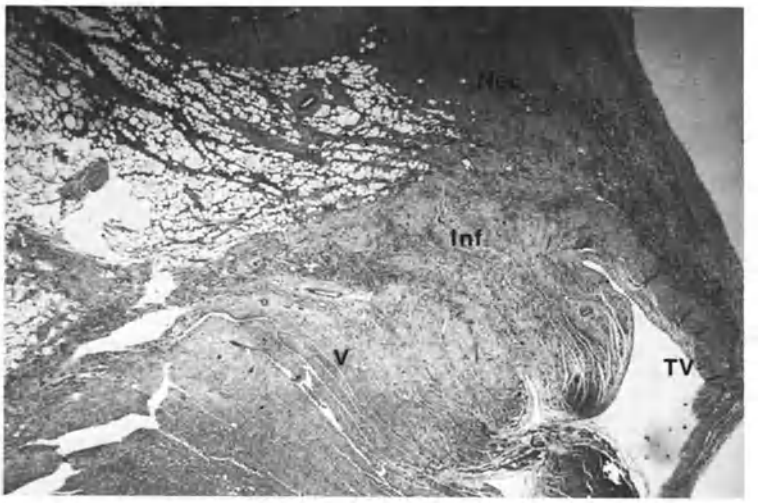

Figure 3–6. Photomicrograph of a cross section through the lesion caused by a 100 joule shock. There is a central area of necrosis with hemorrhage (Nec) closely surrounded by inflammation (Inf). The base of the tricuspid valve (TV) and the ventricular summit (V) are somewhat inflamed. The fat in the coronary sulcus is necrosed but, on higher magnification, the coronary artery is not involved. (Hematoxylin and eosin, original magnification X 12.5).

Fifteen (71%) of the 21 lesions were near the right coronary artery. With energies less than 200 joules, no evidence of arterial damage was seen. However, 200 joules discharges produced adventitial inflammation of the coronary artery adjacent to the lesion in two dogs (figure 3–7), and a 200 joules shock delivered twice at the same site produced marked inflammation of the media of the artery in another. No intimal involvement was seen in any animal.

Implications

Although ablations of right free wall accessory pathways utilizing high-energy discharges have been attempted [28–31], we were interested in formally studying the safety of shocks delivered near the tricuspid annulus and in assessing a technique by which the extent and location of an intended lesion could be predicted. The technique used consistently produced lesions which might be expected to interrupt anomalous conduction. However, with discharges at or above 200 joules, damage of the adjacent right coronary artery was occasionally seen.

The catheter could be securely placed against the atrial wall more easily by utilizing the internal jugular approach than the femoral. The proximity to the annulus could be estimated by fluoroscopic localization and then finally adjusted by making use of the recorded amplitudes of the endocardial atrial and ventricular electrograms. When the ratio of these amplitudes was be-

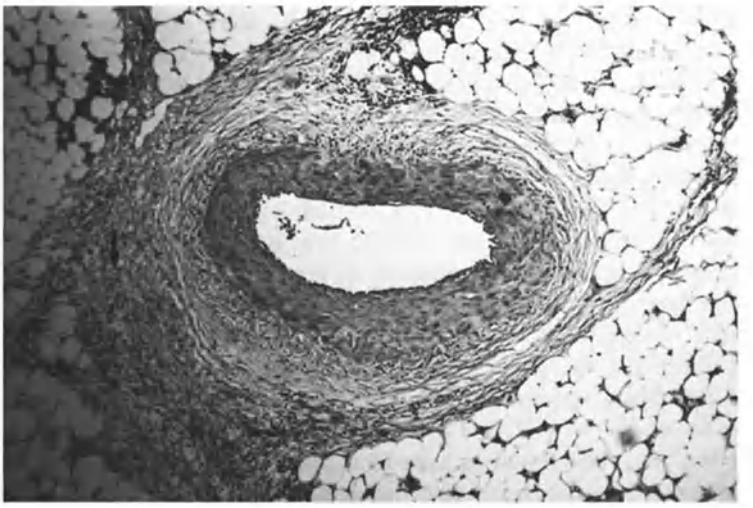

Figure 3–7. High power magnification of a cross section through the lesion caused by a 200 joule shock, delivered at an area near the right coronary artery. The endocardium is to the left, the pericardium to the right. Necrosis and inflammation of the adipose tissue surrounding the artery, especially near the origin of the shock, is seen. The adventitia of the artery is inflamed with cellular infiltrates consisting of polymorphonuclear and mononuclear cells. (Hematoxylin and eosin, original magnification X 64).

tween 1.0 and 1.5, the lesion was centered within 5 mm above the annulus and, histologically, transmural necrosis at the annular level was seen. Because right free wall pathways tend to cross the atrioventricular junction at areas in which the annulus fibrosis is deficient (as opposed to farther out in the adipose tissue) [32], these lesions might prove suitable in disrupting anomalous connections on the right free wall.

The amount of tissue destruction correlated with the cummulative amount of stored energy. This is similar to previous work on discharges within the ventricle [33] as well as near the AV node-His axis [2, 3]. When contact between the tip of the catheter and endocardial surface appeared poor, as measured by pre-shock atrial pacing threshold, the lesions were considerably smaller. This finding may have implications concerning the physical factors involved in tissue destruction with high-energy discharges. Although the pressures generated by the shocks are considerable and barotrauma undoubtedly causes some tissue injury in, for example, the confines of the coronary sinus [9], it would seem unlikely that the destructive energy of barotrauma would be dissipated at such short distances that the size of the lesion produced would be critically dependent on catheter-tissue contact. The suggestion is that electrical current, not barotrauma, causes the desired tissue destruction.

After the shocks and at the time of sacrifice, there was no evidence of right

heart decompensation, tricuspid regurgitation, myocardial perforation, or pericarditis. Similarly, ventricular arrhythmias were not inducible after the shock. However, the effects of the discharges on the coronary artery are of concern. Brodman et al found evidence of vessel wall fibrosis and some luminal narrowing of the circumflex coronary artery resulting from high-energy discharges delivered in the coronary sinus [8]. In our study, adventitial and medial inflammation occasionally occurred with energies at or greater than 200 joules. No significant intimal involvement or luminal reduction was seen, but the mild inflammation might progress, with time, to significant narrowings. It would appear prudent to restrict ablation attempts to those pathways that are not adjacent to a coronary artery.

The AV block seen transiently after the discharges uniformly resolved. It appears likely that this phenomenon is similar to the temporary disruption of normal AV nodal conduction after catheter ablation of posteroseptal accessory pathways in man [27]. The cause of the short-lived AV block is not known but may be related to transient changes in transmembrane voltage gradients caused by the enormous current flows associated with the shocks or by barotrauma.

In summary, delivering high-energy discharges near the tricuspid annulus consistently produced a lesion which might prove suitable for disrupting anomalous conduction in man. The site of the lesion was predicted by the pre-shock ratio of the amplitudes of the atrial and ventricular endocardial electrograms. The size of the lesion correlated with both the energy delivered and the adequacy of pre-shock electrode-endocardial surface contact. While there were no manifest clinical adverse reactions, inflammation was occasionally seen in the outer wall of adjacent coronary arteries and suggests that ablation attempts of right free wall accessory pathways should be limited to lower energies or to those pathways remote from a coronary artery.

REFERENCES

1. Gonzalez R, Scheinman M, Margaretten W Rubinstein M: Closed-chest electrode-catheter technique for His bundle ablation in dogs. *Am J Physiol* 241: H283, 1981.
2. Gonzalez R, Scheinman M, Bharati S, Lev M: Closed-chest permanent atrioventricular block in dogs. *Am Heart J* 105: 461, 1983.
3. Bardy GH, Ideker RE, Kasell J, Worley SJ, Smith WM, German LD, Gallagher JJ: Transvenous ablation of the atrioventricular conduction system in dogs: Electrophysiologic and histologic observations. *Am J Cardiol* 51: 1775, 1983.
4. Scheinman MM, Morady F, Hess DS, Gonzalez R: Catheter induced ablation of the atrioventricular junction to control refractory supraventricular arrhythmias. *JAMA* 248: 851, 1982.
5. Gallagher JJ, Svenson RH, Kasell JH, German LD, Bardy GH, Broughton A, Critelli G: Catheter technique for closed-chest ablation of the atrioventricular conduction system: A therapeutic alternative for the treatment of refractory supraventricular tachycardia. *N Engl J Med* 306: 194, 1982.
6. Wood DL, Hammill SC, Holmes DR Jr, Osborn MJ. Gersh BJ: Catheter ablation of the atrioventricular conduction system in patients with supraventricular tachycardia. *Mayo Clin Proc* 58: 791, 1983.

7. Nathan AW Bennett DH, Ward DE, Bexton RS, Camm AJ: Catheter ablation of atrioventricular conduction. *Lancet* 1: 1280, 1984.
8. Brodman R, Fisher JD: Evaluation of a catheter technique for ablation of accessory pathways near the coronary sinus using a canine model. *Circulation* 67: 923, 1983.
9. Coltorti F, Bardy GH, Reichenbach D, Green HL. Thomas R, Breazeale DG, Alferness C, Ivey TD: Catheter-mediated electrical ablation of the posterior septum via the coronary sinus: Electrophysiologic and histologic observations in dogs. *Circulation* 72: 612, 1985.
10. Starzl TE, Gaertner RA: Chronic heart block in dogs. A method for producing experimental heart failure. *Circulation* 12: 259, 1955.
11. Starzl TE, Gaertner RA, Baker RR: Acute complete heart block in dogs. *Circulation* 12: 82, 1955.
12. Steiner C, Kovalik TW: A simple technique for production of chronic complete heart block in dogs. *J Appl Physiol* 25: 631, 1968.
13. Smyth NPD, Magassy CL: Experimental heart block in the dog: An improved method. *J Thorac Cardiovasc Surg* 95: 201, 1970.
14. Sealy WC, Hackel DB, Seaber AV: A study of methods for surgical interruption of the His bundle. *J Thorac Cardiovasc Surg* 73: 424, 1977.
15. Harrison L, Gallagher JJ, Kasell J, Anderson RH, Mikat E, Hackel DB, Wallace AG: Cryosurgical ablation of the AV node-His bundle: A new method for producing AV block. *Circulation* 55: 467, 1977.
16. Fisher VJ, Lee RJ, Christianson LC, Kavaler F: Production of chronic atrioventricular block in dogs without thoracotomy. *J Appl Physiol* 21: 1119, 1966.
17. Turina M, Babotai I, Wegmann W: Production of chronic atrioventricular block in dogs without thoracotomy. *Cardiovasc Res* 4: 389, 1968.
18. Beazell J, Tan K, Criley J, Schulman J: The electrosurgical production of heart block without thoracotomy. *Clin Res* 24: 137A, (abstract), 1976.
19. Beazell JW, Adomian GE, Furmanski M, Tan KS: Experimental production of complete heart block by electrocoagulation in the closed chest dog. *Am Heart J* 104: 1328, 1982.
20. Scheinman M, Evans-Bell T: Catheter ablation of the atrioventricular junction: A report of the percutaneous mapping and ablation registry. *Circulation* 70: 1024, 1984.
21. Scheinman M, Bharati S, Wang Y, Shapiro W, Lev M: Electrophysiologic and anatomic changes in the atrioventricular junction of dogs after direct-current shocks through tissue fixation catheters. *Am J Cardiol* 55: 194, 1985.
22. McComb JM, McGovern B, Garan H, Ruskin JN: Modification of atrioventricular conduction using low energy transcatheter shocks. *JACC* 5: 455, (abstract) 1985.
23. Narula OS, Bharati S, Chan M, Embi A, Lev M: Microtransection of the His bundle with laser radiation through a pervenous catheter: Correlation of histologic and electrophysiologic data. *Am J Cardiol* 54: 186, 1984.
24. Huang SK, Bharati S, Lev M, Marcus F: Pathological and electrophysiological observations of chronic atrioventricular block induced by closed-chest catheter ablation with radiofrequency energy. *JACC* 7: 131, (abstract) 1986.
25. Bardy G, Coltorti F, Ivey T, Alferuess C, Rackson M, Hansen K, Stewart R, Greene HL: Some factors affecting bubble formation with catheter-mediated defibrillator pulses. *Circulation* 73: 525, 1986.
26. Fisher JD, Brodman R, Kim SG, Matos JA, Brodman E, Wallerson D, Waspel E: Attempted nonsurgical electrical ablation of accessory pathways via the coronary sinus in the Wolff-Parkinson-White syndrome. *JACC* 4: 685, 1984.
27. Morady F, Scheinman M, Winston S, DiCarlo L, Davis J, Griffin J, Ruder M, Abbott J, Eldar M: Efficacy and safety of transcatheter ablation of posteroseptal accessory pathways. *Circulation* 72: 170, 1985.
28. Weber H, Schmitz L: Catheter technique for closed-chest ablation of an accessory pathway. *N Engl J Med* 308: 653, 1983.
29. Jackman WM, Friday K, Scherlog BJ, Dehning MM, Schechter E, Reynolds DW. Olson EG, Berbari EJ, Harrison LA, Lazzara R: Direct endocardial recording from an accessory pathway: Localization of the site of block, effect of antiarrhythmic drugs, and attempt at nonsurgical ablation. *Circulation* 68: 906, 1986.
30. Kuuze K, Kuck K: Transvenous ablation of accessory pathways in patients with incessant atrioventricular tachycardia. *Circulation* 70: 412, (abstract) 1984.

31. Hartzler GO, Giorgi LV, Diehl AM: Right coronary spasm complicating electrode catheter ablation of a right lateral accessory pathway. *JACC* 6: 250, 1985.
32. Davies MJ, Anderson RH, Becker AE: *The Conduction System of the Heart*. London: Butterworths, p. 189–190, 1983.
33. Davis JC, Finkebeiner W, Ruder MA, DiCarlo L, Matsubara T, Chu W. Winston SA, Bharati S, Scheinman MM, Lev M: Histologic changes and arrhythmogenicity after discharge through transseptal catheter electrode. *Circulation* 74: 637, 1986.

4. EFFECTS OF HIGH-ENERGY ELECTRICAL SHOCKS DELIVERED TO THE ATRIUM OF THE CORONARY SINUS

GUST H. BARDY, FERNANDO COLTORTI, TOM D. IVEY, ROBERT STEWART, H. LEON GREENE

Catheter mediated electrical ablation of posterior septal accessory pathways is appealing not only because of the opportunity to avoid a sternotomy but also because posterior septal accessory pathways are recognized as the most difficult type of accessory pathway to ablate surgically [1]. Previous work has documented that catheter mediated electrical ablation of posterior septal accessory pathways is, indeed, clinically feasible although with variable success [2–8]. The purpose of this chapter is to review our work investigating the histologic effects of single, damped sine wave defibrillator pulses on the canine proximal coronary sinus (CS) in order to gain insight into the factors leading to success or failure of the technique for posterior septal accessory pathway ablation in man [9–12].

INITIAL METHODS OF INVESTIGATION

Our initial work was performed in 12 pentobarbital anesthetized dogs weighing between 23 and 28 kg [9]. Using sterile technique and fluoroscopic guidance, standard pacing and recording catheters were inserted transvenously for evaluation of impulse formation and conduction. The catheter intended to carry the defibrillator pulse was a new, standard 6F USCI quadripolar elec-

This work supported in part by grants from the American Heart Association, Washington Chapter and the Seattle Medic One — Emergency Medical Services Foundation. Dr. Bardy is a recipient of New Investigator Award #36170–01, The National Institutes of Health.

trode catheter with 1 cm interelectrode distance that was inserted via the right external jugular vein and positioned in the proximal CS. Prior to delivery of the defibrillator pulse to the CS catheter, a control 12-lead ECG and baseline PA, AH, and HV intervals were obtained followed by antegrade and retrograde decremental pacing, and by antegrade and retrograde refractory period determinations. Preablation programmed stimulation of the atria and ventricles at two basic cycle lengths (500 ms and 400 ms) from two sites was also performed.

At the end of the stimulation studies, the CS catheter was positioned with the proximal pole at the orifice of the CS. Position of the catheter at the CS orifice was confirmed using the following four criteria: 1) characteristic fluoroscopic appearance in the anteroposterior and lateral views; 2) the presence of negative paced P waves in leads II, III, and aVF; 3) the presence of local bipolar electrograms showing an atrial and a ventricular deflection, with the atrial signal falling between the mid portion and the end of the P wave; and 4) the unipolar electrogram from the proximal pole, situated at the CS orifice, having a loss of the rapid component of the atrial electrogram indicative of a cavitary potential.

When the proximal electrode was at the os of the CS, a single synchronous damped sinusoidal pulse of 200 joules (six dogs) or 360 joules (six dogs) of stored energy was delivered to the two proximal poles of the CS catheter connected in parallel to the positive output of a Physio-Control Life Pack 6A defibrillator. A disc electrode 3.5 cm in diameter was connected to the negative output of the defibrillator and positioned on the anterior chest wall opposite the anode, using fluoroscopic guidance.

The current and voltage waveforms were displayed on a Tektronix 5111A oscilloscope. The voltage was recorded using a 1000:1 input to output ratio resistive voltage divider. The current was recorded with a Tektronix A6303 current probe positioned around the positive output cable of the defibrillator. The experimental schema is shown in figure 4–1.

After delivery of the pulse, the dogs were monitored for a two-hour interval at the end of which a 12-lead ECG was obtained. Serial 12-lead ECG's were recorded again at 24-hour, two-week, and four-week intervals. On each occasion signs of tricuspid insufficiency, pericardial tamponade, and heart failure were sought on physical examination. Four weeks after the defibrillator discharge to the CS, repeat electrophysiologic studies were performed. At the end of the study, the animals were sacrificed, and the hearts were removed and fixed in 10% formalin.

After gross inspection for structural damage, the principal areas of interest (i.e., AV groove and AV conduction system) were removed for detailed examination in two tissue blocks. One block included the AV node/His bundle and the main fascicles. The other block included the AV junction spanning 1.0 cm in front of the CS orifice to 3.5 cm beyond the CS orifice toward the left atrium, and including a 2 cm rim of atrial and a 2 cm rim of

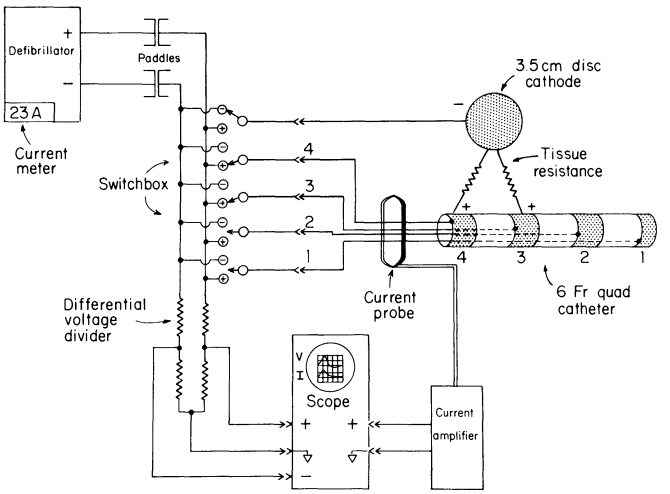

Figure 4–1. Schema for catheter mediated electrical ablation, using a defibrillator and a standard electrode catheter. The proximal pole of the electrode catheter was positioned at the coronary sinus orifice. A damped sine-wave defibrillator pulse was delivered to the two consecutive proximal electrodes (3 and 4) by means of a switch box. These two electrodes, coupled together, served as the anode (positive pole), while a 3.5 cm disc electrode served as the cathode (negative pole). Connections to record current (I) and voltage (V) waveforms are illustrated. A current-sensing transformer built into the Physio-Control defibrillator served as an adjunct to the displayed current waveform, confirming the absence of current leakage outside the catheter. (Reprinted with permission of the American Heart Association, Coltorti, et al. *Circulation* 72: 612, 1985.)

ventricular myocardium above and below the AV groove. Each block was embedded in paraffin and sectioned serially at 1 mm intervals. A section at each interval was stained with Gomori's Trichrome. Verhoeff-Van Gieson stains for visualization of elastic tissue injury were performed at points of maximum injury.

ELECTROPHYSIOLOGIC FINDINGS

Immediately following delivery of the synchronized defibrillator pulse, all dogs showed nonsustained, self-terminating episodes of ventricular tachycardia. Upon cessation of ventricular tachycardia, third degree AV block was observed in five dogs. Complete AV block resolved within 15 minutes in all but one dog, in which it lasted up to 45 minutes. At the end of the two-hour monitoring period, normal resting AV conduction had resumed in all dogs. Other acute electrocardiographic changes included transient PR and ST segment elevation in all dogs, especially evident in the inferior leads. However, at the two-hour observation period the 12-lead ECG did not show any change from control.

An idioventricular rhythm competing with sinus rhythm was noted at 24 hours in six animals. This rhythm showed periods of acceleration and deceleration, with a QRS morphology of right bundle branch block and left axis deviation, consistent with an automatic focus located along the posterior base of the left ventricle.

Later serial 12-lead electrocardiograms and monitoring strips were unremarkable for changes suggestive of ischemia or conduction defects. No arrhythmic episode was detected after the first three days following the defibrillator discharge, and no sudden deaths occurred. Chronic electrophysiologic findings compared to baseline values are summarized in table 4–1. There were no chronic alterations in impulse formation or conduction compared to baseline values in the atria, AV conduction system, or ventricles.

LOCATION OF INJURY AND DEMONSTRATION OF BAROTRAUMA

Anatomic findings are summarized in table 4–2. There was no gross evidence of damage to the tricuspid valve or to the AV node area. Narrowing of the CS orifice was grossly evident in six dogs, and complete occlusion was observed in three dogs. A brownish discoloration due to hemosiderin deposition was found on the endocardium of the posterior left atrium in six dogs (figure 4–2A). No congestion or gross changes in the left ventricle secondary to CS thrombosis was seen.

Sections of the AV node, bundle of His, and proximal bundle branches did not reveal any damage in any dog. Coronary sinus injury, however, was present in all animals. Maximum length of CS injury was 18 ± 6 mm in the 200 joule group and 23 ± 4 mm in the 360 joule group. Injury consisted of circumferential CS fibrosis in all dogs and was associated with loss of CS intimal muscle. Furthermore, the lumen of the CS showed varying degrees of occlusion from thrombus formation (figure 4–3). Finally, although no gross rupture of the CS was seen in this particular study, a constant histologic finding was rupture of the internal elastica of the CS, with abrupt displacement of CS tissue into the atrial wall on its endocardial aspect, as if segments of the CS had been forcefully disrupted due to barotrauma (figure 4–4). No such injury was observed along the epicardial aspect of the CS.

In the left atrial wall, fibrous replacement of atrial myocardium extended for a maximum length of 18 ± 5 mm in the 200 joule group and 26 ± 4 mm in the 360 joule group, reaching a height of 8 ± 3 mm and 11 ± 2 mm, respectively, for the 200 joule and 360 joule pulses. Atrial injury was transmural for a length of 10 ± 5 mm in the 200 joule group and 21 ± 6 mm in the 360 joule group ($p < 0.01$). However, transmural fibrosis near the anulus of the mitral valve was inconstant and scanty (figures 4–3, 4–5).

Maximum length of muscle loss and fibrous replacement in the left ventricle paralleled that of the left atrium, being 15 ± 5 mm long in the 200 joule group and 19 ± 5 mm long in the 360 joule group. However, the depth of

Table 4–1. Electrophysiologic findings before and after delivery of the defibrillator pulse

Dogs 1–6 had 200 joule shocks; 7–12 had 360 joule shocks (numbers are expressed in milliseconds)

	PA		AH		HV		RA DEC P (Wenckebach)		AVN FRP		AVN ERP		RA FRP		RA ERP		AF		VAR	
Dog #	b	a	b	a	b	a	b	a	b	a	b	a	b	a	b	a	b	a	b	a
1	30	30	65	62	35	30	250	260	300	320	160	240	190	180	110	160	NSu	NSu	VF	No
2	28	38	55	45	34	28	260	260	340	340	240	240	180	180	150	150	NSu	NSu	No	No
3	38	40	75	72	35	30	220	240	320	310	220	220	160	170	120	110	NSu	NSu	No	No
4	25	30	60	45	38	36	210	200	270	270	170	190	190	160	170	150	NSu	NSu	No	No
5	30	22	120	74	40	35	410	200	400	270	300	160	180	180	140	140	NSu	NSu	No	VF
6	38	38	58	60	32	35	250	270	340	320	260	250	180	190	150	120	Su	Su	VF	No
mean ± SD	32	33	72	60	36	32	267	238	328	305	225	217	180	177	140	138				
	± 5	± 7	± 24	± 13	± 3	± 3	± 73	± 31	± 44	± 29	± 54	± 35	± 11	± 10	± 22	± 19				
	p=NS		p=NS		P=NS		p=NS		p=NS		p=NS		p=NS		p=NS					
7	37	42	42	40	38	38	210	220	270	280	140	140	170	190	140	140	Su	Su	No	No
8	32	32	50	53	38	38	210	200	260	250	140	180	190	180	140	150	NSu	NSu	No	No
9	46	46	35	38	32	35	190	200	260	270	160	170	190	190	160	160	NSu	NSu	No	No
10	30	25	55	65	32	35	250	250	340	330	240	210	180	140	150	120	NSu	Su	No	No
11	43	38	52	58	45	43	240	340	310	340	250	260	220	200	180	150	NSu	NSu	No	No
12	42	44	48	48	35	33	240	210	270	225	150	150	180	180	130	150	Su	Su	No	No
mean ± SD	38	38	47	50	37	37	223	237	285	283	180	185	188	180	150	145				
	± 6	± 8	± 7	± 10	± 5	± 4	± 23	± 54	± 33	± 45	± 51	± 44	± 21	± 21	± 18	± 14				
	p=NS		p=NS		P=NS		p=NS		p=NS		p=NS		p=NS		p=NS					

Abbreviations: a = after; AF = atrial fibrillation; AH = atrio-Hisian interval; AVN = atrioventricular node; b = before; DEC P = decremental pacing; ERP = effective refractory period; FRP = functional refractory period; HV = His-ventricular interval; NS = nonsignificant; NSu = nonsustained; PA = surface P wave to local AVN atrial electrogram interval; RA = right atrium; Su = sustained; VAR = ventricular arrhythmias; VF = ventricular fibrillation.

Table 4–2. Anatomic changes following delivery of the defibrillator pulse

	Shock	Coronary sinus injury			Atrial injury			Left ventricle injury			Conduction system injury	Left circumflex artery injury
Dog #	Stored Energy (J)	Gross Rupture	Elastic Rupture	Length (mm)	Max Length (mm)	Length of Transmural Injury (mm)	Height (mm)	Length (mm)	Width (mm)	Depth (mm)		
1	200	No	Yes	24	17	7	6	22	4	3	No	No
2	200	No	Yes	18	16	9	12	13	5	5	No	No
3	200	No	Yes	7	10	8	6	7	4	2	No	No
4	200	No	Yes	19	23	20	10	16	3	3	No	No
5	200	No	Yes	17	18	6	5	18	5	3	No	No
6	200	No	Yes	23	23	7	9	12	4	1	No	No
mean ± SD				18 ± 6	18 ± 5	10 ± 5	8 ± 3	15 ± 5	4 ± 1	3 ± 1		
7	360	No	Yes	22	20	16	11	15	3	1	No	No
8	360	No	Yes	23	32	22	12	20	4	3	No	No
9	360	No	Yes	15	24	15	10	14	5	2	No	No
10	360	No	Yes	24	26	20	14	18	4	2	No	No
11	360	No	Yes	24	29	30	8	17	4	1	No	No
12	360	No	Yes	27	26	24	8	27	13	5	No	No
mean ± SD				23 ± 4	26 ± 4	21 ± 6	11 ± 2	19 ± 5	6 ± 4	2 ± 2		

involvement of the left ventricular wall was never greater than 5 mm. Additionally, injury width was at most 5 mm at the point of maximum left ventricular injury, except for one dog (dog 12, table 4–2). Transmural ventricular injury was present only in this one dog and was limited to a length of 3 mm.

Microscopic findings confirmed the absence of injury to the circumflex coronary artery (figure 4–3, 4–5). An occasional finding was the presence of a foreign body reaction with giant cell formation in the areas of maximum injury associated with platinum deposition in the tissue (documented by spectroscopy) (figure 4–6). This is likely due to melting of the electrode at the time of current discharge.

IMPLICATIONS OF THE STUDY

The arrhythmogenic potential of this technique appears to be minimal. No chronic AV block or tachycardias (spontaneous or induced) were seen to occur. The only electrophysiologic abnormalities noted were transient AV block and transient accelerated ventricular rhythms, apparently emanating from the region of the basilar ventricular septum adjacent to the CS site of discharge. When the catheter technique is compared with what is known about the surgical technique for posterior septal accessory pathway ablation, we can at least be optimistic that the catheter approach is less likely to lead to AV block and pacemaker dependency.

Catheter mediated electrical pulses to the CS orifice did not disturb the normal anatomy of the left circumflex coronary artery. However, the anatomic relationship of the CS orifice to the circumflex coronary artery is optimal at the posterior septum, and the implications of these findings should not be extrapolated to other areas along the AV groove. The coronary artery at the location of the CS orifice is usually very small, although a significant right coronary artery extension branch or dominant circumflex coronary artery may make significant arterial injury more likely in man. In the lateral AV groove, delivery of defibrillator pulses to the CS may have an even higher likelihood of coronary arterial injury because of the usual presence of a large circumflex coronary artery in this area and because the coronary artery and the coronary sinus are closer to one another along the lateral AV groove than over the posterior septum [13]. Nevertheless, regardless of where along the AV groove a catheter mediated ablation procedure is to be performed, given the unknown long-term effects of electrical pulses on coronary anatomy, we do not recommend performing the procedure on patients who have inappropriate coronary artery anatomy, regardless of the findings of this animal study. If the technique is to be utilized in man, we believe coronary arteriography is mandatory prior to catheter ablation in order to correlate accessory pathway location with coronary artery anatomy.

The most important observations from this study are twofold. First, trans-

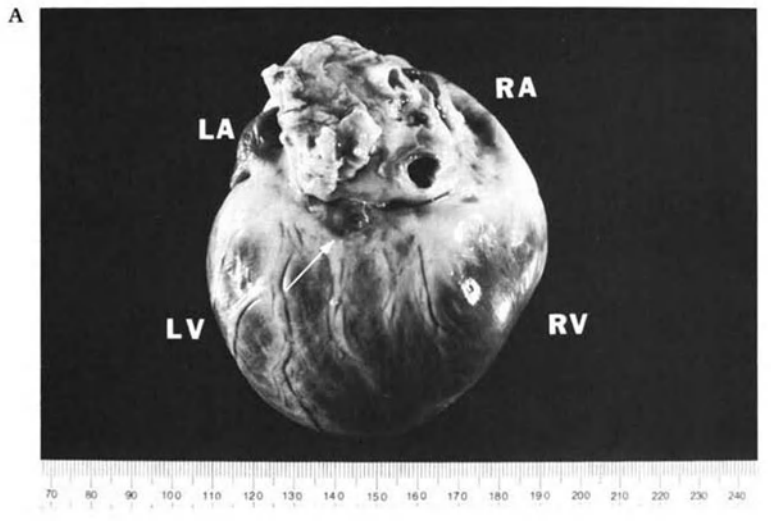
A
RA
LA
LV
RV
70 80 90 100 110 120 130 140 150 160 170 180 190 200 210 220 230 240

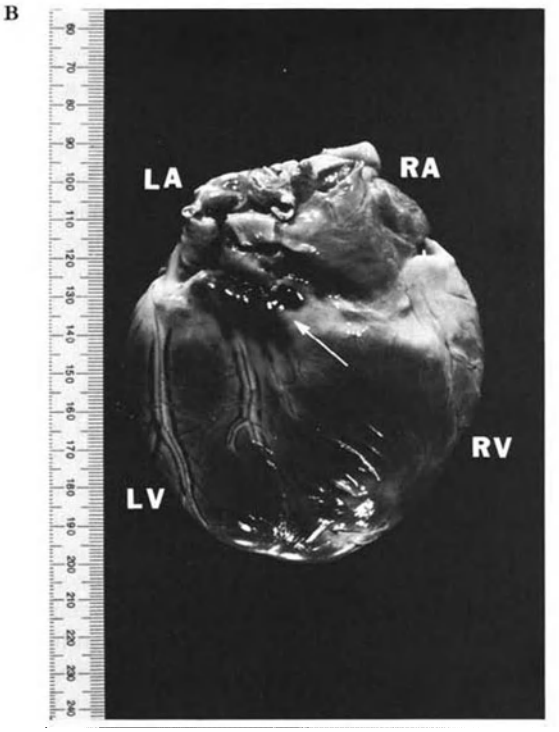
B
LA
RA
RV
LV

mural atrial injury *above but not at* the AV groove could be produced reliably with a single discharge. Second, rupture of the elastica of the CS was observed in each dog, the histologic features of which suggested a barotraumatic mechanism complicating what was thought to be an electrical injury. These findings deserve more detailed consideration, as they give rise to the following questions. What is the mechanism of barotrauma as it relates to intracardiac delivery of high-energy defibrillator pulses? Is barotrauma the sole means of tissue injury or is electrical injury also operative? Can arrhythmias due to accessory pathways be reliably controlled using this technique given the supra-annular location of injury? The remainder of this chapter will be directed to resolving these issues.

THE MECHANISM OF BAROTRAUMA

The answer to the first of these questions, what causes barotrauma with this technique, has actually been known for many years in the nonmedical fields of plasma physics and high-speed pulse technology. Barotrauma is due to an electric arc induced high-pressure shockwave. This phenomenon can be summarized as follows.

Shock-wave generation is initiated by the process of electrolysis, as illustrated in figure 4–7. A clue to the manner in which shock waves arise can be gleaned first from changes observed in the voltage waveform. We have noted distortions or rises in what should otherwise be a smooth Edmark voltage waveform during those pulses resulting in arcs (figure 4–8). These irregularities in the waveform contour indicate changes in impedance following the initial gas formation that results from electrolysis. This process probably begins with the electrolytic decomposition of H_2O to H_2 and O_2, and with the heating of water (figure 4–7) [14, 15]. The quantities of gas generated by electrolysis are quite small and serve only as a catalyst to subsequent events. When enough gas is generated by electrolysis to create a bubble large enough to envelop and insulate the electrode from the blood, current flow to the surrounding blood is transiently interrupted and impedance rises [14]. Despite the rise in impedance, current continues uninterrupted to the elec-

---

Figure 4–2A. Posterior view of the heart four weeks following delivery of a 200 joule defibrillator pulse to a catheter electrode positioned at the os of the coronary sinus. Grossly, there is no evident tissue damage, except for a brownish discoloration at the crux of the heart (arrow). This is due to hemosiderin deposition from previous interstitial hemorrhage (see figure 2B) that occurred immediately after the defibrillator discharge presumably due to barotrauma (see figures 4–4, 4–11, 4–12). Abbreviations: LA = left atrium; LV = left ventricle; RA = right atrium; RV = right ventricle.

Figure 4–2B. Demonstration of subepicardial, interstitial hemorrhage at the crux of the heart two hours following a 200 joule defibrillator pulse to the coronary sinus os of a dog. This hemorrhage occurs routinely as evidenced by the hemosiderin deposition that is observed in the chronic preparations (figure 4–2A, above). The mechanism is probably related to barotraumatic tissue injury (see figures 4–4, 4–11, 4–12).

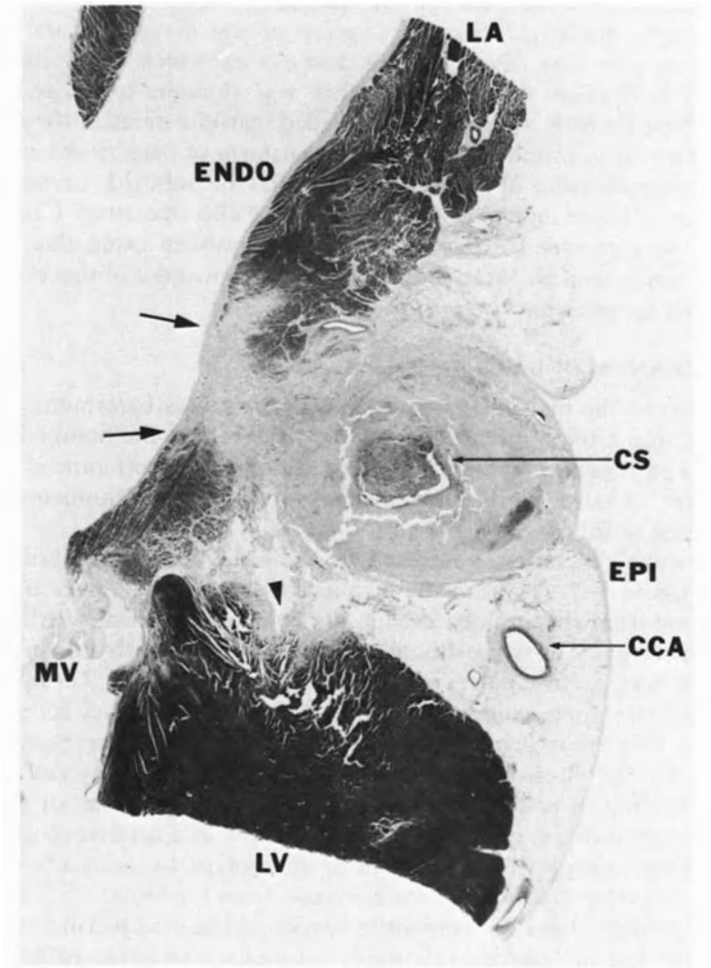

Figure 4–3. Photomicrograph of a cross section of the left atrioventricular groove at the site of maximum injury in dog 7, table 4–1 (360 joules). This section is taken 8 mm within the coronary sinus orifice. The coronary sinus lumen is occluded by an organized thrombus. The coronary sinus wall shows loss of muscle and replacement by circumferential fibrosis. Transmural fibrosis of the atrial wall is present (arrows). There is no fibrosis immediately above the annulus fibrosus. The left ventricular wall shows a very limited area of muscle loss and fibrous replacement (arrowhead). The circumflex coronary artery is patent and no wall abnormalities are present. (Gomori's Trichrome, X 5.7). Abbreviations: arrows = site of myocardial fibrosis; CCA = circumflex coronary artery; CS = coronary sinus; ENDO = endocardium; EPI = epicardium; LA = left atrium; LV = left ventricle; MV = mitral valve. (Reprinted with permission of the American Heart Association, Coltorti, et al. *Circulation* 72: 612, 1985.)

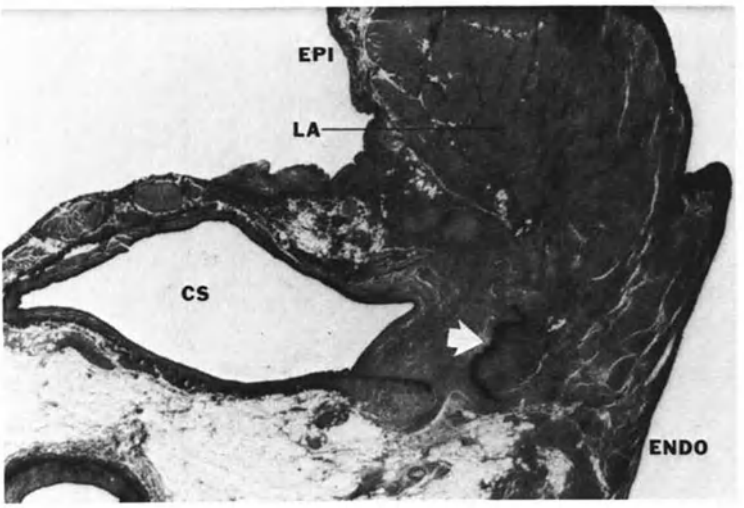

Figure 4–4. Cross section of the left coronary sulcus (Verhoeff-Van Gieson elastic tissue stain, X 26), taken from dog 4, table 4–1 (200 joules), 16 mm within the coronary sinus orifice. Rupture of the internal elastica of the coronary sinus is observed on the endocardial aspect, with a detached part of the elastica itself displaced toward the atrial wall (white arrowhead). The integrity of the elastic membrane around the rest of the circumference of the coronary sinus is maintained. Rupture of the elastic membrane suggests a barotraumatic mechanism of tissue injury. Abbreviations: arrowhead = disrupted elastic membrane; CS = coronary sinus; ENDO = endocardium; EPI = epicardium; LA = left atrium. (Reprinted with permission of the American Heart Association, Coltorti, et al. *Circulation* 72: 612, 1985.)

trode because of the inertia inherent in the defibrillator inductor, which leads to a rise in voltage between the bubble insulated electrode and the surrounding blood. Because of this bubble insulator, an overvoltage is generated between electrode and blood, as the defibrillator current continues to be delivered to the electrode. As the electric field strength increases, more and more electrons enter the bubble that surrounds the electrode until an electron avalanche occurs [16–18]. Eventually, electron density is strong enough to sustain an arc [16–18]. With sufficient electron density, current arcing between the electrode and the surrounding blood occurs, followed by a flash, which can result in an enormous temperature rise in the bubble (as high as 6000°K) [14–19]. Such high temperatures result in a very rapidly expanding bubble volume and an extremely rapid change in the thermodynamic state of the gas. By definition, this phenomenon is a shock wave [20]. The shock wave thus generated can be as high as 50,000 atmospheres, although it is usually less (10 atmospheres to 20 atmospheres) [14, 15]. This sequence of events may repeat following the initial bubble expansion, depending upon

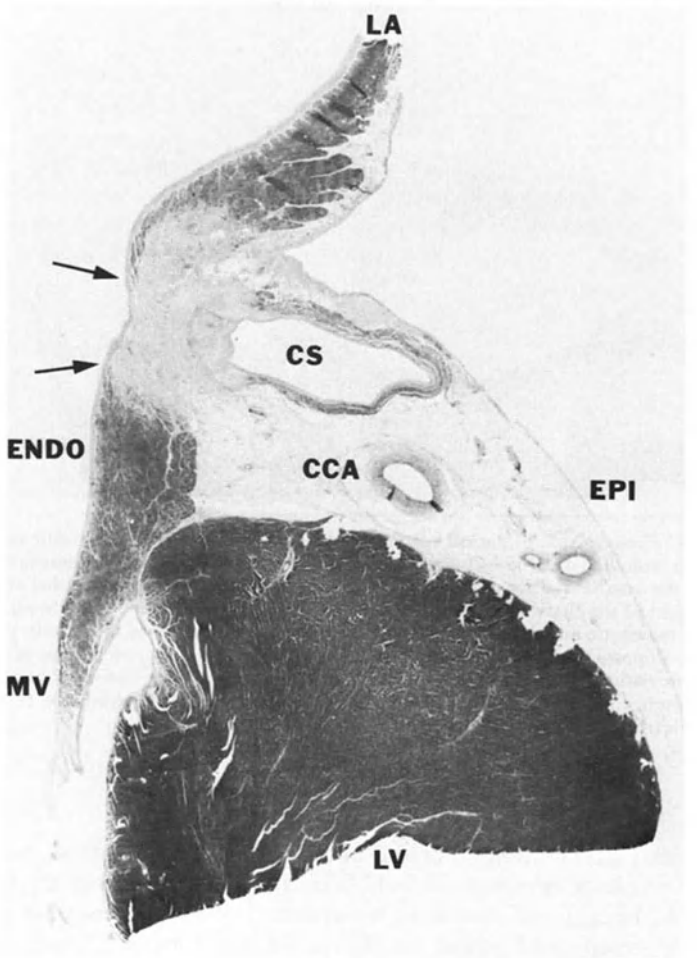

Figure 4–5. Cross section of the left atrioventricular groove, taken 18 mm within the coronary sinus orifice. This dog (#64), table 4–1, received a 200 joule pulse. The left ventricular wall and the coronary artery do not show any damage. Coronary sinus injury is limited. However, transmural atrial fibrosis is present in the atrial wall facing the endocardial aspect of the coronary sinus (arrows). Note undamaged atrial muscle just above the mitral valve. This injury could still leave a bypass tract anatomically intact. Conceivably, however, such a boundary of transmural fibrotic tissue could prevent depolarization wavefronts from entering or exiting the accessory pathway. See text for discussion. (Gomori's Trichrome, X 8.7). Abbreviations: see figures 4–3 and 4–4, legend. (Reprinted with permission of the American Heart Association, Coltorti, et al. *Circulation* 72: 612, 1985.)

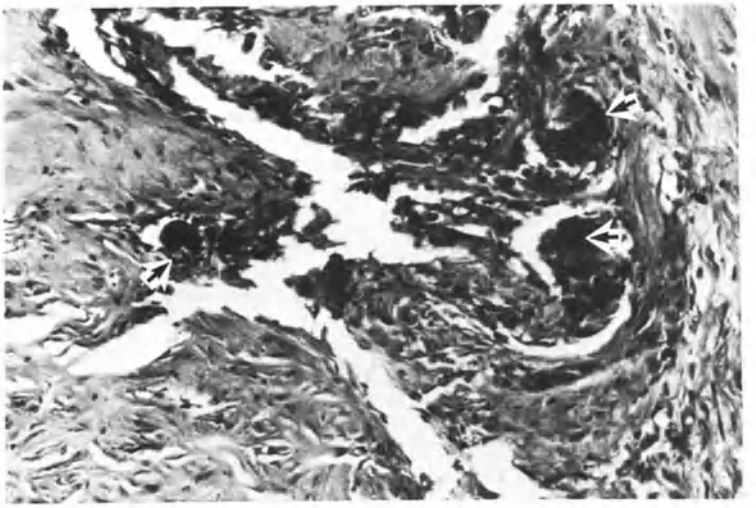

Figure 4–6. High-power photomicrograph from the area of maximum injury in dog 10 (table 4–1). A foreign body reaction with giant cell formation is present in the coronary sinus associated with platinum deposition in the tissue (arrows). See text for discussion. (Gomori's Trichrome, X 300). (Reprinted with permission of the American Heart Association, Coltorti, et al. *Circulation* 72: 612, 1985.)

the amplitude and duration of the electric pulse as well as the electrode surface area, resulting in multiple shock waves.

Although shock waves can arise from rapid bubble expansion, they may also occur as a result of bubble collapse [14, 15, 21, 22]. Bubble collapse occurs following gas bubble overexpansion, which leads to a fall in internal bubble pressure below ambient pressure. As the momentum of the expanding bubble fades and the ambient pressure exceeds internal bubble pressure, the gas volume begins to contract. Upon bubble collapse, a shock wave may again be generated. In some instances, one may actually observe successive shock waves as a consequence of bubble ringing [15].

BAROTRAUMA VERSUS ELECTRICAL INJURY

Given that shock-wave generation with consequent tissue barotrauma were indeed occurring, the question arises whether barotrauma is the sole means of tissue injury during delivery of high-energy defibrillator pulses. We know from previous work during evaluation of transthoracic and epicardial defibrillation that there are factors related to the electric pulse per se that result in cell death [23–26]. Myocyte necrosis with contraction bands, mineralization of necrotic tissue with subsequent macrophage infiltration, and later fibrosis have all been described in the setting of myocardial electrical injury

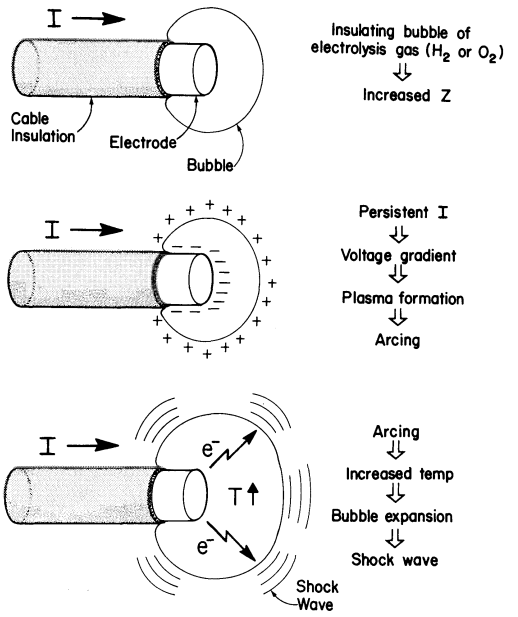

Figure 4–7. Physics of high pressure shock-wave generation. Faraday's Law dictates that a volume of hydrogen and oxygen gas can be generated by electrolysis of water in direct proportion to the amount of charge delivered to the electrodes. The type of gas generated at the electrode, hydrogen (H_2) or oxygen (O_2), depends on polarity. Positive or anodal electrodes generate oxygen, while negative or cathodal electrodes generate hydrogen. The volume of gas generated, regardless of polarity, is trivial but is sufficient to serve as a catalyst for a series of events leading to shock-wave generation.
Top panel. As current (I) is being delivered to the electrode, enough gas is generated to result in an increased impedance (Z) to current flow by insulating the electrode from the surrounding blood. *Middle panel.* Although there is a rise in impedance, current continues to be delivered to the electrode because of the inertia inherent in the type of electric pulse produced by the Physio-Control inductor driven capacitor discharge. As a result, the continued current to the bubble-insulated catheter tip results in a voltage gradient across the bubble, between the catheter electrode and the blood. The resultant electric field is of such a magnitude that the bubble gas can be transformed into a plasma. The plasma then becomes the immediate precursor to arcing (bottom panel). Once a plasma forms, arcing follows as an electron (ē) avalanche from the catheter tip to the bubble surface (in the case of a cathodal electrode). The arc, in turn, produces a large, rapid temperature (T) rise that results in a high velocity bubble expansion and generation of the shock wave. These high-pressure shock waves, in turn, lead to gas generation far in excess to the quantities of gas expected from electrolysis alone. The underlying mechanism is believed to be extrusion of dissolved air in the ambient blood by the high pressure wave [10].

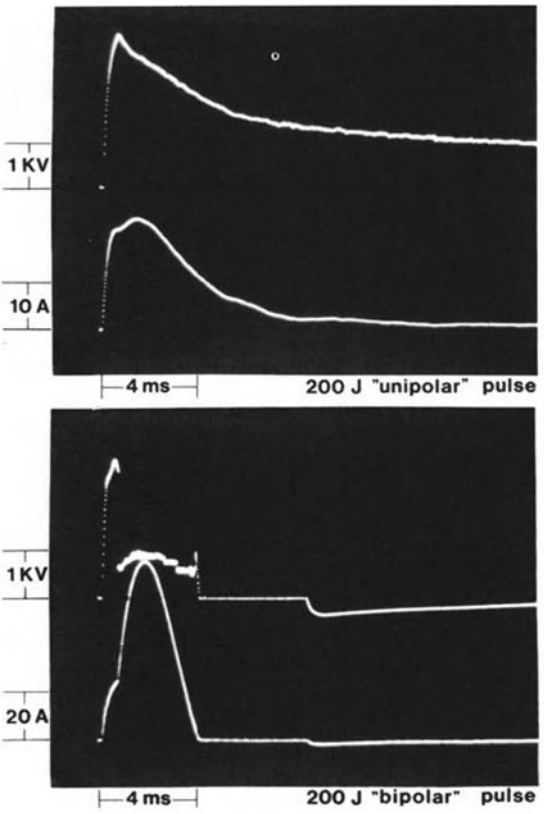

Figure 4–8. Representative examples of the voltage and current waveforms obtained for a unipolar (dog 10, table 4–3) (upper panel) and a bipolar (dog 15, table 4–3) (lower panel) discharge. The voltage waveform is displayed above the current waveform. The defibrillator is set at 200 J for either configuration. The unipolar pulse results in a peak voltage of 3.3 kV, a peak current of 24 A, and a delivered energy of 249 J. The bipolar pulse results in a peak voltage of 3.0 kV, a peak current of 75 A, and a delivered energy of 174 J. Note that the upstroke of the voltage waveforms is similar for both electrode configurations until a break in the curves occurs. It is believed that at this point of the discharge a bubble of electrically nonconductive gas envelops and insulates the electrode, thereby resulting in a sudden rise in impedance to current flow (see figure 4–7). The voltage, on the other hand, continues to rise, triggering an electron avalanche, which eventually transforms the insulating gas into an ionized conductive gas. Given the presence of a conductive medium, current flow can be re-established, resulting in a spark. The spark, in turn, results in large pressure surge (see figure 4–13), thus explaining the coronary sinus elastica rupture observed in figures 4–4, 4–11, and 4–12. Thereafter, the waveforms smoothly and slowly decline. In the case of the unipolar pulse, this slow decline probably reflects high tissue resistance to current flow. In the case of the bipolar pulse, the voltage drops dramatically following the arc, associated with rising current, consistent with a very low resistance to current flow between two electrodes situated in blood only 15 mm apart. The abrupt cessation of current flow observed with the bipolar pulse after approximately 4 ms into the waveform is automatically determined by a mechanical relay switch built into the defibrillator. This relay switch is subject to some bounce, allowing for some current to flow again briefly. (Reprinted with permission of the American Heart Association, Coltorti, et al. *Circulation* 73: 1321, 1986.)

induced by extracardiac countershocks [25, 27, 28]. In such experiments, barotrauma could not possibly be operative. Our study did not allow us to evaluate sequential ultrastructural changes of the kind seen from electric injury, but the observation in our study of areas of macrophage infiltration with giant cell formation is in keeping with those earlier transthoracic/epicardial defibrillation studies [29, 30] and with previous observations made in dogs undergoing transvenous ablation of the AV node [31]. Nevertheless, all these changes could merely represent a general pattern of response of the myocardial cell to injury [32], rather than being specific for electric injury. Therefore, these findings seem unable to clarify the mechanism by which endocavitary discharges produce their effects. Consequently, we attempted to resolve the question about barotrauma versus electrical tissue injury by performing a comparative study between unipolar and bipolar discharges within the CS. By varying the electrode configuration, we expected to determine whether there was any directionality to the amount of tissue injury by virtue of changes in the pattern of current flow and to determine whether there would be any difference in barotraumatic injury.

Unipolar versus bipolar discharges within the coronary sinus: The role of shock waves and electricity in tissue injury

Twenty dogs were randomly divided into two groups of ten dogs each. Under fluoroscopic guidance, quadripolar electrode catheters were positioned in the heart for performance of baseline electrophysiologic studies. A Medtronic 6992A lead was inserted through the jugular vein and positioned in the CS as the catheter receiving the defibrillator pulse. This catheter has high dielectric strength (greater than 5000 volts) and is capable of containing high energy pulses unlike the standard pacing and recording catheters we initially used [12, 33]. Prior to stimulation studies, impulse formation and conduction in the atrium and in the ventricle were studied using the same technique described earlier.

Methods of energy delivery and quantification

When the proximaly ring electrode was at the ostium of the CS, the standard stainless steel stylets were inserted into the leads to minimize line resistance (70 ms without, 4 ms with stylet). A single stylet was passed to the proximaly ring electrode if a unipolar discharge was administered. Two stylets, each for either electrode, were inserted if a bipolar discharge was administered. A single damped sine-wave pulse (200 joule energy setting) was discharged synchronously with the QRS from a Physio-Control Life Pack 6A defibrillator. For unipolar discharges, the proximal ring electrode was the anode and a disc electrode, 3.5 cm in diameter, positioned over the anterior chest fluoroscopically opposite the anode, served as the cathode (figure 4–9A). For bipolar discharges, the proximal ring electrode served as the anode and the distal ring electrode served as the cathode, (figure 4–9B). The total energy

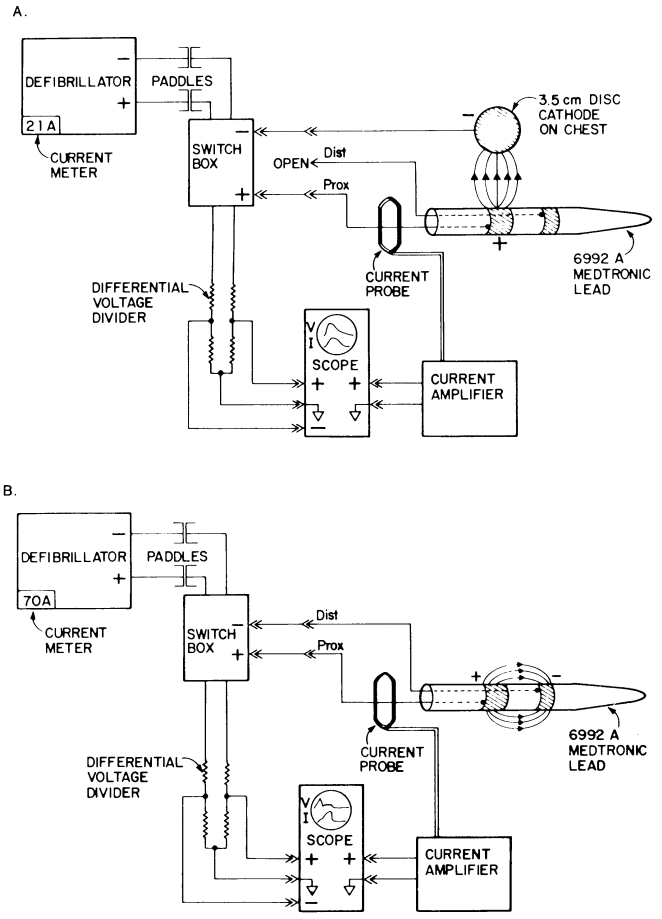

Figure 4–9. Schema for catheter mediated electric ablation using a unipolar (panel A) or a bipolar (panel B) electrode configuration. The proximal electrode of a Medtronic 6992A lead, positioned at the coronary sinus orifice, served as the anode (positive pole) for either configuration. In the case of the unipolar configuration, the cathode (negative pole) was a 3.5 cm diameter disc electrode positioned over the anterior chest fluoroscopically opposite the anode. In the case of a bipolar configuration, the cathode was the distal electrode of the Medtronic lead. A damped sine-wave pulse was discharged from a defibrillator (set at 200 joules) to the electrodes by means of a switch box. Current (I) and voltage (V) waveforms were recorded during delivery of the electric pulse by means of a current probe and a voltage divider connected to an oscilloscope. A current-sensing transformer built into the defibrillator provided an additional reading of the peak delivered current. (Reprinted with permission of the American Heart Association, Coltorti, et al. *Circulation* 73: 1321, 1986.)

delivered was calculated by integrating the voltage and the current waveforms with a computerized digitizer. After the electric discharge, the animals underwent the electrophysiologic evaluation described earlier prior to sacrifice and anatomic evaluation.

Electrocardiographic and electrophysiologic findings

ECG and electrophysiologic findings are summarized in table 4–3. No significant changes in AV conduction or induced atrial or ventricular arrhythmias were found from baseline findings. In general, there were no differences compared to our earlier study regarding impulse formation and conduction. However, there was one electrophysiologic finding that differed in the two groups. At 24 hours, eight of the nine surviving dogs in the unipolar group transiently exhibited an accelerated idioventricular rhythm with a QRS morphology, consistent with origin from the posterior ventricular septum. In contrast, only in one dog (# 15) of the eight surviving in the bipolar group, was this rhythm observed at 24-hour electrocardiograpic observation. No further episodes of spontaneous atrial or ventricular arrhythmias were observed in subsequent electrocardiographic observations. This finding suggests that perturbations in impulse formation of the basilar ventricular myocardium were more likely following unipolar pulses.

Anatomic findings

Anatomic changes are summarized in table 4–4. Two dogs in the bipolar group (dogs 13 and 19) and one in the unipolar group (dog 8), developed hemodynamic deterioration 10–20 minutes after the discharge and subsequently died within three hours (dog 13) and 12 hours (dogs 8 and 19) of pericardial tamponade. Perforation of the CS at the level of the crux of the heart associated with a large, fresh thrombus that partly occupied the lumen of the CS was demonstrated in each of the three dogs. Another animal (dog 5) showed a marked drop in arterial pressure ten minutes after receiving a unipolar pulse that spontaneously resolved within one hour. This dog had an organized thrombus on the epicardial aspect of the CS, consistent with a healed rupture of the vessel. The remainder of the dogs did not suffer any complications. No sudden death was observed during the follow-up period. Gross inspection of the epicardial aspect of the heart was remarkable in the three dogs that had pericardial tamponade. A clot was found to envelop the base and the diaphragmatic surface of the heart. A large subepicardial ecchymotic area extended from the crux of the heart for several centimeters over the left AV groove. The surrounding myocardium was congested and had enlarged venous collaterals in the two animals that survived for a longer period. The CS showed a sharply delineated tear about 5 mm–7 mm long with irregular margins that were not burned. Viewed from the endocardial aspect, the tear started between 3 mm and 10 mm within the ostium of the CS. In the remainder of the dogs, gross examination of the epicardial aspect

Table 4–3. Electrophysiologic findings before and after a 200 joule defibrillator pulse

Dogs 1–10 unipolar; #22–20 bipolar (numbers are expressed in milliseconds)

Dog #	PA b	PA a	AH b	AH a	HV b	HV a	1:1 AV Cond b	1:1 AV Cond a	AVN ERP b	AVN ERP a	AVN FRP b	AVN FRP a	RA ERP b	RA ERP a	RA FRP b	RA FRP a	A Fib b	A Fib a	VAR b	VAR a
1	30	35	50	45	42	42	200	210	140	160	240	240	140	160	180	190	NSu	NSu	No	No
2	25	32	50	42	38	35	270	210	250	200	360	270	130	140	200	180	NSu	NSu	No	No
3	28	22	72	84	45	40	320	260	170	210	360	340	170	150	280	160	NSu	NSu	No	No
4	48	38	45	46	32	32	250	260	130	120	330	280	120	110	180	180	NSu	NSu	No	No
5	25	28	60	50	35	33	200	240	120	230	280	300	120	110	180	170	NSu	NSu	NSuVT	No
6	40	40	46	56	32	40	230	220	150	150	280	290	150	150	190	190	NSu	NSu	No	No
7	38	38	55	68	35	38	230	300	160	250	290	350	150	160	180	250	NSu	NSu	VF	No
9	52	32	42	40	42	40	230	180	150	140	260	210	150	140	190	170	Su	Su	No	No
10	38	32	46	53	40	38	210	180	160	170	250	250	160	170	200	200	NSu	NSu	No	No
mean	36	33	52	54	38	38	238	229	159	181	294	281	143	143	198	188				
± SD	± 10	± 6	± 9	± 14	± 5	± 3	± 38	± 40	± 38	±44	± 45	± 45	± 17	± 21	± 32	± 26				
	p=NS		p=NS		p=NS		p=NS		p=NS		p=NS		p=NS		p=NS					
11	48	30	120	73	42	40	500	290	430	280	520	330	120	110	200	190	NSu	NSu	No	No
12	35	42	52	45	38	32	230	220	180	120	290	290	120	120	180	180	NSu	NSu	No	No
14	38	30	52	50	40	35	260	200	120	150	290	260	120	150	190	190	NSu	NSu	NsuVT	NsuVT
15	36	35	68	65	40	40	260	220	120	140	280	260	120	140	180	170	NSu	NSu	No	No
16	32	32	53	42	35	35	260	260	230	210	340	340	130	140	190	210	NSu	NSu	No	No
17	32	30	50	55	35	37	230	270	140	140	290	290	140	140	200	200	NSu	NSu	No	No
18	35	42	50	55	42	40	240	260	140	130	250	270	140	130	200	170	Su	Su	VF	VF
20	35	40	50	52	30	32	210	240	110	120	240	270	110	120	160	170	Su	Su	No	No
mean	36	35	62	55	38	36	273	245	190	161	313	289	125	131	188	185				
± SD	± 5	± 5	± 24	± 10	± 4	± 3	± 93	± 30	± 124	± 56	± 89	± 31	± 11	± 14	± 14	± 15				
	p=NS		p=NS		p=NS		p=NS		p=NS		p=NS		p=NS		p=NS					

Abbreviations: a = after; AF = atrial fibrillation; AH = atrio-Hisian interval; AV Cond = atrioventricular conduction; AVN = atrioventricular node; b = before; ERP = effective refractory period; FRP = functional refractory period; HV = His-ventricular interval; NSu = nonsustained; PA = surface P wave to local AVN atrial electrogram interval; RA = right atrium; Su = sustained; VAR = ventricular arrhythmias; VF = ventricular fibrillation.

* Dogs #8, #13, and #19 are missing from the sequence because they died acutely from pericardial tamponade.

Table 4–4. Anatomic changes following a 200 joule defibrillator pulse

Dogs # 1–10 unipolar; 11–20 bipolar

						Coronary sinus injury			Atrial injury		LV injury		
Dog #	Current (A)	Voltage (V)	Delivered energy (J)	Gross rupture	Elastic rupture	Max length (mm)	Extent of circumferential injury (mm)	Max length (mm)	Transmural injury (mm)	Max height (mm)	Max length (mm)	Max depth (mm)	Max width (mm)
1	21	3300	248	No	Yes	39	14	25	15	12	14	4	2
2	15	3500	234	No	Yes	27	15	17	9	14	13	3	5
3	23	3400	241	No	Yes	34	30	22	14	9	18	5	3
4	17	3400	246	No	Yes	21	8	15	5	5	16	3	10
5	13	3600	241	Yes	Yes	30	15	21	10	7	18	3	9
6	20	3400	241	No	Yes	26	9	15	9	11	12	4	9
7	26	3400	311	No	Yes	31	12	29	6	4	9	1	5
8*	23	3200	221	Yes	Yes	27	18	23	20	9	22	4	11
9	23	3200	301	No	Yes	31	12	21	14	9	16	2	4
10	24	3300	249	No	Yes	40	17	23	14	8	21	3	7
mean ± SD	21 ± 4	3370 ± 125	253 ± 29			31 ± 6	15 ± 6	21 ± 4	12 ± 5	9 ± 3	16 ± 4	3 ± 1	7 ± 3
11	66	3100	141	No	Yes	33	16	15	0	4	7	3	4
12	66	3100	131	No	Yes	35	13	26	0	1.5	25	2.5	3
13*	73	3100	145	Yes	Yes	33	13	23	0	11	14	5	3
14	72	3100	139	No	Yes	29	6	14	11	6	4	1	2
15	75	3000	174	No	Yes	32	16	13	0	3	7	2	3
16	75	3000	139	No	Yes	35	5	5	0	2	4	1	3
17	62	3000	168	No	Yes	32	14	15	0	4	6	2	7
18	74	2900	143	No	Yes	31	4	22	0	3	20	2	4
19*	70	3000	109	Yes	Yes	32	15	30	5	15	17	7	4
20	68	2800	153	No	Yes	39	0	27	0	4	24	2	4
mean ± SD	70 ± 4	3010 ± 99	144 ± 18			33 ± 3	10 ± 6	19 ± 8	2 ± 4	5 ± 4	13 ± 8	3 ± 2	4 ± 1
	$p<0.001$	$p<0.001$	$p<0.001$			p=NS	p=NS	p=NS	++p=0.0004	p=NS	p=NS	p=NS	$p<0.02$

* Dogs #8, 13, and 19 died acutely from pericardial tamponade.
++ Fisher's exact test.

of the heart was unremarkable for changes suggestive of hemorrhagic effusion or previous inflammation.

Gross damage to the circumflex coronary artery or changes in the ventricles were not found. Except for the three dogs that died acutely, no sign of congestion secondary to CS thrombosis was seen.

The endocardial aspect of the right atrium, the tricuspid valve, and the AV node area were normal at gross inspection in all animals. The endocardium of the posterior left atrium occasionally showed a brownish discoloration due to hemosiderin deposits. The ostium of the CS was narrowed or occluded by fibrotic tissue in eight of the nine long-term survivors receiving unipolar pulses. In one, the CS was unobstructed. Among the eight long-term survivors receiving bipolar pulses, four showed narrowing or complete occlusion of the CS, up to 1 cm within the orifice, while in the remaining four the CS was patent, although some endocardial thickening was present around the ostium.

Microscopic examination of the sections taken from the AV groove, showed CS injury in all animals, starting from 2 mm before to 10 mm within the os of the CS. In general, in the acute dogs injury consisted of selective myocardial necrosis associated with contraction bands and areas of hemorrhage interspersed between damaged fibers. In the chronic dogs, injury consisted of loss of myocardium, with replacement by fibrous tissue.

In the one dog that had gross CS rupture following a unipolar discharge, the rupture itself consisted of multiple tears toward both the epicardial and the endocardial aspect of the CS, and extended for about 20 mm within the ostium. The communication with the epicardium was limited to a length of 5 mm. In the two dogs that had CS rupture from bipolar pulses, the CS was ruptured on its superior and endocardial aspects for a length of about 15 mm. The communication with the epicardium extended for 7 mm.

Measurements of histologic tissue injury are listed in table 4–4. The most significant finding was that atrial injury was transmural in all ten dogs receiving a unipolar pulse (figure 4–10A, 4–12A), but only in two dogs (dogs 14 and 19, table 4–4) receiving a bipolar pulse (figures 4–10B, 4–12B). Maximum length of total atrial injury (not necessarily transmural) was not significantly different in the two groups. Also, maximum height of atrial injury did not differ significantly. Regardless of injury to the atrial wall, however, injury to the peri-anular myocardium was inconstant and not transmural (figure 4–10). The length of total and circumferential CS injury was not significantly different in the two groups.

Although gross rupture was present only in four dogs, sections stained for demonstration of elastic tissue constantly showed microscopic rupture of the internal elastic membrane of the CS, regardless of electrode configuration (figure 4–11). Segments of the elastica appeared to have been forcefully displaced toward the endocardial aspect of the atrial wall (figure 4–12), suggesting a role for barotrauma in the genesis of this type of injury.

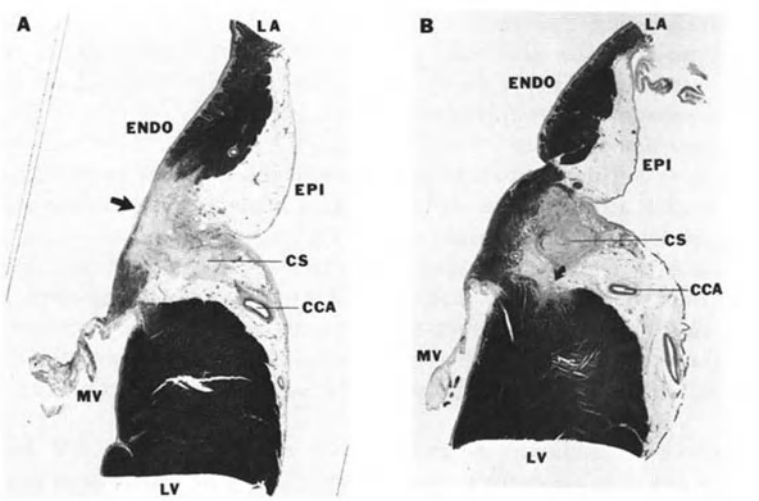

Figure 4–10. Panels A and B are cross sections of the left atrioventricular groove taken at the site of maximum injury and prepared with Gomori's Trichrome stain. Section A is taken 9 mm within the coronary sinus orifice from a dog (#10, table 4–4) that received a unipolar pulse. Section B is taken 12 mm within the coronary sinus orifice from a dog (#12, table 4–4) that received a bipolar pulse. The lumen of the coronary sinus is occluded by an organized thrombus, and the wall of the coronary sinus shows loss of muscle and replacement by circumferential fibrosis in both sections. Fibrosis of the left atrial wall is transmural (arrow, section A) only in the case of the unipolar pulse. Note that neither the unipolar nor the bipolar configuration results in fibrosis adjacent to the annulus of the mitral valve. The left ventricular wall at the level of the coronary sulcus is not injured in the case of the unipolar discharge, while it shows a very limited area of fibrosis in the case of the bipolar discharge (arrow, section B). The circumflex coronary artery is patent, and no coronary artery wall abnormalities are present in either section. (Original magnification X 5.2, for section A; original magnification X 5.7, for section B). CCA = circumflex coronary artery; CS = coronary sinus; ENDO = endocardium; EPI = epicardium; LA = left atrium; LV = left ventricle; MV = mitral valve. (Reprinted with permission of the American Heart Association, Coltorti, et al. *Circulation* 73: 1321, 1986.)

Injury to the left ventricle was limited in all dogs (figure 4–10). There was no statistically significant difference in maximum length or depth of left ventricular injury in the two groups. However, maximum width of left ventricular injury was significantly greater after unipolar than after bipolar discharges. Transmural ventricular injury was present only in one dog (dog 8, unipolar pulse, table 4–4), although limited to a length of 2 mm.

Microscopic examination confirmed the absence of injury to the circumflex coronary artery (figure 4–10).

Energy delivery characteristics

Values for current, voltage, and delivered energy are summarized in table 4–4. Delivery of a pulse at a setting of 200 joules resulted in a peak voltage of

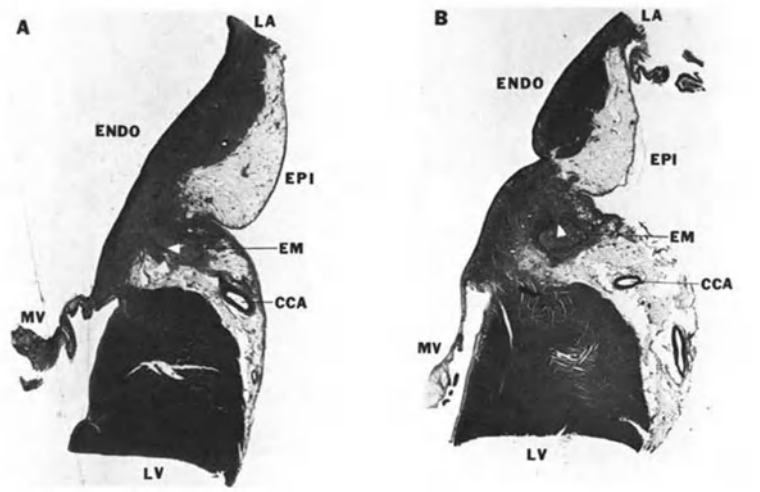

Figure 4–11. The same sections as the ones in figure 4–10 are shown using a Verhoeff-Van Gieson stain for elastic tissue. Section A (unipolar pulse) and section B (bipolar pulse) correspond to sections A and B of figure 4–10. Note that, regardless of electrode configuration, the internal elastic membrane (seen as a thin black line) of the coronary sinus is ruptured and fragmented (arrowheads) on the endocardial aspect of the coronary sinus in both sections. These histologic findings are consistent with a barotraumatic mechanism as the cause of coronary sinus elastica rupture. (Original magnification X 5.2, for section A; original magnification X 5.7, for section B). EM = elastic membrane of the coronary sinus. Other abbreviations are as in figure 4–10. (Reprinted with permission of the American Heart Association, Coltorti, et al. *Circulation* 73: 1321, 1986.)

3370 ± 125 V, a peak current of 21 ± 4 A, and a delivered energy of 253 ± 29 J for the unipolar configuration, as compared with 3010 ± 99 V, 70 ± 4 A, and 144 ± 18 J for the bipolar configuration ($p < 0.001$, for each value). An example of current and voltage waveforms with either electrode configuration is given in figure 4–8. In both cases it can be seen that current and voltage are out of phase (much more so in the case of a bipolar pulse), with voltage peaking earlier than current, consistent with a nonlinear resistance during energy delivery. The upstroke of the curves is similar for both electrode configurations, until a break in the continuity of the curves occurs about one-third of the way through the discharge. At this point of discontinuity in the discharge, gas formation occurs around the electrodes, which leads to arcing (see previous discussion). Thereafter, in the case of a unipolar pulse, the waveforms smoothly and slowly decline, probably reflecting high tissue resistance encountered by current flow. In the case of a bipolar pulse, however, the voltage is seen to drop dramatically, and the current to continue to rise until its peak, consistent with an extremely low resistance to current flow between two electrodes 1.6 cm apart. The abrupt cessation of the pulse after about 4 ms, with some current again flowing shortly thereaf-

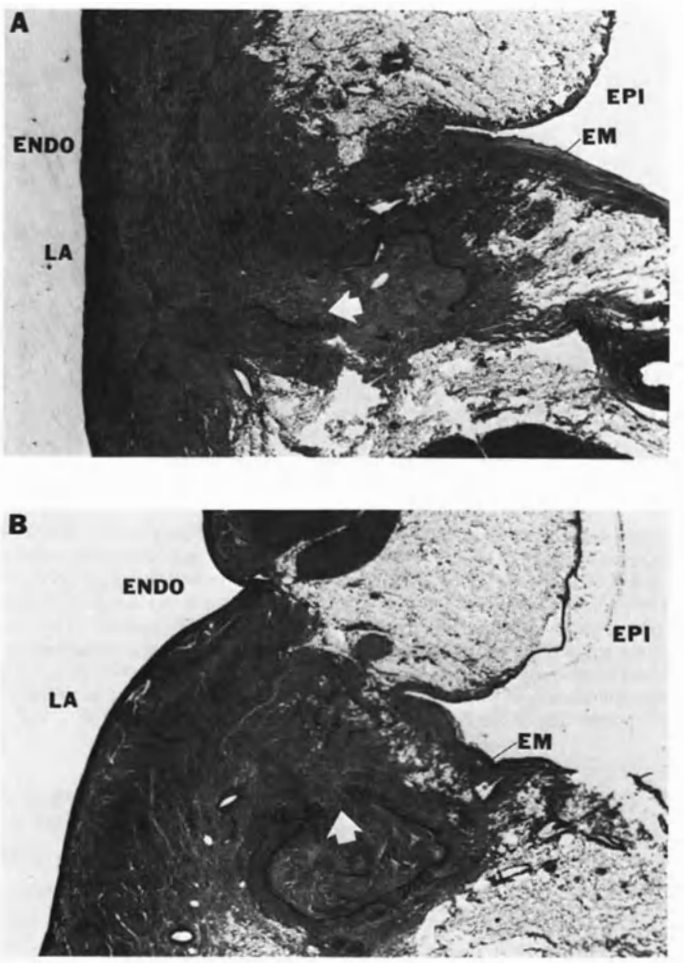

Figure 4–12. These are higher power magnifications of the sections shows in figure 4–11. They show details of the barotraumatic rupture of the coronary sinus elastica (arrows), which is stained as a thin black membrane. Section A is from a dog receiving a unipolar pulse. Section B is from a dog receiving a bipolar pulse. (Verhoeff-Van Gieson: original magnification X 12, for section A; original magnification X 13.8 for section B). Abbreviations are as in figures 4–10 and 4–11. (Reprinted with permission of the American Heart Association, Coltorti, et al. *Circulation* 73: 1321, 1986.)

ter, probably relates to the relay switch built into the defibrillator, which first determines cessation of the pulse and then is subjected to some bounce in the course of rapidly changing resistances as the bubble contracts.

Pressure changes

Peak pressures observed in an in vitro saline preparation for the unipolar pulse were 142 ± 13 atm (108,000 ± 10,000 mm Hg) as compared with 137 ± 8 atm (103,900 ± 6,300 mm Hg) for the bipolar pulse (p = NS). Figure 4–13 shows pressure recordings for each electrode configuration.

CONCLUSIONS REGARDING ANODE-CATHODE CONFIGURATION AND TYPE OF INJURY

The anatomic results of the present study show that electrode configuration is an important factor in determining the extent and the distribution of injury. This is demonstrated by the inconsistency of transmural atrial injury obtained with a bipolar configuration, as compared to the constancy of transmural atrial injury after delivery of unipolar pulses, despite evidence of similar barotraumatic injury.

The extent of tissue injury observed in the part of this study using unipolar discharges confirms the results obtained in the earlier study [9]. Unlike the previous study, not only was intramural rupture of the CS elastica present in all animals, irrespective of electrode configuration, but also gross epicardial rupture occurred in two dogs of each group. It is conceivable that the higher current densities (and therefore larger shock waves) achieved with the use of a single anodal electrode compared to the use of two electrodes coupled in parallel, as used in the previous study, are responsible for such an occurrence. In either the bipolar or unipolar case, barotraumatic rupture of the CS (grossly or histologically) occurred equally. However, unipolar pulses constantly produced atrial transmural injury only noted in two of the ten dogs receiving bipolar discharges. This last observation, in particular, helps substantiate that barotrauma is more of a deleterious phenomenon that does not result in useful tissue injury. This conclusion is confirmed also by the observation that, with either electrode configuration, in vitro pressure recordings were of similar magnitude. From this observation we can conclude that electric factors must be responsible for the useful tissue injury.

CAN TACHYCARDIA DUE TO ACCESSORY PATHWAYS BE RELIABLY PREVENTED?

It is important to emphasize, with respect to ablation techniques, that accessory AV pathways usually skirt the annulus fibrosus in close approximation to it [34–36]. This information pertains to the expectations we might have from catheter mediated ablation techniques. This is an important consideration given that in both our dogs and in previous studies in man [13] the CS occupies a relatively high position in the pyramidal space and left free wall

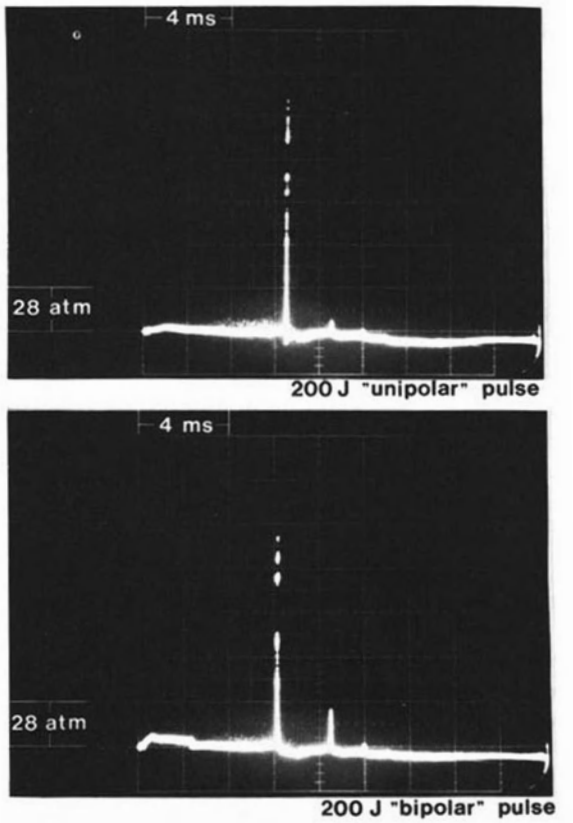

Figure 4–13. Pressure tracings obtained in a saline bath using a piezoelectric transducer placed 2 cm from the proximal ring electrode of a Medtronic 6992A lead. A defibrillator pulse was discharged at a setting of 200 joules in a unipolar fashion (proximal electrode as the anode to a disc electrode 10 cm away serving as the cathode) (upper panel) or in a bipolar fashion (proximal electrode as the anode to distal electrode 1.5 cm away as the cathode) (lower panel). Pressure rises of comparable magnitudes are recorded with either electrode configuration, measuring 150 atm (114,000 mm Hg) for the unipolar pulse and 132 atm (100 mm Hg, 200 mm Hg) for the bipolar pulse. While these marked pressure surges can explain the barotraumatic injury of the coronary sinus observed with either electrode configuration, the similarity in pressure rises would not account for the difference in transmural atrial injury seen between unipolar and bipolar pulses. This suggests that barotrauma is not the only mechanism of injury and that differences in distribution of electric factors play an important role in determining the extent of tissue injury seen with the two electrode configurations. (Reprinted with permission of the American Heart Association, Coltorti, el al. *Circulation* 73: 1321, 1986.)

with respect to the mitral annulus. Our studies show that delivery of high-energy defibrillator pulses in proximity to the CS orifice principally produces damage to the wall of the CS and to the wall of the left atrium *above* the AV groove but not at the annulus proper. (This statement applies only for unipolar pulses, as bipolar pulses are ineffectual). Accessory pathways, therefore, are unlikely to be damaged directly using the technique we describe for unipolar discharges. Nevertheless, an area of delay could be created above the accessory pathway such that the accessory connection would become functionally silent. Impulses entering the accessory pathway antegradely or exiting it retrogradely may be blocked. At least in theory, this kind of injury may be all that is necessary or indeed safely possible from a clinical perspective using this particular technique.

Another consideration in whether catheter mediated electric pulses will be effective is the understanding that accessory pathways may extend over a zone of myocardium larger than simply the punctate site which might be expected from catheter mapping. Early surgical experience with posterior septal and left-sided accessory pathways seems to confirm the impression that accessory AV fibers are often not discrete and can occur over several centimeters [1]. As a consequence, an injury able to prevent accessory pathway conduction ideally should involve an area wider than the precise area of earliest activation. It may be that a single unipolar pulse at one site is inadequate if entry into or exit from the accessory pathway is to be avoided.

A final consideration is the question of safety and controlability given the evidence of barotrauma. Changes in the procedure, therefore, will be necessary for safe application. These effects will predominantly focus on elimination of shock-wave generation. We have begun work on this problem and have already demonstrated that modulation of the current waveform can eliminate barotrauma [37–41]. The technique is not, however, ready for human application. At this time, successful catheter modification via the CS of tachycardia using posterior septal accessory pathways may depend on the ability of transmural atrial injury above the annulus proper to effectively block depolarization wavefronts from entering or exiting the accessory pathway.

CONCLUSIONS

Catheter mediated electric ablation techniques using damped sinusoidal defibrillator pulses applied to the CS orifice result in electrical as well as barotraumatic tissue injury, with the barotraumatic component being more deleterious than helpful. More useful tissue injury occurs with a unipolar electrode configuration than with a bipolar configuration. However, the deleterious barotraumatic effects of the technique are present with either method.

Histologic evidence suggests that direct interruption of the accessory AV

pathway, even with the unipolar technique, is unlikely because of the anatomic relationship of the CS with respect to the mitral annulus. Left atrial tissue above but not at the AV groove is affected. We believe, however, that such an injury can result in a functional interruption of the activation wavefront during tachycardia, utilizing an accessory pathway by preventing entry to or exit from the accessory pathway. Direct interruption of the accessory pathway itself probably will not occur.

Coronary artery injury adjacent to the site of CS discharge is a problem that has not been resolved. Although catheter mediated defibrillator pulses delivered to the proximal coronary sinus may be effective for therapy of arrhythmias associated with accessory pathways, such a technique is not recommended for patients who have accessory pathways adjacent to coronary arteries. Both short-term and long-term effects on coronary artery blood flow are open to question. Therefore, if the technique is to be used in man, coronary arteriography is necessary to correlate accessory pathway location with coronary anatomy. Significant coronary arteries within 2 cm probably should serve as a relative contraindication to catheter mediated ablation.

In general, we can state that the possibility of barotraumatic rupture and limitations in the source of electric energy, in the type of electrodes used, and in the need to avoid coronary artery injury should be carefully weighed before applying this technique in humans.

REFERENCES

1. Gallagher JJ, Sealy WC, Cox JL, German LD, Kasell JH, Bardy GH, Packer DL: Results of surgery for preexcitation caused by accessory atrioventricular pathways in 267 consecutive cases. In: *Tachycardias: Mechanisms, Diagnosis, Treatment.* ME Josephson, HJJ Wellens, ed. Philadelphia Lea & Febiger, p. 259, 1984.
2. Critelli G, Monda V, Perticone F, Coltorti F, Scherillo M, Condorelli M: Closed chest ablation of accessory pathways. Experimental model and successful application in a patient with incessant supraventricular tachycardia. *G Ital Cardiol* 14/I: 181, 1984.
3. Morady F, Scheinman MM: Transvenous catheter ablation of a postero-septal accessory pathway in a patient with the Wolff-Parkinson-White syndrome. *N Engl J Med* 310: 705, 1984.
4. Fisher JD, Brodman R, Kim SG, Matos JA, Brodman E, Wallerson D, Waspe LE: Attempted nonsurgical electrical ablation of accessory pathways via the coronary sinus in the Wolff-Parkinson-White syndrome. *JACC* 4: 685, 1984.
5. Bardy GH, Poole JE, Coltorti F, Ivey TD, Block TA, Greene HL: Catheter ablation of a concealed postero-septal accessory pathway. *Am J Cardiol* 54: 1366, 1984.
6. Ward DE, Camm JA: Treatment of tachycardias associated with the Wolff-Parkinson-White syndrome by transvenous electrical ablation of accessory pathways. *Br Heart J* 53: 64, 1985.
7. Nathan AW, Davies DW, Creamer JE, Camm J: Successful catheter ablation of abnormal atrioventricular pathways in man. In: *Cardiac Pacing: Electrophysiology, Tachyarrhythmias.* F Perez-Gomez, ed. Madrid: Editorial Group, p. 1588, 1985.
8. Morady F, Scheinman MM, Winston SA, Di Carlo LA Jr., Davis JC, Griffin JC, Ruder M, Abbott JA, Eldar M: Efficacy and safety of transcatheter ablation of posteroseptal accessory pathways. *Circulation* 72: 170, 1985.
9. Coltorti F, Bardy GH, Reichenbach D, Greene HL, Thomas B, Breazeale DG, Alferness C, Ivey TD: Catheter mediated electrical ablation of the posterior ventricular septum via the coronary sinus: Electrophysiologic and histologic observations in dogs. *Circulation* 72: 612–622, 1985.

10. Bardy GH, Coltorti F, Ivey TD, Alferness C, Rackson M, Hansen K, Stewart R, Greene HL: Some factors affecting bubble formation during catheter mediated electrical pulses. *Circulation* 73: 525–538, 1986.
11. Coltorti F, Bardy GH, Reichenbach D, Greene HL, Thomas R, Breazeale DG, Ivey TD: Electrophysiologic and histologic observations following catheter-mediated defibrillator pulses at the coronary sinus orifice in dogs: Effects of varying electrode configuration. *Circulation* 73: 1321–1333, 1986.
12. Bardy GH, Coltorti F, Ivey TD, Yerkovich D, Greene HL: Effect of damped sine-wave shocks on catheter dielectric strength. *Am J Cardiol* 56: 769–772, 1985.
13. MacAlpine WA: *Heart and Coronary Arteries*. Berlin: Springer-Verlag, pp. 50, 63, 1975.
14. Früngel FBA: *High speed Pulse Technology*, Vol 1. New York: Academic Press, pp. 476–483, 1965.
15. Tidd MJ, Webster J, Cameron Wright H, Harrison IR: Mode of action of a surgical electronic lithoclast — high speed pressure, cinematographic and Schlieren recordings following an ultrashort underwater electronic discharge. *Biomed Eng* (London) II: 5, 1976.
16. Cobine JD: *Gaseous Conductors. Theory and Engineering Applications*. New York: McGraw-Hill Book Co, pp. 143–204, 1941.
17. Cobine JD: *Gaseous Conductors. Theory and Engineering Applications*. New York: McGraw-Hill Book Co, pp. 290–293, 1941.
18. Brown SC: *Basic Data of Plasma Physics*. New York: John Wiley & Sons, pp. 270–271, 1959.
19. Brown SC: *Basic Data of Plasma Physics*. New York: John Wiley & Sons, pp. 319, 1959
20. Bradley JN: *Shock Waves in Chemistry and Physics*. London: Butler and Tanner Ltd, pp. 1–2, 1962.
21. Bell CE, Landt JA: Laser-induced high pressure shock waves in water. *Appl Physics Lett* 10: 46, 1967.
22. Martynenko OG, Stolovich NN, Rudin GI, Levchenko SA: Shock waves in water induced by focused laser radiation. In: *Shock Waves, Explosions, and Detonations. Progress in Astronautics and Aeronautics*. JR Bowen, N Manson, AK Oppenheim, RI Soloukhin, ed. New York: AIAA, vol 87, pp. 64–70, 1981.
23. Dahl CF, Ewy GA, Warner ED, Thomas ED: Myocardial necrosis from direct current discharge: Effect of paddle electrode size and time interval between discharges. *Circulation* 50: 956, 1974.
24. Doherty PW, McLaughin PR, Billingham M, Kernoff R, Goris ML, Harrison DC: Cardiac damage produced by direct current countershocks applied to the heart. *Am J Cardiol* 43: 225, 1979.
25. Anderson HN, Reichenbach D, Steinmetz GP, Merendino KA: An evaluation and comparison of effects of alternating and direct current electrical discharges on canine hearts. *Ann Surg* 160: 251, 1964.
26. Ewy GA, Taren D, Bangert J, McClung S, Hellman DA: Comparison of myocardial damage from defibrillator discharges at various dosages. *Med Instrum* 14: 9, 1980.
27. Van Vleet JF, Tacker WA Jr, Geddes LA, Ferrans VJ: Sequential cardiac morphologic alterations induced in dogs by single transthoracic damped sinusoidal waveform defibrillator shocks. *Am J Vet Res* 39: 271, 1978.
28. Van Vleet JF, Tacker WA Jr, Geddes LA, Ferrans VJ: Sequential ultrastructural alterations in ventricular myocardium of dogs given large single transthoracic damped sinusoidal waveform defibrillator shocks. *Am J Vet Res* 41: 493, 1980.
29. Barker-Voelz MA, Van Vleet JF, Tacker WA Jr, Bourland JD, Geddes LA, Schollmeyer MP: Alterations induced by a single defibrillating shock applied through a chronically implanted catheter electrode. *J Electrocardiol* 16: 167, 1983.
30. Lerman BB, Weiss JL, Bulkley BH, Becker LC, Weisfeldt ML: Myocardial injury and induction of arrhythmia by direct current shock delivered via endocardial catheters in dogs. *Circulation* 69: 1006, 1984.
31. Bardy GH, Ideker RE, Kasell J, Worley SJ, Smith WM, German LD, Gallagher JJ: Transvenous ablation of the atrioventricular conduction system in dogs: Electrophysiologic and histologic observations. *Am J Cardiol* 51: 1775, 1983.
32. Reichenbach D, Benditt EP: Myofibrillar degeneration: A response of the myocardial cell to injury. *Arch Pathol Lab Med* 85: 189, 1968.
33. Fisher JD, Brodman R, Johnston DR, Waspe LE, Kim SG, Matos JA, Scavin G: Nonsurgi-

cal electrical ablation of tachycardias: Importance of prior in vitro testing of catheters. *PACE* 7: 74, 1984.
34. Lunel AAV: Significance of annulus fibrosus of heart in relation to AV conduction and ventricular activation in cases of Wolff-Parkinson-White syndrome. *Br Heart J* 34: 1263–1271, 1972.
35. Becker AE, Anderson RH, Durrer D, Wellens HJJ: The anatomical substrates of Wolff-Parkinson-White syndrome. A clinicopathologic correlation in 7 patients. *Circulation* 57: 870–879, 1978.
36. Klein GJ, Hackel DB, Gallagher JJ: Anatomic substrate of impaired antegrade conduction over an accessory atrioventricular pathway in the Wolff-Parkinson-White syndrome. *Circulation* 61: 1249–1256, 1980.
37. Bardy GH, Coltorti F, Rackson MM, Hansen K, Greene HL, Ivey TD. Current waveform modulation to avoid plasma-arcing and barotrauma with catheter mediated electric discharges. American Heart Association. Washington D.C., November 11–14, 1985.
38. Bardy GH, Coltorti F, Rackson MM, Hansen K, Greene HL, Ivey TD. Multiple vs single pulses to avoid voltage breakdown and shock-wave generation with catheter mediated electrical pulses. American College of Cardiology. Atlanta, GA. March 9–13, 1986.
39. Bardy GH, Coltorti F, Rackson MM, Hansen K, Greene HL, Ivey TD. Catheter mediated electrical ablation: The relation between current and pulse width on voltage breakdown and shock-wave generation. American College of Cardiology. Atlanta, GA March 9–13, 1986.
40. Bardy GH, Coltorti F, Stewart R, Hansen K, Greene HL, Ivey TD: The role of duty factor in preventing voltage breakdown during delivery of modulated electric pulses to a catheter. North American Society of Pacing and Electrophysiology. New Orleans, LA May 15–17, 1986.
41. Bardy GH, Coltorti, Greene HL, Ivey TD: Catheter mediated electrical ablation: The relation between current and pulse width on voltage breakdown and shock-wave generation. Cardiostim 86, Monaco June 19–21, 1986.

5. THE EFFECTS OF HIGH-ENERGY DC SHOCKS DELIVERED TO VENTRICULAR MYOCARDIUM

GUY FONTAINE

Endocardial catheter fulguration is a new method for the treatment of cardiac arrhythmias which has been used to interrupt the AV conduction system, to prevent rapid ventricular rates originating in the atrium. It could also be applied to atrial or ventricular myocardium to directly modify the arrhythmogenic substrate. Clinical successes obtained with this technique have spurred its clinical applications before systematic studies of the equipment [1–4], physics [5–13], and its biological consequences have been sufficiently investigated in the animal laboratory [14–25]. The present work reports the canine experiments performed in the Laboratoire de Chirurgie Experimentale of Pr. C. Cabrol's group at Hospitalo-Universitaire Pitie-Salpetriere in Paris between April 1982 and March 1984 [18].

VENTRICULAR MYOCARDIAL FULGURATION

At the beginning of our studies, electrical shocks were delivered on the epicardium because this method allowed for very precise localization of the shock site [26]. The first step was to correlate the histological effects with the delivered energies.

Supported in part by grants from Centre de Recherche sur les Maladies Cardiovasculaires de l'Association Claude Bernard — Paris and The ODAM Company, Wissembourg, France.

Epicardial fulguration

Method

Mongrel dogs with a mean weight of 25 kg were anesthetized with 30 mg/kg of penthotal and ventilated. Curare-type drugs were injected as needed by the anesthesiologist. The arterial blood pressure was monitored by a catheter inserted in the radial artery. The electrocardiogram was monitored continuously using three frontal plane leads. The ECG and the arterial blood pressure signals were recorded on an EMI SE 7000 magnetic tape recorder. The animals were kept at the appropriate temperature by a mattress with circulating warm water, which also provides proper insulation from the operating table.

The core temperature was monitored by a rectal probe. In some experiments, the blood pH was measured. A right-sided thoracotomy was performed and the heart exposed using a pericardial cradle. The animals were sacrificed at the end of the experiment. The anatomical samples were analyzed by direct view and pictures taken from the most affected areas. Tissue samples were processed using standard histological techniques.

Electrical shocks ranging from 10 joules to 80 joules were provided by a modified defibrillator (ODAM, Wissembourg France). This defibrillator results in a peak voltage of approximately 2 kV, impulse duration of 6 ms and rise-time of 2 ms.

Generally, several shocks were delivered in most of the cases through a USCI bipolar catheter. The distal pole of the catheter was used as the anode and was connected to a large metallic place coated with a conductive jelly positioned under the left side of the animal. Better manual control of the catheter position was achieved by surrounding the catheter with a tube of plastic.

Shocks were delivered near the base of the heart, the strongest being delivered at the level of the left ventricle, and less intense shocks were delivered to the infundibular area.

Results

GROSS PATHOLOGIC ALTERATIONS. With a shock of 80 joules, a transmural perforation of the myocardium was observed (figure 5–1). The epicardial surface showed an area of white coagulation approximately one centimeter in diameter in the middle of which was a hole which was approximatively the size of the distal electrode. Blood spurted out of this orifice during each systole. However, hemorrhage could be easily controlled by a single stitch. With a shock of 50 joules, incomplete perforation was obtained and there was no hemorrhage. For energies of 30 joules to 40 joules, it was again possible to observe a modified whitish area at the epicardial surface, surrounded by a zone which was darker and which was approximately 7 mm in diameter. The area located beneath the active electrode showed vaporization of the subepi-

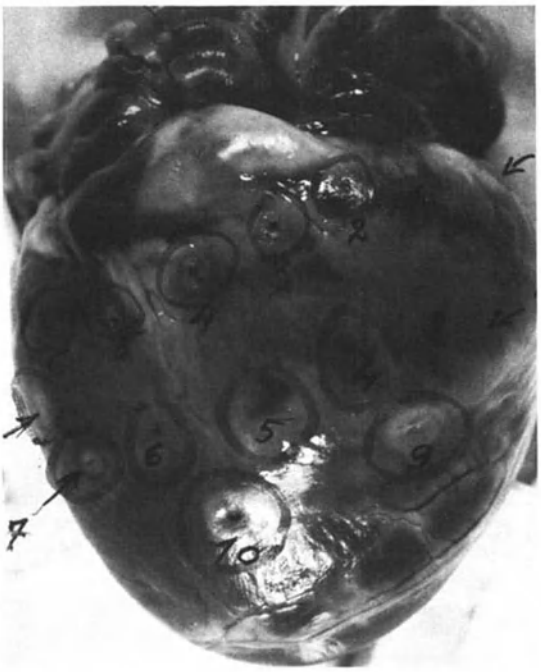

Figure 5–1. Shocks delivered with a USCI catheter on the left and right ventricle. The energy was delivered close to the base of the heart. With shocks of 50 joules and 80 joules, perforation of the myocardium was observed. (The second line indicates the effect on myocardium performed by another physical agent).

cardial layers and coagulation of tissue in close vicinity. With a 20 joule shock, it was still possible to observe a small modification of the epicardial surface. With a shock of 10 joules, which is not synchronized on the QRS complex, ventricular fibrillation was induced, however, defibrillation was easily achieved. These shocks of small magnitude did not leave any visible changes on the epicardial surface.

HISTOLOGICAL ALTERATIONS. For the weakest shocks (i.e., 10 joules), only small islands of "prenecrosis" were found. This term is used to indicate that only a certain percentage of cells are damaged, as shown by their acidophilic behavior. For these shocks acidophilic cells with pycnotic nuclei were observed in approximately 40% of sample cells. For a stronger shock (20 joules), the pattern was quite similar to the previous one, but in addition, areas close to the fulguration electrode may show complete coagulation necrosis. Here, again, the lesions were in the magnitude of 40% of the involved area. These lesions were less and less marked as tissue was examined remote from the fulgurating electrode. With shocks of 30 joules to 40 joules,

Figure 5–2. Almost complete perforation of the myocardium produced by a shock of 50 joules. The arrow points to the area where the epicardial electrode was located.

a definite pattern of acidophilic necrosis with loss of nuclei was observed. The pattern of injury appeared more homogeneous. In addition, the epicardium showed a pattern of coagulation necrosis of about 50% of cardiomyocytes associated with 10% of transmural prenecrosis lesion. With shocks of 50 joules, the area of necrosis was more extensive with a larger acidophilic area, and some areas showed borderline myocardial perforation. In about 50% of the sample, it was possible to see areas of prenecrosis and transmural injury. With shocks of 80 joules, in addition to the previous abnormalities, there was a large hemorrhagic zone, surrounding the transmural perforation (figure 5–2). The necrotic surface was now in the range of 60% with a prenecrotic area of 30%. Here, again, a transmural pattern was observed.

In conclusion, unipolar shocks greater than 50 joules delivered with a USCI catheter will perforate the left ventricular myocardium. However, this experiment was considered somewhat artificial because of the absence of a conductive medium around the electrode. Therefore, the shocks were delivered the same way but with the active electrode immersed in saline.

Epicardial fulguration with immersed electrode

Method

A new series of epicardial shocks ranging from 30 joules to 200 joules were delivered at the base of the left ventricle in dogs weighing 25 kg. In this study, the shock was delivered through a round stainless steel electrode with outside diameter of 4 mm.

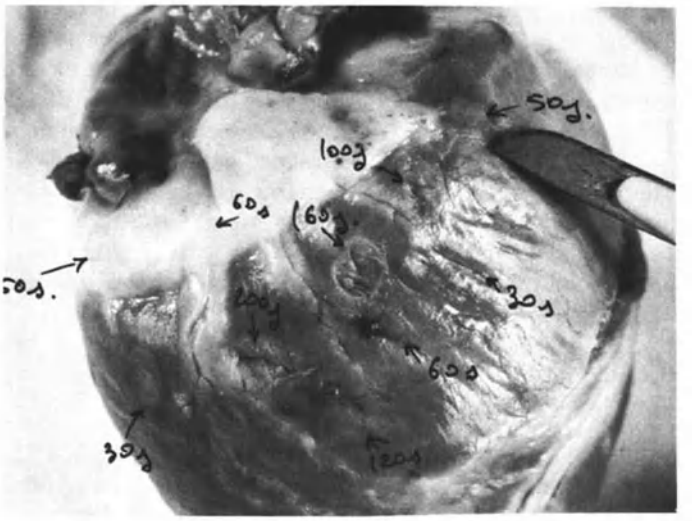

Figure 5–3. Shocks delivered in the pericardial cradle filled with saline using an electrode of 4mm in diameter. Note that even shocks of 200 joules and 160 joules produce less extensive damage without perforation. There is no effect when the shocks are applied on the AV groove.

Results

GROSS PATHOLOGIC ALTERATIONS. With shocks of 30 joules and 50 joules, the macroscopic damages were very localized and showed only an irregular zone of change (figure 5–3). With amplitudes above 50 joules, there was a definite whitish pattern, indicating the position of the electrode, but there was no perforation.

HISTOLOGIC ALTERATIONS. With shocks of 80 joules, areas of acidophilic complete necrosis were observed. The surface involved by this process was in the range of 10%. The surrounding zone consisted of a peripheral prenecrotic pattern in 40% of the cells (with pycnotic nuclei) mixed with cells only partially damaged. The topography of the lesion was typically triangular in form, the base being on the epicardium. With a shock of 100 joules, it was possible to observe more complete acidophilic necrosis than in the previous experiments. The involved surface was now in the range of 15%, associated with 60% of prenecrosis with a transmural orientation extending to the subendocardial layers. Shocks of 160 joules again showed a triangular acidophilic necrotic zone. The surface of the abnormal zone was in the range of 40% and was associated with 50% of prenecrosis.

The distribution showed a transmural pattern. With shocks of 200 joules, the areas of true necrosis were mixed with degenerative lesions. The surface of the involved area was in the range of 50%, with 40% of prenecrosis and hypercontraction bands in the subendocardial regions.

Conclusion

Electrical shocks delivered in saline cause less damage in the 160 joule to 200 joule range as compared to direct epicardial placement of the electrode where perforation is observed for energies above 50 joules. When the electrode is immersed in saline, a part of the current is dissipated in the saline, and less is delivered to the myocardium. On the other hand, the size of the electrode used to apply the shock is larger, therefore reducing the current density beneath the electrode and consequently the damage to myocardium.

In summary, shocks delivered in saline with a large electrode are able to produce a transmural damage with energies in the range of 160 joules to 200 joules without perforation.

Endocardial fulguration

Method

Endocardial fulgurations were delivered through a 7F, USCI bipolar catheter, selected to withstand the peak of current and voltage according to a method previously described [4, 27]. The catheter was introduced through the femoral artery for left ventricular endocardial fulguration and from the internal jugular vein for right ventricular endocardial fulguration. The endocardial contact was assessed by analysis of the injury current from the endocardial electrogram recorded with an amplifier with a long time constant. The weights of the dogs were comparable to those of the previous experiments. Endocardial fulguration (which was done without fluoroscopy) was limited by difficulties in locating precisely the shocked area. It was, however, possible to determine at least two completely different locations which were verified by palpation through the myocardium after a right lateral thoracotomy. The thorax was closed before delivering the shocks in order to not disturb the spread of the electrical field.

Assessment of the risk for perforation with endocardial fulguration at the ventricular level

The catheter was introduced through a vein into the right ventricle and an injury current, as well as manual compression, indicated that the catheter was tightly applied against the wall. A fulgurative shock of 240 joules was delivered to a dog of 19 kg (13J/kg or approximately 6 amps/kg), and ventricular fibrillation followed the fulguration shock. It was not possible to defibrillate the heart despite several defibrillating shocks delivered from external paddles.

The macroscopic examination of the heart showed subepicardial hemorrhage of the right ventricular apex with extension to the free wall and septum.

In the next series of experiments, shocks of 32, 51, 70, 150 (twice), 205, and 262 joules were delivered to the distal electrode of a catheter positioned

Figure 5–4. Craters produced at the base of a papillary muscle in the left ventricle of a dog with multiple delivery of 6 J/kg shocks. Note the deep necrosis of the tissue with complete destruction of the endocardium.

against the left ventricular endocardium. The energy corresponds to a value of around 8 J/kg per shock.

Macroscopic examination localized the hemorrhagic zone at the subepicardial area opposite the catheter. The catheter probably migrated by advancing progressively after each shock from the endocardium toward the epicardium so that its distal end was lodged 2 mm from the surface. All along the catheter trajectory, there was a transmural hemorrhagic pattern with edema of 1 cm width.

In another experiment, a series of shocks of 107, 150, 205, and 262 (twice) joules were applied to the left ventricular endocardium. This amount of energy corresponds to a value of about 6 J/kg per shock.

Macroscopic examination showed that in this particular case, the catheter was stuck in the angle formed by the free wall of the left ventricle and the posterior papillary muscle. Around the papillary muscle, in addition to the lesion caused directly by the catheter, subendocardial hemorrhage was observed over a distance of 2 cm to 3 cm, which involved the complete surface of the posterior part of the papillary muscle. A crater was localized on the endocardial surface (figure 5–4) near the papillary muscle.

In another experiment, a series of high-energy shocks were delivered through a Medidyne catheter introduced into the left ventricle. The catheter was not applied against the endocardium, as shown by complete disappearance of the injury current during catheter withdrawal. Fulguration energies

Figure 5–5. Ultrastructural study of the effects of fulgurating shocks half a centimeter from the fulgurated area showing destruction of the myofibrils, large vacuoles, and mitochondria (acute study). This pattern could only be related to the shock wave generated by the shock.

were in the range of 144, 200 (X3), and 300 joules, as well as four shocks of 400 joules. The last one led to ventricular fibrillation which was successfully defibrillated. In the same dog, shocks were delivered to the right ventricle, with the same kind of catheter, with two shocks of 200 joules and one of 260 joules, and led to an episode of ventricular fibrillation which was successfully defibrillated.

Gross pathological examination indicated extensive subendocardial hemorrhage on the diaphragmatic endocardium of the right ventricle, without any coagulation necrosis pattern or more specific lesions. This feature was similar in the two ventricles. This experiment indicates that when the catheter is not applied against the wall, the histological lesions are minor and are quite different from those obtained when the catheter is firmly applied against the wall. The histology confirmed the presence of minor endocardial injury.

An electron microscopic study was performed in three dogs. The sample was taken half a centimeter from the fulgurated zone and immediately processed (within 20 minutes after death). The tissue showed a very specific pattern, figure 5–5. The myofibrils were disrupted, with diffuse alterations of mitochondria and vacuolization. There was also damage to the nuclei and contraction bands appeared at the periphery.

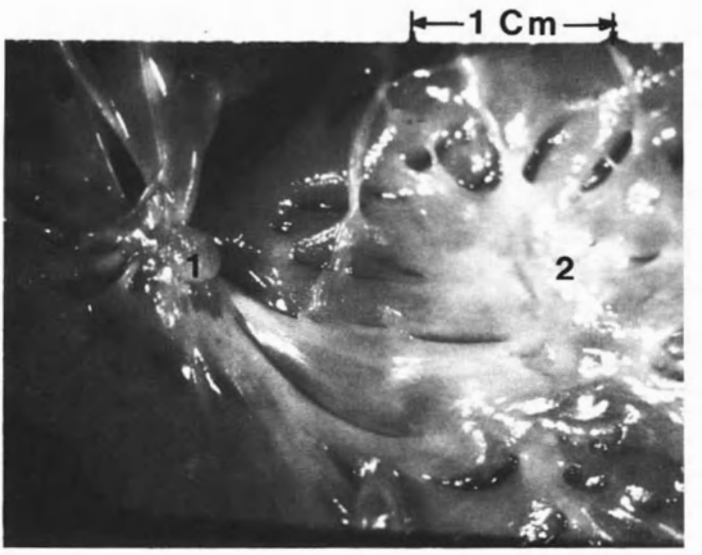

Figure 5–6. Chronic study of the effect of fulguration. Two shocks [1–2] were delivered to the endocardium, one of 107 joules and two shocks of 144 joules. The animal was sacrificed three weeks after the experiment. Note the whitish starlike pattern 1 cm in diameter. Note that the central part has a hemorrhagic pattern without thrombus formation.

CHRONIC STUDY

Chronic observations were possible in one dog. The chronic lesions induced by endocardial catheter fulguration shocks were also assessed. Shocks of 107 joules (X 2) and 144 joules (X 2) were delivered to the right ventricle. One shock of 150 joules and two shocks of 107 joules were delivered to the left ventricle. The animal was sacrificed after three weeks. The macroscopic examination of the right ventricular endocardium indicated two zones of endocardial fibrosis with a starlike pattern 1.5 cm in diameter (figure 5–6). The middle of these lesions showed fibrosis extending for a depth of approximately 2 mm. In the left ventricle, the involved area showed a zone of whitish depressed tissue (figure 5–7). The histological studies confirmed the fibrous pattern, with ramifications going over the epicardium and following the interstitial spaces (figure 5–8A and 5–8B). In addition, it was possible to find inflammatory lesions with mononuclear cells. Contraction bands were found peripheral to the fulguration zone. During endocardial fulguration, the globe of ionized vapor created at the beginning of the shock increased the apparent size of the injured zone, making the modified area larger than the electrode tip.

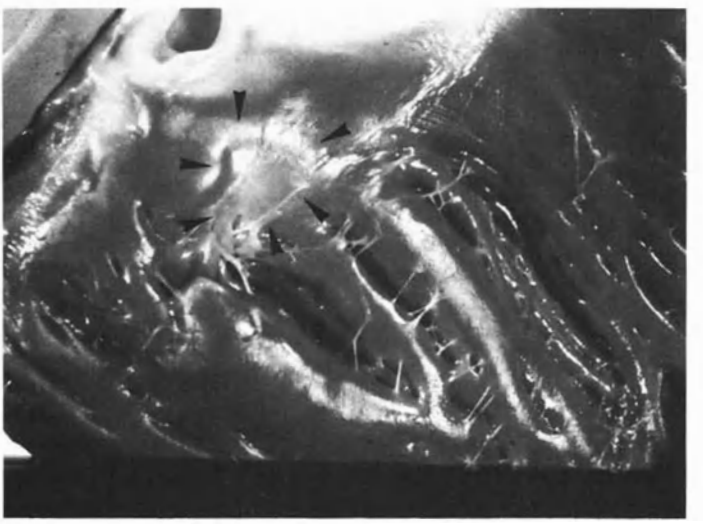

Figure 5–7. Same dog as figure 5–6. In the left ventricle, two shocks of 107 joules and one shock of 150 joules show fibrous tissue with a depressed scar. The shock was delivered against the flat part of the endocardium. There is no crater formation.

Opened thorax fulguration

Experiments were performed to evaluate the differences between open versus closed chest shocks. In the closed chest preparation it was not possible to perforate the right ventricle with a single shock. Perforation was observed in open chest preparations when the catheter was applied along the anterior part of the interventricular septum with a shock of 160 joules. In this experiment, the catheter was guided manually against the wall and manipulated so that pressure against the wall was identical to that used during closed chest experiments. With the open chest procedure, the catheter tip was clearly seen from the surface by a slight bulging of the wall. Therefore, the exact position of the catheter was easy to determine.

Three other shocks of 185 joules performed along the right ventricle in the vicinity of the infundibulum did not produce perforation. However, in two of these shocks the electrode tip showed a whitish coagulum of a tissue which might have been contraction bands observed at histological study. Very similar patterns were obtained in the atrial appendage with delivery of 205 joules (figure 5–9). However, in this case, the current was in the range of 6.9 amperes to 8.7 amperes if the shock was delivered in the atrium, instead of up to 25.5 amperes when the current was delivered within the cavity close to the sinus node. It was, therefore, more comparable with shocks delivered inside the right ventricles, where currents of 13.9 amperes and 14.1 amperes

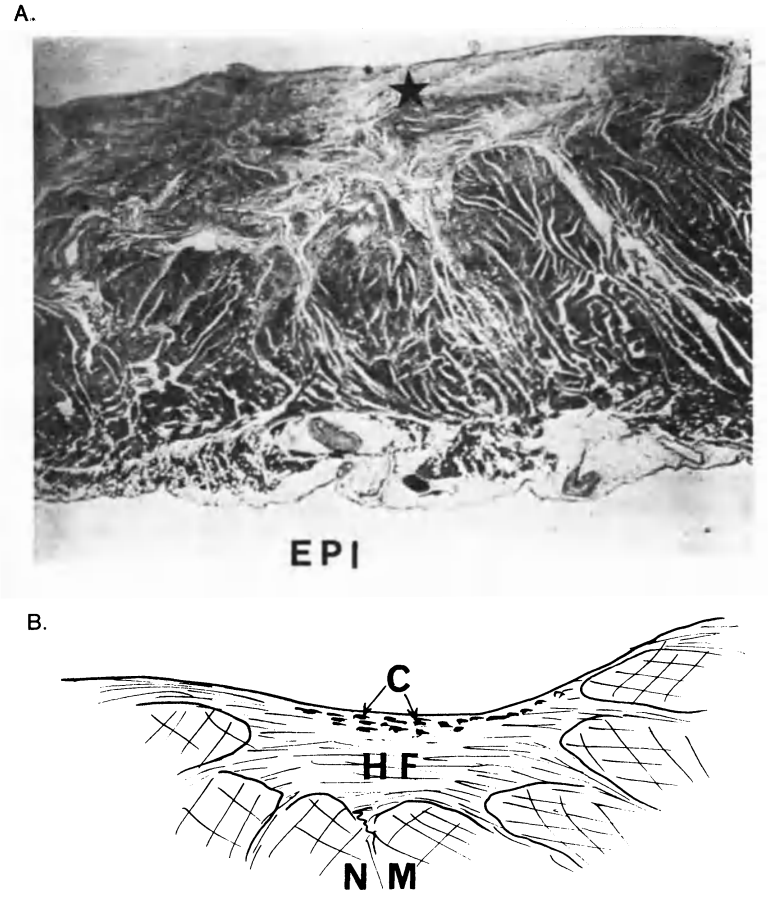

Figure 5–8A and 5–8B. Histological study of the fulgurated area presented in figure 5–7. Modified tissue is stressed by a star. Figure 5–8B shows the interpretation of the histological data. C : Particles of carbon; H : Highly fibrosed area; NM : normal myocardium. Note the relatively clear-cut limit between fibrous tissue and normal myocardium.

were recorded. This suggests that the highest resistance is observed when the flow of current is forced through a relatively narrow isthmus.

Histological studies

Whatever the involved structures, all these experiments indicated patterns of varying degrees of myocardial damage, with or without transparietal hemorrhage. When there was no hemorrhage, it was possible to see on close observation, a very thin border zone suggesting charred particles. A pattern of dense acidophilic necrosis was seen in close proximity to the electrode

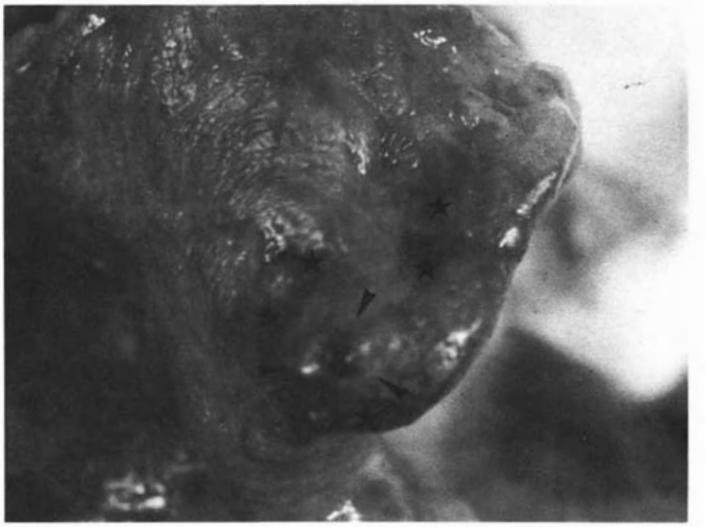

Figure 5–9. Effects of shocks of 250 joules delivered to the right atrial appendage. The star points out the area of hemorrhage. The place of the catheter is visible. Borderline perforation is obtained, but there is not mechanical rupture of the appendage.

where the boundaries between cells were abolished. The percentage of cells showing a pattern of coagulation necrosis decreased with distance from the shock delivery site. More distantly, contraction bands were interspersed with normal cells (figure 5–10). When there was hemorrhage, it was prominent in the area where the active electrode was located. This feature was superimposed on the pattern of coagulation necrosis or contraction bands.

Coronary sinus shocks

Fulguration shocks were delivered inside the coronary sinus in five dogs weighing approximately 25 kgs. Rupture of the coronary sinus was formed for shocks of 180 joules delivered in the proximal large portion of the coronary sinus. In the more distal part of the structure, which is narrower, shocks of 80 joules did not result in rupture. However, the size of these vessels are very variable, and the exact positioning of the catheter is more difficult to determine. In any case, when there was a coronary sinus rupture, the macroscopical pattern of the lesions was remarkably constant and is schematically presented in figure 5–11. When the coronary sinus was ruptured, hemorrhage burrowing in the direction of the atrioventricular groove was observed.

During the gross examination of these dog hearts, some showed a blind cavity of up to 3 cm located behind the tricuspid papillary muscles (figure 5–12). This same structure has also been observed in human hearts. Fulgura-

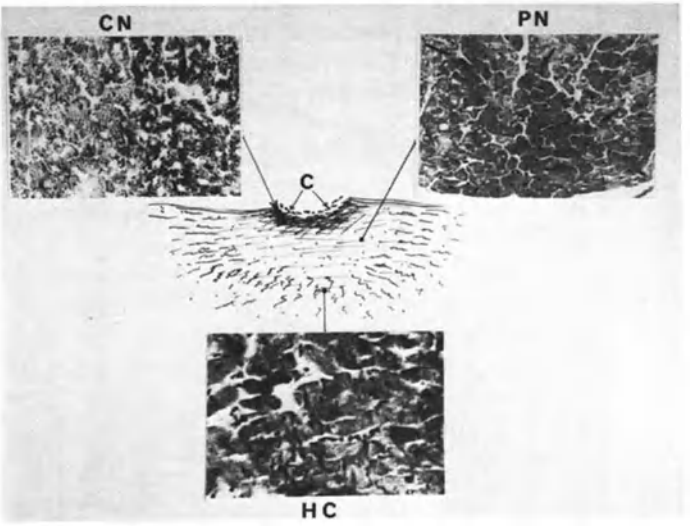

Figure 5–10. Three main parts of the effect of the shock delivered on myocardial tissue.
C: Particles of carbonization
CN: Complete coagulation necrosis (left part of the insert)
PN: Partial necrosis showing the eosinophilic cells interspersed with surviving fibers
HC: Hypercontraction bands

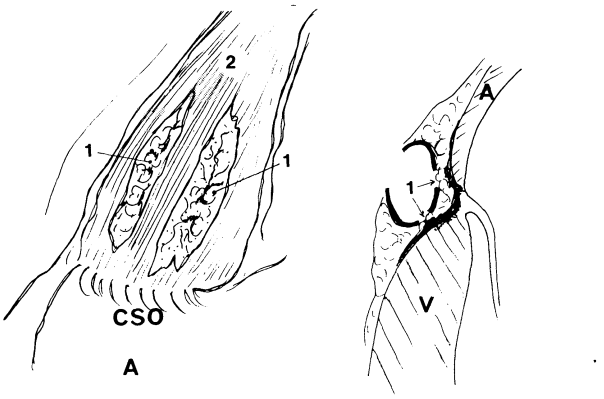

Figure 5–11. Typical pattern of coronary sinus rupture after shocks delivered inside the proximal part
A: atrium
V: ventricle
CSO: coronary sinus ostium
1: fatty tissue of the AV groove in which hemorrhage could be seen.
This hemorrhagic zone extends up to the epicardial aspect of the atrium, ventricle, and annulus.
2: coronary sinus endocardium.
Three areas of rupture are observed on the external part of the coronary sinus and in two places indicated by N°1.

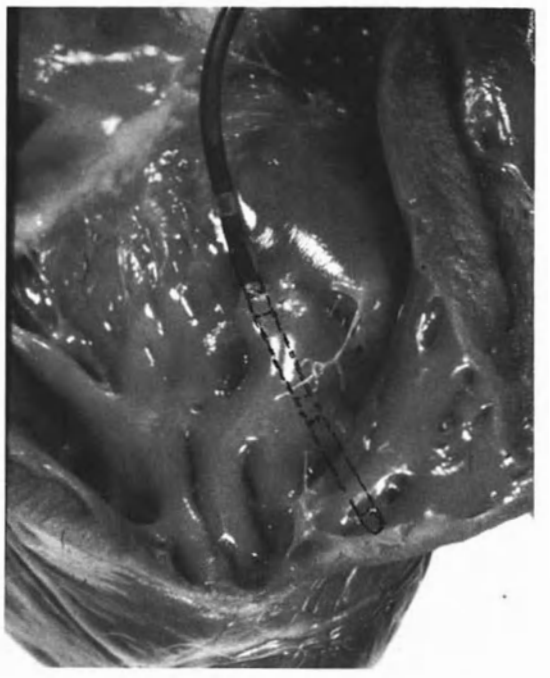

Figure 5–12. A quadripolar USCI 6F catheter was inserted manually behind the papillary muscle in the right ventricle, where a tunnel 2 cm long was found!

tion shocks have not been tested in this structure, and caution should be exercised before this is performed in man.

Physical effects in relationship to tissue damage

After delivery of high energy, it is possible to observe charred particles near the active electrode which are probably related to the high temperature of the electrical arc created during the fulguration procedure [28]. The short duration of this electrical phenomenon (a few milliseconds) could only lead to a very small amount of carbonized tissue. The deflagration and the collapse of the vapor bubble are other mechanical factors which could shear and disperse small charred particles [12, 29, 30].

In general, the amount of heat produced by a fulguration shock of 240 joules is limited [10]. Nevertheless, this energy will be spent in the immediate area around the electrode. This could explain, at least in part, the phenomenon of whitish coagulation observed in the immediate proximity of the electrode. An important factor is also the flow of currents after transthoracic

shocks [31]. The flow of current could probably explain the coagulation necrosis in the immediate vicinity of the electrode. It could also be correlated with the appearance of contraction bands, which decreased in a centrifugal manner. These effects are more important using open-chest dogs, because the lines followed by the current are more concentrated and there is less diffusion of current flow into the surrounding tissues. The same concept is valid for the shocks delivered to the epicardium which led to perforation of the ventricular wall for low shocks (50 joules). The modification of electrical conduction through the blood and through the myocardial tissue also explain the difference between epicardial and endocavitary fulguration. When the fulguration is applied on the epicardium, the blood contained within the ventricular cavity is playing the role of an indifferent electrode, and all the energy is focused between the active electrode and the opposite zone of the endocardium. In contrast, when the shock is delivered to the endocardial surface, the active electrode, being in a milieu which is a good conductor of electricity, results in a sharp decrease of the energy density in the blood and a relatively small amount of current crosses the myocardial structure.

If vessels are involved, the physical effects of the shocks could lead to the deterioration of the vessel wall, leading to hemorrhage. The hemoglobin which is liberated could deteriorate spontaneously, leading to brownish discoloration in the immediate proximity of the electrode. As soon as the ionized vapor bubble is able to grow, the transmission of current through the tissue is not only due to the electrode but also to the area where the globe of ionized vapor is in contact with this tissue in the direction of the indifferent electrode [7, 10]. This could explain, at least partially, the creation of the starlike fibrous zone, which is centered in the contact area between the electrode and the endocardium. However, the mechanical phenomena observed during the growth of the bubble, and later during its collapse, may also play a role. However, the mechanical factor could be particularly important if the electrode is embedded between the trabeculations of the endocardium or when the shock is delivered in a blind cavity, as observed behind the papillary muscles of the right ventricle in dog hearts (figure 5–12). This structure needs to be confirmed in human hearts.

Quantitative aspects of tissue damage related to fulguration shocks

Only a few systematic studies are available in this area [19, 20]. They demonstrated an obvious dose-effect relation. In our acute studies, endocardial delivered energies of more than 100 joules were necessary to obtain a macroscopic modification on the endocardium. It is probable that chronic studies demonstrate more extensive lesions than those seen during acute studies. Perforation is only obtained if a series of high-energy shocks are delivered through a catheter strongly pressed against the endocardial layers, and if the

position remains the same after each shock. In our studies, ventricular perforation has been observed only during the use of open-chest dogs and only in the right ventricle.

CONCLUSION

In this experimental work we systematically explored various physical factors that appear to effect the nature and extent of tissue damage. These factors include not only the amount of electrical energy delivered but whether the energy is delivered in a saline medium in a closed-or open-chested animal, and whether it is delivered in the epicardium or endocardium. Precautions should be taken relating to application of these shocks to confined areas (such as the coronary sinus) or when the catheters are embedded in myocardial tissue.

REFERENCES

1. Bardy CH, Coltorti F, Ivey TD, Yerkovich D, Greene HL: Effect of damped sine-wave shocks on catheter dielectric strength. *Am J Cardiol* 56: 769–772, 1985.
2. Fisher JD, Brodman R, Johnson D, Waspe LE, Kim SG, Matos JA, Scavin G: Nonsurgical electrical ablation of tachycardia : Importance of in vitro testing of catheter leads. *PACE* 7: 74–81, 1984.
3. Fontaine G, Cansell A, Lechat P, Frank R, Tonet JL, Grosgogeat Y: Les chocs electriques endocavitaires. Problemes lies au materiel. *Arch Mal Coeur* 77: 1307–1314, 1984.
4. Fontaine G, Cansell A, Lechat P, Grosgogeat Y: A non destructive method to select catheters for ablation technique. *Eur Heart J* 5: (SPI); 258 (abstract), 1984.
5 Bardy GH, Coltorti F, Ivey TD, Alferness C, Rackson M, Hansen K, Stewart R, Greene HL: Some factors affecting bubble formation with catheter-mediated defibrillator pulses. *Circulation* 73: 525–538, 1986.
6. Downar E, Harris L, Parson I, Easty A: Characterisation of catheter ablation with high speed cinematography *JACC* 7: 131–A (abstract), 1986.
7. Boyd EG, Holt PM: An investigation into the electrical ablation technique and a method of electrode assessment. *PACE* 8: 815–824, 1985.
8. Boyd EG, Holt PM: Haematological effects of the ablation technique: A comparison between anodal and cathodal delivery *JACC* 7: 131–A (abstract), 1986.
9. Boyd EG, Holt PM, Sowton E: Patient impedance-time characteristics during unipolar ablation: A critical factor in the energy delivery system specification *PACE* 9: 298 (abstract), 1986.
10. Fontaine G, Volmer W, Nienaltowska E, Aaddaj S, Cansell A, Grosgogeat Y: Approach to the physics of fulguration. In: *Ablation in Cardiac Arrhythmias*, G Fontaine, MM Scheinman, eds. Mount Kisco: Futura Publishing Company, 1987, p. 101.
11. Wetherbee JN, Chapman PD, Klopfenstein HS, Troup PJ: Is the truncated exponential waveform safer for catheter ablation? *Circulation* 72: (Suppl III); 390 (abstract), 1985.
12. Nienaltowska E, Fruman DH, Fontaine G: Cavitation within the heart: A treatment of cardiac arrhythmias. In: *Proceedings of the American Society of Mechanical Engineers – Atlanta, May 1986.*
13. Lee BI, Rodriguez ER, Notargiacomo A, Ferrans VJ, Chen YW, Fletcher RD: Thermal effects of laser and electrical discharge on cardiovascular tissue: Implications for coronary artery recanalization and endocardial ablation. *JAAC* 8: 193–200, 1986.
14. Westveer DC, Nelson T, Stewart JR, Thornton EP, Gordon S, Timmis GC: Sequelae of left ventricular electrical endocardial ablation. *JACC* 5: 956–960, 1985.
15. Ruder MA, Davis JC, Eldar M, Scheinman MM: Effects of electrode catheter shocks delivered near the tricuspid annulus in dogs *JACC* 7: 7 (abstract), 1986.
16. Levine JH, Spear JF, Weisman HF, Prood C, Kadish AA, de Langen C, Moore EN:

Abnormal impulse conduction and initiation are present in a large border zone after high energy ablation *JACC* 7: 37 (abstract), 1986.
17. Levine JH, Spear JF, Prood C, Kadish AA, de Langen C, Moore EN: The importance of current pathway in ablation: In vitro and in vivo correlates *Circulation* 72 (Suppl III): 390 (abstract), 1985.
18. Lechat P, Fontaine G, Cansell A, Grosgogeat Y: Epicardial and endocardial myocardial damage related to catheter ablation techniques *Eur Heart J* 5 (Suppl 1): 258, 1984.
19. Kempf F, Falcone RA, Iozzo RV, Josephson ME: Anatomic and hemodynamic effects of catheter-delivered ablation energies in the ventricle. *Am J Cardiol* 56: 373–377, 1985.
20. Hauer RN, Straks W, Borst C, Robles de Medina EO: Electrical catheter ablation in the left and right ventricular wall in dogs: Relation between delivered energy and histopathologic changes. *JACC* 8: 637–643, 1986.
21. Coltorti F, Bardy GH, Reichenbach DD, Greene HL, Thomas RC, Breazeale DG, Ivey TD: Effects of varying electrode configuration with catheter-mediated defibrillator pulses at the coronary sinus orifice in dogs. *Circulation* 6: 1321–1333, 1986.
22. Chapman PD, Klopfenstein HS, Troup PJ, Brooks HL: Evaluation of a percutaneous catheter technique for ablation of ventricular tachycardia in a canine model. *Am Heart J* 110: 1, 1985.
23. Brodman R, Fisher JD: Evaluation of a catheter technique for ablation of accessory pathways near the coronary sinus using a canine model. *Circulation* 67: 923–929, 1983.
24. Beazell JW, Adomian GE, Furmanski M, Tan KS: Experimental production of complete heart block by electrocoagulation in the closed chest dog. *Am Heart J* 104: 1328, 1982.
25. Bardy GH, Kasell JH, Ideker RE, Worley SJ, Smith WM, German LD, Gallagher JJ: Transvenous catheter ablation of the atrioventricular conduction system for treatment of refractory supraventricular tachycardia. Electrophysiologic and pathologic observations in dogs. *Am J Cardiol* 49: 1012, 1982.
26. Fontaine G, Volmer W, Nienaltowska E, Aaddaj S, Cansell A, Grosgogeat Y: Approach to the physics of fulguration. In: *Ablation in Cardiac Arrhythmias*, G Fontaine, MM Scheinman, eds. Mount Kisco: Futura Publishing Company, 1987, p. 101.
27. Fontaine G, Cansell A, Lechat P, Frank R, Grosgogeat Y: Method of selecting catheters for endocavitary fulguration. *Stimucoeur* 12: 285–289, 1984.
28. Lee BI, Notargiacomo A, Fletcher RD, Rodriguez ER, Ferrans VJ, Chen YW: The thermal response of ventricular endocardium to laser and electrical ablation and the disparate effects of different superfusion media *JACC* 7: 37 (abstract), 1986.
29. Plesset MS, Prosperetti A: Bubble dynamics and cavitation. *Ann Rev Fluid Mech* 9: 145–185, 1977.
30. Tidd MJ, Webster J, Cameron Wroght H, Harrison IR: Mode of action of a surgical electronic lithoclast high speed pressure, cinematographic and schlieren recordings following an ultrashort underwater electronic discharge. *Biomed Engin* 1: 5–11, 1976.
31. Van Vleet JF, Tacker WA, Geddes LA, Ferrans VF: Acute cardiac damage in dogs given multiple transthoracic shocks with a trapezoidal waveform defibrillator. *Am J Vet Res* 38: 617–626, 1977.
32. Dahl CF, Ewy GA, Warner ED, Thomas ED: Myocardial necrosis from direct current countershock. Effect of paddle electrode size and time interval between discharges. *Circulation* 50: 956–961, 1974.
33. Laniado S, Buckley NM, Frank CW, Kambosos D: Effects of DC electric countershock on ventricular function, cation balance and endogenous norepinephrine in the dog heart. *Cardiology* 59: 253–267, 1974.
34. Mac Lean LD, Van Tyn RA: Ventricular defibrillation. An experimental investigation of voltage requirements and effect of electrode size. *JAMA* 175: 471–474, 1961.
35. Pansegrau DG, Abboud FM: Hemodynamic effects of ventricular defibrillation. *J Clin Invest* 49: 282–297, 1970.
36. Reichenbach DD, Benditt EP: Myofibrillar degeneration : A response of the myocardial cell to injury. *Arch Physiol* 85: 189–199, 1968.
37. Reichenbach DD, Benditt EP: Myofibrillar degeneration : A common form of cardiac muscle injury. *Ann NY Acad Sci* 156: 164–176, 1969.
38. Schuder JC, Rahmoeller GA: Transthoracic ventricular defibrillation with triangular and trapezoidal waveforms. *Circ Res* 19: 679–684, 1966.

39. Schuder JC, Stoeckle H, Gold JH: Effectiveness of transthoracic ventricular defibrillation with square and trapezoidal waveforms. In: *Proceedings Purdue Cardiac Defibrillation Conference*, Purdue Univ Engineering Experiment Station Document 00147, 109–114, 1975.
40. Tacker WA, Geddes LA, Cabler PS, Moore AG: Electrical threshold for defibrillation of canine ventricles following myocardial infarction. *Am Heart J* 88: 476–481, 1974.
41. Tacker WA: Trans-chest ventricular defibrillation of heavy subjects using trapezoidal current waveforms. *J Electrocardiol* 8: 237–240, 1975.
42. Tonet JL, Baraka M, Nieto J, Frank R, Lilamand M, Fontaine G, Cansell A, Grosgogeat Y: Criteria for induction of chronic complete heart block by His bundle fulguration. *JACC* 9: 251–A, 1987.
43. Levy S, Bru P: Interruption electrique par voie percutanee de la conduction atrioventriculaire normale. Resultats d'une etude multicentrique francaise. *Arch Mal Coeur* 79: 1145, 1986.
44. Scheinman MM, Evans-Bell T: Catheter ablation of the atrioventricular junction : A report of the percutaneous mapping and ablation registry. *Circulation* 70: 1024–1029, 1984.
45. Critelli G, Perticone F, Coltorti F, Monda V, Gallagher JJ: Antegrade slow bypass conduction after closed-chest ablation of the His bundle in permanent junctional reciprocating tachycardia. *Circulation* 67: 687–692, 1983.
46. Morady F, Scheinman MM, Winston SA, DiCarlo LA, Jr, Davis JC, Griffin JC, Ruder MA, Abbott JA, Eldar M: Transcatheter ablation of posteroseptal accessory pathway. In: *Ablation in Cardiac Arrhythmias*, G Fontaine, MM Scheinman, eds. Mount Kisco: Futura Publishing Company, 1987, p. 191.
47. Fisher JD, Brodman R, Kim SG, Matos JA: Nonsurgical kent bundle ablation via the coronary sinus in patients with the WPW syndrome. *Circulation* 66: (Suppl II); 375, 1982.
48. Gillette PC, Wampler D, Garson A, Zinner A, Ott DA, Cooley DA: Treatment of atrial automatic tachycardia by ablation procedures. *JACC* 6: 405–409, 1985.

6. HISTOLOGIC EFFECTS OF LASER-INDUCED MYOCARDIAL DAMAGE

SANJEEV SAKSENA

The continuing development of ablative procedures for tachyarrhythmia control has directed research efforts towards evaluating different types of ablative energies in an effort to find the optimal physical technique [1–4]. Recently, the use of laser energy for myocardial ablation has been extensively examined in experimental studies, and this has led to clinical application of this technique [3–20]. The experimental basis for the clinical technique has been under study in our laboratory since 1984 and has resulted in clinical application in patients with malignant supraventricular and ventricular tachycardias. The clinical efficacy and safety of the laser ablation technique is now being evaluated for intraoperative and transcatheter myocardial ablation. The technique itself is influenced by three variables, namely, the physical aspects of the laser energy source, the energy delivery technique and medium, and the myocardial substrate for ablation [21]. While our experimental studies have examined a variety of issues relating to all of these variables, current clinical trials will need to establish the methodology, efficacy, and safety of the technique in the clinical arena.

The author gratefully acknowledges the collaboration of Doctors Arun Gadhoke, and Isaac Gielchinsky, and Mr. Demetris Pantopoulos in the clinical and experimental studies. The continuous assistance and support of Mr. Dennis J. Bruschi was invaluable in the performance of this research project. The patient and outstanding secretarial assistance of Ms. Ruth Harrison permitted preparation of this manuscript.

PHYSICAL CONSIDERATIONS IN LASER ABLATION TECHNIQUES

The theoretical basis for the development of laser energy emission was initially formulated by Albert Einstein in 1917. He postulated that altering energy states of atoms or molecules would result in emission or absorption of electromagnetic radiation. A large number of identical atoms undergoing a similar change in energy level should emit radiation with similar characteristics. This type of stimulated energy emission, now referred to as laser radiation, is usually monochromatic (due to a narrow range of frequencies), coherent (electromagnetic waves are in the same phase), and collimated (electromagnetic waves are parallel). Laser energy can be theoretically produced with any wavelength within the electromagnetic spectrum, depending on the chemical reaction used to generate the energy emission. The substrate involved in the reaction is referred to as the lasing medium and can be solid, liquid, or gaseous. This medium is energized to a higher level by another energy source, e.g., electricity. The higher energy state is usually unstable, and the atoms fall back to their original energy level, emitting a photon whose wavelength is determined by the difference in the two energy levels. The emitted photons are usually reflected repeatedly within the lasing medium, which is enclosed in a resonator with reflective surfaces. This results in continuation of the laser reaction and sustained laser emission. Laser beams can be precisely controlled. They can be focused, reflected, and transmitted using optical systems to produce exact effects at a desired site of application. The delivered energy range of laser-based systems is remarkable, varying from miniscule doses employed in cellular biology to enormous power densities in industrial applications.

Medical lasers employ a variety of substances for laser action. Commonly used lasers include gas lasers (argon ion, carbon dioxide), liquid dye lasers, and solid elements (neodymium-doped yttrium aluminum garnet). Molecular gas lasers (krypton or xenon fluoride) are currently under investigation but need optical transmission systems, limiting their current clinical application. Each laser has specific emitted energy wavelengths ranging from the infrared to the ultraviolet region of the electromagnetic spectrum.

The laser systems currently under investigation employ a laser energy source coupled to an optical transmission system. One commonly used system, the argon ion gas laser, has been extensively used in our experimental laboratory and intraoperatively during cardiac surgery (figure 6–1). The system consists of a 15-watt water-cooled argon laser (Laser Ionics, Orlando, FL). The laser beam is directed by optical mirrors and prisms into an optical coupler (Trimedyne, Inc, Santa Ana, CA), which focuses the laser beam into a 300 micron diameter quartz core optical fiber with a length of 4 meters. This optical fiber can be housed within a standard cardiac catheter, suction electrode catheter, or a fiberoptic angioscopic system for energy delivery without or with electrical and optical monitoring, respectively, at the site of application (figures 6–2A, 6–2B and 6–2C). Continuous

Figure 6–1. Prototype clinical laser system for cardiac application. The power supply, laser tube and head, along with a pulse modulator are mounted on a mobile cart. (Reproduced with permission form The Futura Publishing Co, Inc, Mt Kisco, NY, 1986.)

wave argon laser discharges frequently result in fiberoptic tip deterioration. This becomes a major limitation for catheter application of the laser technique. We have determined that fiberoptic tip damage is minimized by pulsed laser delivery techniques and is markedly reduced with pulse durations of less than one second [12, 15, 20]. In addition, direct tissue contact during lasing enhances tip damage and may need to be avoided.

Alternative experimental laser systems employ an 80-watt Nd-YAG laser energy source (Molectron Medical Model 8000) coupled to a 0.9 mm quartz core fiber (Molectron Medical Model 8200) [9]. The emitted laser beam has a wavelength of 1060 nm. While carbon dioxide laser sources have been available for some time, optical transmission systems had not been developed. A recent report employed a CO_2 laser source (Sharplan 743, Tel Aviv, Israel) coupled to a new silver halide optical fiber [22, 23]. These fibers are 0.9 mm in diameter, 90 cm long, and continually cooled by circulation of CO_2 through a surrounding sheath. The emitted laser beam has a wavelength of 10,600 nm. The use of pulsed excimer laser radiation in cardiovascular disease has been examined by Isner et al [8]. Excimer lasers use a mixture of a rare gas, e.g., krypton or xenon, and a halogen, e.g., fluorine, as the laser medium to produce laser radiation in the ultraviolet range of the electromagnetic spectrum. The electrical excitation of the halogen results in its bonding with the rare gas, resulting in the formation of an excited dimer

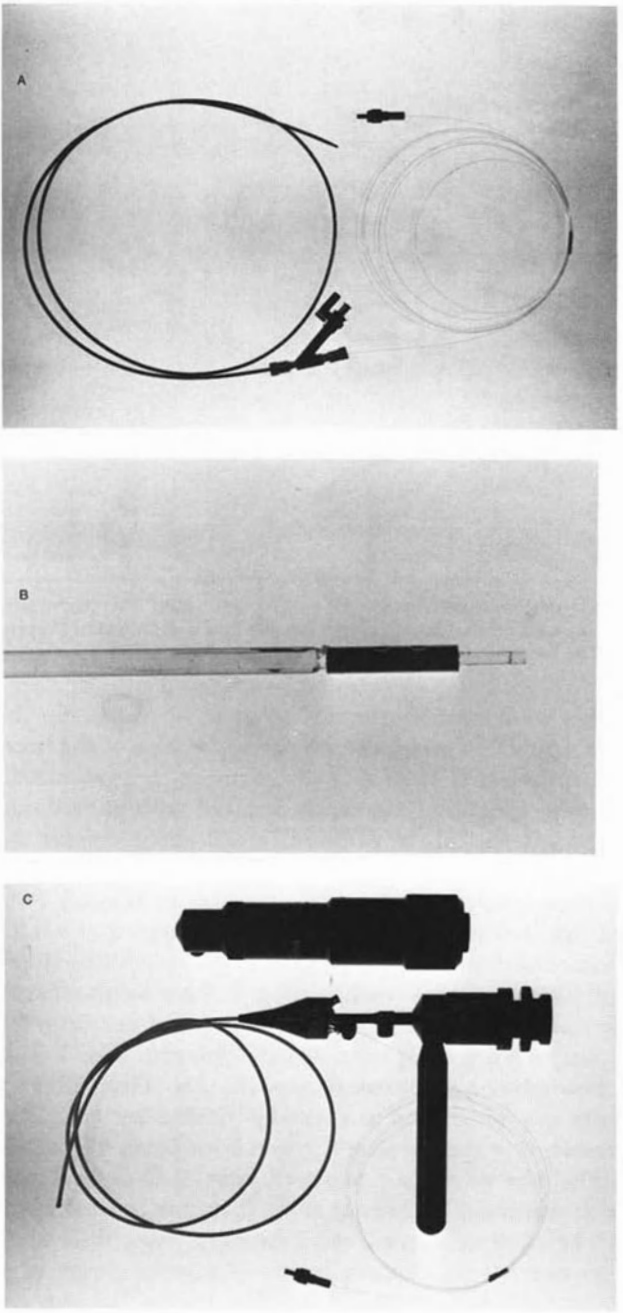
A
B
C

molecule, or excimer. During recovery to the basal energy level, the molecule emits a photon with high energy in the ultraviolet spectrum. Early studies have emphasized the high degree of precision in industrial and biological applications employing excimer laser radiation [8]. A typical excimer laser system employed in experimental cardiovascular studies uses a krypton-fluoride gas mixture with an emitted laser radiation wavelength of 248 nm. High power outputs (up to 50 W) and discharge repetition rates (up to 200 Hz) can be achieved. However, fiberoptic transmission systems are currently being examined for excimer lasers, and interfacing with catheter systems awaits the development of such systems for this laser. The potential carcinogenicity of ultraviolet radiation also needs to be carefully studied.

EXPERIMENTAL BASIS FOR LASER ABLATION TECHNIQUES

The anatomic and physiologic effects of laser radiation on cardiac tissues involved in arrhythmogenesis have been studied in a variety of experimental models. Initial studies employed normal bovine or canine myocardium [3, 4]. Subsequently, we extended these studies to normal and diseased human ventricle excised from patients with sustained ventricular tachycardia [7, 12–17]. Recently we have examined the effects of laser radiation on human atrium and the atrioventricular groove region [24]. A variety of laser energy delivery modes and transmission media have been examined both qualitatively and quantitatively. Finally, limited comparative data exist on the cardiac lesions obtained with different laser energy sources.

Anatomic and histologic effects of laser radiation in cardiac tissues

Continuous wave argon laser radiation was the initial laser energy delivery mode. In animal studies, this type of laser discharge induced a circular, moderately well-circumscribed lesion with a central crater. There was a surrounding area of whitish discoloration with a congealed appearance. During laser discharge, the tissue surface consistently swelled and then ruptured with a popping sound and release of an underlying gas bubble. Histologic examination of such a lesion in canine ventricle is shown in figure 6–3. There is a central crater due to tissue vaporization with a narrow mouth, and this is lined by charred cellular remnants with vacuolization. This is surrounded by a zone of coagulation necrosis for 1 mm to 3 mm around the crater margins. Figures 6–4A and 6–4B are scanning electron micrographs of a lesion obtained in normal bovine ventricle in our laboratory. At low magnification (figure 6–4A) the irregular surface of the vaporized tissue and ruptured cells

Figure 6–2. *Panel A*: Optical fiber and cardiac catheter assembly used for early clinical application. A connector controls the extent of fiber tip extrusion.
Panel B: Optical fiber tip (magnification 50 X).
Panel C: Prototype fiberoptic balloon flotation angioscopic system with three lumina which can be used for viewing, balloon inflation, and guiding laser fiber to site of energy delivery.

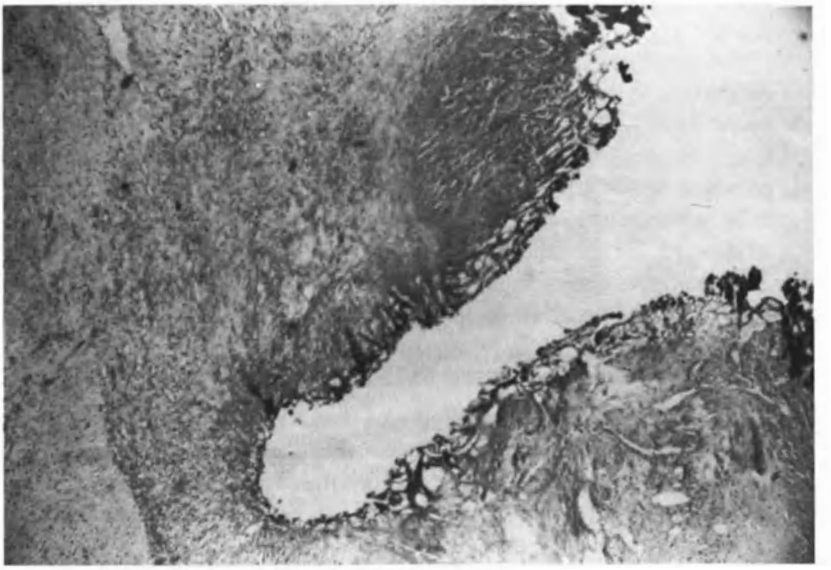

Figure 6–3. Histologic section of a myocardial lesion induced by continuous wave argon discharge in canine ventricle. Note the central crater due to tissue vaporization with surrounding tissue carbonization and coagulation. (Original magnification 30 X.) (Reproduced with permission from The Futura Publishing Co, Inc, Mt Kisco, NY, 1986.)

produce a pockmarked appearance. At greater magnification (figure 6–4B) we observe that the crater is lined with cells with disrupted surface membranes, leaving behind a congealed tissue surface. Similar lesions are observed in atrium exposed to argon laser irradiation.

The effects of laser radiation on myocardium can be best explained by absorption of the delivered energy by intracellular and extracellular water [25]. The energy is transformed into heat, and this results in instantaneous vaporization of water with subsequent cell rupture. Lee and coworkers recorded the tissue temperature changes associated with laser discharges [25]. They noted an immediate increase (approximately 30°C) at the site of laser discharge in isolated tissue. The extent of increase would be expected to be greater in vivo.

The effects of *continuous wave* argon laser radiation on the specialized atrioventricular conduction system have been examined in canine experiments by Narula and coworkers [6]. The gross appearance at the site of laser discharge shows a small hemorrhagic area in the vicinity of the septal leaflet of the tricuspid valve. Similar appearances may be noted in the vicinity of the noncoronary cusp of the aortic valve. The laser discharge produces tissue vaporization with transection of the His bundle into superior and inferior segments. Surrounding areas of coagulation necrosis, hemorrhage, and pyk-

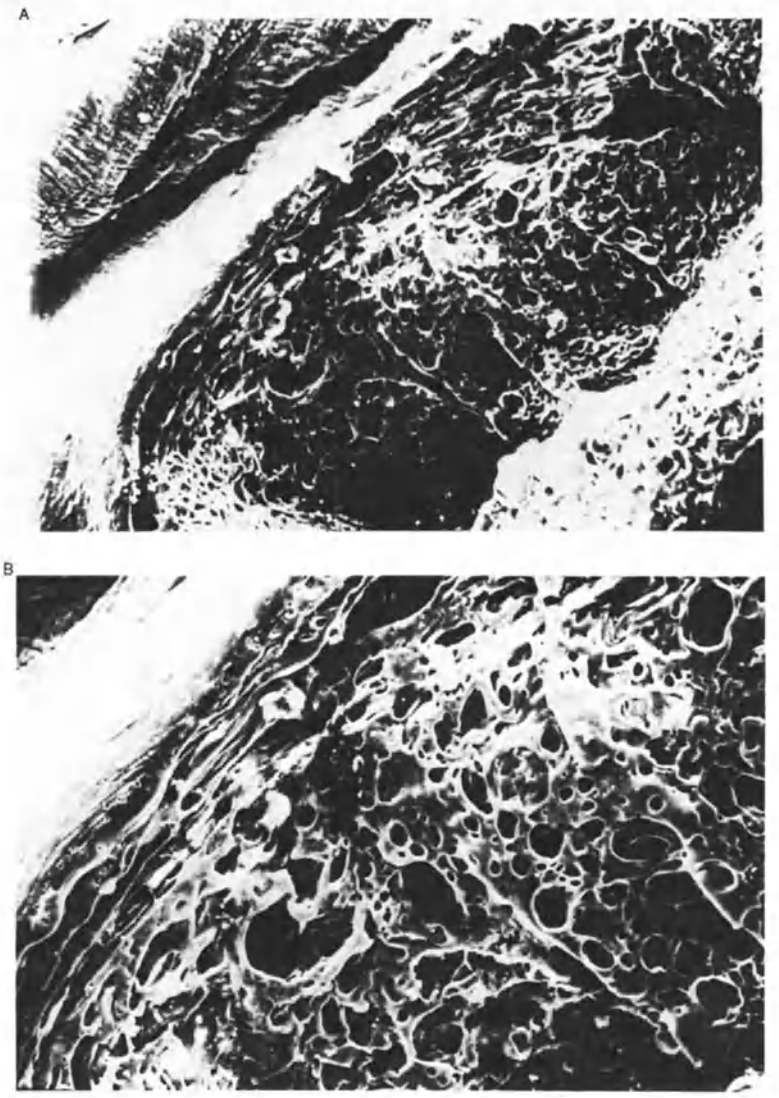

Figure 6–4. Scanning electron micrograph of an argon laser discharge induced lesion in bovine myocardium. Note the irregular surface and ruptured cells due to vaporization of cell water. (Reproduced with premission from The Futura Publishing Co, Mt Kisco, NY, 1986.)
Panel A: Low magnification (50 X).
Panel B: High magnification (300 X).

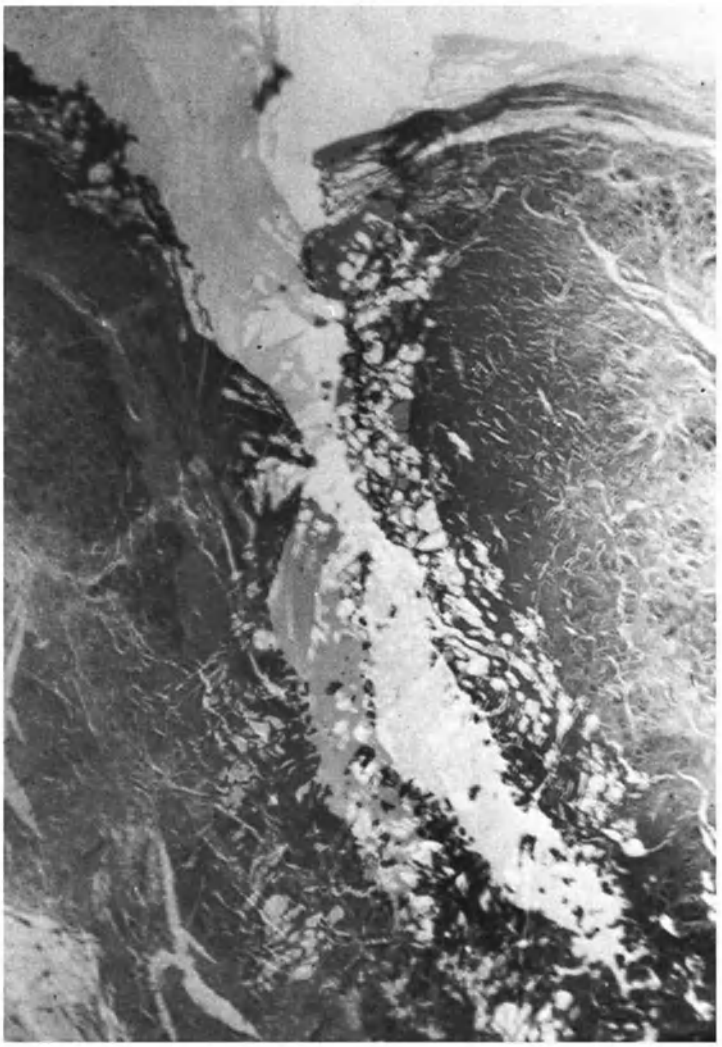

Figure 6–5. Histologic appearance of lesion induced by argon laser discharges in normal human ventricle. Note the deep crater with surrounding coagulation and carbonization. (Reproduced with permission from *The American Heart Journal*, (CV Mosby Co, St. Louis, MO, 1986.)

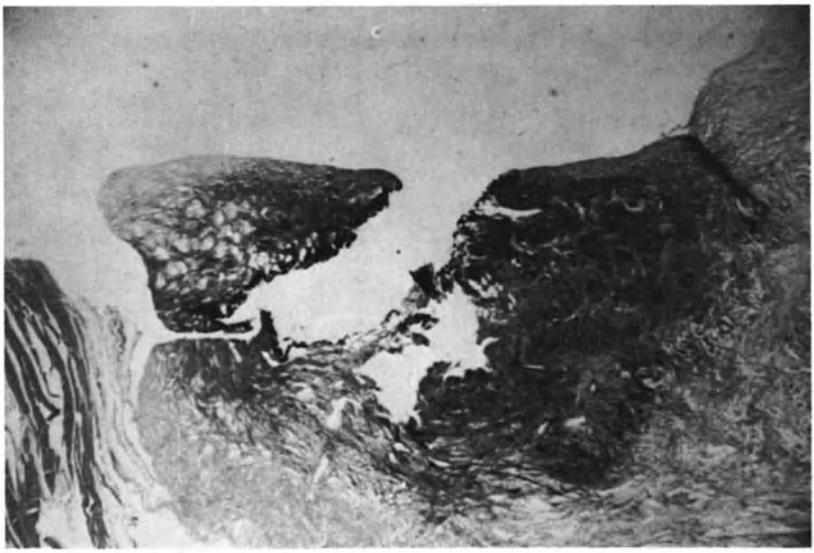

Figure 6–6. Histologic section of a lesion induced by continuous argon laser discharge in diseased human ventricle. Note the shallower crater and the surrounding fibrosis with limited coagulation. (Magnification of photograph 30 X). (Reproduced with permission from *The American Heart Journal*, (CV Mosby Co, St. Louis, MO, 1986.)

nosis of cells of the conduction system are noted along with leukocyte infiltration. The adjoining atrium and ventricle in the septum are often totally unaffected by the laser discharge, indicating the precision of the injury.

Argon laser irradiation of excised human ventricle and atrium has been studied in our laboratory [24]. The lesions observed in normal human ventricle with argon laser irradiation show the central linear crater and surrounding charring and coagulation necrosis (figure 6–5). The nature of the lesion in diseased human ventricle is significantly altered by the nature of the substrate [7, 11] (figure 6–6). The lesion is more superficial, often wider than deeper, and has a limited zone of surrounding coagulation necrosis. Pulsed argon laser ablation of human atrium shows tissue vaporization with crater formation and minimal tissue coagulation (figure 6–7). These lesions in different myocardial tissues are all characterized by the precise and focal nature of the injury without extensive surrounding effects.

The qualitative nature of the lesions obtained with other laser energy sources has also been analyzed. Nd-YAG laser induced lesions have been noted to produce coagulation necrosis of ventricular myocardium at moderate energies and at higher energies produce tissue vaporization and crater formation with charring and coagulation of the surrounding areas [9, 25]. The CO_2 laser produces tissue vaporization, creating channels in ventricular

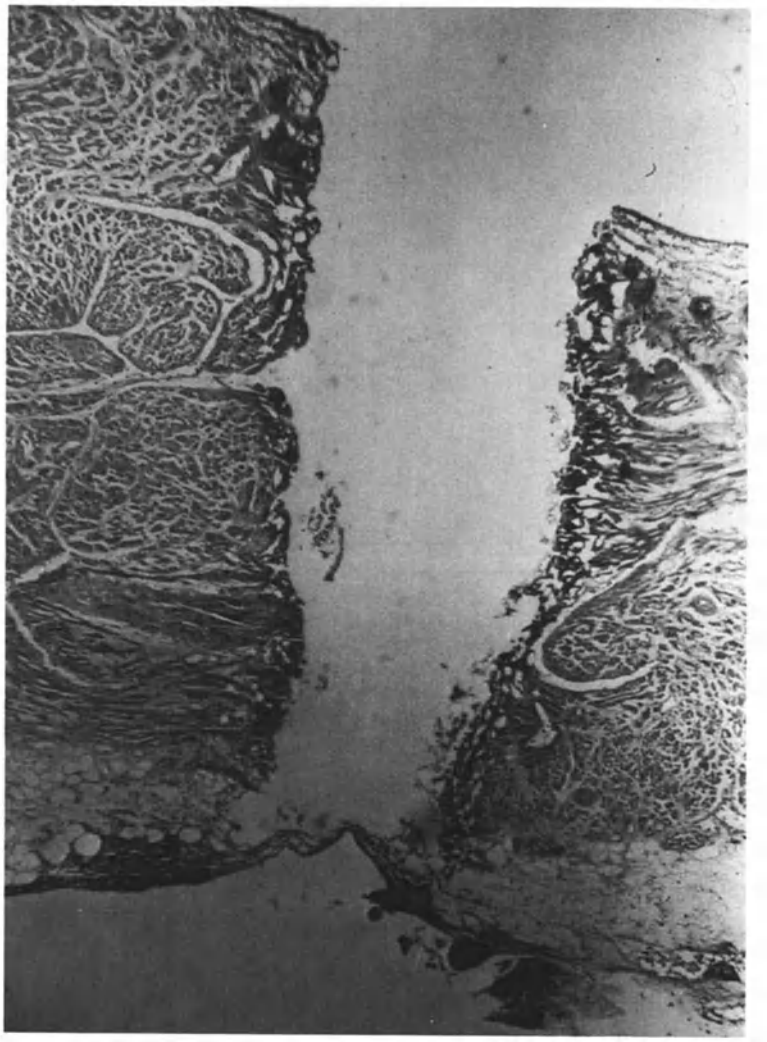

Figure 6–7. Histologic appearance of lesion induced by pulsed argon laser discharges in human atrium. Note the central vaporized region, surrounded by carbonization and coagulation, with preservation only of the epicardial atrial myocardium. (Original magnification 30 X.)

myocardium with little surrounding coagulation necrosis [26, 27]. The excimer laser produces only tissue vaporization with no tissue charring and coagulation necrosis in excised normal ventricular myocardium [8]. Downar et al performed endocardial photoablation using a xenon chloride excimer laser and were able to produce rapid and precise vaporization of normal

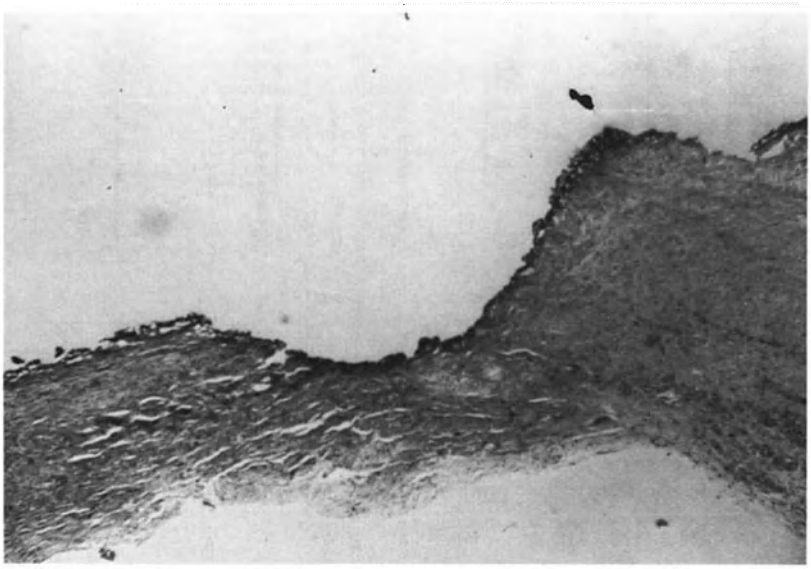

Figure 6–8. Histologic section of a lesion induced by pulsed argon laser discharges in a patient undergoing intraoperative laser ablation of ventricular tachycardia. Note the crater with little carbonization in diseased human ventricle (magnification of photograph 30 X).

porcine myocardium [28]. However, they noted a marked attenuation of ablative effect in diseased ventricle after myocardial infarction. Thus, there appears to be a spectrum of tissue lesions which ranges from photocoagulation to vaporization of myocardial tissue. The qualitative nature of the lesion to be created can be selected by the use of the appropriate laser energy source. Alternatively, in the case of certain laser energy sources, e.g., argon, lesion characteristics can be modified by altering the laser energy delivery technique or the medium of application [14–16, 20]. *High-power pulsed* argon laser discharges reduce the extent of carbonization and coagulation and permit vaporization of normal and abnormal myocardium [16, 20]. Pulse durations below one second markedly reduce the extent of tissue carbonization and coagulation. However, *low-power* short duration pulses can be used to produce tissue coagulation without vaporization. This may be useful in specific tissues, e.g., atrium, when excessive vaporization may result in perforation.

Clinical application of argon laser ablation in man has confirmed the nature of the acute lesion obtained in vivo. Figure 6–8 is a histologic section of a ventricular lesion produced by pulsed argon laser discharges during intraoperative ablation of a ventricular tachycardia focus in a patient with refractory sustained ventricular tachycardia. Note that the actual lesion obtained has great similarity to those observed during experimental studies. There is

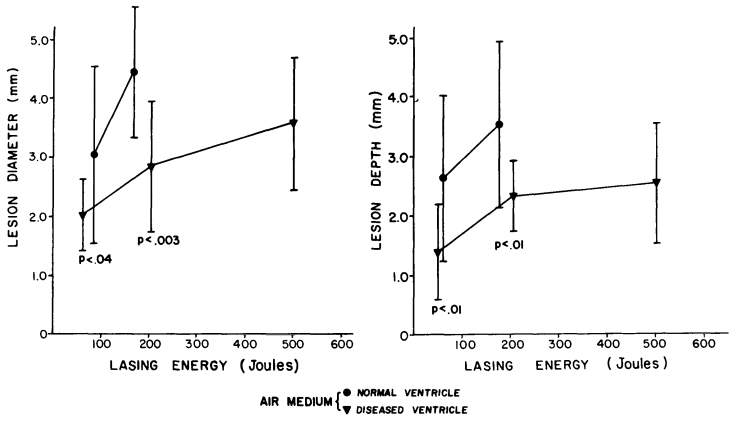

Figure 6–9. Laser energy dose-lesion dimension relationship in normal and diseased human ventricle. The lesion size increases with increasing delivered energy but is larger in normal than diseased ventricle. (Reproduced with permission from *The American Heart Journal*, CV Mosby Co, St. Louis, MO, 1986.)

minimal carbonization, and vaporization of diseased myocardium results in a superficial crater.

The quantitative aspects of argon laser discharge energy and tissue lesion dimensions have been examined in animal and human ventricle [3, 4, 7, 11]. The effects of different superfusing media have been examined [7, 11]. Similar data have been generated in experimental animal studies for an Nd-YAG laser energy source, but human data are not currently available. For argon laser discharges, increasing lesion dimensions are observed with increasing laser energy in the 10 joule to 300 joule range [7, 11]. These dimensions are substantially greater in normal human ventricle than in diseased human ventricle (figure 6–9). Furthermore, little or no increase is observed with energies over 300 joules in diseased human ventricle. The use of different superfusing media, e.g., saline, can reduce the lesion depth significantly. The use of a blood medium, however, produces little or no alteration of lesion size but in vivo may enhance lesion size [7, 20, 25]. The effect of varying argon laser power output has also been examined [14, 15]. Lesion dimensions remain largely comparable in human ventricle at comparable total delivered energies with laser power below or above 5 watts. This implies that high power discharges can be employed for rapid laser ablation in myocardial tissues, e.g., diseased human ventricle.

The photoproducts of laser irradiation of human myocardium have been analyzed [29]. These are consistent with thermal degradation and include protein and heterocyclic ring fragments of myoglobin, and gaseous products including hydrogen, carbon monoxide, and some organic gases. These products are water soluble and rarely result in bubble formation.

The possibility of myocardial perforation with the argon laser discharges can be defined from our experimental data [7, 11, 20]. In human atrium, perforation can be observed with delivery of energies over 25 joules at one site [24]. In normal human ventricle, delivered energies up to 300 joules at a single site do not produce perforation. In diseased human ventricle, perforation is not observed even with energies up to 1000 joules. Intraoperatively, we have employed energies up to 339 J/cm^2 in myocardial tissues without adverse effects.

The healing of laser-induced lesions in human tissues has been examined [30]. Limited data are available in cardiovascular tissues [31]. Argon laser irradiation of canine ventricle produces little scarring, with reendothelialization of the irradiated region and no aneurysm formation [32]. Nd-YAG laser discharges induce greater degrees of fibrosis [9]. Endocardial and subendocardial interstitial fibrosis is observed with replacement of normal myocardium [9]. Mural thrombosis is rarely observed during short-term and long-term follow-up [9, 32]. Thus, the risk of embolization appears small.

Physiologic effects of laser radiation in cardiac tissues

The functional effects of laser radiation in cardiac tissues are presently under active investigation. Experimental studies have examined the electrophysiologic and hemodynamic effects of laser discharges. Recently, clinical studies performed at our institution have also evaluated the electrophysiologic and hemodynamic effects in patients with recurrent supraventricular and ventricular tachycardias [20, 32, 33].

Electrophysiologic effects

The electrophysiologic effects of laser irradiation of myocardial tissues are due to loss of electrical activity in the exposed tissue. This may be due to disruption of cellular structure by tissue vaporization and/or coagulation necrosis. In elegant in vitro microelectrode studies, Merillat and coworkers demonstrated loss of electrical activity using recordings of single cell and extracellular cardiac action potentials after laser irradiation of animal ventricle [34]. This effect was extremely precise, being localized to the immediately exposed tissue with preservation of normal electrical function of surrounding ventricular myocardium. In contrast, electrical ablation shocks produced loss or alteration of electrical activity at the site of application and for varying distances from this site. Thus, the theoretical advantage of laser ablation would be absence of a significant border zone of delayed conduction which could provide a substrate for future reentrant arrhythmias. Laser ablation interrupts conduction and suppresses automaticity. Laser irradiation of the canine specialized atrioventricular conduction system results in the immediate production of atrioventricular block, which can persist during long-term follow-up [6]. In addition, incomplete transection of the bundle of His can

result in second and first degree atrioventricular block, which may permit controlled modification of atrioventricular conduction rather than total interruption of atrioventricular conduction [6]. In animal experiments, in vivo application of laser discharges can result in induced ventricular premature depolarizations and short bursts of nonsustained ventricular tachycardia [9]. The incidence of induced ventricular fibrillation by the laser discharge in an animal model was low (4%). Pacing induced ventricular tachycardia in a canine infarction model has been successfully suppressed after laser ablation [10]. The chronic electrophysiologic effects of laser irradiation of myocardium are not well studied. Narula et al noted persistence of induced atrioventricular block by laser irradiation for periods of up to one year after laser ablation of the specialized conduction system [31].

Hemodynamic effects

The hemodynamic effects of laser ablation have been examined in experimental studies by Lee and coworkers [9]. They performed two-dimensional echocardiograms before, during, and after laser discharge in normal dogs. During laser discharge there was echocardiographic evidence of intracavitary microcavitation, i.e., bubble formation within the blood pool in the majority (66%) of laser discharges. This finding was unaffected by the amount of energy or catheter type used at the time of discharge and was felt to represent the effects of laser energy on the blood pool in its path or in adjoining areas. These microcavitations occurred initially at the fiber tip and then resulted in opacification of the left ventricular blood pool. Subsequently, the left ventricular myocardium was opacified, probably related to coronary artery perfusion by the microcavitations. No wall motion abnormalities were detected with energies of 40 joules to 80 joules in the majority of animals. Minimal hypokinesis occurred in 26% of animals and akinesis in 6% at the site of laser discharge. Overall left ventricular function was minimally depressed or unchanged after laser discharge at these energies and was unaffected by myocardial opacification by microcavitations.

CLINICAL APPLICATION OF LASER ABLATION TECHNIQUES

The laser technique has been employed in patients with recurrent tachyarrhythmias for intraoperative arrhythmia ablation. Early reports have employed argon and neodymium-YAG laser energy sources. In our studies, the argon laser was coupled to a quartz optical fiber ensheathed in a cardiac catheter. Thus, a hand-held intraoperative laser catheter technique was employed (figure 6–10). Our initial clinical experience with intraoperative laser ablation was obtained in five patients with refractory sustained ventricular tachycardia. These patients had failed five to seven electrophysiologically-guided drug trials prior to surgery. All patients had coronary artery disease and four had left ventricular aneurysms. The mean left ventricular ejection

Figure 6–10. Intraoperative laser ablation of a ventricular tachycardia focus in a patient with coronary artery disease and refractory ventricular tachycardia. The surgeon employs a hand-held argon laser catheter to ablate an endocardial region in the left ventricle. Note the tissue vaporization observed during the procedure.

fraction for this patient group was 31 ± 13%. Preoperative and intraoperative mapping was employed for localization of the ablation site. Presystolic electrical activity during induced ventricular tachycardia was mapped, and endocardial sites exhibiting these potentials were ablated. High-power pulsed argon laser discharges were employed. A laser ventriculotomy was performed in four patients, followed by endocardial mapping and laser ablation in all patients. After ablation, reinduction of ventricular tachycardia was attempted. If additional ventricular tachycardia morphologies were induced, these were also mapped and ablated. Mapping-guided laser ablation was performed alone at six sites and in combination with subendocardial resection at one site. The total delivered energies ranged from 85 J/cm^2 to 339 J/cm^2. Five of the seven ventricular tachycardia sites of origin in the original patient group were considered unresectable by standard surgical techniques. Laser ablation of these five ventricular tachycardia sites within the posterior papillary muscle (three patients) or high intraventricular septum (two patients) was performed. All patients had inducible sustained ventricular tachycardia preoperatively and suppression of spontaneous inducible ventricular tachycardia was achieved in all patients postoperatively. Six of the seven ventricular tachycardia morphologies were not inducible in the absence of antiarrhythmic therapy postoperatively. One morphology was suppressed with

a previously ineffective drug (procainamide). In this patient, the lowest laser energy dose (85 J/cm^2) was delivered due to concern regarding disruption of the posterior papillary muscle site of origin and postoperative mitral valvular dysfunction. Figures 6–11A and 6–11B are examples of a preoperative and postoperative electrophysiologic study, respectively, in a patient who underwent intraoperative laser ablation of two ventricular tachycardia sites. One site was in the lateral left ventricle and the other in the high intraventricular septum. Note the suppression of inducible ventricular tachycardia after laser ablation. Inferior and septal ventricular tachycardia foci are frequent (up to 70% in a recent series) [35]. The surgical resectability and success in arrhythmia ablation at these sites is low [35–37]. The intraoperative laser ablation approach could enhance efficacy of surgical ablation procedures for ventricular tachycardia by making these sites accessible for ablation [35, 37].

The clinical electrophysiologic effects of laser ablation have been examined during intraoperative studies in our patients with sustained ventricular tachycardia [32]. Intraoperative ventricular electrograms recorded from the laser ablation site in patients with ventricular tachycardia prior to ablation often demonstrated delayed and fragmented potentials. After laser ablation, subjacent tissues showed preservation of normal ventricular electrogram recordings (figure 6–12). This indicates the limited nature of the electrophysiologic effects in surrounding tissues, which is consistent with experimental data [34]. Transmural needle electrode recordings of epicardial ventricular activity during laser ablation showed no change during endocardial ablation on the epicardial electrograms.

In our initial patient with malignant supraventricular tachyarrhythmias and the Wolff-Parkinson-White syndrome, a laser atriotomy and interruption of a left posterolateral accessory atrioventricular connection was performed. Figures 6–13A, 6–13B, and 6–13C show the preoperative electrocardiograms and electrophysiology study in this patient. Preoperatively, a typical preexcitation ECG pattern was observed (figure 6–13A). The patient presented with spontaneous atrial fibrillation with antegrade bypass tract conduction and rapid ventricular rates varying from 250 beats per minute to 300 beats per minute. The shortest RR interval was 180 ms (figure 6–13B). This resulted in a cardiac arrest requiring electrical cardioversion. Electrophysiologic studies performed preoperatively showed induction of paroxysmal supraventricular tachycardia by single ventricular extrastimuli during ventricular pacing (figure 6–13C). This rapidly degenerated into atrial fibrillation with antegrade accessory bypass tract conduction and was associated with hemodynamic collapse. The earliest retrograde atrial activation during supraventricular tachycardia was observed in the distal coronary sinus. During laser ablation, a 4 cm incision was performed above the mitral annulus using *low-power* pulsed argon laser discharges to detach the atrium from the annulus followed by mechanical dissection. The postoperative electrogram showed

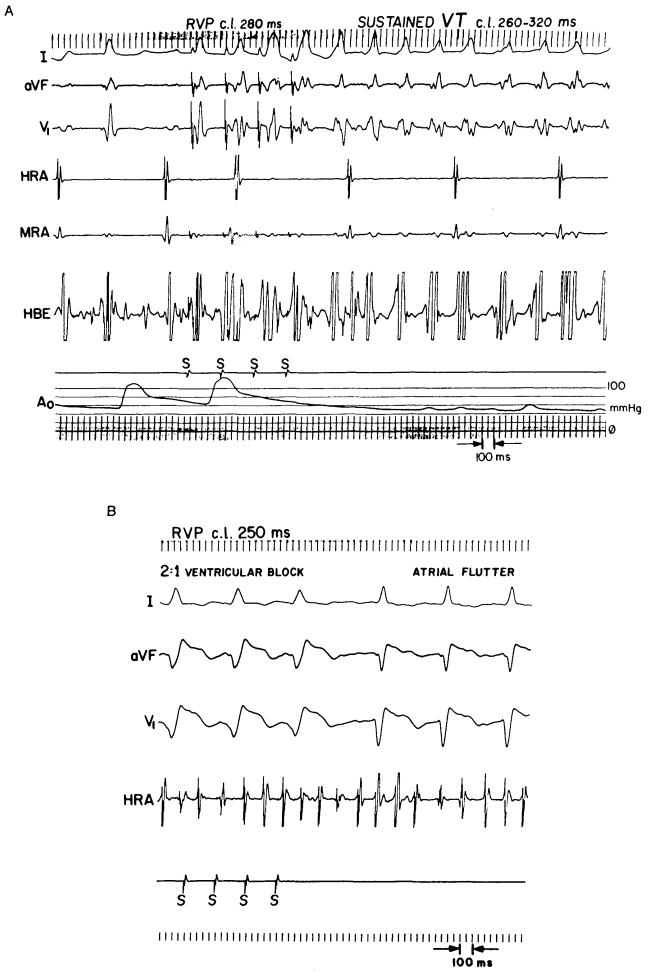

Figure 6–11. *Panel A*: Preoperative electrophysiologic study in a patient with refractory sustained ventricular tachycardia, showing induction of sustained ventricular tachycardia with rapid ventricular pacing.
Panel B: Postoperative electrophysiologic study in the same patient showing no inducible ventricular tachycardia with rapid ventricular pacing up to ventricular refractoriness.
Abbreviations: RVP = rapid ventricular pacing; VT = ventricular tachycardia; C.L. = cycle length; HRA = high right atrium; MRA = mid-right atrium; HBE = His bundle electrogram; Ao = aorta; S = pacing stimulus.

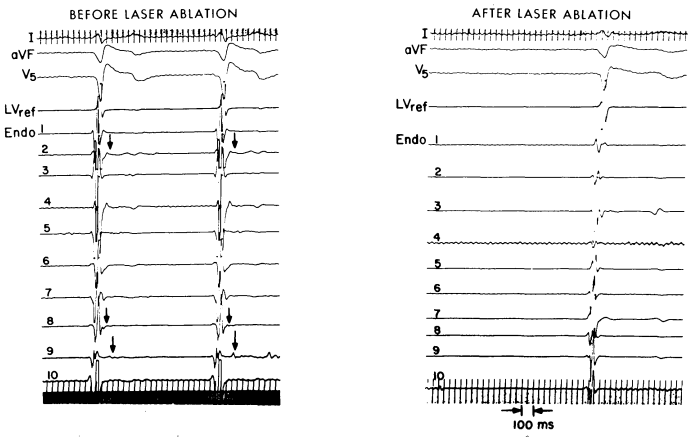

Figure 6–12. Bipolar ventricular electrogram recordings from the endocardial ablation site during sinus rhythm before and after intraoperative laser ablation in a patient with refractory sustained ventricular tachycardia. Abbreviations: LVref = reference electrode; Endo = endocardial ventricular electrograms from ablation site.

disappearance of the delta wave and reappearance of normal atrioventricular conduction (figure 6–14A). Postoperative electrophysiologic study showed resumption of normal retrograde ventriculoatrial nodal conduction, which decremented during ventricular extrastimulation. There was no inducible supraventricular tachycardia during atrial or ventricular stimulation, and abolition of antegrade and retrograde bypass tract conduction (figure 6–14B).

Mesnildrey and coworkers first reported the use of non-map-guided Nd-YAG laser encircling ventriculotomy in 12 patients with sustained ventricular tachycardia [38]. Continuous Nd-YAG laser discharges were employed. Successful ventricular tachycardia suppression was achieved with this approach in nine patients, but two patients died of a low cardiac output state postoperatively. The investigators ascribed the success of this technique in these nine patients to thermoexclusion of the arrhythmogenic substrate by

Figure 6–13. *Panel A*: Preoperative ECG in a patient with malignant supraventricular tachyarrhythmias and the Wolff-Parkinson-White syndrome. Note the preexcitation pattern in sinus rhythm.
Panel B: Preoperative spontaneous atrial fibrillation with antegrade bypass tract conduction resulting in cardiac arrest in this patient. The slowest RR interval was 180 ms.
Panel C: Preoperative electrophysiologic study in the same patient. Note the induction of sustained reciprocating tachycardia with programmed ventricular extrastimulation. The earliest retrograde atrial activation is shown in the distal coronary sinus recording. The reciprocating tachycardia degenerated rapidly into atrial fibrillation, which resulted in hemodynamic collapse. Abbreviations: CSp = proximal coronary sinus; CSd = distal coronary sinus; RVP = rapid ventricular pacing; VT = ventricular tachycardia; C.L. = cycle length; HRA = high right atrium; MRA = mid-right atrium; HBE = His bundle electrogram; Ao = Aorta; S = pacing stimulus; EPS = electrophysiologic study.

A

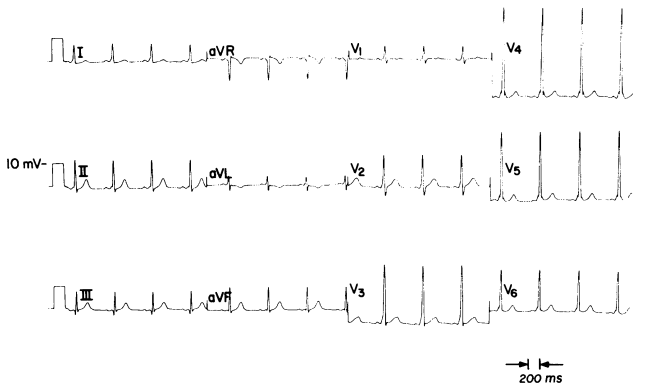
I
aVR
V1
V4
10 mV
II
aVL
V2
V5
III
aVF
V3
V6
200 ms

B

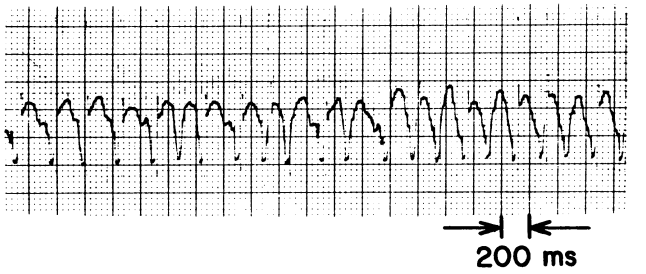
200 ms

C

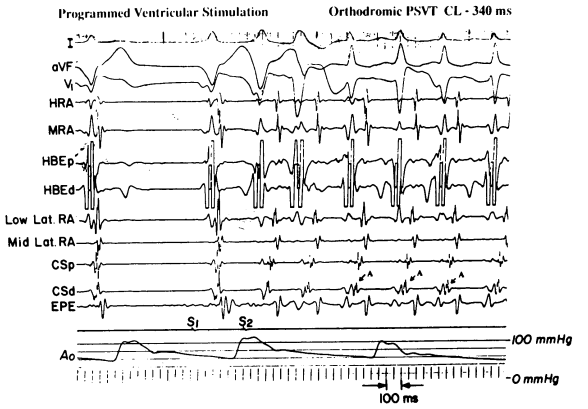
Programmed Ventricular Stimulation
Orthodromic PSVT CL - 340 ms
I
aVF
V1
HRA
MRA
HBEp
HBEd
Low Lat. RA
Mid Lat. RA
CSp
CSd
EPE
S1
S2
Ao
100 mmHg
0 mmHg
100 ms

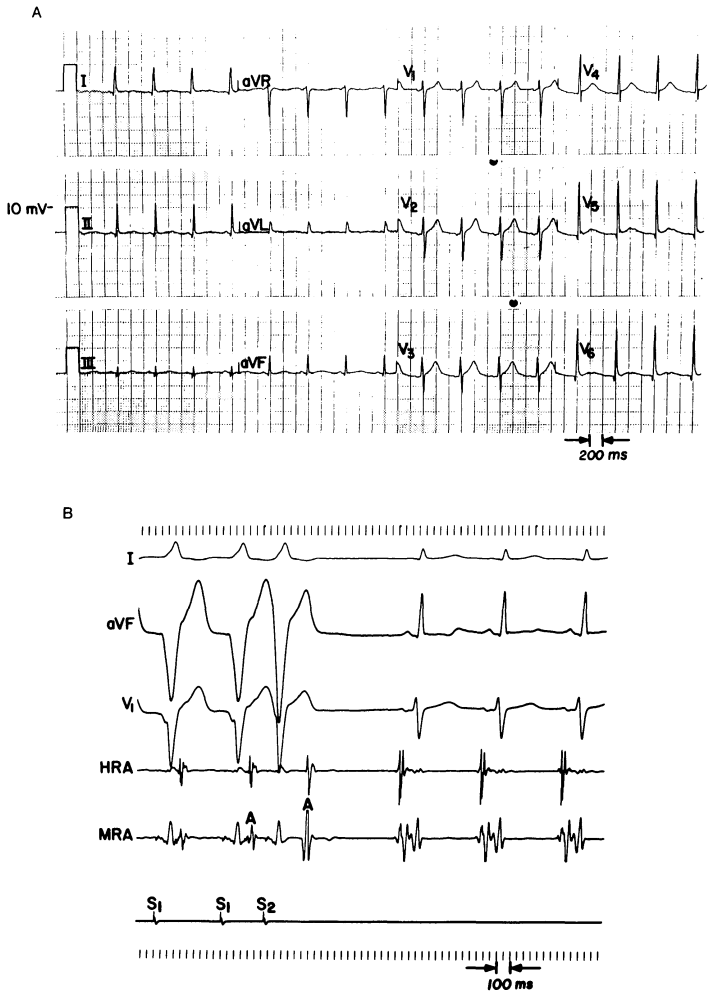

Figure 6–14. *Panel A*: Postoperative ECG in the same patient as in figure 6–13. Note disappearance of delta wave.
Panel B: Postoperative electrophysiologic study in the same patient shown in figure 6–12 with no inducible supraventricular tachycardia. Note the reappearance of normal decremental retrograde ventriculoatrial conduction.

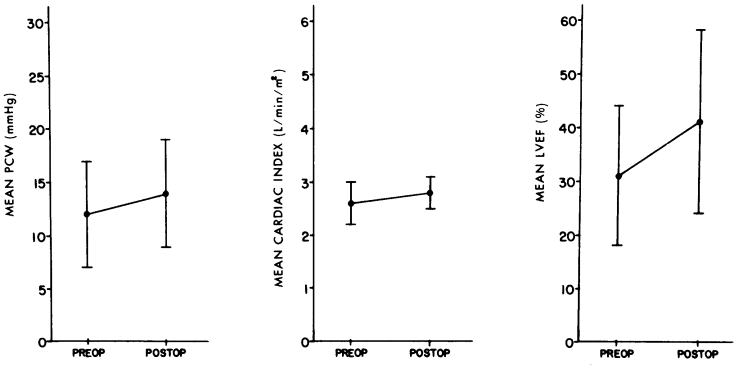

Figure 6–15. Hemodynamic indices before and after laser ablation in the initial five patients with coronary artery disease and refractory ventricular tachycardia. Abbreviations: PCW = pulmonary capillary wedge pressure.

the Nd-YAG laser technique. Similarly, Svenson and coworkers have employed photocoagulation with an Nd-YAG laser during intraoperative resection of ventricular tachycardia foci in five patients with encouraging results [39]. The long-term electrophysiologic and hemodynamic effects of these two approaches need to be evaluated.

Clinical studies on left ventricular function preceding and after argon laser ablation in patients with sustained ventricular tachycardia have been performed at our center. Figure 6–15 shows our initial experience using standard indices of hemodynamic function in these patients. Mean pulmonary capillary wedge pressure, cardiac index, and global left ventricular ejection fraction are unchanged after argon laser ventriculotomy and ablation of ventricular tachycardia foci. Two-dimensional echocardiograms after ablation do not show any new wall motion abnormality, mitral regurgitation by Doppler, or mural thrombosis. Postoperatively, all patients have been discharged in functional class II. In the patient with supraventricular tachycardia and the Wolff-Parkinson-White syndrome, no wall motion abnormality or mitral regurgitation was observed. He was discharged in functional class I. While information on the long-term hemodynamic effects of Nd-YAG laser photoablation is more limited, there appears to be no change in left ventricular ejection fraction in patients with ventricular tachycardia [39]. Its effects in patients with supraventricular tachycardia are presently unknown.

POTENTIAL ROLE OF LASER ABLATION TECHNIQUES

Laser ablation techniques have been applied intraoperatively and have the potential to be developed for catheter ablation of tachycardias. In the former application, they would serve as an adjunct to conventional surgical resection

techniques. They could be valuable when mechanically unresectable ventricular tachycardia foci are present, particularly when mitral valve replacement or interventricular septal disruption needs to be avoided. This is particularly important since posterior, inferior, and septal foci constitute up to two-thirds of all foci encountered [35]. Their limited hemodynamic effects may be useful in patients with multiple disparate ventricular tachycardia foci requiring ablation and poor left ventricular function. The bloodless nature of the incision may be useful for patients with accessory bypass tracts. It is more precisely controlled and rapid than cryothermal ablation and can be visually and electrically guided. This may be particularly useful in accessory pathway or conduction system ablation. The risk for myocardial perforation appears to be considerably lower than for coronary artery perforation [40]. However, the need for careful adherence to experimentally developed laser energy dose-tissue response relationships should be emphasized. In other surgical arenas, serious complications have been encountered when safe parameters for laser power and time of application have been exceeded using the Nd-YAG laser [41]. These are presumed to be due to the uncontrolled thermal effects of the laser. The continuous wave mode is difficult to control and pulsed delivery techniques appear preferable.

Catheter ablation using laser energy can be feasible when appropriate guiding catheter systems are developed for directing the laser beam [6, 9]. These could include electrically-guided or visually-guided systems alone or in combination. The ability for active fixation with such a catheter system would be highly desirable. The efficacy of the catheter ablation technique will also be dependent on the amount and type of myocardium to be ablated. Intraoperative studies will be extremely valuable for delineating the future needs for catheter ablation techniques. The extent of ablation required for conduction system or accessory tract ablation will be considerably smaller than for ventricular tachycardia ablation. Specific steerable catheter systems will need to be designed for use in different cardiac locations, particularly with laser energy, to obtain clinical efficacy and safety. With catheter techniques, the time required for laser ablation will be of greater importance. For this purpose, high-power laser discharges may be required in diseased human ventricle. High-power pulsed laser energy delivery offers rapid ablation [15]. However, safety issues may limit the use of the pulsed mode to moderate rates and ultrarapid pulsing may offer lesser degrees of control. Due to the substantial cost of laser energy sources, adaptation of the same source to supraventricular and ventricular tachycardia ablation will require continued careful evaluation of different energy delivery techniques. Flexibility of use will be important, and very high power lasers may be disadvantageous in these respects. Finally, a greater understanding of the biologic phenomena involved in the interaction of laser energy and human myocardium will help refine the technique for clinical application.

REFERENCES

1. Gonzalez R, Scheinman MM, Margaretten W, Rubeinstein M: Closed chest electrode catheter techniques for His bundle ablation in dogs. *Am J Physiol* 241: 283–289, 1981.
2. Harrison L, Gallagher JJ, Kasell J, Anderson RH, Mikat E, Hackel DB, Wallace AG: Cryosurgical ablation of the A-V node-His bundle — A new method for producing A-V block. *Circulation* 55: 463–470, 1977.
3. Lee, G, Ikeda RM, Theis J, Stobbe D, Ogata C, Lui H, Reis RL, Mason DT: Effects of laser irradiation delivered by flexible fiberoptic system on the left ventricular internal myocardium. *Am Heart J* 106: 587–590, 1983.
4. Saksena S: Cardiovascular applications of laser technology. *Cardio* 1: 27–31, 1984.
5. Abela GS, Griffin JC, Hill JA, Normann S, Conti CR: Transvascular argon laser induced atrioventricular conduction ablation in dogs. (abstract) *Circ* 68 (Suppl III): II–145, 1983.
6. Narula OS, Bharati S, Chan MC, Embi AA, Lev M: Microsection of the His bundle with laser radiation through a pervenous catheter: Correlation of histologic and electrophysiologic data. *Am J Cardiol* 54: 186–192, 1984.
7. Saksena S, Ciccone JM, Chandran P, Rothbart ST, Pantopoulos D, Lee B: Laser ablation of normal and diseased human ventricle. (abstract) *JACC* 5: 473, 1985.
8. Isner JM, Donaldson RF, Deckelbaum LI, Clarke RH, Laliberte SM, Ucci AA, Salem EN, Konstam MA: The excimer laser: Gross, light microscopic and ultrastructural analysis of potential advantages for use in laser therapy of cardiovascular disease. *JACC* 6: 1102–1109, 1985.
9. Lee B, Gottdiener JS, Fletcher RD, Rodriguez ER, Ferrans VJ: Transcatheter ablation: Comparison between laser photoablation and electrode shock ablation in the dog. *Circulation* 71: 579–586, 1985.
10. Vincent JM, Hunter J, Dixon J, Fox J: Neodymium YAG laser ablation of stimulated ventricular tachycardia in a canine model. *Lasers in Surg & Med* 5: 168–172, 1985.
11. Saksena S, Ciccone J, Chandran P, Pantopoulos D, Lee B, Rothbart ST: Laser ablation of normal and diseased human ventricle. *Am Heart J* 112: 52–60, 1986.
12. Ciccone JM, Saksena S, Pantopoulos D. Comparative efficacy of continuous and pulsed argon laser ablation of human diseased ventricle. *PACE* 8: 318, 1986.
13. Saksena S: Argon laser ablation of human ventricle: Dose response studies in normal and diseased tissues. In: *Fulguration and Laser*, G Fontaine, MM Scheinman, eds. (in press), 1986.
14. Saksena S, Rothbart ST, Calvo RA, Pantopoulos D: Effects of varying laser power output on laser ablation of human diseased ventricle. (abstract) *Clin Res* 34: 341A, 1986.
15. Saksena S, Calvo RA, Rothbart ST, Pantopoulos D: High power rapid pulsed argon laser ablation of diseased human ventricle. (abstract) *PACE* 9: 299, 1986.
16. Saksena S, Calvo RA, Gadhoke A, Pantopoulos D: Comparison of continuous wave and high power pulsed argon laser ablation in diseased human ventricle. (abstract) *Clin Res* 34: 340A, 1986.
17. Saksena S, Gadhoke A, Hussain SM: Feasibility of intraoperative laser ablation of ventricular tachycardia: Studies in intact animal ventricle and diseased human ventricle resected from patients with ventricular tachycardia. *New Trends in Arrhythmias* 2: 285–292, 1986.
18. Ben-Shachar G, Sivakoff MC, Bernard SL, Sahms BB, Reimenschneider TA: Acute continuous argon-laser induced tissue effects in the isolated canine heart. *Am Heart J* 110: 65–70, 1985.
19. Lee G, Ikeda RM, Stobbe D, Ogata D, Theis J, Hussein H, Mason DT: Laser irradiation of human atherosclerotic obstructive disease: Simultaneous visualization and vaporization achieved by a dual fiberoptic catheter. *Am Heart J* 195: 163–164, 1983.
20. Saksena S, Gadhoke A: Laser therapy for tachyarrhythmias: A new frontier. *PACE* 9: 531–550, 1986.
21. Fenoglio JJ, Pham TD, Harken AH: Recurrent sustained ventricular tachycardia: Structure and ultrastructure of subendocardial regions in which tachycardia originates. *Circulation* 68: 518–533, 1983.
22. Eldar M, Battler A, Neufeld HN, Gaston E, Aneli R, Akelsrod S, Levite A, Katziz A: Transluminal carbon dioxide laser catheter angioplasty for dissolution of atherosclerotic plaques. (abstract) *J Am Coll Cardiol* 3: 135, 1984.

23. Eldar M, Battler A, Gad D, Rath S, Rotstein Z, Neufeld HN, Akelsrod S, Katziz A, Gaton E, Wolman M: The effects of varying lengths and powers of CO_2 laser pulses transmitted through an optical fiber on atherosclerotic plaques. *Clin Cardiol* 9: 89–91, 1986.
24. Gadhoke A, Saksena S: Laser ablation of human atrium: Implications for therapy of supraventricular tachycardia. (Submitted for publication), 1986.
25. Lee BI, Rodriguez ER, Notargiocomo A, Ferrans VJ, Chen Y, Flether RD: Thermal effects of laser and electrical discharges on cardiovascular tissue: Implications for coronary artery recanalization and endocardial ablation. *JACC* 8: 193–200, 1986.
26. Mirhoseini M, Cayton MM: Revascularization of the heart by laser. *J Microsurg* 2: 253–260, 1981.
27. Owen ER, Canfield P, Bryand K, Hopwood PR: Observations on the effects of CO_2 laser on rat myocardium. *Microsurgery* 5: 140–143, 1984.
28. Downar E, Butany J, Jares A, Storcheff BP: Endocardial photoablation by excimer laser. *JACC* 7: 546–550, 1986.
29. Isner JM, Clarke RH, Donaldson RF, Aharon A: Identification of photoproducts liberated by in vitro argon laser irradiation of atherosclerotic plaque, calcified cardiac valves and myocardium. *Am J Cardiol* 55: 1192–1196, 1985.
30. Yellin AE, Dwyer RM, Craig JR, Blass M, Cherlow J: Endoscopic argonion laser phototherapy of bleeding gastric lesions. *Arch Surg* 111: 750–754, 1986.
31. Narula OS, Boveja BK, Cohen DM, Tarjan PP: Laser catheter induced AV nodal delays and block: Acute and chronic studies. (abstract). *Circulation* 70 (Suppl II): II–99, 1984.
32. Saksena S, Hussain SM, Gielchinsky I, Gadhoke A, Pantopoulos D: Intraoperative mapping-guided argon laser ablation of malignant ventricular tachycardia. *Am J Cardiol* (in press), 1986.
33. Saksena S: Laser ablation of tachycardias — experimental basis and preliminary clinical application. *Proc Internat Symp Non-Pharmacol Ther Tachyarrhythmias, Dusseldorf*, (in press), 1986.
34. Merillat JE, Levine JH, Weisman HF, Stern MD, Spear JF, Moore EN, Kadish AA, Fonger J, Guzman R, Guarnieri T: Laser ablation leads to more focal electrophysiologic effects compared to catheter delivered high energy ablation. (abstract). *JACC* 7: 237A, 1986.
35. Borgreffe M, Breithardt G: Multicenter study on the surgical ablation of ventricular tachycardia. *Proc Intl Symp Non-Pharmacol Ther Tachyarrhythmias, Dusseldorf*, (in press), 1986.
36. Miller JM, Kienzle MG, Harken AH, Josephson ME: Subendocardial resection for ventricular tachycardia: Predictors of surgical success. *Circulation* 60: 624–631, 1984.
37. Saksena S, Hussain SM, Wasty N, Gielchinsky I, Parsonnet V: Long-term efficacy of subendocardial resection in refractory ventricular tachycardia: Relationship to site of arrhythmia origin. *Ann Thor Surg* (in press), 1986.
38. Mesnildrey P, Laborde F, Piwmica A, Larboisiere F: Encircling thermoexclusion by the Nd-YAG laser without mapping: A new surgical technique for ischemic ventricular tachycardia. (abstract). *Circulation* 72 (Suppl III): III–389, 1986.
39. Svenson R, Gallagher JJ, Selle JG, Sealy WC, Zimmern SH, Fedor JM, Marroun MC, Tatsis GP, Seifert KT, Robisek F: Successful intraoperative mapping-guided Nd-YAG laser ablation of ventricular tachycardia. *JACC* 237A, 1986.
40. Lee G, Seckinger D, Chan MC, Embi AA, Stobbe D, Thompson RV, Sanchez NA, Ikeda RM, Reis RL, Mason DT: Potential complications of coronary laser angioplasty. *Am Heart J* 108: 1577–1579, 1984.
41. Jain KK: Complications of the use of the neodymium-yttrium-aluminum-garnet laser in neurosurgery. *Neurosurgery* 16: 759–761, 1985.

7. RADIOFREQUENCY ENERGY FOR CATHETER ABLATIVE PROCEDURES

FRANK I. MARCUS

Radiofrequency energy is generally considered to range from 150,000 cycles per second or hertz (Hz) or 150 kHz to about 1,000,000 Hz or one megahertz (MHz). There are no finite limits to the radiofrequency range, which can extend up to the infrared range. One terminology used in medicine is to provide specific designations for the various ranges of radiofrequency energy according to their use (table 7–1). All frequencies between 100 kHz and 4 MHz can cut, coagulate, and desiccate tissue, and there appears to be little significant differences in performance. Frequencies below 100 kHz can stimulate muscles and nerves and are not used in electrosurgery. It is difficult to confine electrical currents to wires at frequencies above three to four MHz. Therefore, energy in the radiofrequency range, usually 500 kHz to 750 kHz are most commonly employed in electrosurgical devices. This type of device is often mistakenly called electrocautery. In electrocautery, electrical current not in the radiofrequency range remains in the wire that is heated by the current passing through the wire. In electrosurgery, the electrical current actually passes through the tissue. The radiofrequency current is delivered between an active electrode and a dispersive electrode, usually a large conductive pad placed on the patients skin or the radiofrequency current may pass between bipolar electrodes. The tissue offers resistance to the transmission of the radiofrequency waves, and heat is developed between the electrodes.

Electrosurgical devices can generate a variety of wave forms that are

Table 7–1. Terminology used for various frequencies of electrical energy

Alternating current	50 Hz–60 Hz (cycles/sec)
Audible sound	20 Hz–20,000 Hz
Radiofrequency	150,000 Hz–1,000,000 Hz (150 kHz–1000 kHz)
Ultrasound	1,000,000 Hz–10,000,000 Hz (1 MHz–10 MHz)

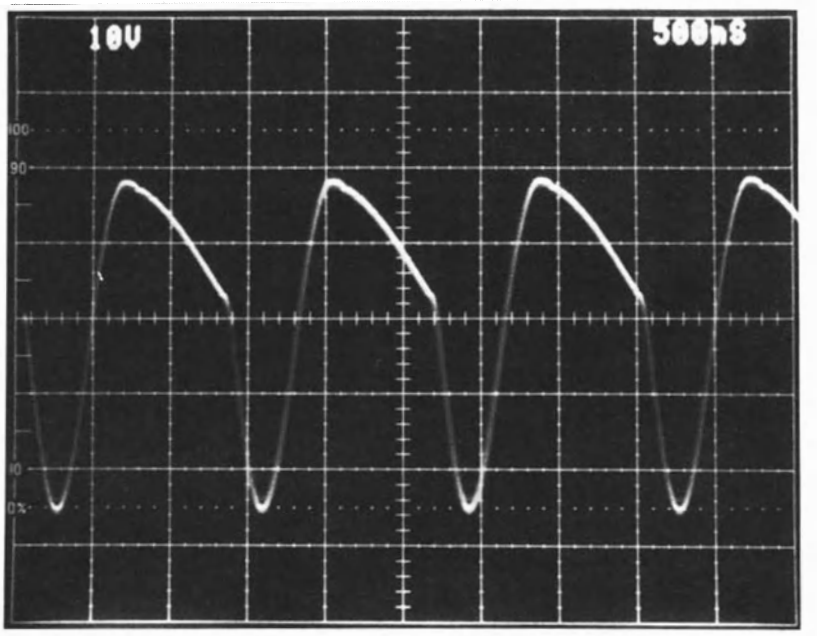

Figure 7–1. A radiofrequency sinusoid wave form at 750 kH^2 at high voltages (maximum peak-to-peak voltage of 2500 V, open circuit). This type of RF energy is used for cutting. At lower voltage (maximum peak-to-peak voltage of 400 V, open circuit), the RF energy is suitable for cardiac ablation. (Reproduced with permission) [1].

used for cutting, coagulation, or ablating tissue. Waveforms used for cutting tissue are sine wave delivered at a high power or watts (figure 7–1) [1]. Cutting involves sparking to tissues. To achieve coagulation, the same frequency sine waves (500 kHz to 750 kHz) are used but in rapid intermittent bursts (20,000 to 35,000 times per second). (figure 7–2) [1]. Since the radiofrequency waves are delivered intermittently, the total power and heat generated is less than with the mode used for cutting. To produce tissue ablation, continuous sine waves in the radiofrequency range are used but at low voltage. In this application tissue is heated but desiccation is not sufficiently complete to cause sparking. If the tissue in contact with the electrode becomes charred, the result will be a sharp rise in impedance, since dry tissue does not conduct

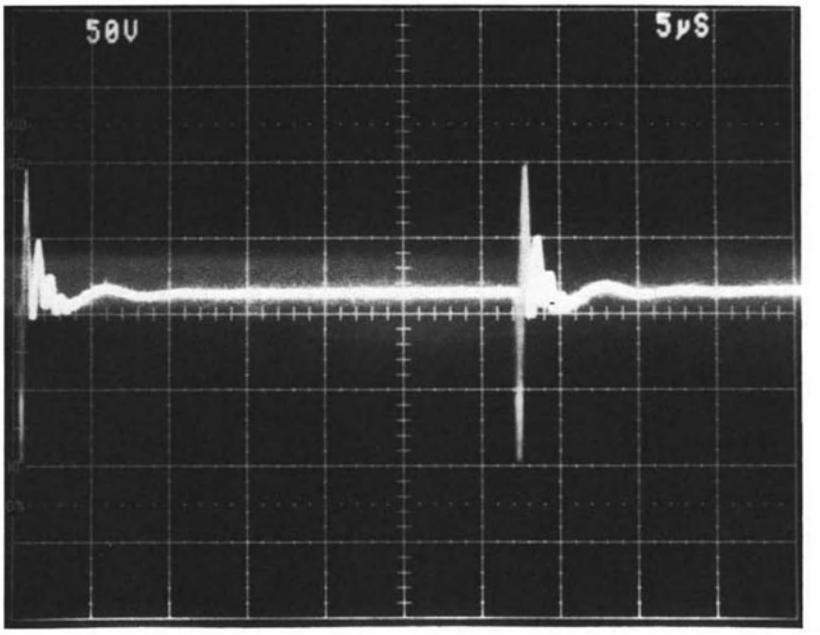

Figure 7–2. 740 kHz damped sinusoid bursts with a repetition frequency of 30 kHz. This illustrates a wave form used for coagulation. The maximum peak-to-peak voltage may be high (900 V, open circuit). This form could cause undesirable charring and adhesion between the catheter tip and cardiac tissue. (Reproduced with permission) [1].

electricity well and current flow will decrease rapidly or stop. It is important to use the minimal amount of current to cause tissue injury. The heat produced in tissue is proportional to the square of the current passing through it. Therefore, if the current is doubled, the rate of heating will increase fourfold [2].

SAFETY OF RADIOFREQUENCY FOR MYOCARDIAL ABLATION

Radiofreqency waves oscillate more than 100,000 times per second, a rate that is too rapid to cause cardiac or skeletal muscle stimulation. The fact that RF energy does not cause ventricular fibrillation was dramatically shown by d'Arsonval in 1893 when he passed one to three amperes of radiofrequency current through two human subjects each holding one wire of a light bulb [3]. The bulb glowed brillantly. The subjects reported only a sensation of warmth (figure 7–3) [4]!

There have been two reports of ventricular fibrillation associated with the use of electrosurgical devices. In one instance, an investigator caused ventricular fibrillation in dogs when the active electrode touched the animal at a

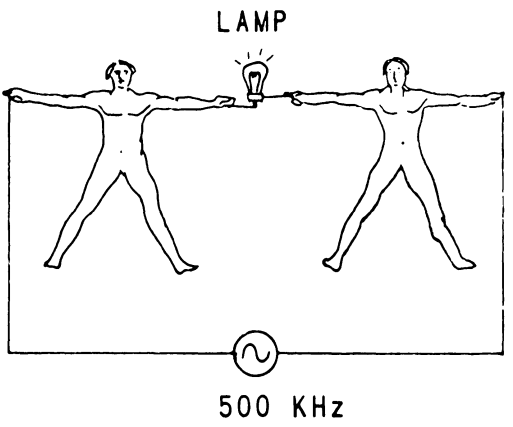

Figure 7–3. d'Arsonval's experiment (1893) in which he passed 1 amperes to 3 amperes of radiofrequency current through human subjects in series with a light bulb that glowed brilliantly. The subjects reported only a sensation of warmth [4].

time when the indifferent electrode became disconnected [5]. The dog had a pressure sensing catheter located at the tip of the right ventricle. Ventricular fibrillation was probably due to the particular radiofrequency stimulator used that delivered pulses at a repetitive rate of 60 to 120 times per second. It was thought that a process called rectification occurred; in turn, this caused stimulation similar to AC current at 60 to 120 cycles per second, resulting in ventricular fibrillation. There is one report in humans of ventricular fibrillation in a patient due to the use of radiofrequency current [6]. It is likely that this was due to improper grounding of the electrosurgical unit. With technological improvements in design, modern electrosurgical units should rarely, if ever, cause ventricular fibrillation. Also it is unlikely that lower frequency currents will be induced when radiofrequency is operated without sparking, as it is used for cardiac ablation [7].

USE OF RADIOFREQUENCY ENERGY TO INDUCE AV BLOCK

Meijler et al were the first to use radiofrequency energy to ablate the AV node [8]. Ablation was done by direct intracardiac inspection after opening the atrium in the open-chest dog. Later, radiofrequency ablation of the AV node was performed in the open-chest dog via an atriotomy [9, 10, 11, 12], using a small puncture in the atrial wall [13], or using a disc electrode applied to the epicardium adjacent to the node [14]. In 1987, Huang et al showed that AV ablation could be produced in the closed-chested dog using radiofrequency energy directed through an intracardiac catheter. Huang et al evaluated the use of 750 kHz RF energy to ablate the AV junction in 13 dogs [15, 16]. The RF energy was delivered by a 6F quadripolar or 7F tripolar USCI electrode

catheter inserted percutaneously into a femoral vein and advanced under fluoroscopy to the region of the His bundle. There were 1–13 ablation attempts per dog, with 100 joules to 700 joules delivered with bipolar ablation and 10 joules to 100 joules with unipolar ablation. Catheter damage occurred only after repeated uses delivering in excess of 1500 joules of total energy. No ventricular arrhythmias were observed. Initially, complete AV block occurred in 11 dogs and second degree AV block in 2. Complete AV block persisted during the four to seven day follow-up period in 9 of the 11 dogs; the other 2 had return of AV conduction; one had persistent 2:1 AV block and the other had persistent first degree AV block. Of the two dogs that initially had second degree AV block, one developed complete AV block and the second reverted to 1:1 AV conduction with a normal PR interval. Pathological examination showed well delineated necrosis of the AV junction without surrounding hemorrhage or mural thrombus. The authors concluded that RF ablation of the AV junction is safe and that it is effective in producing discrete areas of necrosis and various degrees of AV block.

Marcus et al investigated the efficacy and safety of inducing partial AV nodal ablation in six dogs using radiofrequency energy applied through standard USCI catheters [17]. In four of six dogs, first degree AV block was produced and persisted for the four month follow-up. The average increase in PR interval was 48%. The A_2–H_2 intervals were increased, but there was no consistent change in the AV nodal refractory period. The PR interval could not be prolonged in one dog and persistent AV block occurred in the other dog, necessitating permanent pacemaker implantation. It was concluded that modification of AV block can be produced in a majority of dogs using radiofrequency energy through an intracardiac catheter. This report indicates that AV nodal conduction can be impaired in the dog without producing complete AV block. This study raises the possibility that this procedure may be applicable to treat patients with supraventricular tachycardias refractory to antiarrhythmic drugs without the need for pacemaker implantation.

Recently AV block using radiofrequency energy through a catheter was successfully applied to two patients, one with disabling chronic atrial fibrillation and the other who had recurrent junctional tachycardia related to AV nodal reentry [18]. A specially designed suction catheter was used. It was reported that the application of radiofrequency energy was painless and hemodynamically well tolerated. Sustained ventricular arrhythmias were not recorded during the procedure or during the subsequent 48 hours of ambulatory ECG monitoring. Complete AV block persisted in one of the two patients. Similar success with AV ablation using radiofrequency energy with standared USCI catheters has been reported by M. Borggrefe et al [19].

From these preliminary data it seems that radiofrequency energy applied through an intracardiac catheter may become the treatment of choice for patients with supraventricular tachyarrhythmias refractory to antiarrhythmic drugs.

USE OF RADIOFREQUENCY ENERGY TO ABLATE ACCESSORY BYPASS TRACTS

Catheter ablation of accessory bypass tracts using DC shock has been associated with serious complications, particularly coronary sinus rupture and/or pericardial tamponade. Deaths have resulted from this type of procedure. Coronary sinus rupture is undoubtedly due to DC energy that causes shock waves. The coronary sinus, a thin-wall vessel with relatively small volume, cannot tolerate this barotrauma. Since radiofrequency energy does not cause barotrauma, it has a great advantage as compared with DC energy for ablation of accessory pathways, particularly left-sided pathways. Both Huang et al and Langberg have studied the effect of closed-chest catheter desiccation in the coronary sinus using RF energy in dogs [20, 21]. Coronary rupture did not occur. Langberg et al found that there was occlusion of the coronary sinus in one dog [21]. Pathological examination showed well circumscribed lesions. None of the hearts showed involvement of the endocardium or damage to the circumflex coronary artery or mitral valve. An alternate approach to ablation of left-sided accessory pathways would be by passing a catheter retrograde to the left ventricle and positioning it at the mitral annulus. Another catheter could be passed into the coronary sinus. Ablation could then be carried out between the two catheters. This approach was explored by Jackman et al in 15 dogs [22]. Total energy utilized ranged between 51 joules to 446 joules. At the time of sacrifice, the coronary sinus was not ruptured, but there was thrombosis of the coronary sinus in one dog. In one experiment, there was evidence of injury to the circumflex coronary artery. The authors concluded that they could consistently produce epicardial LA and LV necrosis adjacent to the mitral annulus when the left ventricular lead was positioned against the annulus.

Thus it appears that radiofrequency energy has the potential for safely ablating accessory bypass tracts. However, it may be difficult to ablate some accessory pathways since they may involve a broad band of tissue. This anatomic observation may prevent successful ablation of left-side accessory pathways in at least some patients.

Ablation of right-sided accessory pathways, particularly paraseptal and posterior pathways, may well be more readily approached using this technique. Indeed, M. Borggrefe et al have successfully ablated an accessory right-sided free wall pathway in humans using radiofrequency energy [19].

USE OF THE RADIOFREQUENCY ENERGY TO ABLATE ATRIAL AND/OR VENTRICULAR TACHYARRHYTHMIAS

Hoyt et al evaluated the effect of 750 kHz radiofrequency energy on excised segments of bovine left ventricle [23]. Standard quadripolar 5F, 6F or 7F USCI electrophysiological electrode catheters were used for all ablations in this study. Four variables — pulse power (1 watt to 50 watts), pulse duration (2 seconds to 20 seconds), catheter contact pressure (0 grams to 20 grams),

and catheter size (5F to 7F) were studied in 150 ablations. The data showed that a zone of desiccation in the shape of a spherical cap develops around the catheter tip, that RF energy induces myocardial damage at energy levels of about 20 joules and greater, and that the volume of damaged myocardium injured correlates with the delivered energy. Finally, the diameter and depth of the zone of injured myocardium paralleled increments of power, catheter contact pressure, and catheter size. Huang et al studied closed-chest RF catheter ablation of the ventricular myocardium in six dogs [24]. These investigators delivered 750 kHz RF energy with a 6F or 7F USCI tripolar or quadripolar catheter. Energies ranging between 100 joules and 300 joules were delivered to both left ventricular and right ventricular sites. No ventricular arrhythmias were observed during the procedure. Programmed ventricular stimulation did not induce VT or VF following the procedure, except in one dog who had inducible VT before the procedure. There were occasional premature ventricular beats and rare episodes of transient ventricular tachycardia recorded using 24-hour ambulatory ECG monitoring for 13 to 14 hours after the procedure. The dogs were sacrificed four to five days later. Pathology showed well demarcated lesions. Mural thrombus was found in one dog, and transmural necrosis appeared occasionally in the thin right ventricular wall when higher energies were used. There was a loss of catheter integrity in two of the ten catheters after repeated use.

Similar studies testing the safety as well as observing the damage done with the use of radiofrequency energy delivered through a catheter tip to the right and left ventricle in dogs was reported by Nacarelli et al [25]. They induced ventricular fibrillation using RF energy delivered transseptally in 1 of 11 dogs. Saksena et al studied the effect of radiofrequency energy on excised normal as well as diseased left ventricular tissue [26]. They found that it requires multiple pulses of RF energy to cause tissue injury in diseased ventricles that was similar in extent to that induced by single pulses of RF energy in normal ventricles. Arai et al studied the effect of radiofrequency energy of 13.56 MHz applied through an electrode pin stuck directly into the myocardium of dogs [27]. They found that a generator output of 5 watts to 15 watts kept the electrode temperature at 50°C to 90°C. The border between the necrosed and normal tissue was sharp and smooth. They did not find arrhythmias or hemodynamic changes.

The first use of radiofrequency energy to ablate intractable ventricular tachycardia in humans was reported in 1971 by Petitier et al [28]. They reported a case of a patient 63-years-old who had almost continuous ventricular tachycardia refractory to all medical therapy. After nine months, ventricular tachycardia became continuous. The patient was taken to surgery and had a thoracotomy. The area thought to represent the earliest activation of the tachycardia was treated with transmural electrocoagulation over a surface of 1 cm^2. This procedure appeared to be successful during a follow-up period of four months, since ventricular tachycardia did not recur during

that time. Fontaine et al used radiofrequency in an attempt to ablate an area or areas in the right ventricle in a patient with right ventricular dysplasia [14]. They appeared to have a successful result. However, they were not certain that the application of radiofrequency energy was responsible for eradicating ventricular tachycardia, since ventriculotomy had also been performed in the same zones. Klein et al recently reported a lack of success with radiofrequency energy applied through an intracardiac catheter in all six patients, three of whom had incessant ventricular tachycardia and in two of 22 patients with recurrent ventricular tachycardia [29].

Considerable research will have to be done before radiofrequency energy can be successfully used to treat ventricular tachycardia, particularly, in patients who have coronary disease and endocardial fibrosis. Radiofrequency energy will not penetrate scar tissue readily, and the type of energy required for RF ablation of VT in hearts scarred as a result of coronary ischemic heart disease will require modification. Most importantly, presently available techniques of intracardiac mapping will require extensive improvement to localize the area to be ablated. Improvement in catheter design to effectively transfer radiofrequency energy to diseased myocardium is also needed.

In summary, research in the use of radiofrequency energy for ablation is in its infancy. It is a promising technique, particularly for modification or ablation of AV nodal pathways. It is premature to attempt to apply this technique for the treatment of ventricular tachycardia in humans.

REFERENCES

1. Marcus FI: The use of radiofrequency energy for intracardiac ablation; historical perspectives and results of experiments in animals. In: *Non-Pharmacological Therapy of Tachyarrhythmias*, G Breithardt, M Borggrefe, DP Zipes, eds. Mt. Kisko, New York: Futura Publishing Co, 1987.
2. Barlow DE: Endoscopic applications of electrosurgery: A review of basic principles. *Gastrointestinal Endoscopy* 28: 73–76, 1982.
3. d'Arsonval: Action physiologique des courants alternatifs a grand frequence. *Arch Physiol Norm Path* 5: 401–408, 789–790, 1893.
4. Geddes LA, Silva LF, DeWitt DP and Pearce JA: What's new in electrosurgical instrumentation? *Medical Instrumentation* 11: 355–359, 1977.
5. Geddes LA, Tacker WA and Cabler P: A new electrical hazard associated with the electrocautery. *Medical Instrumentation* 9: 112–113, 1975.
6. Hungerbuhler RF, Swope JP and Reves JG: Ventricular fibrillation associated with the use of electrocautery. *JAMA* 230: 432–435, 1974.
7. Tucker RD, Schmitt OH, Sievert CE and Silvis SE: Demodulated low frequency currents from electrosurgical procedures. *Surg Gynecol Obstet* 159: 39–43, 1984.
8. Meijler FL, Wieberdink, J and Durrer D: L'importance de la position des electrodes stimulatrices au cours du traitement d'un bloc auriculo-ventriculaire postoperatif total. *Arch des Mal du Coeur* 55: 690–698, 1962.
9. Brutsaert D: Influence of different stimulation frequencies on the cardiac output at rest and during moderate exercise in dogs with chronic atrioventricular heart block. *Acta Cardiologica* 20: 469–498, 1965.
10. Wieberdink J: Experimental production of permanent heart block (total or bundle branch block) without circulatory arrest or extracorporeal circulation. *Thorax* 21: 401–404, 1966.
11. Macdonald IB: A simple method of producing experimental heart block in dogs. *J Thorac Cardiovasc Surg* 53: 695–697, 1967.

12. Smythe NPD and Magassy CL: Experimental heart block in the dog: An improved method. *J Thorac Cardiovasc Surg* 59: 201–205, 1970.
13. Shiang HH, Kupersmith J, Wiemann GF, Rhee CY and Litwak RS: Creating permanent complete heart block by indirect cauterization without atriotomy. *Am J Physiol* 233: H723–H726, 1977.
14. Fontaine G, Lechat PH, Cansell A, Guiraudon G, Linares-Cruz E, Koulibali M, Chomette G, Auriol M, and Grosgogeat Y: Advances in the treatment of cardiac arrhythmias in the last decade: Definition and role of ablative techniques. In: *Ablation in cardiac arrhythmias*, G Fontaine, MM Scheinman, eds. Mt. Kisko, New York: Futura Publishing Co, pp 5–20, 1987.
15. Huang SK, Bharati S, Graham AR, Lev M, Marcus FI and Odell RC: Closed-chest catheter desiccation of the atrioventricular junction using radiofrequency energy — A new method of catheter ablation. *JACC* 9: 349–358, 1987.
16. Huang SK, Bharati S, Lev M, Marcus FI: Pathological and electrophysiological observations of chronic atrioventricular block induced by closed-chest ablation with radiofrequency energy. *PACE* 10: 805–816, 1987.
17. Marcus FI, Blouin LT, Wharton K and Bharati S: Electrophysiological and pathological assessment of chronic first degree atrioventricular block caused by closed-chest catheter ablation with radiofrequency. *JACC* 9(2): 95A (abstract), 1987.
18. Lavergne T, Guize L, Letleuzey J-Y, Cousin M-T, Carcone P, Geslin J, Khaznadar G, Couetil J-P and Ourbak P: Transvenous ablation of the atrio-ventricular junction in human with high-frequency energy. *JACC* 9(2): 99A (abstract), 1987.
19. Borggrefe M, Budde T, Podczfck A, Breithardt G: Application of transvenous high frequency alternating current ablation in humans. *PACE* 10(3): Part I, 603 (abstract), 1987.
20. Huang SK, Graham AR, Lee MA, Gorman G: Closed-chest catheter ablation of the canine coronary sinus using radiofrequency energy. *PACE* 10(2): 410 (abstract), 1987.
21. Langberg J, Griffin JC, Bharati S, Lev M, Chin M, Scheinman MM: Radiofrequency catheter ablation in the coronary sinus. *JACC* 9(2): 99Q (abstract), 1987.
22. Jackman WM, Kuck K-H, Naccarelli GV, Pitha J and Carmen L: Catheter ablation at the mitral annulus using RF current in canines. *PACE* 10(2): 410 (abstract), 1987.
23. Hoyt RH, Huang SK, Marcus FI, Odell RC: Factors influencing trans-catheter radiofrequency ablation of the myocardium. *J Appl Cardiol* 1: 469–487, 1986.
24. Huang SK, Graham AR, Hoyt RH and Odell RC: Transcatheter desiccation of the canine left ventricle using radiofrequency energy — a pilot study. *Am Heart J* (in press).
25. Naccarelli GV, Kuck K-H, Pitha J, Carmen L, Jackman WM: Selective catheter ablation of canine ventricular myocardium with radiofrequency current. *JACC* 9: 2, 1987.
26. Saksena S, Furman R, Gadhoke A and Osypka P: Feasibility of radiofrequency ablation of supraventricular and ventricular tachyarrhythmias. *PACE* 10: 410 (abstract), 1987.
27. Arai Y, Masani F, Kato H, Sasagawa Y, Shibata A, Eguchi S, Nemoto K, Makino H, Saitoh Y: Experimental study of myocardial ablation by radio-frequency current. *PACE* 10: 426 (abstract), 1987.
28. Petitier H, Polu JM, Dodinot B, Sommelet P, Mathieu P and Faivre G: Tachycardie ventriculaire irreductible traitement par electrocoagulation apres localisation du foyer. *Arch Mal du Coeur* 64: 331–351, 1971.
29. Klein H, Schroder E, Trappe HJ and Kuhn E: Catheter ablation of ventricular tachycardia — Special emphasis on the incessant form of tachycardia. *PACE* 427 (abstract), 1987.

8. CLINICAL ROLE OF CATHETER ABLATION OF ATRIOVENTRICULAR JUNCTION

MELVIN M. SCHEINMAN AND G. THOMAS EVANS, JR.

In the 94 years since the discovery of the atrioventricular (AV) conduction system, many therapeutic modalities have been developed to alter or abolish AV conduction in order to treat patients with symptomatic supraventricular tachyarrhythmias (SVT). The mainstay of therapy has been, and remains, pharmacologic agents. For a very select subgroup of patients with disabling or life-threatening SVT who are refractory to either conventional or experimental drug therapy, alternative techniques involving antitachycardia pacemakers and both open-and closed-chest surgical and catheter approaches have been developed. Preliminary animal studies to interrupt AV conduction involved direct mechanical crushing [1, 2], surgical incision [3, 4], cautery, [4], ligation of septal arteries [5], injection of caustic material [6–8], cryosurgical ablation [9], and electrode catheter ablation [10]. The earliest cases of therapeutic production of third-degree AV block in man involved direct incision of the AV junction or ligature of the AV node [11, 12]. Later techniques involved open-chest procedures utilizing needle electrocoagulation [13], excision of the AV node [14], and what ultimately has proven to be the surgical procedure of choice, cryoablation of the AV junction [9]. In recent years, closed-chest electrode catheter ablation techniques have been developed which have largely supplanted open-chest techniques for management of selected patients. This chapter will discuss the clinical role of catheter ablation of the AV junction. The various types of rhythm disturbances necessitating ablation will be discussed, as will future trends in catheter ablation for therapy of drug or pacemaker refractory SVT.

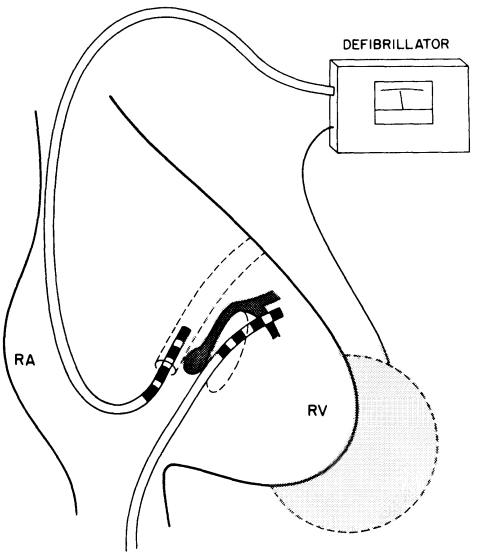

Figure 8–1. The AV node-His axis is shown in grey and is bracketed by a catheter inserted into the coronary sinus (top electrode catheter) and one positioned just across the tricuspid valve (bottom electrode catheter). The latter is manipulated in order to obtain the largest unipolar His bundle potential. The shock is delivered from the electrode showing the largest His bundle potential to a patch over the left scapulae from a standard direct-current defibrillator.

HISTORICAL PERSPECTIVES AND TECHNIQUE OF CATHETER ABLATION THE AV JUNCTION

Beazell et al [10] first described an electrode catheter technique for induction of complete AV block in a canine preparation. The technique involved the use of an insulated wire positioned fluoroscopically in the region of the AV junction. The AV junctional area was electrocoagulated by delivery of high-energy direct-current shocks through the catheter. Gonzalez et al [15] refined this technique by positioning an electrode catheter in proximity to the AV junction using His bundle recordings. A similar technique was introduced into clinical medicine by Scheinman et al [16] and Gallagher et al [17].

Patients are brought to the electrophysiology laboratory in a post-absorptive state. A temporary electrode catheter is inserted percutaneously into a peripheral vein and positioned against the right ventricular apex. A femoral arterial catheter is inserted for continuous blood pressure monitoring. A previously unused standard 6F or 7F tripolar or quadripolar (USCI) catheter is inserted into the right femoral vein and positioned across the tricuspid valve. Bipolar filtered 40 Hz–500 Hz and unfiltered unipolar low atrial and His bundle potentials are recorded, and the electrode which demonstrates the largest unipolar His bundle deflection is then connected to the cathodal output of a standard defibrillator (figure 8–1). This connection utilizes a special

Table 8–1. Types of rhythm disturbances amenable to catheter ablation of the atrioventricular junction

1. Sinus node rentrant tachycardia
2. Intra-atrial reentrant tachycardia
3. Automatic atrial tachycardia
4. Atrial flutter
5. Atrial fibrillation
6. AV nodal reentrant tachycardia
7. Atrioventricular reentrant tachycardia utilizing an accessory atrioventricular bypass tract
8. Permanent junctional reciprocating tachycardia
9. Junctional ectopic tachycardia

switching box which allows for rapid conformation of a stable unipolar His deflection immediately prior to the shock. A patch electrode or lubricated plate electrode is then placed securely over the left scapula and connected as the anode. In preparation for the shock, patients are anesthetized with short-acting anesthetic agents. The defibrillator is then charged and direct-current shocks synchronized to the QRS complex are delivered through the electrode showing the largest unipolar His deflection, since Dick [18] and coworkers have shown that clinically recognizable His bundle electrograms can only be recorded in close proximity to this structure (within 3 mm). After delivery of the shock, a period of ventricular asystole usually occurs, necessitating temporary demand pacing. The amplitude of the His bundle potential is usually significantly reduced or absent after the first shock, making precise catheter localization difficult. Most investigators deliver two or more shocks of at least 200 joules. The patients are observed in the laboratory and then transferred to the coronary care unit for continuous ECG monitoring. Routine in-hospital follow-up also includes determination of both total CPK and CPK-MB fractions, echocardiograms, and ambulatory electrocardiographic Holter monitor recordings. After 24 hours of stable chronic third-degree AV block, a permanent pacemaker is implanted. The hospital stay for an uncomplicated procedure is usually four or five days. Routine follow-up procedures should include Holter recordings and routine checks of pacemaker function.

PATIENT SELECTION AND MANAGEMENT STRATEGIES

A wide variety of arrhythmias constitute what is presently diagnosed as supraventricular tachycardia. A listing of these arrhythmias is found in table 8–1. The initial approach to management of patients with these arrhythmias remains pharmacologic. It is clear that the current pharmacologic armamentarium allows for arrhythmia control in most of these patients. This includes use of class IA drugs, IC drugs, a variety of beta blockers, calcium channel blockers, and amiodarone. A subset of patients may prove refractory or intolerant to drug therapy. In addition, younger patients may opt for

Table 8–2. Management options in therapy of refractory supraventricular tachycardias

1.	Surgical excision of an automatic focus
2.	Surgical isolation of the left atrium for left atrial tachycardia foci
3.	Surgical construction of a corridor of internodal tissue for patients with atrial fibrillation
4.	Surgical division of an accessory atrioventricular pathway
5.	Surgical disconnection of perinodal tissue in reentrant AV nodal tachycardia
6.	Cryoablation of the His bundle
7.	Automatic antitachycardia pacemaker for reentrant tachycardias
8.	Catheter electrocoagulation of an automatic focus
9.	Catheter electrocoagulation of the AV junction

nonpharmacologic arrhythmia control in preference to a lifelong requirement for drug therapy. The latter considerations are of especial import to females in the child-bearing age whose arrhythmia may be controlled with agents whose teratogenetic potential is unknown.

Nonpharmacologic options — antitachycardia pacemakers

A variety of nonpharmacologic options have been introduced depending on the type of cardiac arrhythmia (table 8–2). One option that has been used for patients with reentrant mechanisms involves antitachycardia pacemakers. The rationale behind use of these techniques is the ability of an electrical impulse to result in both antidromic and orthodromic collision within the pathway (figure 8–2).This technique has been used for patients with AV nodal reentry as well as in selected patients with AV reentrant tachycardia and, rarely, in patients with atrial flutter. Clearly, not all patients with reentrant arrhythmias are candidates for antitachycardia pacing since arrhythmias may be very frequent or incessant, ready tachycardia termination may be unreliable, and pacemaker sensing may not be able to distinguish the arrhythmia from sinus tachycardia, leading to inappropriate pacing and the possibility of initiating the arrhythmia. Moreover, patients with the Wolff-Parkinson-White syndrome with short effective refractory periods of the bypass tract are not candidates for antitachycardia pacing, since pacing induced atrial fibrillation or flutter may lead to life-threatening cardiac arrhythmias.

Surgery for patients with supraventricular tachycardia

A variety of exciting surgical procedures have been introduced for management of patients with supraventricular tachycardia. The most widely used procedure is surgical ablation of accessory bypass tracts in patients with the Wolff-Parkinson-White syndrome. This technique involves careful epicardial mapping at the time of open-heart surgery in order to precisely locate the accessory pathway. The pathway is destroyed by either direct surgical incision and/or cryosurgical techniques. The standard surgical approach introduced by Sealy et al [14] involves performance of an atriotomy and dissection

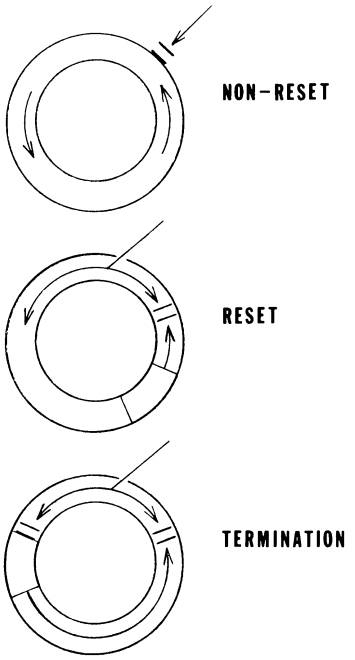

Figure 8–2. Schema illustrating the effects of pacing on a reentrant circuit. The top panel illustrates an electrical impulse which fails to penetrate a reentrant circuit. The second panel shows an electrical impulse that penetrates the circuit but results in tachycardia reset. The bottom panel illustrates tachycardia termination with block of the induced pacing stimulus in both clockwise and counterclockwise directions.

through the atrial wall in the region of the AV grooves. A newer approach (closed-heart approach) introduced by Guiraudon et al [19] allows for interruption of the accessory pathway by external dissection of the AV groove without entering the cardiac chambers. Both the traditional as well as the newer procedure have been associated with remarkable efficacy as well as acceptable mortality and morbidity.

Surgical ablation of the AV junction

A number of surgical teams have reported the use of surgical techniques for direct ablation of the AV junction. Garcia [20] successfully ligated the AV junction in a patient with disabling drug-refractory atrial flutter. The most extensive experience was provided by Sealy et al [21], who used predominantly a cryosurgical procedure for interrupting the His bundle in 42 patients. They reported a success rate of 87%, with one death occurring in a patient one month after a failed attempt at His bundle interruption. Similarly, Camm et al [22] reported production of complete AV block in three of four

patients undergoing cryoablation of the His bundle. The disadvantage of complete interruption of AV conduction involves the need for lifelong chronic cardiac pacing. More specific procedures have been introduced allowing for surgical interruption of supraventricular tachycardia foci or pathways which leave the normal conduction system intact. These procedures have obvious advantages compared with permanent ablation of the His bundle.

Surgery for patients with atrial tachycardia, atrial fibrillation and AV nodal reentry

A variety of ingenious surgical techniques have been introduced for management of patients with drug-refractory atrial or AV nodal arrhythmias. Ross et al [23], for example, have introduced a surgical technique involving disarticulation of atrial muscle bundles inserting into the AV junction. Preliminary experience with this technique has shown it to be very effective in abolishing arrhythmias relating to AV junction reentry without interference with normal AV conduction. Application of this technique involves careful assessment of the potential benefits and risks of surgery compared with alternative approaches (i.e., drug and/or antitachycardia pacing). In patients with discrete atrial foci of abnormal automaticity or in whom an atrial reentrant circuit can be identified, primary excision or interruption of the abnormal area may result in arrhythmia control. Unfortunately, some of these patients may subsequently develop arrhythmic foci in atrial areas remote from the surgical site. Other procedures include a left atrial isolation procedure for patients with left atrial foci [24] or construction of a tissue corrider linking the sinus and AV nodes for patients with atrial fibrillation [25]. A left atrial isolation procedure has been proposed for patients with atrial fibrillation and a dilated left atrium owing to mitral stenosis. While the canine experience appears promising, this procedure has to date yet to be performed in patients.

Catheter ablation of the AV junction in man

Catheter ablation of the AV junction has been used primarily for control of supraventricular arrhythmias in which the AV junction acts to funnel impulses into the ventricle. It has proven especially effective for patients with paroxysmal or chronic atrial fibrillation or flutter resistant to antiarrhythmic agents. After successful ablation and initiation of third degree AV block, a permanent cardiac pacemaker is required. The latter remains an important limitation for widespread use of this procedure. Catheter ablation has also been used for patients with extranodal accessory pathways. In these patients, the most common arrhythmia involves antegrade conduction over the AV node His pathway with retrograde conduction over the AV node His pathway with retrograde conduction over the accessory pathway (figure 8–3). Successful catheter ablation of the AV junction would be expected to result in arrhythmia control, since the AV junction is a critical component of the reentrant circuit. Catheter ablation of the AV junction should not, however, be

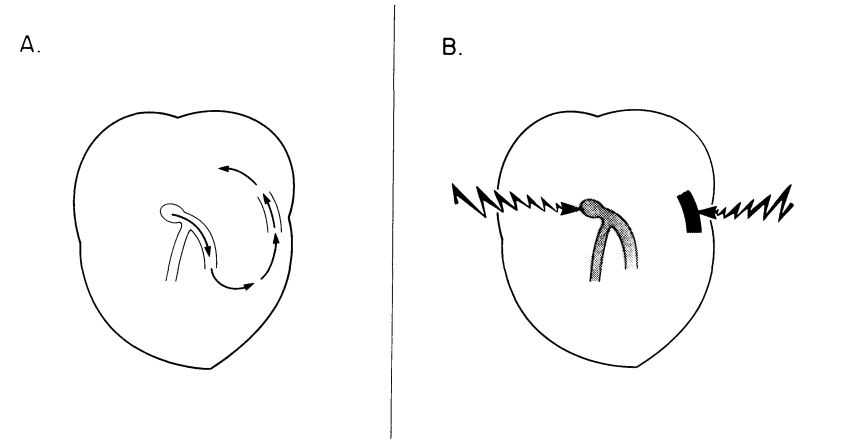

Figure 8–3A. Schema showing the mechanism of orthodromic AV reentrance in patients with an accessory pathway. The electrical impulse proceeds antegrade over the AV node-His axis and retrogradely over the accessory pathway.

Figure 8–3B. Catheter ablation of either the AV junction (left flash mark) or the accessory pathway (right flash mark) should result in tachycardia control since both of these pathways are critical for maintenance of the tachycardia.

used for those patients with short effective refractory periods of the accessory pathway, since atrial fibrillation may still result in potentially life-threatening arrhythmias. In addition, even though accessory pathway conduction is intact, a permanent ventricular pacemaker is indicated, since the natural history of conduction over an accessory pathway is not completely known. A small number of patients with nodo-ventricular pathways have undergone catheter ablation of the AV junction. This technique should provide arrhythmia control, provided it is proven that the AV junction is a critical component of the tachycardia circuit. It is recognized that in some patients with nodo-ventricular pathway the tachycardia mechanism may be AV nodal reentry with the Mahaim tract (nodo-ventricular) acting as an innocent bystander. In this situation, His bundle destruction alone would not result in tachycardia control.

CATHETER ABLATION REGISTRY

In 1982, a worldwide voluntary registry was established in order to chart the course of patients undergoing various ablative procedures. Centers throughout the world were urged to send data to a central registry in order to allow for rapid determination of the efficacy and adverse effects of catheter ablation. Data were collected relative to the type of arrhythmia found, previous therapy applied, and underlying cardiac diagnosis. In addition, procedural

Table 8–3. Clinical findings in patients with drug and/or pacemaker resistant supraventricular tachycardia

Heart disease (type/% of patients)	Arrhythmia (type/% of patients)	Symptoms (type/% of patients)	Prior treatment (type/% of patients)
No organic disease/48	Atrial fibrillation/flutter/60	Palpitations/70	Digitalis/82
Coronary artery disease/16	Atrioventricular node reentry/22	Dizziness/36	Type I/77
Cardiomyopathy/14	Atrial tachycardia/13	Dyspnea/40	Beta blockers/72
Valvular heart disease/12	Accessory pathway/11	Syncope/25	Calcium-channel blockers/71
Hypertensive cardiovascular disease/8	Permanent JRT/2	Chest pain/17	Amiodarone/56
Cor pulmonale/2	Other/4	Fatigue/17	Other experimental drugs/24
Other/6		Angina/11	Antitachycardia pacemaker/7
		Other/6	

The percentages total more than 100% since more than one parameter may have been present in a given patient. Abbreviations: JRT = junctional reciprocating tachycardia, Type I = type I antiarrhythmic agents.

details relating to the types of catheters used, energy delivered, complications, and follow-up data were obtained. Periodic follow-up evaluation were requested and causes of death were tabulated.

Results of worldwide catheter ablation registry

To date, data from 475 patients who underwent catheter ablation of the AV junction have been submitted. In this report, data from the first 367 patients are analyzed. The clinical descriptors for this patient cohort are summarized in table 8–3. The patients were described as being very symptomatic from their arrhythmias, with presyncope (36%) or frank syncope (25%) being the most common presenting complaint. Nine patients suffered a cardiac arrest, and 61 required at least one external direct-current countershock for arrhythmia control. Over half the patients had organic cardiac disease, with coronary artery disease the most common diagonsis.

Patients failed or proved intolerant to a mean of 3.5 antiarrhythmic drugs. A majority failed digitalis (82% of patients), beta blockers (72%), calcium channel blockers (71%), type I antiarrhythmic drugs (77%), and 56% failed chronic amiodarone therapy. The primary rhythm disturbance requiring ablation was paroxysmal or chronic atrial fibrillation or flutter, which occurred in 60% of the reported cases. Other major arrhythmias included AV nodal reentry tachycardia (22%), AV tachycardia (11%), atrial tachycardia (13%), and a lesser number of patients with the permanent form of junctional reentrant tachycardia, junction ectopic tachycardia, and sinus node reentrant tachycardia.

Procedural data

A single ablative session was used for 80% of patients, while two or more sessions were used in the remainder. The stored energy per shock ranged

from 50 joules to 500 joules but was usually in the range of 200 joules to 300 joules. The mean stored cumulative energy used was 603 ± 453 joules. There was no significant difference in stored energy between those in whom complete AV block was achieved compared to those who showed resumption of AV conduction. Data were available in 113 patients relative to the maximal unipolar His bundle and atrial deflections. The mean maximal recorded unipolar His bundle deflection was 0.38 ± 0.29 mV and the atrial deflection was 0.87 ± 0.83 mV. There was a significant increase in the recorded amplitudes of these deflections between responders (third degree AV block) and nonresponders.

Clinical response

Immediately after delivery of the shock(s) 90% of patients showed either complete AV block (or maximal preexcitation in those with accessory pathways). The average rate of the escape pacemaker was 45 ± 15 beats/minute. The escape pacemaker was infra-Hisian in 58%, supra-Hisian in 32%, and indeterminate in the remainder. Patients were followed over a mean of 11 ± 10 months, and 63% maintained chronic stable third degree AV block and required no antiarrhythmic drugs. The remaining patients showed resumption of AV conduction, which occurred at a mean of 6 ± 18 days after the procedure. Ten percent of patients who had resumption of AV conduction were asymptomatic without drug therapy, while another 12% had arrhythmia control but required resumption of antiarrhythmic drug therapy. The procedure was judged unsatisfactory in 15% of patients.

Complications of the AV junctional ablation

Immediate complications

The most frequent acute complications occurring after delivery of the electrical shocks were arrhythmic in nature. Six patients developed ventricular tachycardia or fibrillation after application of the shock and required external direct-current cardioversion. Two additional patients developed ventricular tachycardia within 24 hours of the procedure. Transient sinus arrest, atrial tachycardia, atrial flutter, or nonsustained ventricular tachycardia (17 patients) were reported, but no specific therapy was required. Hypotension, post shock, was reported in six patients, three of whom required pressor support. The hypotensive episode was transient in five and persisted for 72 hours in one. No deaths have been reported in the immediate post-shock period (within 24 hours). Three patients developed cardiac tamponade due to myocardial perforation. Thromboembolic complications included a pulmonary embolus in one, thrombosis of the left subclavian vein in one, and thrombophlebitis in four patients. One patient developed a large right atrial thrombus despite prior anticoagulant therapy. In addition, infections complications, all related to pacemaker insertion, were recorded in four patients.

One patient with a presumed immunodeficient state died of overwhelming sepsis. One patient had diaphragmatic pacing and ventricular tachycardia, which resolved on repositioning of the temporary pacing electrode.

Late complications

Late complications included a cerebrovascular accident 17 months after ablation in patient with atrial fibrillation; another had a probable arterial embolus after the procedure. Long-term pacemaker complications included a pacemaker-mediated tachycardia in three, pacemaker tracking of supraventricular tachycardia in two, pacemaker inhibition due to myopotential sensing in one, and two patients had symptoms due to acute pacemaker failure. A slow underlying pacemaker emerged in the latter two patients.

Follow-up mortality statistics after AV junctional ablation

A total of 19 patients died in the follow-up period. The death was sudden and of natural causes in eight and occurred from three days to 13 months after ablation. Seven of these patients had underlying organic cardiac disease, and one was free of known heart disease. Four patients died of severe congestive heart failure, which was present prior to the ablative procedure. One patient died two years after procedure from infective endocarditis, and one died from surgery after attempted accessory pathway division. Noncardiac deaths were recorded due to sepsis (after pacemaker revision in one), severe chronic lung disease (1), and cerebral hemorrhage in one patient. The cause of death was unknown in one.

PERSONAL EXPERIENCE WITH CATHETER ABLATION OF THE AV JUNCTION

From March 1981 through January 1987, a total of 39 patients underwent attempted ablations of the AV junction at the University of California Medical Center. Complete AV block was achieved in 30 (77%). Of the remaining nine patients in whom AV conduction resumed, five have achieved arrhythmia control either without drugs (one patient) or with drugs that previously proved ineffective (four patients). Two patients who suffered symptomatic recurrences of arrhythmia underwent uneventful section of the His bundle during open-heart surgery. One of these patients with hypertrophic cardiomyopathy died of congestive heart failure six months after surgery. Two patients remain symptomatic in spite of maximum drug therapy and have declined repeat ablative procedures or surgery. In summary, approximately 90% of our patients have benefited from the procedure, either showing complete arrhythmia control without need for antiarrhythmic drugs (31/39) or arrhythmia control using previously ineffective drugs (4/39). The procedure proved ineffective in approximately 10% of patients.

Procedural data

Based upon our canine experience [15], we used large amounts of stored energy for our initial ablative attempts (300–500 joules/shock). With further experience, we have found that lesser amounts of energy are equally effective. We now seldom use more than 300 joules/shock and deliver at least two shocks per session. In contrast to the data presented for the worldwide registry, we found no correlation between the amplitude of the His or atrial deflection and induction of complete AV block. The only factor found to be predictive of an unsuccessful outcome was end-diastolic volume; failed attempts were more common in those with larger left ventricular end-diastolic volumes.

Complications

Thus far, no serious complications, i.e., cardiac tamponade or persistent hypotension, have occurred in the course of, or following, the ablation procedure. One patient developed ventricular tachycardia, which resolved with repositioning of the permanent pacemaker wire. The most serious complication occurred in the second patient undergoing catheter ablation. One month after the procedure, she sustained ventricular fibrillation and could not be resuscitated. This patient had an idiopathic cardiomyopathy, and it is not clear whether the death was related to the ablative procedure or to underlying myocardial disease. An additional patient developed ventricular fibrillation approximately one year after catheter ablation. This patient was hospitalized for evaluation of an unrelated medical problem (peripheral neuropathy) and was successfully resuscitated. Complete evaluation, including coronary angiography, left ventriculography, and myocardial biopsy show no evidence of organic disease. She is presently being treated with amiodarone. In the latter case and in at least one other patient from the world registry, it would appear that sudden death occurred in the absence of organic cardiac disease and, until proven otherwise, must be considered related to the ablative procedure. It should be appreciated that current methods produce lesions in the AV junction as well as in the summit of the ventricular septum. It is conceivable that such lesions may form the nidus for malignant ventricular arrhythmias following attempted ablative procedure.

CATHETER ABLATION VERSUS SURGICAL ABLATION OF THE AV JUNCTION

No control data are available to compare efficacy and complications of catheter versus direct surgical attempts at AV junctional ablation. German et al [26] reviewed the experience at Duke University Medical Center (nonconcurrent series). They reported 42 attempted surgical ablations with complete AV block achieved in 36 (86%), modification of AV nodal function in one

(2%), and no AV block in five (12%). Of 31 patients undergoing catheter ablation of the AV junction, 26 had complete AV block (84%). One (3%) showed modification of AV function, and four showed resumption of AV conduction (13%). Postoperative morbidity and mortality was significantly higher for the operated group. The authors concluded that the catheter technique appeared to show equal efficacy with lesser morbidity and mortality. The difficulties in comparing retrospective nonconcurrent patient series are appreciated.

SUMMARY AND FUTURE PERSPECTIVE

Catheter ablation of the AV junction has supplanted the direct surgical approach for His bundle ablation, since the catheter approach appears to be equally effective but associated with lesser morbidity, mortality, and cost. Surgery is primarily reserved for failed catheter ablative attempts or for those patients requiring surgical correction of other cardiac problems (i.e., valve replacement or aorta coronary bypass procedures). Catheter ablation is not the ideal procedure for patients with AV reentrant arrhythmias incorporating a bypass tract, since the patient is not protected from future development of other atrial arrhythmias. It is appreciated that surgical or catheter ablation (where feasible) of the accessory pathway is the preferred approach. However, catheter ablation of the AV junction may yet have a role for patients with AV reentrant arrhythmias who are considered high risk surgical candidates by virtue of the presence of associated medical conditions. The primary drawback to wide application of catheter ablative procedures is the induction of a pacemaker dependent state. These patients, of course, require careful pacemaker follow-up. Of equal concern is the approximately 2% incidence of sudden death that has been reported following application of this procedure. Although this figure compares favorably with the surgical mortality following His bundle section, it must be carefully assessed when consideration is given to applying the catheter technique to patients with drug-resistant supraventricular arrhythmias.

Future development of catheter ablative procedures rests with development of catheter and energy delivery systems that allow for modification of AV conduction without complete disruption and hence need for chronic pacemaker therapy. Such modifications might allow for wider use of these techniques in patients with AV nodal reentry arrhythmias or in those with atrial fibrillation who prove resistant to drug therapy.

REFERENCES

1. Erlanger J, Blackman JR: Further studies on the physiology of heart block in mammals. Chronic auriculoventricular heart-block in the dog. *Heart* 1: 177, 1910.
2. Meakins J: Experimental heart block with atrioventricular rhythm. *Heart* 5: 281, 1913.
3. Starzl TE, Gaerthner RA, Baker RR: Acute complete heart block in dogs. *Circulation* 2: 82–9, 1955.

4. Sealy WC, Hackel DB, Seaber AV: A study of methods for surgical interruption of the His bundle. *J Thorac Cardiovasc Surg* 73: 424–30, 1977.
5. Hashiba K, Katayama T, Takahashi A, Ona A, Matsuo S, Fujita J, Yamaguchi Y, Tazima N. Yoshioka M, Miura K: Atrio-ventricular block produced by ligation of septal arteries in the dog. *Jpn Heart J* 6: 256, 1967.
6. Randall OS, Westerhof N, Van den Bos GC, Sipkema P: Production of chronic heart block in closed-chest dogs: An improved technique. *Am J Physiol* 241: H279–82, 1981.
7. Baum T, Peters JR, Butz F, Much DR: A method for the placement of His bundle electrodes and production of atrioventricular block in dogs. *J Appl Physiol* 38: 932–3, 1975.
8. Fisher VJ, Lee JR, Christianson LC, Kavaler F: Production of chronic atrioventricular block in dogs without thoracotomy. *J Appl Physiol* 21: 1119–20, 1966.
9. Harrison L, Gallagher JJ, Kassell J, Anderson RH, Mikat E, Hackel DB, Wallace AG: Cyrosurgical ablation of the A-V node-His bundle: A new method for producing A-V block. *Circulation* 55: 463–70, 1977.
10. Beazell J, Tan K, Criley J, Schulman J: The electrosurgical production of heart block without thoracotomy. *Clin Res* 24: 137A (abstract), 1976.
11. Cole JS, Wills RE, Winterscheid LC, Reichenbach DD, Blackmon JR: The Wolff-Parkinson-White syndrome. Problems in evaluation and surgical therapy. *Circulation* 42: 111–121, 1970.
12. Giannelli S Jr, Ayres SM, Gomprecht RF, Conklin EF, Kennedy RJ: Therapeutic surgical division of the human conduction system. *JAMA* 199: 123–8, 1967.
13. Edmonds JH, Jr, Ellison RG, Crews TL: Surgically induced atrioventricular block as treatment for recurrent atrial tachycardia in Wolff-Parkinson-White syndrome. *Circulation* 39: I–105–111, 1969.
14. Sealy WC, Anderson RW, Gallagher JJ: Surgical treatment of supraventricular tachyarrhythmias. *J Thorac Cardiovasc Surg* 73: 511–22, 1977.
15. Gonzalez R, Scheinman MM, Margaretten W, Rubinstein M: Closed-chest electrode-catheter technique for His bundle ablation in dogs. *Am J Physiol* 241: H283–7, 1981.
16. Scheinman MM, Morady F, Hess DS, Gonzalez R: Catheter-induced ablation of the atrioventricular junction to control refractory supraventricular arrhythmias. *JAMA* 248: 851–85, 1982.
17. Gallagher JJ, Svenson RH, Casell JH, German LD, Bardy GH, Broughton A, Critelli G: Catheter technique for closed-chest ablation of the atrioventricular conduction system: A therapeutic alternative for the treatment of refractory supraventricular tachycardia. *N Engl J Med* 306: 194–200, 1982.
18. Dick M, Antar RE, Hoffman BF, Bowman FO Jr, Malm JR, Krongrad E: Sensitivity of His bundle (HB) recording technique during open heart surgery in man. *Circulation* 50: III–81 (abstract), 1974.
19. Guiraudon Gm, Klein GJ, Gulamhusein S, Jones DL, Yee R, Perkins DG, Jarvis E: Surgical repair of Wolff-Parkinson-White syndrome: A new closed-heart technique. *Ann Thorac Surg* 37(1): 67, 1984.
20. Garcia R, Arciniegas E: Recurrent atrial flutter: Treatment with a surgically induced atrioventricular block and ventricular pacing. *Arch Int Med* 132: 754–7, 1973.
21. Sealy WC, Gallagher JJ, Kasell J: His bundle interruption for control of inappropriate ventricular responses to atrial arrhythmias. *Ann Thorac Surg* 32: 429–38, 1981.
22. Camm J, Ward DE, Spurrell RAJ, Rees GM: Cryothermal mapping and cryoablation in the treatment of refractory cardiac arrhythmias. *Circulation* 62: 67–74, 1980.
23. Ross DL, Johnson DC, Denniss AR, Cooper MJ, Richards DA, Uther JB: Curative surgery for atrioventricular junctional ("AV nodal") reentrant tachycardia. *JACC* 6: 1383–92, 1985.
24. Williams JM, Ungerleider RM, Lifland GK, Cox J: Left atrial isolation. New technique for the treatment of supraventricular arrhythmias. *J Thorac Cardiovasc Surg* 80: 373, 1980.
25. Guiraudon G, Klein G, Jones DC, McClellan PG: Combined sinoatrial node and atrioventricular node isolation: A surgical alternative to His bundle ablation in patients with atrial fibrillation. *Circulation* 72: III–220 (abstract), 1985.
26. German LD, Pressley J, Smith MS, O'Callaghan WG, Ellenbogen KA: Comparison of cryoablation of the atrioventricular node versus catheter ablation of the His bundle. *Circulation* 70: II–412 (abstract), 1984.

9. CATHETER ABLATION OF ACCESSORY PATHWAYS

FRED MORADY AND MELVIN M. SCHEINMAN

Patients who have either the Wolff-Parkinson-White syndrome or a concealed accessory atrioventricular (AV) connection may be appropriate candidates for nonpharmacologic treatment for one or more of the following reasons: 1) the occurrence of rapid and potentially life-threatening tachycardias, for example, atrial fibrillation with a ventricular rate of 250 beats/minute, associated with loss of consciousness or a cardiac arrest; 2) inefficacy of antiarrhythmic drugs; 3) intolerance to antiarrhythmic drugs; or 4) patient preference. Up until the recent past, if it was decided that a patient was an appropriate candidate for definitive therapy, surgery provided the only means by which an accessory AV connection could be ablated. However, the transcatheter ablation technique now provides a potential alternative to surgical ablation of at least some types of accessory AV connections. This chapter shall review the current status of transcatheter ablation of posteroseptal, left free-wall, and right free-wall accessory AV connections. Because the largest amount of experience and the highest success rate has been reported for accessory AV connections that are posteroseptal in location, this type of accessory AV connection will be discussed first.

TRANSCATHETER ABLATION OF POSTEROSEPTAL ACCESSORY ATRIOVENTRICULAR CONNECTIONS

Experimental background

In patients who have a posteroseptal accessory AV connection, mapping in the electrophysiology laboratory characteristically demonstrates early

atrial activation during orthodromic reciprocating tachycardia at the os of the coronary sinus. Therefore, transcatheter ablation techniques have involved delivery of shocks at the os of the coronary sinus. Electrophysiologic and histologic effects in dogs of shocks delivered to the region of the os of the coronary sinus were studied by Coltorti et al [1]. The proximal two electrodes of a quadripolar electrode catheter were positioned at the os of the coronary sinus and served as the anode, and a disc electrode on the anterior chest wall served as the cathode. A 200 joule shock (stored energy) was delivered in six dogs and a 360 joule shock in another six. Transient AV block and idioventricular rhythms occurred in five and six dogs, respectively. However, at the time of an electrophysiology study four weeks after the shocks, AV conduction was normal in all dogs, there was no spontaneous or inducible ventricular tachycardia, and ventricular fibrillation was inducible in only one dog.

Histologic examination demonstrated transmural atrial injury at the level of the coronary sinus over a 10 ± 5 mm length (mean ± standard deviation) with the 200 joule shock and 21 ± 6 mm length with the 360 joule shock. Localized intramural atrial rupture of the endocardial aspect of the coronary sinus wall was found in each dog, but there were no cases of cardiac tamponade and there was no evidence of damage to coronary arteries or to the conduction system.

Therefore, Coltorti et al demonstrated that it was possible, without serious complications, to produce atrial injury potentially capable of blocking atrial conduction through an accessory AV connection by delivering a shock at the os of the coronary sinus.

In a later study, Coltorti et al compared the effects of unipolar and bipolar shocks delivered at the os of the coronary sinus [2]. In ten dogs a single 200 joule shock was delivered with an electrode at the os serving as the anode and a disc electrode on the anterior chest serving as the cathode; in another ten dogs, the 200 joule shock was delivered with the proximal electrode of a bipolar catheter (1.5 cm interelectrode distance) serving as the anode and the distal electrode serving as the cathode.Transmural atrial scarring occurred in each of the ten dogs that received a unipolar shock but in only two dogs that received a bipolar shock. Therefore, unipolar shocks may be more likely than bipolar shocks to result in transmural atrial injury sufficient to prevent conduction through an accessory AV connection.

Of note is that Coltorti et al observed gross rupture of the coronary sinus in two dogs who received a bipolar shock and also in two dogs who received a unipolar shock [2]. In contrast, in their prior study, no instances of coronary sinus rupture occurred with shocks of 200 joules to 360 joules when two electrodes in parallel served as the anode [1]. These investigators suggested that the use of two electrodes in parallel may avoid the high concentration of energy to a small area that may occur when a single electrode serves as the anode [2].

Technique

Several different techniques have been used to ablate posteroseptal accessory AV connections. The technique that will be described in detail here is the technique which has been successful in the largest series, to date, of patients with posteroseptal accessory AV connections undergoing transcatheter ablation [3, 4].

Before transcatheter ablation is attempted, a detailed electrophysiology study is mandatory to establish the presence of a posteroseptal AV connection, which either is a necessary component of a reciprocating tachycardia circuit or which is responsible for a rapid ventricular response during atrial fibrillation or atrial flutter. In some patients who have symptomatic tachycardias, a posteroseptal accessory AV connection may be a innocent bystander. It is important to identify these patients, since ablation of the posteroseptal accessory AV connection will not eliminate the symptomatic tachycardia.

Approximately 30% of patients who have a posteroseptal accessory AV connection also have a right free wall accessory AV connection [5]. Therefore, the electrophysiologic study should include detailed mapping of the tricuspid annulus to rule out the presence of a second accessory AV connection.

At the time of the ablation procedure, surgical back-up should be arranged in the event of coronary sinus rupture and cardiac tamponade. An electrode catheter is positioned against the right ventricular apex for use as a temporary pacemaker should transient AV block occur after delivery of the shocks. A short arterial cannula is inserted to allow continuous monitoring of the blood pressure. Using a left subclavian approach, a central lumen catheter is positioned within the coronary sinus and contrast material is injected to visualize the location of the coronary sinus os. This catheter is then removed, and a 6F or 7F quadripolar electrode catheter (1 cm interelectrode distance) is inserted into the coronary sinus such that the proximal two electrodes straddle the os. These two electrodes are made electrically common and connected to the cathodal output of a defibrillator and a patch electrode (16 cm) positioned on the anterior or posterior chest is connected to the anodal sink of the difibrillator (figure 9–1). After the induction of general anesthesia by an anesthesiologist, correct catheter position is verified by fluoroscopy and a 300 joule shock (stored energy) is delivered. If the patient's hemodynamic status and AV conduction through the AV node-His-Purkinje axis remain normal, a second shock is delivered to minimize the chance that conduction through the accessory AV connection will return at a later date.

After the ablation procedure, the patient should be monitored in a coronary care unit setting for 24–48 hours and should have continuous ambulatory electrocardiographic monitoring in a ward setting for an additional four to five days. Patients who have uncomplicated course are generally discharged from the hospital five to seven days after the ablation procedure.

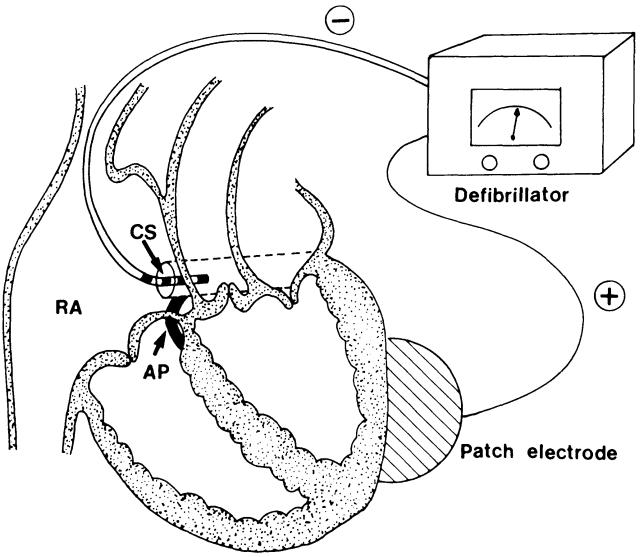

Figure 9–1. A schematic illustration of the technique used for transcatheter ablation of a posteroseptal accessory atrioventricular connection. A quadripolar electrode catheter is positioned within the coronary sinus such that the proximal pair of electrodes straddles the os. These two electrodes are connected to the cathodal output of a defibrillator. A patch electrode positioned over the midthoracic spine serves as the anode. Transcatheter shocks are delivered after the patient is anesthetized. Not shown is an electrode catheter positioned in the right ventricle for backup pacing if needed. (From reference 3, with permission from the American Heart Association.)

Results

The largest published series of patients with a posteroseptal accessory AV connection who underwent trancatheter ablation consists of eight patients and was reported in 1985 [4]. This series has now been expanded to 16 patients and will be described here.

Among the 16 patients who had a posteroseptal accessory AV connection, nine had an overt and seven had a concealed posteroseptal accessory AV connection. The mean age of these patients was 29 years, with a range of 15 to 48 years. Five of the 16 patients had a second accessory AV connection located in the right free wall. In each case, mapping during orthodromic reciprocating tachycardia demonstrated that the earliest site of atrial activation was at the os of the coronary sinus. The mean ventricular-atrial conduction time during orthodromic reciprocating tachycardia was 98 ms, with a range of 77 ms to 130 ms.

After delivery of the shocks, there was complete elimination of conduction through the posteroseptal accessory AV connection acutely in 14 of the 16

patients. In one case, discussed in detail in the next section, cardiac tamponade occurred after delivery of a single 300 joule shock. In another patient, conduction over the accessory AV connection returned within two to four minutes after the shocks were delivered. The latter patient underwent surgical ablation one week later, at which time intraoperative mapping demonstrated that he did indeed have a posteroseptal accessory AV connection.

Among the 14 patients who had good results acutely, long-term follow-up has been available in 13. Follow-up evaluation was performed during an electrophysiologic study four months after delivery of the shocks or by an intraoperative electrophysiologic study at the time of surgical ablation of the right free wall accessory AV connection in three patients who had dual accessory AV connections. Conduction over the posteroseptal assessory AV connection was found to be completely absent in ten of the 13 patients, and present in three (figure 9–2). In these three patients, conduction over the accessory AV connection initially was eliminated, but returned six days to six weeks later. In two of these three patients, conduction over the accessory AV connection was unchanged compared to baseline. However, in the other patient, retrograde conduction was found to be absent, and, although anterograde conduction over the accessory AV connection was present, it was slowed compared to baseline; atrial fibrillation was associated with a ventricular rate of 200 beats/minute before the ablation procedure, but only 150 beats/minute several months afterwards (figure 9–3). In addition, delta waves disappeared during exercise. The patient has remained asymptomatic without antiarrhythmic drug therapy.

Comparing the patients in whom the procedure was successful with those in whom it was not, there were no discernible differences in clinical variables, baseline characteristics of the accessory AV connection, or the technique used. The mean number of joules used was 750, with no difference between patients, in whom the ablation was successful and those in whom it was not. In some patients, the external patch electrode which served as the anode was placed on the back and others on the anterior chest. The success rate was equally high with both positions. The inefficacy of the attempted ablation in some patients may be due to variation in the anatomic relationship of posteroseptal AV connections to the os of the coronary sinus.

To summarize the long-term results in the above series of 15 patients in whom transcatheter ablation of a posteroseptal AV connection was attempted, conduction over the accessory AV connection was completely eliminated or modified such that symptomatic tachycardias no longer occurred in 11 of 15 patients (73%).

There has been little other published experience with transcatheter ablation of posteroseptal accessory AV connections. Other reports have consisted of one to three patients, using variations of the technique described above. For example, Nathan et al delivered 10 shocks to 46 shocks of 10 joules to 100 joules in strength at the os of the coronary sinus in three patients who had a

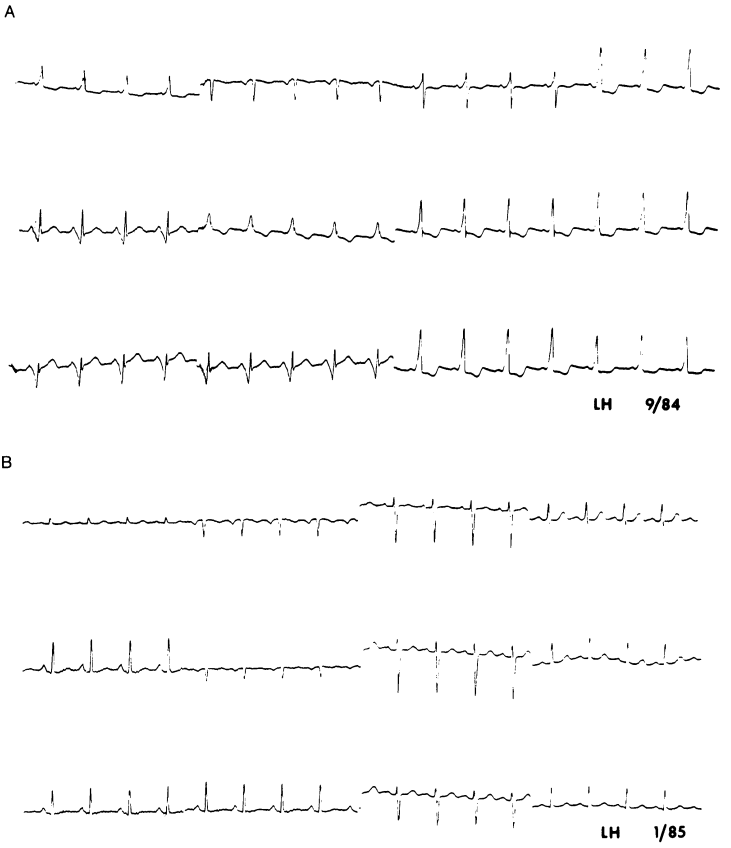

Figure 9–2. Electrocardiograms before and four months after transcatheter ablation of a posteroseptal accessory atrioventricular connection.
(A) The baseline electrocardiogram demonstrated inverted delta waves in leads II, III, and aVF, and upright delta waves in I, aVL, and V_1- V_6. This pattern of delta waves and the transition to a tall R wave between V_1 and V_2 are typical of a posteroseptal accessory atrioventricular connection.
(B) Four months after delivery of two 300 joule shocks at the os of the coronary sinus, the electrocardiogram is normal. Electrophysiologic testing demonstrated the absence of conduction over an accessory atrioventricular connection. (From reference 3, with permission from the American Heart Association.)

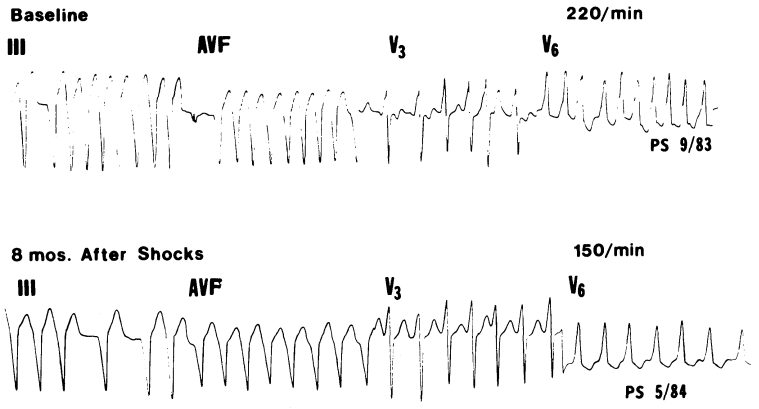

Figure 9–3. Atrial fibrillation induced during an electrophysiologic testing in a patient with a posteroseptal accessory atrioventricular connection.
Top: During a baseline study, the average ventricular rate during atrial fibrillation was 220 beats/minute.
Bottom: Eight months after the delivery of two 300 joules at the os of the coronary sinus there was persisting ventricular preexcitation, but the average ventricular rate during atrial fibrillation was 150 beats/minute. Electrophysiologic testing demonstrated the absence of retrograde conduction over the accessory atrioventricular connection, and the patient has remained free of symptomatic arrhythmias.

posteroseptal accessory AV connection [6]. The attempted ablation was successful in two of the three patients.

Bardy et al reported the successful ablation of a concealed posteroseptal accessory AV connection using two shocks of 200 joules each delivered between an electrode positioned at or near the os of the coronary sinus and an external indifferent electrode [7].

In all of the cases described above, the electrode catheter was positioned within the coronary sinus, with the electrode or electrodes through which the shock was delivered positioned at the os and connected to the cathodal output of the defibrillator. In contrast, Jackman et al localized a posteroseptal accessory AV connection by positioning the catheter across the tricuspid valve and recording an accessory pathway potential [8]. The electrode recording the largest accessory pathway potential was connected to the anodal sink of a defibrillator, and a back plate was used as the cathode. Two shocks of 160 joules and 320 joules were delivered. The attempted ablation was unsuccessful, with conduction through the accessory AV connection initially disappearing but returning 15 minutes later. Because only a single case has been reported using the technique described by Jackman et al, the efficacy of their technique cannot be commented upon.

In patients who have the permanent form of junctional reciprocating tachycardia, the retrograde limb of the tachycardia circuit may be a slowly

conducting posteroseptal accessory AV connection. Gang et al reported the successful transcatheter ablation of this type of posteroseptal accessory AV connection using two shocks of 100 joules and the same electrode configuration show in figure 9–1 [9].

Complications

In the series of 16 patients described above, the only serious complication was cardiac tamponade in one patient after delivery of a single 300 joule shock. The cardiac tamponade was successfully managed by needle pericardiocentesis, and emergent surgery was not required. Examination of the electrode catheter used in this case revealed breaks in the insulation. It was presumed that some energy was inadvertently delivered through the distal electrode within the coronary sinus, resulting in rupture of the coronary sinus. This was borne out when the patient underwent elective surgical ablation of the posteroseptal accessory AV connection one month later and was found to have a small healed perforation of the coronary sinus two to three cm from the os. This case emphasizes the importance of using intact catheters that can withstand the high energy shocks that are used for transcatheter ablation and also the importance of having surgical back-up should cardiac tamponade not responsive to needle pericardiocentesis occur.

As expected, the shocks resulted in release of creatine kinase. The mean peak level of creatine kinase MB fraction was 33 IU/L (upper limits of normal 9 IU/L). Therefore, the extent of myocardial necrosis was limited, as also reflected by the fact that a pyrophosphate scan was mildly positive in only one patient and negative in seven of eight patients who underwent scanning. No new ventricular arrhythmias were noted in any of the patients.

Although most of the 16 patients had up to several minutes of AV block after delivery of the shocks, no patient had persistent AV block. In a follow-up electrophysiologic evaluation four to 11 months after the ablation procedure, the mean AH interval was unchanged compared to baseline, and the response to atrial pacing was normal in each patient. However, retrograde conduction through the AV node-His-Purkinje axis was impaired in four patients; in these patients there was AV dissociation at slow ventricular pacing rates.

Regarding other potential complications of these shocks, no evidence of damage or thrombosis of the coronary sinus was seen angiographically in six patients or by direct intraoperative inspection in four patients. In six patients who underwent coronary angiography four months after the ablation procedure, no abnormalities of the coronary arteries were found.

TRANSCATHETER ABLATION OF LEFT AND RIGHT FREE-WALL ACCESSORY AV CONNECTIONS

Experimental Background

The effects of shocks delivered within the coronary sinus of dogs were studied by Broadman and Fisher [10]. The shocks were delivered through a bipolar or hexapolar electrode catheter positioned within the coronary sinus. In this study, the distal electrode within the coronary sinus was connected to the cathodal output of a defibrillator, and a proximal electrode was connected to the anodal sink. Five dogs received a single shock of 35 joules to 45 joules, and in these dogs gross and microscopic examination six hours later demonstrated that there was extensive ecchymosis and edema surrounding the coronary sinus, extending into the adjacent left atrial and ventricular walls into the coronary sulcus from the mitral annulus into epicardial fat. Perforation of the coronary sinus occurred in one dog who received the low energy shock. Among three dogs that received two or three 240 joule shocks, coronary sinus rupture and perforation occurred in two.

In 16 dogs, one to four 35 joule to 45 joule shocks were delivered in the coronary sinus, and morphologic examination was carried out two to 11 weeks later. In 15 of these 16 dogs, there was dense scarring of the left atrial wall adjacent to the site where the shocks had been delivered. Of note is that the coronary sinus was completely occluded at the shock site in eight of these 16 dogs, and was moderately to markedly stenotic in five. In addition, there was mild to marked intimal hyperplasia of the circumflex coronary artery in three dogs.

This study demonstrated that multiple 35 joule to 45 joule shocks in the coronary sinus may result in a sufficent degree of fibrosis of the adjacent left atrial wall to potentially interrupt conduction through a left-sided accessory AV connection. However, the study demonstrated that low energy shocks of 35 joules to 45 joules frequently result in perforation, occlusion, or stenosis of the coronary sinus.

In regards to the potential applicability of the catheter ablation technique for interrupting conduction in right-sided accessory AV connections, Ruder et al studied the effects of shocks delivered near the tricuspid annulus in dogs [11]. Shocks ranging from 50 joules to 400 joules were delivered to different areas around the tricuspid annulus, using the distal electrode of a catheter in the right atrium as the cathode and a chest wall patch as the anode. Ventricular fibrillation occurred in one dog, but none died, and there were no instances of tamponade. Morphologic examination ten days later demonstrated no damage to the tricuspid valve and no perforations of the right atrium. The size of the endocardial lesion was dependent on the energy of the shocks: 62 mm^2 with 50 joule shocks and 221 mm^2 with 400 joule shocks. Transmural damage was observed with shocks greater than 200 joules. When the ratio of the atrial and ventricular electrograms recorded at the shock site

was one or more, the endocardial lesion extended to the tricuspid annulus. When this rate was less than one, the center of the lesion was below the tricuspid annulus.

Ruder et al concluded that intracardiac shocks have the potential for damaging the right atrial wall adjacent to the tricuspid annulus in such a way as to possibly interrupt right-sided accessory AV connections [11].

Results

The results of attempted transcatheter ablation of ten left-side accessory AV connections in eight patients were reported by Fisher et al [12]. They used two to 26 shocks ranging in strength from 40 joules to 80 joules, except in one patient who received shocks of 100 joules and 150 joules. The electrode configuration used in these patients was variable. In six patients the shocks were delivered between two adjacent electrodes within coronary sinus, and in two patients an electrode within the coronary sinus served as the cathode and an external plate served as the anode. Conduction through the accessory AV connection was acutely eliminated in each patient, however, conduction returned in all patients within ten days. Only one patient remained asymptomatic without antiarrhythmic medication during the follow-up period, and the other patients all either required antiarrhythmic drug therapy or surgical ablation of the accessory AV connection.

Nathan et al reported their experience in a paitent with a left-side accessory AV connection who underwent transcatheter ablation. Twelve shocks ranging in strength from 50 joules to 100 joules were unsuccessful in ablating this pathway [6].

Kunze and Kuck reported their experience with attempted transcatheter ablation of a right free-wall accessory AV connection in five patients [13]. The right-sided accessory AV connection was localized by identification of an accessory pathway potential. Four shocks of 80 joules to 300 joules were then delivered in the right atrium. Persistent conduction block in the accessory AV connection was achieved over the long term in only one of the five patients.

Weber and Schmitz delivered two 150 joule shocks in the right atrium of a patient who had a right-sided accessory AV connection [14]. Although conduction was initially eliminated, conduction through the accessory AV connection had returned by six weeks later.

The successful ablation of two concealed right-sided accessory AV connections was reported in a patient who had a pacemaker-mediated tachycardia incorporating these two aberrant pathways as the retrograde limb of the tachycardia circuit [15]. Each of the two right-sided accessory AV connections were successfully ablated with two 200 joule shocks.

Complications

Delivery of shocks within the coronary sinus in an attempt to ablate a left free-wall accessory AV connection has resulted in at least two cases of cardiac

tamponade. Cardiac tamponade occurred in one patient after two shocks of 150 joules and 100 joules delivered at the junction of the proximal and middle thirds of the coronary sinus; this patient was successfully treated by pericardiocentesis [12]. However, cardiac tamponade and death occurred in another patient who received two shocks of 190 joules in the proximal coronary sinus (Dr. G. Fontaine, personal communication). Postmortem examination demonstrated a 1.5 cm rupture of the proximal coronary sinus.

Coronary sinus occlusion has also occurred as a complication of shocks delivered within the coronary sinus. Coronary sinus occlusion was found in two patients at the time of surgical ablation eight to nine weeks after the delivery of multiple 40 joule to 50 joule shocks within the coronary sinus [12].

Although the published experience with transcatheter ablation of left-sided accessory AV connections is very preliminary, it is apparent that there is a significant risk of coronary sinus perforation or injury when shocks are delivered directly within the coronary sinus.

With regard to complications of transcatheter ablation of right-side AV connection, there were no instances of right atrial perforation when 80 joule to 300 joule shocks were delivered in the right atrium of five patients [13]. However, one patient with a right septal accessory AV connection developed complete AV block necessitating implantation of a permanent pacemaker.

CURRENT STATUS OF TRANSCATHETER ABLATION OF ACCESSORY AV CONNECTIONS

The experience to date with transcatheter ablation of accessory AV connections is much too preliminary to allow conclusions regarding the role of transcatheter ablation techniques in the management of patients with accessory AV connections. The little data that are available suggest that the technique is most promising in patients who have a posteroseptal accessory AV connection. The long-term success rate in ablating posteroseptal accessory AV connections with transcatheter shocks appears to be approximately 75%, and the risk of serious complications appears to be acceptably low. If further experience confirms these preliminary results, transcatheter ablation of posteroseptal accessory AV connections will be an attractive alternative to surgical ablation. Successful transcatheter ablation obviates the need for surgical ablation, which has a lower success rate in patients with posteroseptal accessory AV connections (88%) than in patients with free-wall accessory AV connections (98%) [16]. Compared to surgical ablation, transcatheter ablation is associated with less discomfort to the patient, a shorter convalesence period, and less expense.

At this point in time, the success rate of transcatheter ablation of left free-wall accessory AV connections has been very low, and there has been a siginificant risk of coronary sinus perforation or injury when shocks have been delivered within the coronary sinus. Therefore, current transcatheter ablation techniques appear to be inappropriate for use in patients with left-

sided accessory AV connections. In experienced hands, surgical ablation of left free-wall accessory AV connections has a success rate of 98% and a low morbidity rate [16]. At least at present, surgical ablation is clearly preferable to attempts at transcatheter ablation in patients with a left-sided accessory AV connection.

The limiting factor in successful transcatheter ablation of right free-wall accessory AV connections is the inability to precisely localize these pathways. Improvements in mapping catheters and techniques to record accessory AV connection potentials will most likely greatly increase the potential for successful transcatheter ablation of right-sided accessory AV connections.

REFERENCES

1. Coltorti F, Bardy GH, Reichenbach D, Greene HL, Thomas R, Breazeale DG, Alferness C, Ivey TD: Catheter-mediated electrical ablation of the posterior septum via the coronary sinus: Electrophysiologic and histolgic observations in dogs. *Circulation* 72: 612–622, 1985.
2. Coltorti F, Bardy GH, Reichenbach D, Greene HL, Thomas R, Breazeale DG, Ivey TD: Effects of varying electrode configuration with catheter-mediated defibrillator pulses at the coronary sinus orifice in dogs. *Circulation* 73: 1321–1333, 1986.
3. Morady F, Scheinman MM: Transvenous catheter ablation of a posteroseptal accessory pathway in a patient with the Wolff-Parkinson-White Syndrome. *N Engl J Med* 310: 705–707, 1984.
4. Morady F, Scheinman MM, Winston SA, DiCarlo La, Jr, Davis JC, Griffin JC, Ruder M, Abbott JA, Eldar M: Efficacy and safety of transcatheter ablation of posteroseptal accessory pathways. *Circulation* 72: 170–177, 1985.
5. Morady F, Scheinman MM, DiCarlo LA, Jr., Winston SA, Davis JC, Baerman JM, Krol RB, Crevey BJ: Coexistent posteroseptal and right-sided atrioventricular bypass tracts. *JACC* 5: 640–646, 1985.
6. Nathan AW, Davies DW, Creamer JE, Butrous GS, Camm AJ: Successful catheter ablation of abnormal atrioventricular pathways in man. *Circulation* 70 (Suppl II): 396 (abstract), 1984.
7. Bardy GH, Poole JE, Coltorti F, Ivey TD, Block TA, Trobaugh GB, Greene HL: Catheter ablation of a concealed accessory pathway. *Am J Cardiol* 54: 1366–1368, 1984.
8. Jackman WM, Friday KJ, Scherlag BJ, Dehning MM, Schecter E, Reynolds DW, Olson EG, Berbari EJ, Harrison LA, Lazzara R: Direct endocardial recording from an accessory atrioventricular pathway: Localization of the site of block, effect of antiarrhythmic drugs, and attempt at nonsurgical ablation. *Circulation* 68: 906–916, 1983.
9. Gang ES, Oseran D, Rosenthal M, Mandel WJ, Deng Z, Meesmann M, Peter T: Closed chest catheter ablation of an accessory pathway in a patient with permanent junctional reciprocating tachycardia. *JACC* 6: 1167–71, 1985.
10. Brodman R, Fisher JD: Evaluation of a catheter technique for ablation of accessory pathways near the coronary sinus using a canine model. *Circulation* 67: 923–929, 1983.
11. Ruder MA, Davis JC, Eldar M, Scheinman MM: Effects of electrode catheter shocks delivered near the tricuspid annulus in dogs. *JACC* 7: 7A (abstract), 1986.
12. Fisher JD, Brodman R, Kim SG, Matos JA, Brodman E, Wallerson D, Waspe LE: Attempted nonsurgical electrical ablation of accessory pathways via the coronary sinus in the Wolff-Parkinson-White syndrome. *JACC* 4: 685–694, 1984.
13. Kunze KP, Kuck KH: Transvenous ablation of accessory pathways in patients with incessant atrioventricular tachycardia. *Circulation* 70 (Suppl II): 1649 (abstract), 1984.
14. Weber H, Schmitz L: Catheter technique for closed-chest ablation of an accessory atrioventricular pathway. *N Engl J Med* 308: 653–54, 1983.
15. Weber H, Schmitz L, Hellberg K: Pacemaker-mediated tachycardias: A new modality of treatment. *PACE* 7: 1010–1016, 1984.
16. Gallagher JJ, Sealy WC, Cox JL, Kasell JH: Results of surgery for preexcitation in 200 consecutive cases. In: *Cardiac Arrhythmias, from Diagnosis to Treatment.* S Levy, MM Scheinman, eds. New York: Futura Publishing Co., pp. 540–69, 1984.

10. CATHETER ABLATIVE TECHNIQUES FOR TREATMENT OF PATIENTS WITH AUTOMATIC ECTOPIC ATRIAL OR JUNCTIONAL TACHYCARDIA

PAUL C. GILLETTE, BERTRAND ROSS, VICKIE ZEIGLER

Automatic ectopic tachycardias represent 14% of pediatric supraventricular tachycardia and a somewhat smaller percentage of the adult population [1, 2, 3, 4]. These tachycardias have been shown to result from enhanced automaticity in the atrium or AV junction by catheter electrophysiologic studies.

CLINICAL PRESENTATION

Automatic ectopic atrial tachycardias are chronic, usually nonparoxysmal, narrow QRS tachycardias. They usually present in patients complaining of fatigue, shortness of breath, inability to exercise, or syncope. Rarely, palpitations may be the presenting symptom. The tachycardia may be discovered coincidently during a physical exam for another reason.

Junctional automatic tachycardia usually presents in infants less than a year of age as congestive heart failure [5]. It often occurs in families and has been reported concurrently in nonidentical twins. It has been diagnosed by echocardiography *in utero* in the sibling of a previous patient.

Junctional automatic focus tachycardia also occurs immediately after reparative open heart surgical procedure for congenital heart defects. Low cardiac output and use of antivagal and/or sympathomimetic drugs seem to favor the emergence of this tachycardia. It usually subsides in one to two days if the patient's cardiac output can be maintained. Maneuvers which increase vagal

tone or decrease sympathetic tones help slow this tachycardia. Mortality has been reported associated with this arrhythmia.

NATURAL HISTORY

Spontaneous resolution of atrial automatic or junctional automatic tachycardias is rare. They tend to be chronic and persist for weeks, to months, to years. The rates of atrial automatic tachycardias tend to be slower than paroxysmal supraventricular tachycardias. They have been considered benign. We have found that even tachycardia rates of 130 bpm can cause cardiomyopathy after several years. Junctional automatic ectopic tachycardia has extremely varied rates, with faster rates being found in infants. Severe congestive heart failure and sudden death occurs in greater than 50% of these patients [6]. Some cases of monitored sudden death have documented cardiac asystole.

ELECTROCARDIOGRAPHIC CHARACTERISTICS

Atrial automatic tachycardias are characterized by a P wave rate equal to or faster than the ventricular rate. First and second degree AV block are common. The P wave axis is variable and highly accurate in predicting the site of the focus. In some patients P wave axis and morphology have been virtually indistinguishable from sinus P waves. Foci in the base of the right atrial appendage and above the right upper pulmonary vein are particularly close in ECG morphology to sinus rhythm. Variations in the atrial rate in response to changes in autonomic tone are the rule, although some automatic atrial foci have had absolutely fixed rates day and night. Both permanent automatic atrial tachycardias and intermittent ones have been reported, but the permanent form predominates.

Junctional automatic tachycardias are characterized by a narrow normal QRS with a rate more rapid than the sinus rate. Retrograde (VA) conduction is very rare in junctional automatic tachycardia. Atrial capture beats are common, resulting in an irregular rate.

ELECTROPHYSIOLOGIC CHARACTERISTICS

Electrophysiology characteristics of atrial automatic focus tachycardias are very different from reentrant tachycardias. A reentrant tachycardia is usually stopped by overdrive pacing, whereas atrial automatic tachycardia is characterized by the temporary slowing of the tachycardia in response to overdrive pacing [4, 7, 8]. A reset response is usually seen in atrial automatic tachycardia in response to single premature stimulation. A nonreset response due to entrance block is also possible. The recovery and conduction times of automatic foci have been shorter than those of the sinus node. After overdrive pacing a gradual acceleration of the rate is often seen, i.e., a warm-up response. DC cardioversion does not result in conversion of an automatic

tachycardia. Both atropine and isoproterenol increase the rates of automatic foci.

PHARMACOLOGIC CHARACTERISTICS

Automatic focus supraventricular tachycardias respond very differently to drugs than reentrant tachycardias [4]. Many different antiarrhythmic drugs convert reentrant supraventricular tachycardia to sinus rhythm. Virtually no drugs convert automatic tachycardias to sinus rhythm. Digoxin has little or no effect, and beta blockers slow the rate less than 10%. Type IA (quinidine-like) drugs have no effect. Verapamil increases the rate of many automatic tachycardias. Junctional automatic tachycardias have been accelerated to dangerous levels. Calcium chloride seems to reverse these effects. Amiodarone tends to slow the rate 10% to 15% and in one case has been associated with cessation of an atrial automatic tachycardia and reversion to sinus rhythm. Flecainide and encainide offer the most promise for medical treatment of atrial automatic tachycardias. In our hands, flecainide has completely controlled one of four atrial automatic tachycardias. Propafenone has significantly slowed postoperative junctional automatic tachycardia. Intravenous xylocaine and dilantin have had small beneficial effects on automatic tachycardias. Tocainide and mexiletine have not yet been tried to our knowledge.

EVALUATION

Before deciding on catheter ablation or surgical treatment of an automatic focus, a detailed evaluation is necessary. Symptoms may be elicited in the history and signs of congestive heart failure on physical exam. The chronicity of the tachycardia may be documented by 24–48 hours of ambulatory monitoring, which also documents the rate during day-to-day activity and sleep. Echocardiography or nuclear angiography are useful noninvasive tests of ventricular function. Catheter electrophysiology study documents automaticity by lack of interruption of tachycardia and by the reset response. Mapping can localize the location of the focus (figure 10–1). Transeptal left atrial catheterization is usually necessary to localize left atrial foci. Drug trials other than flecainide or encainide seem ineffective and a waste of time.

DIFFERENTIAL DIAGNOSIS

The differential diagnosis of atrial automatic tachycardias includes sinus tachycardia or some type of reentrant mechanism. Sinus tachycardia is differentiated by its rate variation and by clinical status such as thyrotoxicosis or the discovery of a hyperadrenergic state. Reentrant tachycardias are differentiated by their electrophysiologic and pharmacologic characteristics. The most difficult differentiation is from the permanent form of junctional reciprocating tachycardia (PJRT). The differentiation is made by the response to cardiac stimulation. PJRT will virtually always exhibit some sinus beats, whereas AET does not. Reset defines automaticity. The same atrial activa-

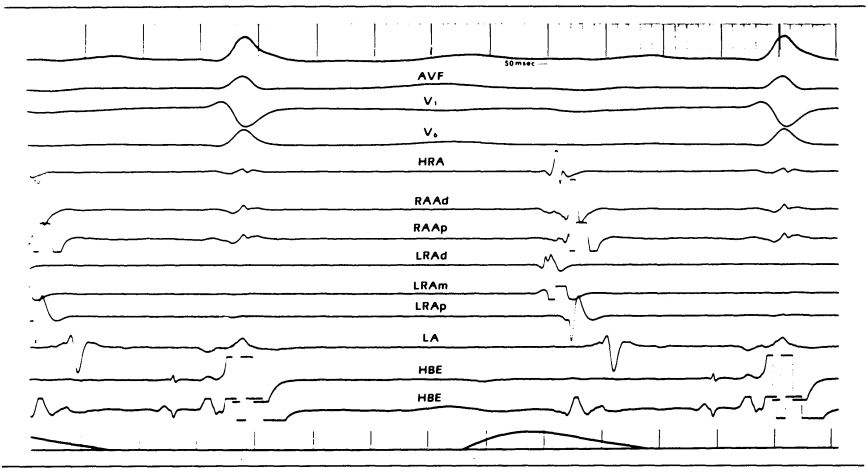

Figure 10–1. Simultaneously recorded surface ECG leads I, AVF, V_1, and V_6 and intracardiac electrograms from the high right atrium (HRA), right atrial appendage (RAA), low right atrium (LRA), left atrium (LA), and His bundle area (HBE) in a patient with a low right atrial automatic ectopic focus tachycardia. The distal low right atrial pair of electrodes shows the earliest activation. The filter settings are $30H_2$ low and 250 H_2 high. The electrograms are also limited.

tion sequence during tachycardia and ventricular pacing favors an accessory connection such as PJRT.

TREATMENT

His bundle ablation is the definitive procedure for junctional automatic tachycardia [9]. It is performed similarly to His bundle ablation intended to create AV block for atrial fibrillation [10, 11]. The major difference is that an attempt is not made to ablate the most proximal His bundle area but rather the more distal bundle. Surgical experience has taught us that the focus is often in the distal bundle [12]. A large unipolar His bundle electrogram is found, and a cathodal discharge is given from the electrode to a back patch using 3–5 watt seconds/kg of body weight [9]. Heavy sedation with diazepam and ketamine is used, and a ventricular catheter is in place for back-up pacing. The shock is synchronized to the QRS. A unit of blood and a surgical team are available if needed in an emergency situation. A permanent pacemaker is implanted the next day or during the same procedure.

Catheter His bundle ablation theoretically could be used for the most severe cases of postoperative JET, but the fresh suture lines might not withstand the barotrauma; so, in this situation, surgical cryoablation is preferred.

His bundle ablation could be used for atrial automatic tachycardias, but it would require that the patient be permanently paced; therefore, atrial ablation of the automatic focus is preferred [13, 14].

Ablation of an atrial automatic focus responsible for a supraventricular tachycardia is dependent upon the precise mapping of the focus. There is not a positive marker that the correct site has been located, as there is for His bundle ablation. Thus it is always possible that an earlier site exists that has yet to be mapped. The earliest site should precede the onset of the surface P wave. The use of multipolar catheters with 10–14 electrodes has facilitated mapping of atrial automatic foci.

TECHNIQUE

The technique of atrial ablation is similar to that of His bundle ablation. The amount of energy used depends on the site of the focus. Right atrial appendage foci are common. The possibility exists of rupturing the appendage, since it is a relatively small, relatively enclosed area with a thin wall. Energies of 50–100 watt seconds (1–2 w-s/kg) are probably the maximum for the right atrial appendage. Shocks of up to 200 watt seconds stored have been delivered to the right atrial free wall in children without perforation. The possibility exists that less energy was delivered to the endocardium because of the construction of the catheters used.

The site of the return patch (R-2 corp) has been varied according to the site of the focus. A right anterior return was used for each right atrial appendage focus, and a right lateral patch used for the right lateral focus. For the low atrial septal focus, a posterior left chest wall patch was utilized for return.

Cathodal damped sine wave shocks from a Statham defibrillator were used, synchronized to the R wave. The patients were premedicated with meperidine and promethazine and further sedated with diazepam and ketamine. General anesthesia or assisted ventilation were not used. A unit of blood previously typed and cross-matched and an operating room team were available in each instance. A ventricular pacing catheter was positioned in each patient in case AV block or sinus bradycardia occurred. After the ablation, the patients were observed in the catheterization laboratory for one hour, during which time hemodynamic monitoring was carried out in addition to the auscultation of the chest for friction rubs. They were further observed in the hospital for two to four days, and echocardiography and chest radiography were performed.

One patient who had a failed ablation of the right atrial free wall with up to 200 watt seconds was observed at surgery 24 hours later. No visible lesions were present on the epicardium. The endocardium was not visualized. The shocks had been delivered 1.5 cm from the true site of the focus.

RESULTS OF ATRIAL AUTOMATIC FOCUS ABLATION

Catheter ablation of atrial automatic focus tachycardia has been attempted five times. It was only successful twice, both times when the focus was in the right atrial appendage. No complications occurred. Free wall foci are more

difficult to precisely map and have not been successfully ablated yet. Left atrial automatic ectopic foci have not been attempted, although they have been successfully approached surgically with cryoablation. The risk of embolization on the left side of the heart is of concern, but results with left ventricular ablation are encouraging in this regard. The approach to left atrial foci is by transeptal puncture, a technique not familiar to most electrophysiologists. It seems prudent at this time to use a surgical approach to left atrial tachycardias. Surgery may also be the preferable approach for right atrial free wall unless mapping techniques can be improved. It seems unwise to induce scarring unless a considerable degree of success can be achieved. The right atrial appendage offers the most chance for success because it is the easiest right atrial site to map and possibly because of its small area. The risk of right atrial appendage ablation remains to be defined.

VENTRICULAR FUNCTION

Definitive treatment with either surgical or catheter ablation should be carried out in any patient with atrial or junctional automatic tachycardia and ventricular dysfunction. The longer the heart rate remains elevated, the more severe the cardiomyopathy becomes and the longer it takes for ventricular function to revert to normal. We have yet to see a case of chronic tachycardia associated with a chronic cardiomyopathy in which ventricular function did not revert to normal if the tachycardia was stopped.

REFERENCES

1. Gillette PC, Garson A, Jr, Porter CJ, Wampler DG: Tachycardia in children. In: *Tachycardias: Mechanisms, Diagnosis, and Treatment.* Philadelphia, PA: Lea & Febiger, 1984.
2. Gillette PC, McVey P, Garson A Jr, Ott D: Advances in the treatment of supraventricular tachycardia in children. In: *Cardiac Electrophysiology and Arrhythmias.* New York, NY: Grune & Stratton, 1985.
3. Gillette PC: The mechanisms of supraventricular tachycardia in children. *Circulation* 54: 133–139, 1976.
4. Gillette PC, Garson A, Jr: Electrophysiologic and pharmacologic characteristics of automatic ectopic atrial tachycardia. *Circulation* 56: 571–575, 1977.
5. Garson A, Jr, Gillette PC: Junctional ectopic tachycardia in children: Electrocardiography, electrophysiology and pharmacologic response. *Am J Cardiol* 44: 298–302, 1979.
6. Garson A, Jr, Gillette PC, McNamara DG: Supraventricular tachycardia in children: Clinical features, response to treatment and long-term follow-up in 217 patients. *J Pediat* 98: 857–882, 1981.
7. Scheinman MM, Basu D, Hollenberg M: Electrophysiologic studies in patients with persistent atrial tachycardia. *Circulation* 50: 266, 1974.
8. Goldreyer BN, Gallagher JJ, Damato AN: The electrophysiologic demonstration of atrial ectopic tachycardia in man. *Am Heart J* 85: 205, 1973.
9. Gillette PC, Garson A, Jr, Porter CJ, Ott D: Junctional automatic ectopic tachycardia: New proposed treatment by transcatheter His bundle ablation. *Am Heart J* 106(4): 619–623, 1983.
10. Scheinman MM, Morady F, Hess DS, Gonzalez R: Catheter-induced ablation of the atrioventricular junction to control refractory supraventricular arrhythmias. *JAMA* 248: 851–855, 1982.
11. Gallagher JJ, Svenson RH, Kasel JH, Germna LD, Bardy GH, Broughton A, Critelli G:

Catheter technique for closed-chest ablation of the atrioventricular conduction system. *N Engl J Med* 306: 194–200, 1982.
12. Gillette PC, Garson A, Jr, Hesslein PS, Karpawich PP, Tierney RC, Cooley DA, McNamara DG: Successful surgical treatment of atrial, junctional, and ventricular tachycardias in infants and children. *Am Heart J* 102: 984–991, 1981.
13. Silka MJ, Gillette PC, Garson A, Jr, Zinner A: Transvenous catheter ablation of a right atrial automatic ectopic tachycardia, *Am J Cardiol* 5: 999–1001, 1985.
14. Gillette PC, Wampler DG, Garson A, Jr, Zinner A, Ott D, Cooley D: Treatment of atrial automatic tachycardia by ablation procedures. *JACC* 6: 405–409, 1985.

11. CLINICAL EXPERIENCE WITH CATHETER ABLATIVE TECHNIQUES FOR PATIENTS WITH VENTRICULAR TACHYCARDIA

GUY FONTAINE

Ventricular tachycardia (VT) is frequently the precursor of ventricular fibrillation. Therefore, preventive treatment of VT is a major goal to reduce sudden death. The possible forms of treatment are palliative or radical, the latter referring to procedures which irreversibly alter the arrhythmogenic medium. Antiarrhythmic drugs are generally the first line of therapy for patients with VT. Treatment by means of antitachycardia pacemakers [1], the cardioverter [2], and the implantable defibrillator [3] are applicable in a limited number of patients. Cardiac electrosurgery is a definite but higher risk form of therapy and is therefore considered when none of the preceding methods are applicable or effective [4]. The surgical technique of endocardial encircling ventriculotomy has resulted in a reasonable success rate [5, 6]. Similarly, simple ventriculotomy has proved to be effective in a small group of patients [7]. The interesting concept introduced by this technique was the demonstration that a very limited surgical procedure precisely guided by epicardial mapping was able to modify enough myocardium to prevent relapse of life threatening VT. As some patients were not able to withstand a major surgical intervention, we sought methods able to modify conduction in a limited area of myocardium by a physical agent [8]. In this particular field new ablative techniques have been considered including cryosurgery [9], radiofrequency

Supported in part by grants from Centre de Recherche sur les Maladies Cardiovasculaires de l'Association Claude Bernard and La Fondation de cardiologie.

waves [4], microwaves, and laser irradiation [10]. Endocardial catheter fulguration (electrode catheter ablation), using the administration of a strong electrical shock by means of an endocavitary catheter positioned in the area to be modified, is a technique whose usefulness has already been extensively demonstrated for the indirect treatment of supraventricular tachycardia [11, 12]. The same electrical energy applied directly to the area of origin of abnormal ventricular activation, determined by endocardial mapping in the treatment of chronic ventricular tachycardia, is a more recent and promising development [13–15].

This chapter reports the results of endocardial catheter fulguration performed at Jean Rostand Hospital on a series of 31 consecutive patients with an average follow-up of 18 months.

PATIENTS

Our clinical series includes 31 patients (26 men and 5 women) between the ages of 14 and 74 (mean age: 48 ± 18). Their clinical features are summarized in table 11–1. The series represents consecutive VT cases encompassing different etiologies: 10 cases of arrhythmogenic right ventricular dysplasia, 13 cases of VT following myocardial infarction (range: 3 months to 10 years), 5 cases of idiopathic dilated cardiomyopathy, 2 cases of idiopathic VT (no structural heart disease), and 1 case of VT following surgical correction of a congenital anomaly. None of the frequent criteria of exclusion such as age, low ejection fraction, and poor general condition were applied. All of these patients were referred from different university medical centers where previous forms of medical treatment were applied. The reason for referral in each of the cases was evaluation of the patient's ventricular arrhythmia, mainly in anticipation of a major intervention.

Because of the unpredictable outcome of the fulguration procedure, as suggested by some reports (13, 16–19), and the conclusions drawn from some laboratory experiments (20–23), our patients selection was particularly cautious at the beginning of our experience. Fulguration was considered as a last resort procedure, and its use was restricted to the most resistant and difficult cases, some patients were even moribunds (24).

Reevaluation of individual response to antiarrhythmic drugs is performed in our institution in virtually all cases before the fulguration is considered. This approach allowed for drug efficacy in 66% of patients considered resistant by the referring centers. Most of these patients were treated with amiodarone at the time of referral, and we evaluated amiodarone with class I and particularly class Ic [25] agents. When amiodarone treatment is considered appropriate, a loading dose is given to shorten the time needed to reach maximal effectiveness. In order to avoid the development of side effects, the dosage of amiodarone should not exceed 400 mg/day. In cases of spontaneous recurrence or induction of monomorphic sustained VT by pro-

Table 11–1. (updated 01 APR 86)

	Age	SX	Dx	LOC	FC	EF	TI	NM	NE	LI	SI	INC	Nb	ENERG	RIP	AR	MT	10D	FOL
1	35	M	ARVD	DIAPH	1	—	>20	1	<2	M	—	−	II	240*1	—	—	—	NP	DCOD
2	62	F		DIAPH	2	—	36	2	>20	M	W	−	I	160*5	RM	O	O	RM	28M
3	74	M		INFUN	2	52%	12	1	3	M	M	−	I	160*1	NI	AMIO	PRO	NI	27M
4	37	M		DIAPH	1	58%	6	1	3	M	<D	−	II	240*6	M	O	O	NI	24M
5	27	M		DIAPH	4	25%	120	4	6	Y	I	+	I	160*17	RM	O	O	NP	DC8D
6	56	M		LV	1	45%	84	5	>20	Y	M	−	III	240*4	R	A+Pr	TH	IN	15M
7	40	F		INFUN	1	59%	48	2	16	M	M	−	II	240*1	TL	O	O	RM	18M
8	32	M		INFUN	1	—	4	1	2	W	<D	−	I	210*4	NI	AMIO	PRO	NI	21M
9	30	M		F.W.	1	56%	12	2	2	M	M	−	I	240*3	TL	A+F1	TH	IN	21M
10	38	M		INFUN		—	1	2	>20	<Y	D	+	II	240*3	NP	—	—	—	DCOD
11	60	M	MI	ANTSEP	2	12%	24	3	>20	W	D	+	II	260*1	NI	AMIO	PRO	NP	33M
12	29	M		INF	1	42%	1	2	4	M	M	−	II	260*7	RM	A+Pr	TH	NP	22M
13	73	M		ANTSEP	2	22%	1	3	>20	M	I	+	II	160*1	NP	AMIO	PRO	NP	26M
14	65	M		ANTSEP	2	—	12	1	2	W	<D	−	I	160*5	NI	O	O	NI	25M
15	55	M		INF	1	—	24	3	10	M	M	−	IV	240*2	NI	AMIO	PRO	NI	19M
16	60	M		ANTSEP	3	<25%	1	1	10	M	M	−	I	240*2	NP	—	—	—	DC4D
17	67	M		ANTSEP	3	<25%	—	2	2	D	D	−	I	240*2	NP	AMIO	PRO	NP	DC1M
18	74	M		ANTSEP		<30%		2	10	M	D	−	I	240*2	NI	AMIO	TH	NI	19M
19	64	M		ANTSEP	2	46%	4	6	14	M	D	+	I	240*2	NC	AMIO	TH	IN	DC22M
20	62	F		ANTSEP	3	26%	3	2	>20	M	I	+	IV	240*3	R	A+Bb	TH	NP	DC9M
21	53	M		ANTPOST	1	—	16	2	7	W	D	−	I	240*2	NC	AMIO	TH	IN	DC4M
22	64	M		INF	3	25%	2	3	>20	Y	D	−	I	240*2	NC	A+PM	TH	NP	14M
23	55	M		INF	1	<30%	12	1	7	W	D	+	I	280*3	NI	AMIO	PRO	NI	14M
24	18	M	IDCM	ANTSEP	2	<30%	168	1	>20	M	I	+	I	260*5	O	AMIO	TH	NI	DC14M
25	14	F		SEPTLV	3	<20%	36	1	>20	I	I	−	I	160*3	O	O	O	NP	DC2M
26	56	M		LV	2	20%		3	6	Y	M	+	I	240*3	NI	AMIO	PRO	NI	DC16MM
27	28	M		RV	1	48%	120	2	>20	<Y	D	−	III	240*1	NI	FLEC	TH	IN	17M
28	58	M		RV+LV	1	—	60	1	>20	M	D	−	III	280*3	NC	QD	TH	NI	13M
29	22	M	IDIO	POSTSEP	1	59%	96	1	>20	M	W	+	I	240*2	NI	O	TH	NP	22M
30	53	F	IDIO	INFUN	1	61%	120	4	>20	M	D	−	II	240*2	NI	O	O	NI	22M
31	21	M	CONG	INFUN	1				10	M	D		I	240*4	NI	AMIO	PRO	NP	27M

Table abbreviations are shown on page 198.

grammed pacing, a class I antiarrhythmic agent is added. Fulguration therapy is finally considered in only those cases where antiarrhythmic therapy proved inapplicable, failed, or was associated with unacceptable side effects.

PROCEDURE

Prior to the procedure, class I antiarrhythmic drug therapy is interrupted for a period equivalent to five half-lives. When used, amiodarone therapy is not discontinued (about 60% of the cases). General anesthesia is used because of the length of the procedure, since in most cases it is necessary to deliver more than one shock in a single procedure. Radial arterial pressure and capillary pressure (using a Swan-Ganz catheter) are continuously monitored. The cardiac output is also studied by the thermodilution technique.

In cases where VT is not incessant, programmed stimulation is used to induce the arrhythmia. ECG leads I, VF, V1, V6 or I, II, III, or VI are recorded from an Electronics for Medicine recorder (VR 12). These data in addition to endocardial signals, are recorded on a EMI 14 channel magnetic tape recorder. Five of the most important persons involved in the procedure are wearing microphones and headsets. All comments are recorded and proved to be of the utmost importance in case of major untoward events. Endocavitary mapping is used (figure 11–1) to localize the presumed area of origin of the VT [26]. Confirmation is sought by trying to reproduce the morphology of the VT [27] by ventricular pacing during sinus rhythm, or VT. In cases of right-sided VT, a tripolar or quadripolar USCI 6F or 7F catheter, preselected to withstand both the fulgurating current and voltage [28], is used for mapping and fulguration as well. Two other catheters, positioned in the infundibulum and apex, are also introduced for endocavitary recording and pacing, in addition to a coronary sinus or atrial catheter. For left-sided VT, the catheter used for fulguration and mapping is introduced by means of femoral or axillary (one case) arterial puncture.

Fulguration is delivered at the end of a checklist followed by a countdown during which every piece of relevant equipment is checked. The shock is synchronized with the surface QRS complexes during either VT or sinus rhythm. In case of poor synchronization, a nonsynchronized shock is automatically delivered 2 seconds after the shock has been ordered (figure 11–2). The shock is applied between the distal electrode of the fulguration catheter used as an anode and an indifferent electrode positioned in the patient's back used as a cathode. The preselected discharge energy varied from 160 joules to 320 joules. Its value was determined from previous experimental studies on animals suggesting that with our equipment an amount of 3 joules per kg was appropriate (figure 11–3). The shock is provided by the Fulgucor ODAM, Wissembourg France. This equipment includes a capacitor of 45F, an inductor of 45 mH, the internal resistance of this latter component being approximately 10 ohms. This equipment also includes an electric circuit

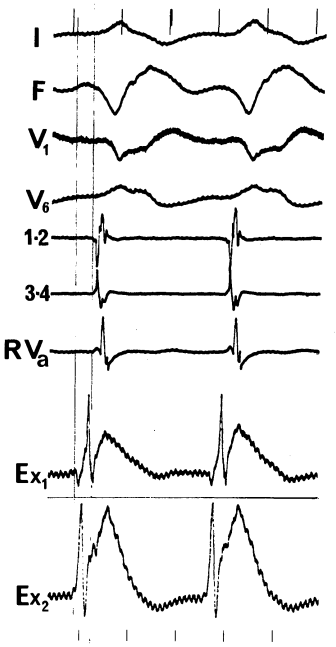

Figure 11–1. Endocardial mapping during ventricular tachycardia. Leads 1–2 and 3–4 represent the electrograms from the infundibular area recorded by a quadripolar catheter. RVa: bipolar lead located at the right ventricular apex. Exploring electrograms EX1 and EX2 near the site of VT origin are recorded. The position of the intrinsic deflection in EX2 suggests that the catheter is closer to the site of origin of ventricular tachycardia.

measuring the current and voltage applied to the fulgurating catheter [29]. Among other things, this measurement proves that the catheter is able to withstand the energy used for each fulguration. In addition, prior to sterilization, all catheters have been checked at a voltage above the peak voltage obtained during the shock by a technique previously reported [28]. A high voltage electromechanical relay automatically switches from recording of the endocardial signals to the capacitor containing the fulgurating energy.

An electrically completely independent emergency defibrillator is incorporated in our equipment. It is left charged at 40 joules in the waiting position connected to an anterior patch electrode (R2 Corporation, Morton Grove, IL, USA) with an adhesive ring on the precordial region. Its other electrode is the same as the indifferent electrode used for the fulguration shock, provided that it is positioned on the left side of the patient's back. After completion of the fulguration shock, provided stability of the fulgurating electrode, it is possible to record flattening of the endocardial potential [29]. In case of atrioventricular block, ventricular pacing is performed by means of

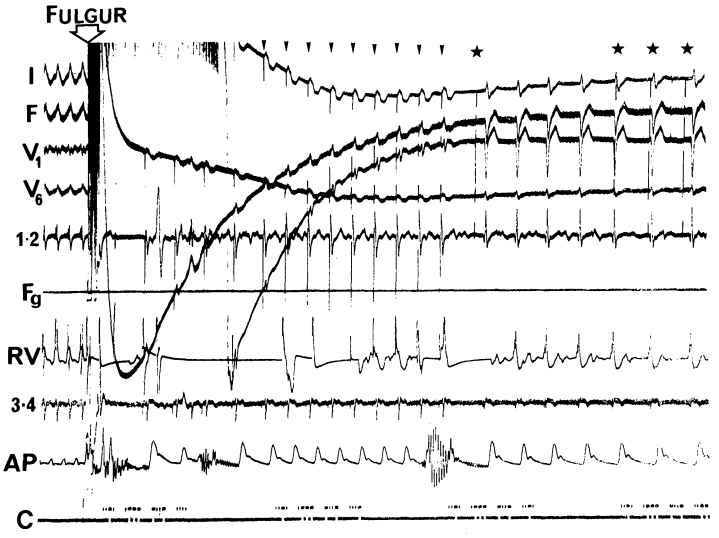

Figure 11–2. Nonsynchronized shock delivered during VT. The shock is followed by complete AV block and catheter pacing is initiated. (The spikes are stressed by downward arrows). On the right of this figure, the spontaneous ventricular rhythm resumes, and the permanent pacemaker (spikes are noted by stars) is temporarily unable to sense or pace. I, F, V1, V6: ECG leads; 1–2, 3–4: Ventricular leads from a quadripolar catheter; Fg: Fulguration lead; RV: Pacemaker signal from the right ventricle; AP: Arterial blood pressure from the radial artery; C: Technical track.

either the infundibular or apical catheter. In case of either acceleration of ventricular tachycardia or its degradation to ventricular fibrillation, a defibrillating external shock is delivered. A few minutes after fulguration, the pacing threshold reverts to a level compatible with stimulation of 20 mA, which represents the highest level of current available on our stimulating equipment. After a 10 minute rest period to permit electrical and hemodynamic stabilization, programmed stimulation is resumed. The main end points of the session are:

Failure to induce a stable, monomorphic VT by a programmed pacing protocol equivalent or more aggressive than that employed for initiating mapping [30].

Spontaneous interruption in less than 30 seconds of a previously sustained VT.

Induction of repeated episodes of acceleration of VT or VF after fulguration.

Repeated induction of VT leading to hemodynamic deterioration.

Time limitation due to technical considerations (procedure lasting more than eight hours).

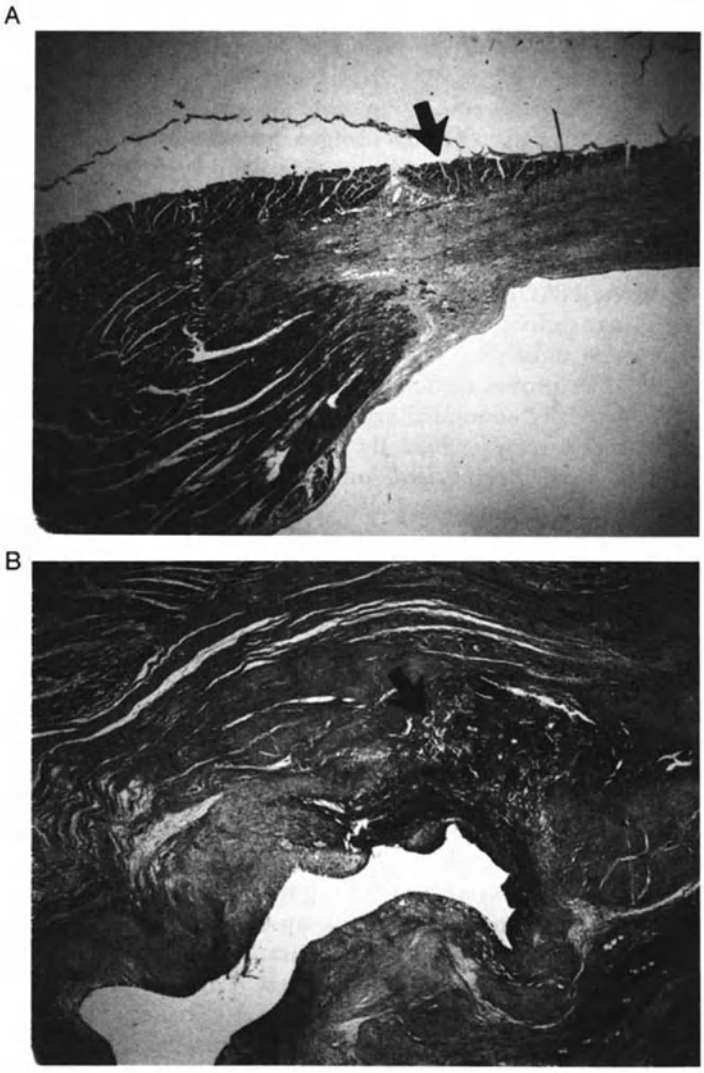

Figure 11–3. (A) Pig heart. The animal has been sacrificed one month after the experiment in which two shocks of 240 joules had been delivered close to the apex of the right ventricle. Note the fibrous tissue as a consequence of the shock. The arrow points out the rim of undamaged subepicardial layers. Note also the relative homogeneity and the clearcut demarcation between the area of fibrosis and normal tissue.
(B) Same animal. Two 360 joules shocks had been delivered in the left ventricle with a catheter firmly pressed within the trabeculae. Note the area of necrosis and hemorrhage surrounded by fibrous tissue (arrow). Normal myocardium interspersed with fibrous tissue is seen at the upper left part of the picture.

POSTPROCEDURE SURVEILLANCE

The patient's radial artery and venous blood pressures are monitored for 24 hours after ablation. A catheter is left at the apex of the right ventricle to permit reassessment of VT reinduction, provided there was no spontaneous recurrence of VT. This is achieved using a programmed pacing protocol incorporating up to three extrastimuli at basic pacing cycle lengths of 600 ms to 400 ms.

Continuous ECG monitoring is achieved by computer during a 10–day interval, either by cable or telemetry (Hewlett-Packard HP 78225 system associated with the NADIA software figure 11–4).

When ventricular tachycardia comparable to previous attacks either recurs spontaneously or is inducible, class I antiarrhythmic drug therapy is reattempted. If the latter proves ineffective, fulguration therapy is reconsidered. Amiodarone is generally continued prophylactically (50% of the cases, dosage - 400 mg/day) in cases where the previous attacks of VT were life-threatening. This is called *prophylactic* antiarrhythmic treatment (table 11–1). This category also includes patients who were taking amiodarone for treatment of extrasystoles. When drugs were necessary to prevent spontaneous or programmed pacing induced episodes of VT, this is called a *therapeutic* antiarrhythmic treatment. Table 11–1 lists the antiarrhythmic drugs administered, whether as therapeutic or as a prophylactic measure.

Effectiveness of fulguration is verified before patient discharge in almost all of the cases by programmed stimulation, 24-hour Holter recording and stress test on a stationary bicycle.

FOLLOW-UP

Complete follow-up is available through our computer data bank. Information obtained from patients, physicians, or family members is permanently updated in the computer system. Direct phone contacts to the patient or family members are used to obtain follow-up data. Follow-up time is computed from the difference between last fulguration procedure to the current date. Each death is investigated in order to know if death was "sudden" (i.e., unexpected death occurring within one hour after the first symptom).

The follow-up period of the various patients ranges from 13 months to 33 months (mean value: 21 ± 5). It should be noted, however, that 12 patients required two or more sessions.

One limitation in the evaluation of arrhythmia control is that after treatment a previously symptomatic patient could become asymptomatic due to a slower rate of tachycardia. Holter monitoring was mainly performed in those patients in whom extrasystoles were present. Reevaluation by invasive methods was performed in one case (N°19) and rehospitalization and monitoring in another (N°28) one year after the procedure. In one case an attempt to reinduce VT was performed by burst pacing through a radiofrequency

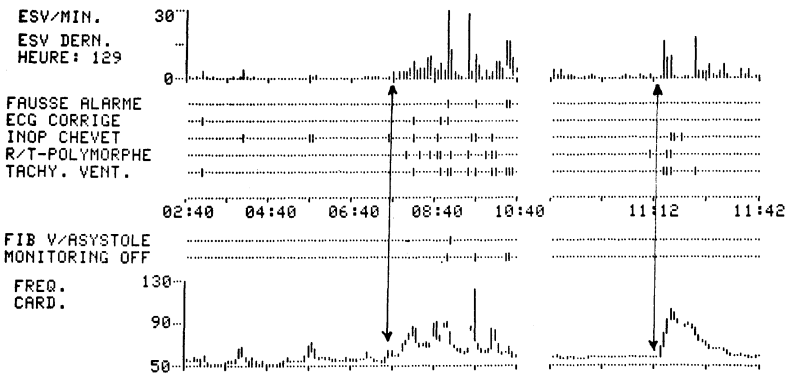

Figure 11–4. Study of arrhythmia by a computerized monitoring system during the early follow-up period. This particular case developed recurrence of ventricular tachycardia after a fulguration procedure (N°20) despite four sessions. Major antiarrhythmic treatment was able to prevent recurrence of VT. However, extrasystoles were still present, especially when the patient was awake or during exercise (lunch time). These extrasystoles were suppressed when 1.25 mg of pindolol was added to a combination of amiodarone 400mg/24 hours and flecainide 150mg/24 hours.

pacemaker connected to a catheter located at the right ventricular apex (N°2) seven months following the procedure.

Assessment of cardiac function was performed seven days after the procedure (in some cases by 2D echo). However, the results of hemodynamic studies demonstrating that the cardiac function reverted to its control values 10 to 15 minutes after the shocks, in addition to the small amount of CPK-MB fraction obtained after the shocks, made this concern less important.

RESULTS

In view of the fact that five (N°5, 11, 13, 20, 22) of the candidates for fulguration therapy were moribund, while two (N°5, 13) were already unconscious, the results were surprisingly favorable. Four (N°1, 5, 10, 16) deaths, however, occurred just after the first or the second session. These deaths will be reported in more detail later; they were related to the procedure (due to low output syndrome in three) but not to an arrhythmia or to the fulguration itself.

This new form of treatment, combined with or without antiarrhythmic drug therapy, prevented recurrence of ventricular arrhythmia in all survivors.

During reevaluation of the rhythm disorder, both during the hospital stay and during the early follow-up period, spontaneous or induced ventricular tachycardia occurred in 18 out of the 29 surviving patients, leading to a success rate of the first fulguration alone of 36% (in this percentage we have included as a success patient N°5, who died after eight days of a noncardiac

cause. This short follow-up was, nevertheless, considered as a success based on the fact that this patient was referred in incessant VT and no arrhythmia recurred until death). Success rate increased up to 57% when therapeutic drug therapy was added after the fulguration procedure.

Two deaths due to either low output failure in a patient with severe cardiomegaly (N°10) or inappropriate attention to protocol (N°1) occurred during the second procedure. Five more patients were brought under control, two requiring no further antiarrhythmic therapy (N°4 and 7), and two took prophylactic antiarrhythmic treatment (N°11 and 13). Therefore, after the second session plus drugs, the success rate for VT prevention reached 78%. Antiarrhythmic drugs having proven ineffective in the five remaining patients, a third fulguration session was again performed. Three patients (N°6, 27, 28) required antiarrhythmic therapy, but the success rate rose to 89% (27 survivors). A fourth fulguration attempt was performed in the two remaining patients. Antiarrhythmic treatment was, however, necessary in both to achieve in-hospital complete prevention of VT. Recurrences of ventricular tachycardia after discharge, although better tolerated, were observed on several occasions in three patients (N°6, 9, 15). In two of them tachycardia recurred in spite of using near toxic levels of antiarrhythmic drugs (N°6, 15). Therefore, these cases were originally considered as fulguration failures. In one case an implantable cardioverter (programmed in the nonautomatic mode) and in the other an automatic implantable defibrillator were considered. However, after a few weeks all these three patients did not experience further episodes, despite progressive reduction of their antiarrhythmic treatment.

In summary, of 27 patients surviving the periablative period, VT was brought under control in all of them by means of one or more fulguration sessions; 12 initially required antiarrhythmic treatment following the fulguration therapy.

Mortality

Over a follow-up period of 35 months, nine deaths were observed. Four were early deaths (less than one month after the procedure), two of the latter occurring during the procedure and due to low cardiac output: the first of these (N°1) was a case of arrhythmogenic right ventricular dysplasia, who underwent surgery seven years previously but developed more recent recurrent episodes of life-threatening VT at 240 bpm. Death was probably the result of lack of appropriate hemodynamic monitoring at the beginning of our experience. The second patient (N°10) succumbed from irreversible low cardiac output associated with severe myocardial failure. A few minutes before the patient succumbed, external cardiac massage was required following a single external defibrillation shock for VT acceleration. A third case of death was observed in a patient (N°16) with a low ejection fraction following

an old myocardial infarction. He had been rejected as a candidate for surgical treatment. Delay in the resuscitation procedures led to irreversible cerebral damage resulting in death four days after fulguration. Although in this case there was no recurrence of VT, the interval before death was too short to permit inclusion of this patient among those in whom fulguration was considered successful. The last case (N°5) was unconscious and in incessant VT upon arrival. A series of low-energy (160 joules) shocks led to the reduction in the rate of VT, which stopped spontaneously several hours later without the need of antiarrhythmic therapy. The patient, nevertheless, succumbed eight days later of preexisting refractory hypoxemia due to extensive pulmonary infection. No recurrence of VT was observed until death.

Anatomic and histologic examinations were performed for cases N°1, 5, and 10. They revealed modifications similar to the histological lesions observed in experimental animals [31] following the application of endocavitary shocks superimposed on the underlying pathology.

Five late deaths were observed, one (N°17) occurred one month following discharge due to acute pulmonary edema without recurrence of VT. The patient, suffering from severe coronary artery disease with poor distal vessels, low ejection fraction, cardiomegaly, and left-sided ventricular failure was considered inoperable. One (N°25) had idiopathic dilated nonobstructive cardiomyopathy: death resulted from pulmonary edema three months following fulguration, with no recurrence of rhythm disturbances. One (N°20) died of cardiac failure ten months after fulguration procedure, while on therapeutic antiarrhythmic drug treatment.

Two cases died suddenly. Case (N°24) died suddenly 14 months after fulguration during an episode of heart failure, due to end-stage idiopathic dilated cardiomyopathy. Patient (N°21) had two forms of sustained VT elicited during programmed pacing. The fulguration procedure was performed and seemed to be effective in one of the two. The *non*fulgurated VT was still inducible at the time of discharge, but the attack was slower and better tolerated. Undocumented sudden death occurred four months after the procedure, and we do not know if it was due to recurrence of the fulgurated VT, to the *non*fulgurated VT, or to a different complication.

Complications

Acute pulmonary edema was observed in two cases (N°13, 15) during the first ten minutes following fulguration. The edema was, however, brought under control using standard therapy.

In one case (N°6) during the second fulguration session, the patient experienced chest pain associated with ST segment changes and transient right bundle branch block. The rise in the CPK, and particularly the CPK MB fraction, was 140 IU higher than that observed in the other patients treated (37 ± 15 SD).

Transient complete atrioventricular block was frequently observed in the course of the procedure, immediately after shocks (28 for 167 shocks). Only in two cases (N°11, 13) did it persist after the session, but it disappeared within two hours (N°13). Intraventricular conduction delays of short duration were also noted (14 LBBB and 8 RBBB for 167 shocks). Ventricular tachycardia acceleration or ventricular fibrillation were observed in 15% of the shocks immediately following the initial electrical discharge [32]. No malignant arrhythmia resistant to defibrillation was observed following fulguration. In one case (N°16), however, probably because of hypoxia, numerous defibrillating shocks were necessary.

Long-term relapse of VT

One case (N°29) experienced a syncopal relapse due to VT 14 months after the fulguration. He concealed this event for ten months for personal reasons. The relapses became more frequent and the patient recently underwent a repeat fulguration procedure.

DISCUSSION

Our results confirm the favorable results already reported both by Hartzler [13, 33] in coronary artery disease patients and Puech [14] in a case of arrhythmogenic right ventricular dysplasia. These authors first reported the use of fulguration for treatment of VT [12, 34–37].

Other investigators have reported less favorable results in the management of VT with this technique. We do not think that differences in patient population explain the different results. We think that it might be explained by a difference in the selection of the equipment. We observed at the beginning of our experience that the vast majority of the regular USCI catheters were not able to withstand both the high peak of current and voltage necessary to obtain the desired effects on the endocardium [31]. We developed a technique to select USCI tripolar or quadripolar catheters by a nondestructive high voltage test [28, 38]. As a result, we were able to demonstrate in some cases that a successful outcome could be obtained using a relatively low fulguration energy delivered in a single shock [24].

A second difference is based on the fact that we originally decided to use the active electrode as the anode rather than the cathode because in vitro studies of the effect of shocks demonstrated that anodal shocks provided stronger mechanical effect [39].

Recently we observed that the waveform generated by different defibrillators must also be taken into account. It was observed from limited in vitro experiments that waveforms with rapid risetimes led to stronger mechanical effect and tissue damage.

These three points could therefore make difficult any comparison between our results and others for animal and human use of fulguration.

Ventricular tachycardia morphologies

It is now well accepted that nonsustained or polymorphic VT induced by programmed pacing may not be clinically significant [40]. Therefore, only patients with sustained monomorphic VT were evaluated. However, programmed pacing could also induce VT morphologies not previously documented (nonclinical VTs). Since all class I antiarrhythmic drugs were discontinued several days before the fulguration procedure, they could not be implicated as a cause of different VT morphology induced during the fulguration procedure [41]. We have learned by experience that both clinical as well as nonclinical VTs should be considered for fulguration [44, 17].

Endocardial catheter mapping

In four cases (N°3, 7, 11, 13) a single fulguration shock between 160 joules and 240 joules was sufficient to prevent recurrences of VT without the need for antiarrhythmic treatment. This suggests that the minor injury produced by the shock is at least in some cases able to modify a pathologic substrate which was the basis of a life-threatening arrhythmia. This finding confirms a previously reported similar result when we observed that relatively minor surgical intervention (simple ventriculotomy) was able to prevent recurrence of resistant VT [7, 43]. However, due to the limitations of present techniques for producing endocardial surface damage by the shock, we emphasize that precise endocardial mapping is an important prerequisite for the success of the procedure.

The precise characteristics of the endocavitary potential considered as a marker for determination of the site to be fulgurated remain unclear. However, we came to the conclusion that the absence of presystolic activity led invariably to VT recurrences. In contrast, success was greater in cases where high amplitude early presystolic endocardial potentials were recorded during VT. On the other hand, the concept of VT prevention by delivering one or several blind shocks within the ventricular cavity has never been substantiated.

Mortality

Although we are still in the learning phase in use of the fulguration procedure, the risks involved in this form of therapy appear acceptable. Three patients (N°5, 11, 13) were moribund when effective fulguration was performed. At least nine cases (N°5, 10, 11, 13, 16, 17, 20, 22, 24, 25) involved prohibitive surgical risks. None died of the immediate effect of the shock.

Two accidents terminating in death early in the study could have been avoided: the first (N°1) by more careful hemodynamic surveillance and the second (N°16) by avoiding a modification of our anesthetic protocol. Five deaths (N°5, 10, 17, 20, 25) were the consequence of the evolution of a preexistent severe cardiac pathological condition.

Two patients (N°21, 24) died suddenly. One patient (N°21) was of note. In this patient the nonfulgurated less rapid VT was still inducible at the time of discharge and clinical recurrences were better tolerated. In retrospect, we think that this patient would have been a candidate for either an implantable defibrillator or another fulguration procedure. In case number 24 sudden death was observed 14 months after the procedure, and, despite documented episodes of VT, preterminal deterioration of cardiac function precluded another fulguration attempt.

Recurrences

In some cases, recurrences were likely due to technical difficulties involving the catheter [38]: insufficient energy output (N°11) or fulguration performed remote from the zone of origin of the VT (N°13, 15). Other recurrences are less easily explained but may be related to: inadequate endocardial mapping and/or arrhythmogenic areas extending beyond the zone benefiting from fulguration. Of note was the finding that in some cases remission occurred after a transient period of relapses. Several investigators have documented the late development of His bundle interruption several weeks or months after a seemingly inadequate His bundle-fulguration procedure.

The fulguration process

Fulguration change implies two principal mechanisms: 1) a flow of electric current crossing the myocardium between the active and indifferent electrodes and, 2) the formation of at least two shock waves. The first, is produced by the abrupt surge of vapor generated by the creation of ionized plasma around the active electrode tip and the liquid environment and the second when the vapor globe collapses after the end of the delivery of current [45]. This mechanical perturbation of the electrical discharge is propelled in all directions. The collapse of the vapor globe against the wall of the myocardium could cause a particularly violent impact [46]. While the effect of electrical current on the myocardium has been extensively discussed with respect to external defibrillation [47–51], the same is, however, not true for its endocavitary application [31]. The respective parts played by both electrical and mechanical agents in the process of fulguration remain to be defined.

Secondary effects

Recent experimental data from our laboratory indicate that following endocavitary fulguration delivered to a healthy endocardium (pig weighing 80 kilos), the cardiac output decreases by 10% to 15% for approximately ten minutes. One instance of acute pulmonary edema (N°13) observed in our series was probably related to the fulguration of a nearly normal myocardium.

Episodes of ventricular tachycardia acceleration or fibrillation brought on by fulguration or occurring during programmed VT activation were occa-

sionally observed [32], but these arrhythmias responded immediately to external defibrillation. This experience emphasizes the necessity of prepositioning the defibrillating electrodes in order to avoid disturbance of sterile fields and fluoroscopic equipment.

The case of myocardial infarction (N°6) observed during the fulguration procedure did not result from the endocavitary shock itself but was the consequence of difficulty encountered during manipulation of the catheter across the aortic valve. Review of the magnetic tapes revealed that during catheter insertion, the patient complained of chest pain, which was rapidly followed by progressive ST segment modification and right bundle branch block. Transient ischemia resulted in a definite increase of CPK isoenzyme. MB fraction was therefore produced. Modification of the technique employed subsequently eliminated this risk.

Measurement of the myocardial isoenzyme of the creatine kinases revealed low values (38 ± 15 international units), confirming our experience in experimental studies; the myocardial area altered by the endocavitary shock is limited [31]. Consequently, fulguration may be repeated, if necessary.

A defect in the functioning of one patient's permanent pacemaker at the time of fulguration required replacement of the latter. There is, in fact, a risk that the electrical output of the endocavitary shock may affect the functioning of a unipolar device [52, 53].

THE ROLE OF PACEMAPPING AND VT INDUCTION AFTER FULGURATION

Despite the fact that the pacemapping technique needs to be fully perfected, it nevertheless proved highly valuable in some cases when VT could not be induced during the session; guided exclusively by this method, it was possible to deliver discharges which proved to be effective.

The predictive value of VT reinduction during fulguration sessions is relatively unreliable. Fifty percent of recurrences took place in cases where it was not possible to reinduce VT at the end of the session. However, in all the patients who remained inducible, a spontaneous or subsequent induced recurrence was observed. Better results were, however, obtained ten days following fulguration, although it completely failed in one case (N°15). Reevaluation on the tenth day cannot account for modifications apt to develop over a longer period, since it may be too early for long-term evaluation of chronic changes.

LIMITATIONS OF THE TECHNIQUE

Many questions concerning the treatment of VT by fulguration remain to be answered. Little is still known about the cellular modifications of the arrhythmogenic substrate after the electrical discharge. The various mechanical factors involved need clarification. How important is the positioning of

the indifferent electrode? Which electrical parameters are the most reliable? What should be the size and shape of fulguration electrodes? What are the best criteria for choosing the fulguration target [18]? These questions need to be addressed before the technique meets its full clinical potential.

TABLE ABBREVIATIONS

Dx = Cardiac diagnosis; ARVD: Arrhythmogenic right ventricular dysplasia, MI: Myocardial infarction, IDCM: Idiopathic dilated cardiomyopathy, IDIO: Idiopathic VT (no structural heart disease), CONG: Congenital malformation.
LOC = Location of abnormality; DIAPH: Diaphragmatic, INFUN: Infundibulum, LV: Left ventricle, F.W.: Free wall, ANTSEP: Anteroseptal, ANTPOST: Anterior and posterior, INF: Inferior, SEPTLV: Left ventricular septum, RV: Right ventricle, POSTSEP: Posteroseptal.
FC = Functional class (NYHA).
EF = Ejection fraction (echography, angiography, scintigraphy).
TI = Time interval since the first attack of VT (months).
NM = Number of clinical morphologies of VT.
NE = Total number of VT episodes prior to fulguration.
LI, SI = Longest and shortest interval between two episodes of VT; I: incessant, day, week, month or year.
INC = Incessant VT in the electrophysiological laboratory.
Nb = Number of fulguration sessions.
ENERG = Joules delivered: 160*5 = 5 discharges of 160 joules (value concerning the last procedure).
RIP = Reasons for interrupting the procedure; R: Changes in rate, M: Changes in morphology, NP: Programmed pacing not performed, TL: Time limit, NC: Nonclinical VT, NI: VT not inducible.
AR = Anti-arrhythmic prescription upon hospital discharge; AMIO: Amiodarone, A + Pr: Amiodarone + propafenone, A + Fl: Amiodarone + flecainide, FLEC: Flecainide, A + Bb: Amiodarone + beta-blockers, A + PM: Amiodarone + pacemaker, QD: Quinidine.
MT = Mode of treatment; PRO, TH: Prophylactic or therapeutic treatment.
10D = Provocative test performed 10 days after fulguration; NP: Provocative test not performed, NI: VT not inducible, IN: Inducible by programmed stimulation, RM: Change in rate and morphology of VT morphology.
FOL = Follow-up; DC: Death.

REFERENCES

1. Dulk KD, Bertholet M, Brugada P: Clinical experience with implantable devices for control of tachyarrhythmias. *PACE* 7:548, 1984.
2. Zipes DP, Heger JJ, Miles WM, Prystowsky EN: Synchronous intracardiac cardioversion. *PACE* 7: 522, 1984.
3. Mirowski M, Reid PR, Mower MM, Watkins L, Platia EV, Griffith L, Juanteguy JM: The automatic implantable cardioverter defibrillator. *PACE* 7: 534, 1984.
4. Fontaine G, Guiraudon G, Frank R, Tereau Y, Pavie A, Cabrol C, Chomette G, Grosgogeat Y: Surgical management of ventricular tachycardia not related to myocardial ischemia. In: *Tachycardias: Mechanisms, Diagnosis and Treatment*, ME Josephson, H.J.J. Wellens, eds. Lea & Febiger, pp 451–473, 1984.
5. Guiraudon G, Fontaine G, Frank R, Grosgogeat Y, Cabrol C: Encircling endocardial ventriculotoms, late follow-up results. *Circulation* 62 (Suppl III): 1233, 1980.
6. Fontaine G, Guiraudon G, Frank R, Coutte R, Cabrol C, Grosgogeat Y: Intraoperative mapping and surgery for the prevention of lethal arrhythmias after myocardial infarction. In: *Sudden Coronary Death*, HM Greenberg, EM Dwyer, eds. Ann NY Acad Sci, Vol 382, pp 396, 1982.
7. Fontaine G, Guiraudon G, Frank R, Gerbaux A, Cousteau JP, Barillon A, Gay RJ, Cabrol C, Facquet J: La cartographie epicardique et le traitement chirurgical par simple ventriculotomie de certaines tachycardies ventriculaires rebelles par reentree. *Arch Mal Coeur* 68: 113–124, 1975.
8. Fontaine G: Les methodes ablatives. *Arch Mal Coeur* 77: 1299–1300, 1984.

9. Gallagher JJ, Anderson RW, Kasell JH, Rice JR, Pritchett EL, Gault JH, Harrison LA, Wallace AG: Cryoablation of drug-resistant ventricular tachycardia in a patient with a variant of scleroderma. *Circulation* 57: 190, 1978.
10. Mesnildrey P, Laborde F, Beloucif S, Mayolini P, Piwnica A: Tachycardies ventriculaires d'origine ischemique. Traitement chirurgical par thermo-exclusion circonferentielle au laser Nd-Yag. *Presse Med* 15: 531–534, 1986.
11. Scheinman MM, Evans-Bell T: Catheter ablation of the atrioventricular junction: A report of the percutaneous mapping and ablation registry. *Circulation* 70: 1024–1029, 1984.
12. Gallagher JJ, Svenson RH, Kasell JH, German LD, Bardy GH, Broughton A, Critelli G: Catheter technique for closed-chest ablation of the atrioventricular conduction system. *N Engl J Med* 306: 194–200, 1982.
13. Hartzler GO, Giorgi LV: Electrode catheter ablation of refractory ventricular tachycardia: Continued experience. *J Am Coll Cardiol* 3: 512, 1984.
14. Puech P, Gallay P, Grolleau R, Koliopoulos N: Traitement par electrofulguration endocavitaire d'une tachycardie ventriculaire recidivante par dysplasie ventriculaire droite. *Arch Mal Coeur* 77: 826–835, 1984.
15. Fontaine G, Tonet JL, Frank R, Gallais Y, Farenq G, Grosgogeat Y: La fulguration endocavitaire. Une nouvelle methode de traitement des troubles du rythme? *Ann Cardiol Angeiol* 33: 543–561, 1984.
16. Hartzler GO, Giorgi LV, Diehl AM, Hamaker WR: Right coronary spasm complicating electrode catheter ablation of a right lateral accessory pathway. *J Am Coll Cardiol* 6: 250–253, 1985.
17. Gallagher JJ: Ablation by transcatheter shock. Current Status. *Chest* 88: 804–806, 1985.
18. Josephson ME: Catheter ablation of arrhythmias. *Ann Intern Med* 101: 234–237, 1984.
19. Bharati S, Scheinman MM, Morady F, Hess DS, Lev M: Sudden death after catheter-induced atrioventricular junctional ablation. *Chest* 88: 883–889, 1985.
20. Lerman BB, Weiss JL, Bulkley BH, Becker LC, Weisfeldt ML: Myocardial injury and induction of arrhythmia by direct current shock delivered via endocardial catheters in dogs. *Circulation* 69: 1006–1012, 1984.
21. Bardy GH, Coltorti F, Ivey TD, Greene HL: Some factors affecting bubble formation during catheter ablation *PACE* 8: 311 (abstract), 1985.
22. Kempf F, Falcone RA, Waxman HL, Marchlinski FE, Josephson ME: Anatomic and hemodynamic effects of electrical discharges in the ventricle. *Circulation* 68 (Suppl III): 696, 1983.
23. Holt PM, Boyd EG: Hematologic effects of the high-energy endocardial ablation technique. *Circulation* 73: 1029–1036, 1986.
24. Fontaine G, Tonet JL, Frank R, Lacroix H, Farenq G, Gallais Y, Drobinski G, Grosgogeat Y: Traitement d'urgence de la tachycardie ventriculaire chronique apres infarctus du myocarde par la fulguration endocavitaire. *Arch Mal Coeur* 78: 1037–1043, 1985.
25. Frank R, Fontaine G, Tonet JL, Grosgogeat Y: Treatment of severe chronic ventricular arrhythmias by flecainide combined with amiodarone. *Eur Heart J* 5 (Suppl I): 181 (abstract), 1984.
26. Josephson ME, Horowitz LN, Spielman SR, Waxman HL, Greenspan AM: Role of catheter mapping in the preoperative evaluation of ventricular tachycardia. *Am J Cardiol* 49: 207, 1982.
27. O'Keefe DB, Curry PV, Prior AL, Yates JK, Deverall PB, Sowton E: Surgery for ventricular tachycardia using operative pace mapping. *Br Heart J* 43: 116, 1980.
28. Fontaine G, Cansell A, Lechat P, Frank R, Grosgogeat Y: Method of selecting catheters for endocavitary fulguration. *Stimucoeur* 12: 285–289, 1984.
29. Fontaine G, Tonet JL, Frank R, Touzet I, Dubois-Rande JL, Gallais Y, Grosgogeat Y: Traitement des tachycardies ventriculaires rebelles par fulguration endocavitaire associee aux anti-arythmiques. *Arch Mal Coeur* (in press), 1986.
30. Tonet JL, Fontaine G, Frank R, Gosgogeat Y: Treatment of refractory ventricular tachycardias by endocardial fulguration *Circulation* 72 (Suppl III): 388, 1985.
31. Lechat P, Fontaine G, Cansell A, Grosgogeat Y: Epicardial and endocardial myocardial damage related to catheter ablation techniques *Eur Heart J* 5 (Suppl 1): 258 (abstract), 1984.
32. Tonet JL, Baraka M, Fontaine G, Abdelali S, Frank R, Menezes-Falcao L, Funck-Brentano C, Grosgogeat Y: Ventricular arrhythmias during endocardial catheter fulguration of ventricular tachycardias. *JACC* 7(2): 236A, 1986.

33. Hartzler GO: Electrode catheter ablation of refractory focal ventricular tachycardia. *JACC* 2: 1107–1113, 1983.
34. Gonzalez R, Scheinman MM, Margaretten W, Rubinstein M: Closed chest electrode-catheter technique for His bundle ablation in dogs. *Am J Physiol* 241: H283–H287, 1981.
35. Scheinman MM, Morady F, Shen EN: Interventional electrophysiology: Catheter ablation technique. *Clin Prog Pacing Electrophysiol* 1: 375–381, 1983.
36. Scheinman MM, Morady F, Hess DS, Gonzalez R: Catheter-induced ablation of the atrioventricular junction to control refractory supraventricular arrhythmias. *JAMA* 248: 851–855, 1982.
37. Scheinman MM, Morady F, Hess DS, Gonzalez R: Transvenous catheter technique for induction of damage to the atrioventricular junction in man. *Am J Cardiol* 49: 1013 (abstract), 1982.
38. Fontaine G, Cansell A, Lechat P, Frank R, Tonet JL, Grosgogeat Y: Les chocs electriques endocavitaires. Problemes lies au materiel. *Arch Mal Coeur* 77: 1307–1314, 1984.
39. Hoffman BF, Cranefield PF: *Electrophysiology of the Heart.* Mount Kisco NY: Futura Publishing Co, 1976.
40. Brugada P, Green M, Abdollah H, Wellens HJ: Significance of ventricular arrhythmias initiated by programmed ventricular stimulation: The importance of the type of ventricular arrhythmia induced and the number of premature stimuli required. *Circulation* 69: 87–92, 1984.
41. Horowitz LN, Vetter VL, Harken AH, Josephson ME: Electrophysiologic characteristics of sustained ventricular tachycardia occurring after repair of tetralogy of fallot. *Am J Cardiol* 46: 446–452, 1980.
42. Tonet JL, Baraka M, Frank R, Fontaine G, Gallais Y, Abdelali S, Grosgogeat Y: Endocardial catheter fulguration of ventricular tachycardias: Pitfalls of the clinical and nonclinical approach. *Circulation* 72: (Suppl III): 388, 1985.
43. Fontaine G, Frank R, Bonnet M, Cabrol C, Guiraudon G: Methode d'etude experimentale et clinique des syndromes de Wolff-Parkinson-White et d'ischemie myocardique par cartographie de la depolarisation ventriculaire epicardique. *Coeur Med Interne* 12: 105, 1973.
44. Mason JW, Stinson EB, Winkle RA, Oyer PE, Griffin JC, Ross DL: Relative efficacy of blind left ventricular aneurysm resection for the treatment of recurrent ventricular tachycardia. *Am J Cardiol* 49: 241–248, 1982.
45. Tidd MJ, Webster J, Cameron Wroght H, Harrison IR: Mode of action of a surgical electronic lithoclast high speed pressure, cinematographic and schlieren recordings following an ultrashort underwater electronic discharge. *Biomed Engin* 1: 5–11, 1976.
46. Chanine GL: Etude locale du phenomene de cavitation. Analyse des facteurs regissant la dynamique des interfaces. *These de Doctorst es Sciences*, Paris, 1979.
47. Van Vleet JF, Tacker WA Geddes LA, Ferrans VF: Acute cardiac damage in dogs given multiple transthoracic shocks with a trapezoidal waveform defibrillator. *Am J Vet Res* 38: 617–626, 1977.
48. Dahl CF, Ewy GA, Warner ED, Thomas ED: Myocardial necrosis from direct current countershock. Effect of paddle electrode size and time inteval between discharges. *Circulation* 50: 956–961, 1974.
49. Ehsani A, Ewy GA, Sobel BE: Effects of electrical countershock on serum creatine phosphokinase (CPK) isoenzyme activity. *Am J Cardiol* 37: 12–18, 1976.
50. Slodki SJ, Falicov RE, Katz MJ, West M, Zimmerman HJ: Serum enzyme changes following external direct current shock therapy for cardiac arrhythmias. *Am J Cardiol* 17: 792–797, 1966.
51. Mandecki T, Giec L, Kargal W: Serum enzyme activities after cardioversion. *Br Heart J* 32: 600–602, 1970.
52. Fontaine G, Touil F, Frank R, Cansell A, Gorins D, Tonet JL, Grosgogeat Y: Defibrillation, fulguration et cardioversion: Effets sur les pacemakers. *Stimucoeur* 12: 91–101, 1984.
53. Bowes RJ, Bennett DH: Effect of transvenous atrioventricular nodal ablation on the function of implanted pacemakers. *PACE* 8: 811–814, 1985.

INDEX